

Desulphurisation in 21st century iron- and steelmaking

Schrama, F.N.H.

DOI

[10.4233/uuid:4f1e8ff6-e910-4048-8a17-2a959c74f508](https://doi.org/10.4233/uuid:4f1e8ff6-e910-4048-8a17-2a959c74f508)

Publication date

2021

Document Version

Final published version

Citation (APA)

Schrama, F. N. H. (2021). *Desulphurisation in 21st century iron- and steelmaking*. [Dissertation (TU Delft), Delft University of Technology]. <https://doi.org/10.4233/uuid:4f1e8ff6-e910-4048-8a17-2a959c74f508>

Important note

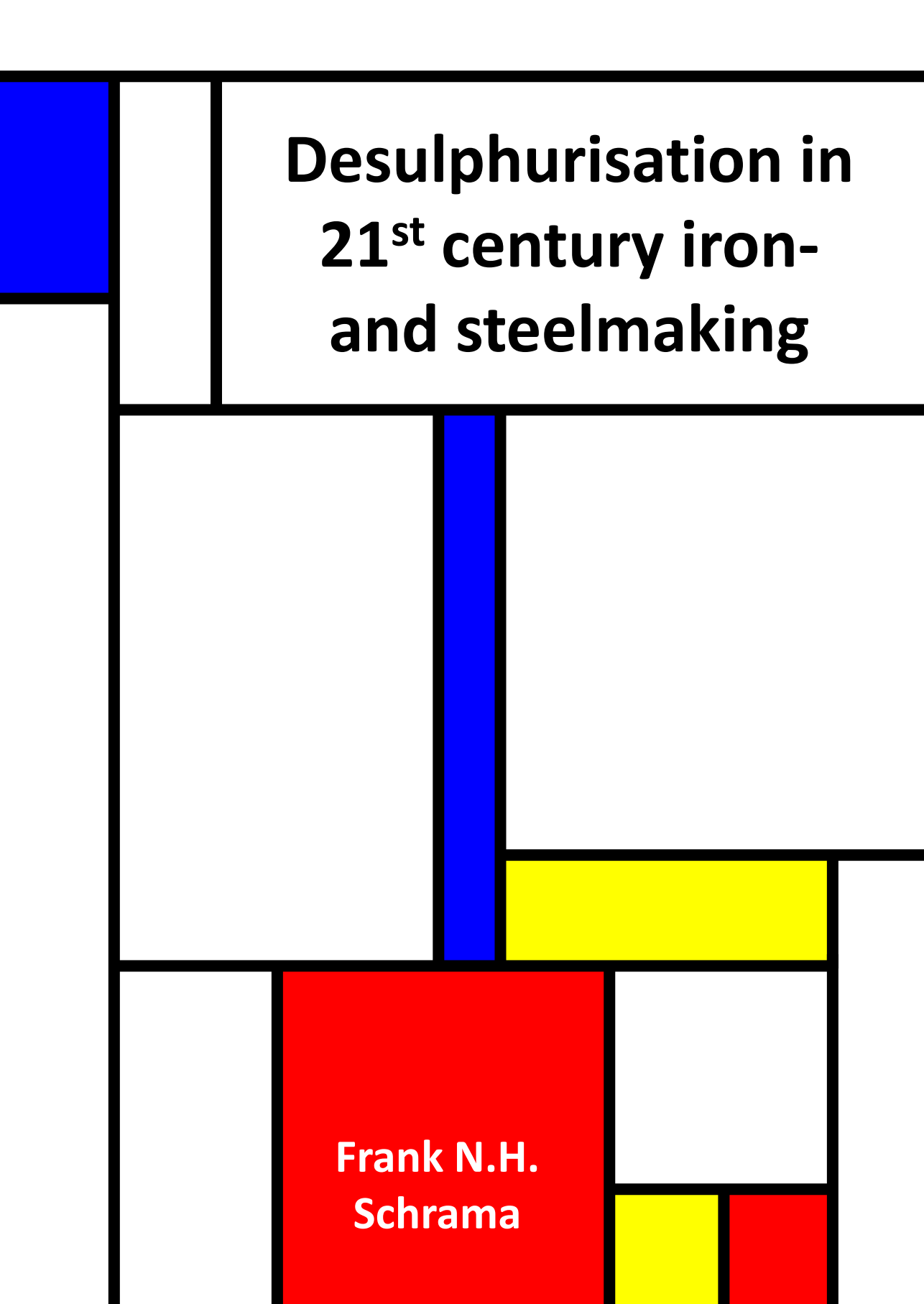
To cite this publication, please use the final published version (if applicable).
Please check the document version above.

Copyright

Other than for strictly personal use, it is not permitted to download, forward or distribute the text or part of it, without the consent of the author(s) and/or copyright holder(s), unless the work is under an open content license such as Creative Commons.

Takedown policy

Please contact us and provide details if you believe this document breaches copyrights.
We will remove access to the work immediately and investigate your claim.



**Desulphurisation in
21st century iron-
and steelmaking**

**Frank N.H.
Schrama**

Desulphurisation in 21st century iron- and steelmaking

Proefschrift

Ter verkrijging van de graad van doctor
aan de Technische Universiteit Delft,
op gezag van de Rector Magnificus, prof.dr.ir. T.H.J.J. van der Hagen,
voorzitter van het College voor Promoties,
in het openbaar te verdedigen op maandag 4 oktober 2021 om 15.00 uur

door

Frank Nicolaas Hermanus SCHRAMA

Master of Science in Chemical Engineering, Universiteit Twente,
geboren te Enschede

Dit proefschrift is goedgekeurd door de promotoren.

Samenstelling promotiecommissie bestaat uit:

Rector Magnificus, Dr. Y. Yang	voorzitter Technische Universiteit Delft, promotor
Prof.dr.ir. J. Sietsma	Technische Universiteit Delft, promotor

Onafhankelijke leden:

Prof.dr. M.J. Santofimia Navarro	Technische Universiteit Delft
Prof.dr.ir. J.L. Schenk	Montan Universiteit Leoben, Oostenrijk
Prof.dr. T. Fabritius	Universiteit Oulu, Finland
Prof. B. Björkman	Technische Universiteit Luleå, Zweden
Prof.dr.ir. J.M.C. Mol	Technische Universiteit Delft, reserve lid

Overige leden:

Prof.dr. R. Boom	Technische Universiteit Delft
Dr.ir. E.M. Beunder	Tata Steel Europe, IJmuiden

Cover: Ontzwaveling in Stijl (*Desulphurisation in Stijl*)

Cover design: Frank Schrama

Copyright © 2021 by Frank Schrama

Printed in Enschede by Gildeprint (www.gildeprint.nl)

ISBN 978-94-6419-301-5

This research was funded by Tata Steel Nederland Technology BV.

*Voor
Jantsje, Rein en Wende*

Table of contents

Part I: Introduction

1	General introduction	3
1.1	Steelmaking	4
1.2	Sulphur and desulphurisation	6
1.3	Slag in hot metal desulphurisation	7
1.4	HIIsarna hot metal	8
1.5	This thesis: desulphurisation in 21 st century iron- and steelmaking	10
1.6	References	12
2	Sulphur removal in ironmaking and oxygen steelmaking	15
2.1	Introduction	16
2.2	Sulphur distribution flow	17
2.3	Thermodynamics	20
2.3.1	Introduction	20
2.3.2	Lime	20
2.3.3	Calcium carbide	22
2.3.4	Magnesium	23
2.3.5	Resulphurisation	25
2.4	Kinetics	26
2.5	Sulphur removal in the blast furnace	27
2.6	Hot metal desulphurisation	28
2.6.1	Torpedo desulphurisation	28
2.6.2	Co-injection	29
2.6.3	Kanbara reactor	30
2.6.4	Magnesium mono-injection	31
2.7	Sulphur removal in the converter	32
2.8	Steel desulphurisation	33
2.8.1	Vacuum based processes	34
2.8.2	Ladle furnace	35
2.8.3	Other secondary metallurgy processes	35
2.9	Outlook	36
2.10	Concluding remarks	37
2.11	References	38

Part II: Optimal hot metal desulphurisation slag

3	Optimal hot metal desulphurisation slag: fundamentals	45
3.1	Introduction	46
3.2	Sulphur removal capacity	47
3.2.1	Desulphurisation process	47
3.2.2	Sulphide capacity	50
3.2.3	C_S in an industrial HMD	56
3.2.4	Basicity	58
3.3	Iron loss	59
3.3.1	Types of iron loss	59
3.3.2	Iron droplets	61
3.3.3	Viscosity of the slag	63
3.3.4	Solid fraction of the slag	67
3.3.5	Interfacial tension	69
3.4	Optimal slag	70
3.5	Conclusions	71
3.6	References	72
4	Optimal hot metal desulphurisation slag: evaluation	79
4.1	Introduction	80
4.2	HMD slag thermodynamic evaluation	81
4.2.1	Monte Carlo simulation input	81
4.2.2	Solid fraction	82
4.2.3	Sulphur removal capacity	84
4.2.4	Discussion	87
4.3	Plant data analysis	87
4.3.1	Introduction	87
4.3.2	Temperature	87
4.3.3	Slag weight	88
4.3.4	Slag composition	89
4.3.5	Silicon and titanium	91
4.3.6	Discussion	93
4.4	Viscosity and melting range experiments	94
4.4.1	Introduction	94
4.4.2	Melting point measurements	95
4.4.3	Apparent viscosity	96
4.5	Discussion	100
4.5.1	Validation	100

4.5.2	Industrial implications	101
4.6	Conclusions	102
4.7	References	103
5	Slag modifiers without fluoride	105
5.1	Introduction	106
5.2	Theory	106
5.2.1	HMD slag	106
5.2.2	Iron loss	108
5.2.3	Basicity	108
5.2.4	Slag modifiers	109
5.3	Experiments	111
5.3.1	Slag preparation	111
5.3.2	Viscosity measurements	112
5.3.3	Melting point measurements	113
5.4	Results	113
5.4.1	Viscosity measurements	113
5.4.2	Melting point measurements	116
5.5	Discussion	117
5.5.1	Experimental results	117
5.5.2	Industrial use of slag modifiers	119
5.6	Conclusions	120
5.7	References	121

Part III: Desulphurisation of HIsarna hot metal

6	The hampering effect of precipitated carbon on hot metal desulphurisation	125
6.1	Introduction	126
6.2	Theoretical evaluation	127
6.2.1	HMD reactions	127
6.2.2	Specific magnesium consumption	127
6.2.3	Carbon saturation of hot metal	128
6.2.4	Graphite formation in hot metal	129
6.2.5	The hampering effect of graphite on HMD	130
6.3	Measurements and discussion	131
6.3.1	Plant measurements	131
6.3.2	Influence of the hot metal composition	133
6.3.3	The magnitude of the effect	137
6.4	Conclusions and recommendations	138
6.4.1	Conclusions	138
6.4.2	Recommendations	138
6.5	References	139

7	Desulphurisation of high-sulphur Hisarna hot metal	141
7.1	Introduction	142
7.2	Theoretical evaluations	144
7.2.1	HMD process	144
7.2.2	Oxygen	145
7.2.3	Influence of hot metal composition on HMD	147
7.2.4	Temperature	149
7.2.5	Slag	150
7.2.6	Summary	151
7.3	Thermodynamic simulations	152
7.4	Plant data analysis	154
7.5	Discussion	158
7.6	Conclusions and outlook	161
7.6.1	Conclusions	161
7.6.2	Outlook	161
7.7	References	162
8	A novel process for continuous hot metal desulphurisation	167
8.1	Introduction	168
8.2	Process overview	169
8.2.1	CHMD process	169
8.2.2	Earlier continuous HMD processes	170
8.3	Theory	171
8.3.1	Desulphurisation reactions	171
8.3.2	Slag chemistry	172
8.3.3	Ideal reactors	173
8.4	Process design and characteristics	173
8.4.1	Reactor volume	173
8.4.2	Reagent consumption	176
8.4.3	Residence time and temperature loss	178
8.4.4	Slag removal and iron loss	179
8.4.5	Environmental consequences	180
8.4.6	Steel plant logistics	181
8.5	Business case	182
8.5.1	Financial comparison	182
8.5.2	Qualitative comparison	184
8.6	Conclusions and outlook	185
8.7	References	186

Part IV: Conclusions and outlook

9	Conclusions and recommendations	191
9.1	Conclusions	192

9.1.1	Optimal HMD slag	192
9.1.2	Desulphurisation of HIsarna hot metal	193
9.2	Recommendations	194
10	Outlook	197
10.1	Climate change and the steelmaking industry	198
10.2	The year 2025	200
10.3	The year 2030	202
10.3.1	Lowering the CO ₂ emission	202
10.3.2	Optimising scrap	203
10.3.3	Alternative ironmaking processes	204
10.3.4	CCS and CCU	206
10.3.5	Conclusion	207
10.4	The year 2050	207
10.4.1	Zero CO ₂	207
10.4.2	Scrap recycling	208
10.4.3	CO ₂ compensation and capture	208
10.4.4	Hydrogen steelmaking	209
10.5	Conclusion	210
10.6	References	211

Appendices

Summary	217
Samenvatting	223
Nomenclature	229
Symbols	231
Abbreviations	232
Curriculum vitae	233
List of publications	235
Journal publications	235
Publications in conference proceedings	237
Patents	238
History and acknowledgements	239
History	239
Acknowledgements	240
References	242

Part I

Introduction

Part I Introduction

1 General introduction

This thesis consists of four parts. In Part I, a general introduction on the topic of this thesis, sulphur removal in 21st century iron- and steelmaking, is given, followed by a more detailed introduction of the current state of the art of desulphurisation in iron- and steelmaking. Part II focusses on the optimal slag for the current hot metal desulphurisation (HMD) process via magnesium-lime co-injection, regarding the sulphur removal capacity of the slag and iron losses. In Part III, the consequences of a new ironmaking process, HIsarna, for the HMD process are investigated. Here both the consequences for the current state-of-the-art HMD of HIsarna hot metal, as well as the development of a new continuous hot metal desulphurisation process are discussed. Finally, in Part IV, the conclusions of this study are presented and an outlook for desulphurisation processes in the coming decades is given. In the outlook the focus is on the consequences of the measures for climate change mitigation and the resulting drastic changes in the iron- and steelmaking processes for the desulphurisation processes.

1.1 Steelmaking

Steel is an important material in today's world. It is hard to imagine a world without steel, as it is used for a wide variety of products, including buildings, vehicles, tools, machines and equipment. Steel has been an important material for ages. It is not a coincidence that in ancient times, when a culture reached the iron age, it marked a rapid development in many other fields as well, like literature, politics, art, science, economy and growth. Steel tools and ploughs allowed for a larger and more efficient production of food, clothes and other necessities. Steel arms ensured a better defence of the own territory and resources, as well as a higher probability of conquering the territory and resources of others. All this led to an increase in wealth and more time to devote to development.

According to the Oxford dictionary, steel is “A general name for certain artificially produced varieties of iron, distinguished from those known as ‘iron’ by certain physical properties...” [1]. These physical properties have not been commonly agreed upon, but in general the carbon content of the iron alloy should be between 0.002 and 2.0 wt% to be called ‘steel’. At higher carbon concentrations, the material is referred to as ‘pig iron’ or ‘cast iron’. ‘Iron’, on the other hand, refers to the pure element Fe. However, in steel industry, ‘iron’ is also used instead of ‘pig iron’, so the term ‘iron’ can either refer to pure Fe or to an Fe-alloy that contains too much carbon to be called steel. Liquid pig iron, is commonly referred to as ‘hot metal’. Technically, one could describe liquid steel as ‘hot metal’ too, but in steel industry and in this thesis, liquid steel is referred to as ‘liquid steel’. In short: ‘hot metal’ is liquid iron with more than 2 wt% carbon and ‘liquid steel’ is liquid iron with less than 2 wt% carbon.

Steelmaking is done by humans since the iron age, which means that in some parts of Asia and Europe, steelmaking started almost 4000 years ago. From the very beginning of steelmaking, the most important raw materials are iron ore and a carbon source (usually coal or wood). Iron ore is essentially oxidised iron, or FeO_x (oxidised iron can be FeO , Fe_3O_4 and Fe_2O_3 , so x is a number between 1 and 1.5). To produce steel, the iron in the oxides needs to be reduced. For practical reasons, like availability and density, carbon is the best candidate for the reducing agent. For the reduction of iron, energy, in the form of heat, is required as well. As carbon is already present in the process, the required heat can be generated by oxidising (burning) carbon.

Although the methods and efficiency improved over the centuries, steelmaking 4000 years ago and today are both based on the above described principles. The liquid iron that is produced in this way is very hot (the temperature is at least 1200 °C, but in modern blast furnaces typically around 1500 °C) and saturated with

1. General Introduction

carbon [2]. At these high temperatures, 4-5 wt% carbon can be dissolved in the liquid iron, so it is called 'hot metal'. When the hot metal cools down, it results in solid pig iron. Since 200 years, the dominant method to produce hot metal, or pig iron, from iron ore is the blast furnace (BF) process. In the BF alternating layers of iron ore (in the form of pellets, sinter and lump ore) and coke (which is essentially pyrolysed coal) are stacked from the top and are slowly descending inside the furnace. At the lower part of the BF, air (enriched in oxygen) is injected. The oxygen from the air reacts with the carbon from the coke to form CO and heat. The CO moves upwards through the stacked layers as in a counter-current reactor, thus reducing the FeOx in the ore. As a result of the heat, the reduced iron melts and forms a liquid at the lower end of the BF. Impurities (gangue and ash) from ore and coke form, together with additions like lime, a slag phase. Because the slag has a lower density than the hot metal, it floats on top of it in the BF. Hot metal is retrieved from the BF by regularly drilling a hole at the lower end of the BF and tapping the hot metal. Depending on the size of the BF, tapping takes 1-3 hours, after which the hole is filled with clay and the hot metal is allowed to build up again for at least 30 minutes. During tapping, slag is tapped as well. Most of the slag is separated from the hot metal in the iron runner, but some 'carryover slag' (typically 0.5-1 wt% of the hot metal) remains with the hot metal. The temperature of the hot metal when it is tapped is typically 1450-1500 °C and its carbon concentration is 4.5-5.0 wt% (close to the hot metal's carbon saturation point) [2, 3].

Pig iron from the BF is too brittle for most practical use. To make it more ductile, the carbon concentration of the pig iron should be lowered to less than 2 wt%, so that it becomes the hard, strong and formable material called 'steel'. In the past, the decarbonisation of pig iron was done by the blacksmith, who would heat it on a fire, blow air (which contains oxygen) on it with bellows and hammer it. Since the industrial revolution, the steelmaking process has become more advanced: oxygen is added to the (liquid) hot metal, to remove the surplus of carbon. In the early 1950's, the current decarburisation process, the basic oxygen furnace (BOF), was developed at Linz and Donawitz in Austria (the process is therefore also referred to as the LD process) [4, 5]. In this process, the hot metal is converted to steel by blowing oxygen on top of it, the BOF or LD process is therefore most commonly known as 'converter process'. The blown oxygen does not only remove the unwanted dissolved excess carbon, but also removes most of the unwanted other impurities, such as silicon, phosphorus and manganese. After the converter process, the liquid steel can be further fine-tuned at the secondary metallurgy stations, where elements can be added or removed, depending on the specifications and requirements of the steel. When the liquid steel has the desired

composition, it is cast in a solid slab, bloom, beam or thread, which can be further processed at the rolling mills and then finally send to a customer who turns the steel into an end product.

1.2 Sulphur and desulphurisation

In the previous section, it was briefly mentioned that the hot metal contains impurities, other than carbon. Most of these impurities are introduced in the hot metal during the ironmaking process via the iron ore and coke. The most important impurities are silicon, phosphorus, manganese and sulphur. The first three can be removed during the converter process, by blowing oxygen, but it is difficult to remove sulphur by oxidation. Even though the exothermic reaction between oxygen and sulphur to SO_2 gas is possible under steelmaking conditions (temperatures 1300-1600 °C), the oxidation of iron is thermodynamically favoured over the oxidation of sulphur. This means that sulphur dissolved in hot metal can best be removed by other means than oxidation. Since sulphur and oxygen are both members of the chalcogen family in the periodic table of the elements, oxygen will compete with sulphur to react with any other element that could be used to form sulphides in order to remove the sulphur from the hot metal. This means that sulphur can best be removed when there is no oxygen present, and therefore sulphur removal requires a separate process before the converter process: the hot metal desulphurisation process.

Sulphur is an unwanted element in the steel because it changes the steel's properties; it lowers the formability and weldability and it makes the steel more brittle [6]. Furthermore, sulphur can form MnS in steel, leading to internal weak spots in the rolled steel. More than 400 years ago, metallurgists already considered sulphur an unwanted impurity that needs to be removed [7]. Nowadays, certain steel types (for example hydrogen induced cracking resistant, or HIC, steel) require sulphur concentrations below 10 ppm, while typical steel grades contain 50-200 ppm sulphur.

Sulphur can be removed at different steps during the steelmaking process route (see Figure 1.1). Already in the blast furnace, roughly 90 % of the sulphur is removed. After that, the remaining sulphur is removed during the dedicated hot metal desulphurisation (HMD) process. Different hot metal desulphurisation processes are currently in operation around the world, of which the co-injection process [5, 6, 8–12] and Kanbara reactor (KR) process [8–10, 13, 14] are the most commonly used. During the converter process, new sulphur is introduced in the hot metal via the scrap and other additions. Therefore, in the secondary metallurgy (for example in the ladle furnace or in the vacuum degasser), additional desulphurisation is often required.

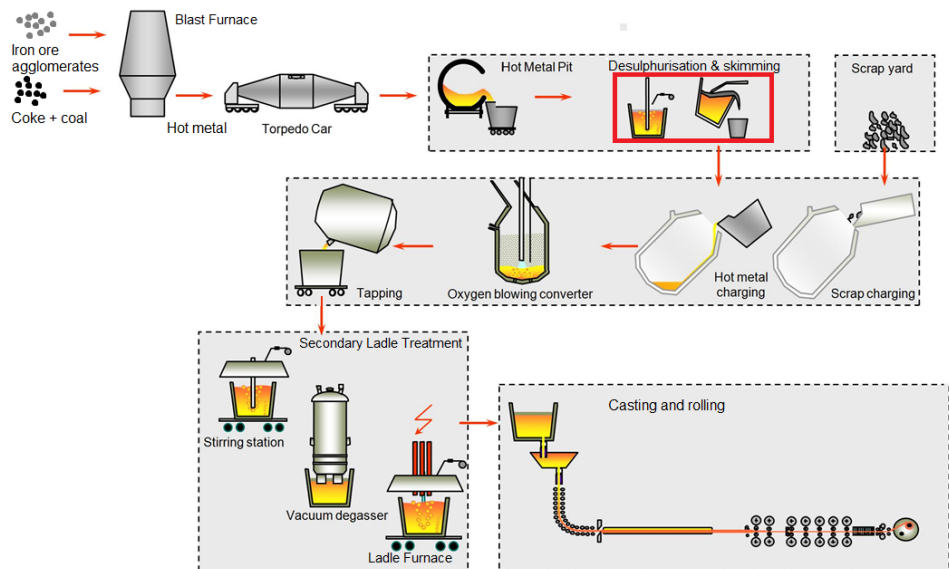


Figure 1.1: Overview of the integrated ironmaking and steelmaking process route, starting from iron ore and coke (pyrolysed coal) and ending with rolled steel.

1.3 Slag in hot metal desulphurisation

Steelmaking slags are by-products of the steelmaking processes, consisting of oxides, sulphides and carbides, and sometimes fluorides and chlorides as well. Slag is immiscible with hot metal and liquid steel and, in a stationary situation, due to its lower density, floats on top of the hot metal or liquid steel. Depending on the temperature and composition, slag can be liquid, solid or a mixture of both [5]. In different steelmaking processes, the slag is used as the phase to capture removed impurities in the form of oxides and sulphides. For desulphurisation, the slag is used to capture the removed sulphur in the form of sulphides (usually calcium sulphide, CaS). Because the slag floats on top of the metal bath, it is relatively easy to separate it from the metal. When the slag is separated from the metal, the removed sulphur cannot go back into the hot metal or liquid steel. It should be noted that sulphur can also leave the process in the gas phase, but typically only 2.5 % of the sulphur in the hot metal leaves the system in the gas phase (SO_2 and H_2S) over the entire steelmaking route. Therefore, the focus of desulphurisation in steelmaking is on the slag phase.

During the HMD process, sulphur is removed from the hot metal by causing it to react with reagents, like magnesium or lime, forming sulphides that go into the slag layer. When the reaction with the reagents stops, the slag, including the sulphides, is raked off with a large rake, the so called ‘skimmer’ (see Figure 1.2).

Slag plays an important role in the HMD process: it should absorb the formed sulphides and it should be easily separated from the hot metal. However, the separation of slag and hot metal during the HMD process is not perfect. During the skimming, hot metal gets entrained by the slag when it is raked off. Also, small hot metal droplets can get caught in the slag, in a colloidal form, and are removed from the process together with the slag. The hot metal that is removed together with the slag is referred to as ‘iron loss’. On the other hand, slag does not always have the capacity to contain all the sulphides. Therefore, it is important for the steelmaking industry to know the optimal slag composition and condition to have a sufficient sulphur removal capacity and the lowest possible iron loss.



Figure 1.2: a) Slag in a hot metal ladle prior to HMD. b) Slag skimming at an HMD station (photos: Alison Tuling, 2020).

One way to lower iron losses is to add slag modifiers to the slag to lower its viscosity. In industry, typically fluorine-containing materials (like KAlF_4 or CaF_2) are used as slag modifiers. However, it was found that the fluorine, apart from being harmful for the environment and human health, decreases the desulphurisation efficiency of magnesium [15]. Therefore, alternative, fluorine-free slag modifiers are investigated. In 2020 and 2021, fly ash is tested at the Tata Steel plant in Port Talbot, UK, to replace a fluorine-containing slag modifier.

1.4 Hisarna hot metal

For roughly 4000 years carbon has been essential for steelmaking. There are steelmaking processes that use electricity to produce steel, like the electric arc furnace (EAF) process, but these processes use either direct reduced iron (DRI), which again requires carbon to reduce the iron ore, or recycled steel (scrap) as raw material [16]. Given the rapid economic development in Asia and Africa, recycling steel will not be sufficient to meet the growing worldwide steel demand for the coming decades. Therefore, production of ‘virgin iron’ by reduction of iron ore remains inevitable in the foreseeable future. The problem of reducing

iron ore with carbon is that it produces CO₂ as a by-product. CO₂ is one of the greenhouse gasses that causes global warming, so its emission should be reduced, as was internationally promised via the Paris agreement in 2015 [17]. The steel industry worldwide emits around 2000 Mt/y of CO₂ (2019) [18], which is roughly 5.5 % of the total global annual CO₂ emission (in 2019 roughly 38 Gt/y [19]). Therefore, lowering the CO₂ emission of the steel industry is crucial for the global climate change mitigation. Consequently, the necessity to use carbon to produce enough steel to meet the growing global demand, places the steel industry for an enormous challenge.

In theory, iron ore can be reduced by hydrogen as well. If steel can be produced with hydrogen, assuming that the hydrogen is produced with green energy, steel can be produced with a very low CO₂ emission. Besides, hydrogen does not come with any sulphur, therefore much less sulphur will need to be removed for hydrogen-based steel, as scrap and iron ore contain roughly ten times less sulphur than coal. Nevertheless, even an hydrogen-based steelmaking process requires carbon (steel contains carbon), therefore some sulphur will enter the process together with the carbon. Worldwide, several hydrogen-based steelmaking processes are being developed. However, it will take another 10-20 years before these processes are mature enough to take over some of the production of the current blast furnaces [20]. Until hydrogen-steelmaking is mature, the steel industry should focus on processes that minimise the CO₂ emission of the carbon-based steelmaking. One of the most promising processes is the HIsarna process. HIsarna produces hot metal with a 20 % lower direct CO₂ emission. The CO₂ emission can be lowered further by 80 % when using carbon capture and storage (HIsarna is better suited for that than a BF) [20–24]. On paper the CO₂ emission can be decreased even further when biomass is used as a carbon source, instead of coal (assuming that the used biomass is replaced by planting new plants). However, a disadvantage of HIsarna is that its hot metal contains 3-4 times more sulphur than hot metal from the BF, since HIsarna has a higher sulphur input (instead of coke, coal, which contains more sulphur, is used) and has a more oxidising environment (which hampers desulphurisation) than a blast furnace. Therefore, in order to make HIsarna a more successful low-CO₂ alternative to the BF, it should be possible to desulphurise its hot metal to the same level as is currently possible for conventional BF hot metal.

Apart from having a higher sulphur concentration, HIsarna hot metal also contains less carbon than BF hot metal. A high carbon concentration in hot metal leads to carbon precipitation, which could hamper the desulphurisation process [6]. However, current research showed that, although the mechanism exists, this does not significantly influence the industrial hot metal desulphurisation process

efficiency. The higher sulphur concentration of HIsarna hot metal, compared to BF hot metal, will lead to longer HMD process times. To limit the effects of this on the entire steelmaking process chain, a new continuous hot metal desulphurisation (CHMD) process is being developed at Tata Steel in IJmuiden, the Netherlands, which can be located directly at the hot metal outflow of the HIsarna process. The CHMD process is compatible with the blast furnace as well [25]. At present, the process is still in the early design phase.

1.5 This thesis: desulphurisation in 21st century iron- and steelmaking

The first two decades of the 21st century showed a global focus on process optimisation in iron- and steelmaking: producing better steel at lower cost. For the hot metal desulphurisation process the most important possible improvement lies in optimising the slag conditions. Lowering the iron losses only recently gained the attention it deserves in terms of costs and waste. At the same time the desulphurisation efficiency, via the sulphur removal capacity of the slag, should not be hampered by the new improvements to control the iron losses.

For the coming decades, the focus of the steelmaking industry will be mostly on reducing the carbon footprint and still produce high quality steel at acceptable costs. This change of perception leads to a shift from optimising the current processes to developing new processes. These new processes, of which HIsarna is only one example, will lead to completely new requirements to the desulphurisation processes in iron- and steelmaking.

In this thesis, desulphurisation in 21st century iron- and steelmaking is discussed. Part I of this thesis is the introduction. Chapter 1, the current chapter, introduces the current situation of steelmaking in general and desulphurisation in particular, as well as its challenges. In Chapter 2, the state of the art of sulphur removal in iron- and steelmaking is discussed.

Part II of the thesis focusses on the optimal slag composition and condition for HMD, as this is the aspect of today's process where improvements and better understanding can make the highest impact. Chapter 3 discusses the fundamentals of the optimal composition and condition of the HMD slag that lead to the lowest possible iron losses, while maintaining a sufficient sulphur removal capacity. Chapter 4 evaluates the findings from Chapter 3 with a Monte Carlo simulation of thermodynamic calculations from FactSage, viscosity and melting point measurements at laboratory scale and analysis of plant data from Tata Steel in IJmuiden. Finally, Chapter 5 discusses fluorine-free slag modifiers that can be

added to the slag to achieve lower iron losses, while maintaining the sulphur removal capacity of the slag.

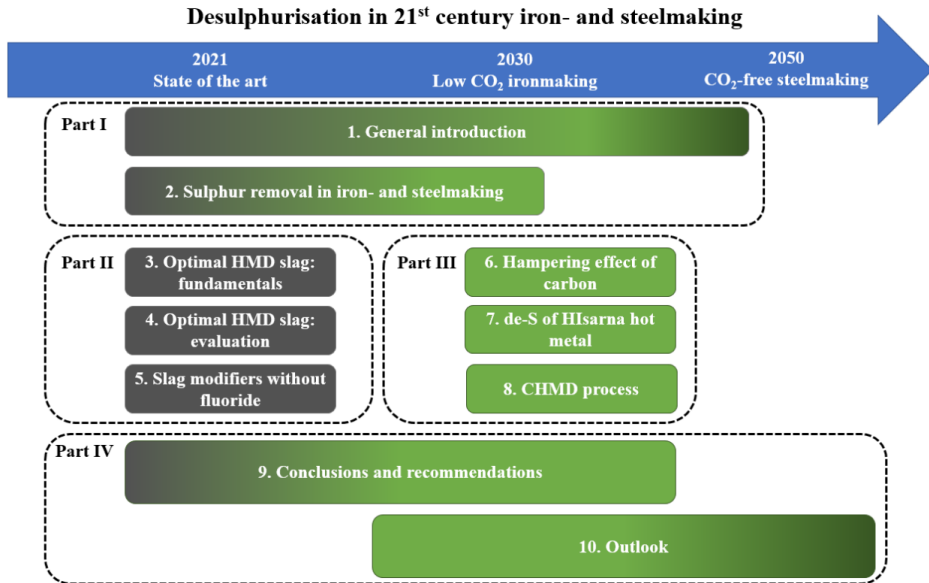


Figure 1.3: Graphical overview of the thesis' content.

In Part III of this work, the consequences are outlined for the HMD process of an industrial HIsarna process, which is one of the most promising methods to achieve the short- to midterm CO₂ emission targets. In Chapter 6, the influence of the lower carbon concentration in HIsarna hot metal, resulting in less or no graphite precipitation, on the HMD process is discussed. Chapter 7 discusses what the consequences are for the current magnesium-lime co-injection process when used for desulphurisation of HIsarna hot metal. A literature study, thermodynamic calculations and plant data analysis are used to predict the consequences of desulphurisation of HIsarna hot metal. Finally, in Chapter 8, the new continuous hot metal desulphurisation process, CHMD, is introduced. The CHMD process is specially designed to solve one of the main challenges of the HIsarna process: its high-sulphur hot metal. The development of the new CHMD process is part of this PhD study.

Finally, in Part IV, in Chapter 9, the desulphurisation in iron- and steelmaking, both the optimisation of the current process and the consequences of the new developments, as discussed in the previous chapters, will be summarised and some recommendations based on the work presented in this thesis are shared. Furthermore, in Chapter 10, an outlook for desulphurisation in iron- and steelmaking for the remainder of the 21st century is given, with a focus on the

consequences of the global climate change mitigation on the desulphurisation processes in iron- and steelmaking.

1.6 References

- [1] “steel, n.1,” *Oxford English Dictionary*. [Online]. Available: <https://www.oed.com/view/Entry/189540?rskey=tbYc4l&result=1#eid>. [Accessed: 12-Mar-2021].
- [2] M. Geerdes, R. Chaigneau, I. Kurunov, O. Lingiardi, and J. Ricketts, *Modern Blast Furnace Ironmaking*, 3rd ed. Delft (NL): IOS Press, 2015.
- [3] Y. Yang, K. Raipala, and L. Holappa, “Ironmaking,” in *Treatise on Process Metallurgy*, vol. 3, S. Seetharaman, Ed. Oxford (UK): Elsevier, 2014, pp. 2–88.
- [4] H. Jalkanen and L. Holappa, *Converter Steelmaking*, vol. 3. Oxford (UK): Elsevier Ltd., 2014.
- [5] B. Deo and R. Boom, *Fundamentals of Steelmaking Metallurgy*, 1st ed. Hemel Hempstead (UK): Prentice-Hall, 1993.
- [6] H.-J. Visser, “Modelling of injection processes in ladle metallurgy,” (PhD thesis) Delft University of Technology, Delft (NL), 2016.
- [7] G. Agricola, *De Re Metallica*. Basel (CH), 1556.
- [8] F.N.H. Schrama, B. van den Berg, and G. Van Hattum, “A comparison of the leading hot metal desulphurization methods,” in *Proceedings of the 6th International Congress on the Science and Technology of Steelmaking*, 2015, pp. 61–66.
- [9] S. Kitamura, “Hot Metal Pretreatment,” in *Treatise on Process Metallurgy*, vol. 3, S. Seetharaman, Ed. Oxford (UK): Elsevier, 2014, pp. 177–221.
- [10] P.J. Koros, “Pre-Treatment of Hot Metal,” in *The Making, Shaping and Treating of steel*, 11th ed., R. J. Fruehan, Ed. Pittsburgh (USA): AISE Steel Foundation, 1998, pp. 413–429.
- [11] N.A. Voronova, *Desulfurization of hot metal by magnesium*. Dayton (USA): The International Magnesium Association, 1983.
- [12] A. Freißmuth, *Die Entschwefelung von Roheisen*, 1st ed. Tisnov (CZ): Almamet GmbH, 2004.
- [13] M. Song and J. Park, “KR Efficiency Improvement Technology by Changing of Impeller Shape and Gas Injection,” in *Proceedings of the 7th*

International Congress on the Science and Technology of Steelmaking, 2018, p. ICS052.

- [14] Y. Liu, Z. Zhang, S. Masamichi, J. Zhang, P. Shao, and T. Zhang, “Improvement of impeller blade structure for gas injection refining under mechanical stirring,” *J. Iron Steel Res. Int.*, vol. 21, no. 2, pp. 135–143, 2014, doi: 10.1016/S1006-706X(14)60022-4.
- [15] F.N.H. Schrama *et al.*, “Effect of KAlF₄ on the efficiency of hot metal desulphurisation with magnesium,” in *European Oxygen Steelmaking Conference (EOOSC)*, 2018, p. EOOSC021.
- [16] J.A.T. Jones, B. Bowman, and P.A. Lefranc, “Electric Furnace Steelmaking,” in *The Making Shaping and Treating of Steel*, 11th ed., R. J. Fruehan, Ed. Pittsburgh (USA), 1998, pp. 525–660.
- [17] United Nations, *Paris agreement*. 2015.
- [18] World Steel Association, “Sustainability indicators 2020 report,” Brussels (BE), 2020.
- [19] United Nations Environment Programme, “Emissions Gap Report 2020,” Nairobi (KEN), 2020.
- [20] J. Zhao, H. Zuo, Y. Wang, J. Wang, and Q. Xue, “Review of green and low-carbon ironmaking technology,” *Ironmak. Steelmak.*, vol. 47, no. 3, pp. 296–306, 2020, doi: 10.1080/03019233.2019.1639029.
- [21] H.K.A. Meijer, C. Guenther, and R.J. Dry, “Hisarna Pilot Plant Project,” *InSteelCon*, no. July, pp. 1–5, 2011.
- [22] C. Zeilstra, J. van der Stel, H.K.A. Meijer, and T. Peeters, “The Hisarna ironmaking process,” 2016.
- [23] J.W.K. van Boggelen, H.K.A. Meijer, C. Zeilstra, and Z. Li, “The Use of Hisarna Hot Metal in Steelmaking,” in *Scanmet V*, 2016, p. 008.pdf.
- [24] M. Abdul Quader, S. Ahmed, S.Z. Dawal, and Y. Nukman, “Present needs, recent progress and future trends of energy-efficient Ultra-Low Carbon Dioxide (CO₂) Steelmaking (ULCOS) program,” *Renew. Sustain. Energy Rev.*, vol. 55, pp. 537–549, 2016, doi: 10.1016/j.rser.2015.10.101.
- [25] A. Emami, F.N.H. Schrama, and J.W.K. van Boggelen, “Device and method for continuous desulphurisation of liquid hot metal,” WO2020/239554A1, 2020.

Part I Introduction

2 Sulphur removal in ironmaking and oxygen steelmaking

This chapter is based on the following publication:

F.N.H. Schrama, E.M. Beunder, B. van den Berg, Y. Yang and R. Boom, “Sulphur removal in ironmaking and oxygen steelmaking”, *Ironmaking and Steelmaking*, Vol. 44, No. 5, **2017**, p 333-343.

In this chapter sulphur removal in the ironmaking and oxygen steelmaking process is reviewed and discussed. A sulphur balance is made for the steelmaking process. There are four stages in the process route where sulphur can be removed: in the blast furnace (BF), during hot metal pre-treatment, in the converter (BOF) and during the liquid steel treatment (secondary metallurgy). In order to achieve the quality demands of the current market, sulphur has to be removed in more than one process step.

For sulphur removal a very low oxygen activity is desired. Also a basic slag layer is required, both to react with the dissolved sulphur and to absorb the sulphides. Magnesium-, sodium- and calcium-based reagents are used in industry for the slag. In the BF typically 90 % of the sulphur is removed, but the hot metal product usually contains at least 0.03 wt% sulphur. Several hot metal desulphurisation (HMD) processes have been developed and are used worldwide in most steel plants. For HMD with co-injection or Kanbara Reactor (KR) sulphur concentrations below 0.001 wt% are achieved. In the converter oxygen is blown onto the hot metal for decarburisation. This creates an unfavourable environment for desulphurisation. Although the basic slag enhances sulphur removal, the sulphur concentration in the liquid metal can also increase during this process due to addition of sulphur-containing scrap and additions. During secondary metallurgy processes the final composition of the steel is determined. Depending on the desired sulphur concentration in the final product, steel desulphurisation can be applied. For steel desulphurisation the oxygen concentration should be decreased, after which a basic slag is used to bind the sulphur.

2.1 Introduction

In today's world manufacturers and end users demand steel of an ever increasing quality. However, the overall quality of the raw materials (iron ore, coke and coal) is decreasing, because the raw material reserves are not endless and the best materials have mostly been used in the past. This means that the steel industry needs to cope with more impurities, but their final products should contain less impurities.

Today, roughly two third of the world's steel is produced via the integrated blast furnace – basic oxygen furnace (BF-BOF) route. Figure 2.1 gives a schematic overview of the BF-BOF steelmaking process. In this process, iron ore is reduced mainly by coke in the blast furnace. This coke also produces the required heat by reacting with the available oxygen (from the hot blast and the FeO). The liquid hot metal that leaves the BF contains impurities, which have to be removed later in the process. In the hot metal pre-treatment, usually most of the sulphur (and sometimes silicon and phosphorus as well) is removed. The hot metal is then charged to the basic oxygen furnace or converter, together with scrap, where the hot metal is oxidised by blowing pure oxygen on the melt, removing most of the carbon, (remaining) silicon and phosphorus. The produced liquid steel is tapped from the converter and sent to the secondary metallurgy (SM) ladle treatment before being cast at the casting machine (CM). Here remaining impurities are removed and alloying elements and deoxidisers are added. When the steel has the desired chemical composition, it is cast to solid steel [1-5].

BF-BOF steelmaking:

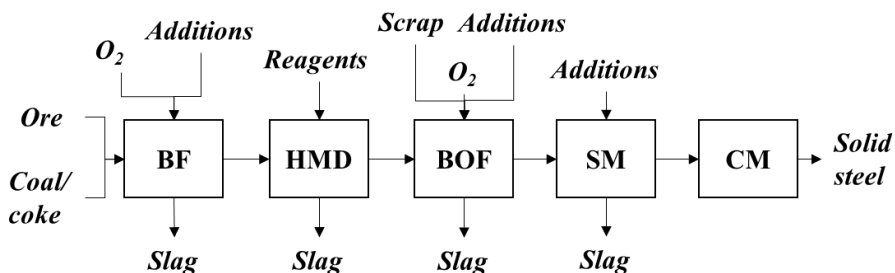


Figure 2.1: Block scheme of the BF-BOF steelmaking process.

2. Sulphur removal in ironmaking and oxygen steelmaking

One of the above mentioned unwanted impurities in the steelmaking process is sulphur (although there are certain steel grades that require sulphur). Sulphur increases the brittleness of steel and decreases the weldability and corrosion resistance [6, 7]. Therefore sulphur needs to be removed to a concentration that is typically below 0.015 %. The main sources of sulphur in the BF-BOF steelmaking process are coke and coal. Even though roughly 40 % of the sulphur in coal is removed in the coking process, typical sulphur levels in coke remain around 0.5 wt%. Iron ore contains typically 0.01 wt% sulphur and is only a minor source of sulphur in the steelmaking process [2, 8].

In the BF-BOF process there are four process steps where sulphur can be removed:

- Blast furnace
- Hot metal pre-treatment
- Converter
- Secondary metallurgy ladle treatment

The other main steelmaking process, the electric arc furnace (EAF) process (roughly 30 % of the world steel production), is not discussed in this chapter. In the EAF the additions (scrap types and DRI) are used to control the sulphur concentration of the liquid steel. The SM ladle treatment processes are comparable for both BF-BOF and EAF steelmaking. However, sulphur removal is less an issue in the EAF process, since its raw materials (scrap, direct reduced iron) contain less sulphur than the raw materials of the BF-BOF process (iron ore, coke and coal) [1, 4].

2.2 Sulphur distribution flow

To get an overview of the sulphur input and output throughout the BF-BOF steelmaking process, a balance of the sulphur flows during the production of a standard steel grade (with a maximum sulphur at casting of 0.01 wt%) at Tata Steel IJmuiden was made (see Figure 2.2). Data of 2548 heats in total of this steel grade, produced in 2015, were analysed. In case data for sulphur concentrations were not measured for every single heat and if these concentrations could not be derived from other measurements of these heats, random samples that were taken in 2015 or best guesses were used. For the BF, data of one month in 2015 were selected. This month had the highest sulphur input of 2015. The hot metal output of the BF and the input of the HMD were

averaged to determine the single stream in this diagram. The average sulphur presence in every process flow (in kg sulphur per tonne produced steel) is given in Table 2.1. A Sankey-type diagram of the sulphur balance of the production of this steel grade is given in Figure 2.2. The balance between sulphur input and output for the BF and the BOF is simply added as an extra flow. This is done because the accuracy of the measured sulphur concentration or the mass flow, is not the same for every flow. For example, the sulphur concentration in the hot metal that leaves the BF is measured more accurately than the sulphur concentration in the slag. For the HMD and the SM, it is assumed that the sulphur that is measured at the station's input and that is not at the station's output in off-gas or liquid metal, is in the slag.

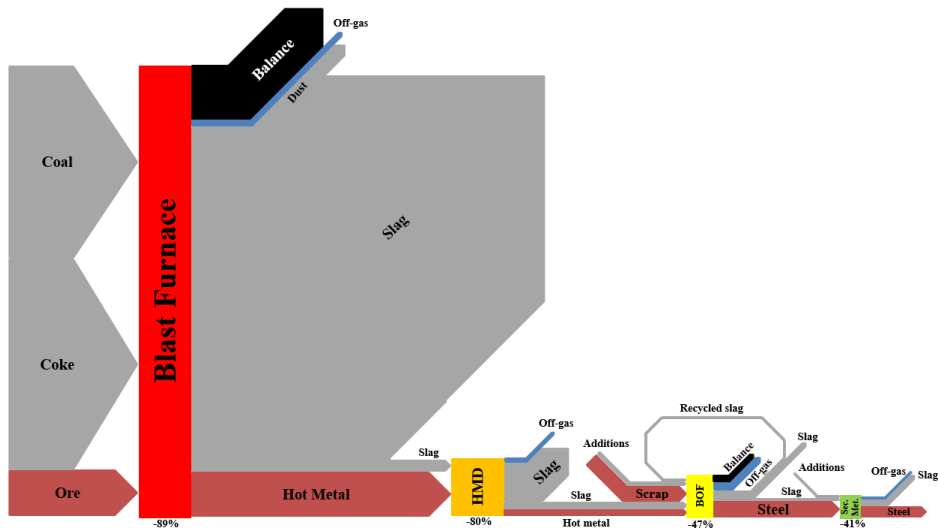


Figure 2.2: Sankey-type diagram of the sulphur distribution flow for a standard steel grade at Tata Steel IJmuiden in 2015 for BF, HMD, BOF and SM. Arrows represent the amount of sulphur present in a flow, necessary per unit of produced steel. Below the process blocks the percentage of sulphur input that is removed in that process step is indicated.

2. Sulphur removal in ironmaking and oxygen steelmaking

Table 2.1: Average values of sulphur streams (in kg sulphur per tonne produced steel) for a standard steel grade at Tata Steel IJmuiden in 2015.

BF				HMD			
In	[kg/t]	Out	[kg/t]	In	[kg/t]	Out	[kg/t]
Coal	1.233	Off-gas	0.029	Slag	0.057	Off-gas	0.019
Coke	1.325	Dust	0.092	Hot metal	0.267	Slag	0.276
Ore	0.280	Slag	2.065			Hot metal	0.028
		Hot metal	0.267				
		Balance	0.384				
Total	2.837		2.837		0.324		0.324

BOF				SM			
In	[kg/t]	Out	[kg/t]	In	[kg/t]	Out	[kg/t]
Rec. slag	0.003	Off-gas	0.035	Additions	0.002	Off-gas	0.006
Additions	0.016	Slag	0.028	Slag	0.002	Slag	0.033
Scrap	0.094	Steel	0.091	Steel	0.091	Steel	0.057
Slag	0.036	Balance	0.022				
Hot metal	0.028						
Total	0.176		0.176		0.096		0.096

The balance shows the enormous desulphurisation capacity of the BF. Around 90 % of the sulphur input is already removed in the BF. It also shows the great importance of the HMD step. When looking at the poor desulphurisation capacity of the converter (for this steel grade the sulphur concentration of the liquid metal even increases), sulphur removal has to take place at the HMD to avoid a too heavy desulphurisation demand from the SM. When more sulphur needs to be removed during SM, that process will take more time. This could lead to a bottleneck in the entire BF-BOF process. Furthermore sulphur removal before the BOF process has lower costs than afterwards.

At the BF more than 40 % of the sulphur input comes from coal. This is because at Tata Steel almost half of the carbon input in the BF originates from coal by pulverised coal injection (PCI). In most blast furnaces the coal input is much lower. Since coal contains more sulphur than coke, the total sulphur input to the BF will increase when more coal instead of coke is added.

After the HMD, more sulphur is added to the converter via the HMD-slag than via the hot metal itself. The total sulphur stream via the slag is less accurate, since it is calculated and not directly measured. However, it does emphasise the importance of good deslagging.

2.3 Thermodynamics

2.3.1 Introduction

Independent of where sulphur removal takes place, it is based on the same chemical equations. The circumstances of the individual processes only have an impact on the importance of the chemical equations. The removal of sulphur is based on one principle: to move the dissolved sulphur from the iron to the slag, after which the slag layer is separated from the metal. This is summarised by the following reaction, for the sulphur transfer between the metal and slag [2, 9]:



In reactions in this thesis, [x] means that element x is dissolved in hot metal and (x) indicates that element x is dissolved in the slag phase. The equilibrium constant of this equation ($K_{2.1}$) can be written as:

$$K_{2.1} = \frac{a_{[O]} \cdot a_{(S^{2-})}}{a_{[S]} \cdot a_{(O^{2-})}} \quad (2.2)$$

Here a_x stands for the activity of element x in the steel or in the slag. This equation shows that for maximal sulphur removal the oxygen activity in the metal phase and the sulphur activity in the slag phase should be as low as possible. Furthermore it is known that an increased basicity leads to a higher sulphur capacity of the slag, which is good for desulphurisation of the metal. In steel plants the basicity is calculated based on the weight ratio of basic oxides (like CaO and MgO) to acid oxides (like SiO₂, Al₂O₃ and P₂O₅). The basicity calculations can differ from plant to plant, since there is no general rule on which oxides are included (this also depends on which oxides can be detected). The basicity has typical values of 1-1.5 (BF) and 2-4 (BOF) [2, 10, 11].

2.3.2 Lime

Desulphurisation of metal can be controlled by adding reagents (via injection or mixing). The most commonly used reagents are lime, calcium carbide and magnesium, but soda ash (Na₂CO₃) and calcium fluoride are still used as well. Lime is the most applied reagent, which can be used in every desulphurisation process from BF to SM. Lime reacts with dissolved sulphur via Reaction 2.3:



2. Sulphur removal in ironmaking and oxygen steelmaking

The thermodynamics of this reaction, expressed as the Gibbs free energy (ΔG^0 [J/mol]) and the equilibrium constant ($\log(K)$), are collected in Table 2.2 valid for the hot metal temperature range 1250-1450 °C. The equations from Hayes [12] and Turkdogan [9] were derived from standard Gibbs free energies of formation of the constituting elements in the reaction (when Hayes did not mention ΔG^0 of a certain step, data from Turkdogan was used instead).

Table 2.2: Overview of ΔG^0 and $\log(K)$ equations for the reaction between CaO and [S] (Reaction 2.3). Temperature is in K. All equations are valid for the temperature range of 1250-1450 °C.

Source	ΔG^0 [J/mol]	Log(K)
Hayes, 1993, [12]	$\Delta G_{2.3}^0 = 109,956 - 31.045T$	$\log K_{2.3} = -\frac{5,744}{T} + 1.622$
Turkdogan, 1996, [9]	$\Delta G_{2.3}^0 = 371,510 - 199.36T$	$\log K_{2.3} = -\frac{19,406}{T} + 10.414$
Grillo, 2013, [13]	$\Delta G_{2.3}^0 = 115,353 - 38.66T$	$\log K_{2.3} = -\frac{6,026}{T} + 2.019$
Tsujino, 1989, [14]	$\Delta G_{2.3}^0 = 105,709 - 28.70T$	$\log K_{2.3} = -\frac{5,522}{T} + 1.499$
Ohta, 1996, [15]	$\Delta G_{2.3}^0 = 114,300 - 32.5T$	$\log K_{2.3} = -\frac{5,971}{T} + 1.70$
Kitamura, 2014, [2]*	$\Delta G_{2.3}^0 = 108,986 - 29.25T$	$\log K_{2.3} = -\frac{5,693}{T} + 1.528$

*: The temperature-independent term in Kitamura's $\log(K)$ equation was written as "1528", but this was considered as a typing error.

The difference between Turkdogan and Hayes is that Turkdogan assumes a lower standard Gibbs free energy of formation of CaO [9, 12].

In order to get a clear overview of the differences between the mentioned sources, the ΔG^0 values are plotted in Figure 2.3 for the temperature range of 1250-1450 °C.

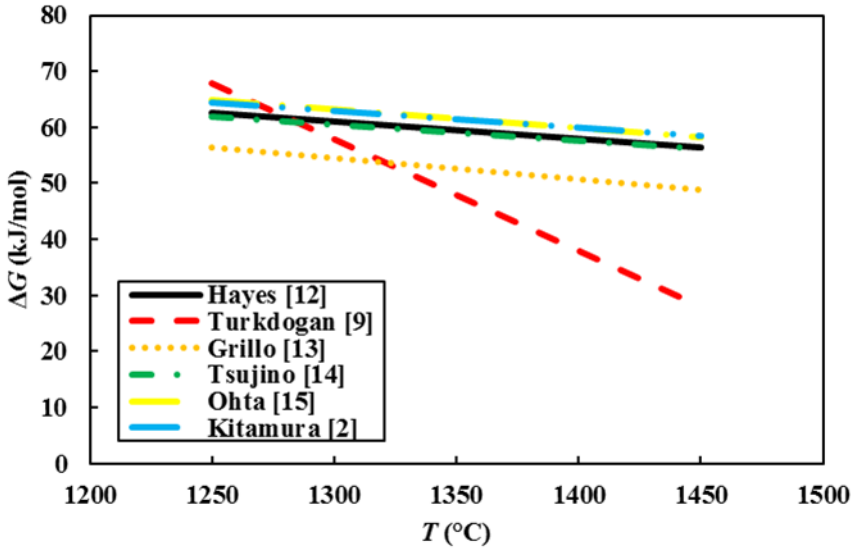


Figure 2.3: Temperature dependence of ΔG^0 for the reaction between CaO and $[\text{S}]$ (Reaction 2.3), according to literature.

Both the Gibbs free energy equation and the chemical equilibrium equation show that the reaction between CaO and $[\text{S}]$ is favoured at higher temperatures. This is in accordance with plant experience.

2.3.3 Calcium carbide

For the reaction of sulphur with calcium carbide (Reaction 2.4) it is assumed that the formed carbon does not dissolve in already carbon-saturated hot metal [16]. When CaC_2 is used in steel desulphurisation, where there is no carbon saturation, the dissolution of carbon in iron should be taken into account.



About the thermodynamics of this reaction, literature is unanimous. The only deviations in literature are when it is assumed that the formed carbon will dissolve in the iron. The equations for ΔG^0 and $\log(K)$ are based on data of Hayes [12] and confirmed by Kitamura [2] and Visser [17] (temperature range: 1250-1450 °C). In Equations 2.5 and 2.6 temperature, T , is in K.

$$\Delta G_{2.4}^0 = -352,790 + 106.65T \quad (2.5)$$

2. Sulphur removal in ironmaking and oxygen steelmaking

$$\log(K_{2.4}) = \frac{18428}{T} - 5.571 \quad (2.6)$$

Both equations indicate that thermodynamically Reaction 2.4 is favoured at lower temperatures. This however is contradictive to industrial experience, where CaC₂ desulphurisation efficiency increases at higher temperatures. As with the reaction with lime (Reaction 2.3), this reaction is controlled by kinetics rather than thermodynamics. Furthermore it should be noted that CaC₂ in industrial practice is only 50-70 % pure (the rest is mainly lime, 20-30 %, and carbon). These impurities have their influence on the process and could partly explain the apparent inconsistency between theoretical behaviour and plant experience [16, 18].

2.3.4 Magnesium

Magnesium is only used for HMD and not for post-converter desulphurisation. It has a boiling point of 1105 °C, so in contact with hot metal (1250-1450 °C) it will vaporise. Magnesium gas dissolves into liquid iron, after which it can react with the dissolved sulphur (Reaction 2.7). The magnesium gas can also react directly with the dissolved sulphur at the bubble-metal interface, but this has only a small contribution as will be further discussed in Section 2.4.



From plant experience it is known that Reaction 2.7 proceeds better at lower temperatures. Figure 2.4 gives the amount of industrial magnesium (the purity is unknown, but typically between 80-97 wt% Mg) required to remove one kg of sulphur in the hot metal set against the hot metal temperature in a Mg-CaO co-injection HMD station in a South American plant for 2158 heats in 2006. The average heat size was 92 t and the average reagent injection ratio CaO to Mg was 4:1. The stoichiometric consumption of Mg to form MgS equals 0.76 kg Mg per 1 kg S.

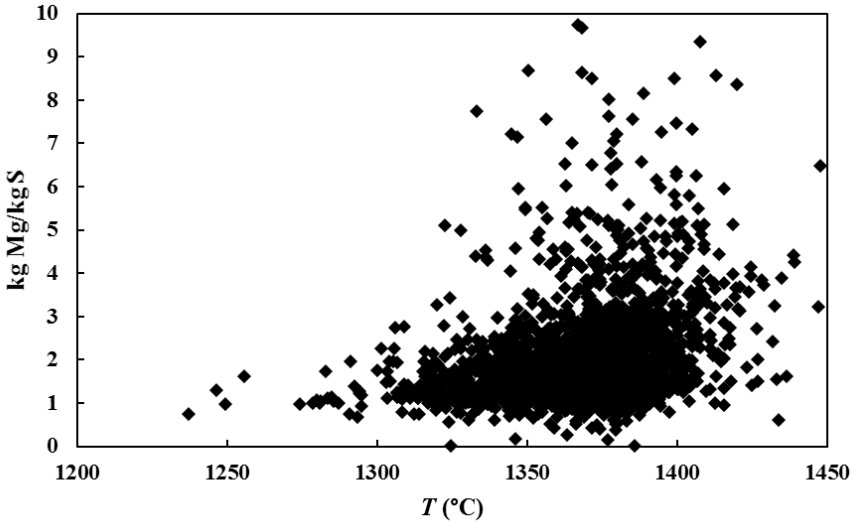


Figure 2.4: Amount of Mg used to remove 1 kg sulphur at different hot metal temperatures. Data of 2158 heats at the HMD in a South American plant.

The plant data clearly show that at lower hot metal temperatures less magnesium is required to remove one kg of dissolved sulphur. The thermodynamics support the observation that lower temperatures have a positive effect on the magnesium desulphurisation efficiency. Table 2.3 gives the equations for ΔG^0 and $\log(K)$ for the desulphurisation reaction with magnesium from literature (T : 1250-1450 °C).

Table 2.3: Overview of ΔG^0 and $\log(K)$ equations for the reaction between [Mg] and [S] (Reaction 2.7). Temperature in K. All equations are valid for the temperature range of 1250-1450 °C.

Source	ΔG^0 [J/mol]	Log(K)
Hayes, 1993, [12]	$\Delta G_{2.7}^0 = -325,986 + 98.82T$	$\log K_{2.7} = \frac{17,028}{T} - 5.162$
Turkdogan, 1996, [9]	$\Delta G_{2.7}^0 = -325,950 + 98.77T$	$\log K_{2.7} = \frac{17,026}{T} - 5.159$
Hino, 2010, [19]	$\Delta G_{2.7}^0 = -260,643 + 115.63T$	$\log K_{2.7} = \frac{13,615}{T} - 6.04$
Saxena, 1997, [18]	$\Delta G_{2.7}^0 = -149,000 + 98.2T$	$\log K_{2.7} = \frac{7,783}{T} - 5.13$
Yang, 2005, [20]	$\Delta G_{2.7}^0 = -325,380 + 98.41T$	$\log K_{2.7} = \frac{16,997}{T} - 5.141$

2. Sulphur removal in ironmaking and oxygen steelmaking

The equations for ΔG^0 of Table 2.3 are plotted in Figure 2.5 to show the differences between the equations from the different sources. The differences between the equations is remarkable. A reason for these large differences could be that experiments with dissolved magnesium in molten metal are difficult to perform as escape of magnesium gas from the metal bath should be prevented. Furthermore, the high flammability of magnesium gas requires extra safety measures.

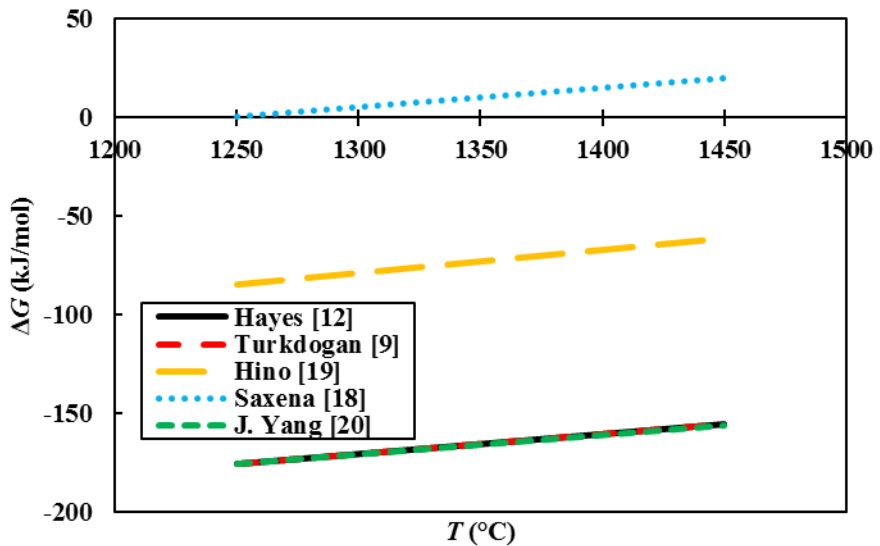


Figure 2.5: Temperature dependence of ΔG^0 for the reaction between $[Mg]$ and $[S]$ (Reaction 2.7), according to literature.

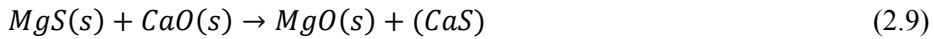
In Figure 2.5 the ΔG^0 values of Hayes [12], Turkdogan [9] and Yang [20], seem to overlap. However, these equations have small differences. The ΔG^0 at 1350 °C determined with Hayes' equation is 45.2 J/mol higher than with Turkdogan's equation and 59.5 J/mol higher than with Yang's equation.

2.3.5 Resulphurisation

A disadvantage of desulphurisation with magnesium is the so called resulphurisation, the net transfer of sulphur from the slag back to the metal. The MgS in the slag reacts with oxygen from the air, or from other sources, forming MgO and unbound sulphur [20]:



In order to avoid resulphurisation, the sulphur should be captured in a more stable compound. CaS is more stable than MgS [1, 20], so by adding calcium (typically in the form of lime) the resulphurisation can be prevented. Reaction 2.9 describes the effect of adding lime:



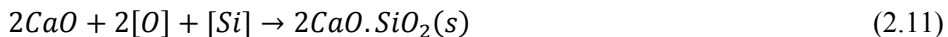
The equation for its Gibbs free energy is ([12]):

$$\Delta G_{2.9}^0 = -100,918 + 8.21T \quad (2.10)$$

From Equation 2.10 it is clear that even at elevated hot metal temperatures of 1400 °C this reaction still takes place. Nevertheless higher temperatures do not only have a negative effect on desulphurisation by magnesium (Reaction 2.7), but also on the stabilisation reaction (Reaction 2.9). For magnesium desulphurisation lower temperatures are favourable.

2.4 Kinetics

Desulphurisation by CaO or CaC₂ is in reality controlled by kinetics rather than thermodynamics [2, 18, 21]. When CaO reacts with sulphur, CaS is formed (Reaction 2.3). This CaS forms a layer around the CaO particle, through which dissolved S atoms need to permeate before they can react with CaO. Since also oxygen is formed in this reaction, the oxygen activity increases around the CaO particle. This oxygen reacts with either carbon (forming CO) or silicon, which leads to the formation of 2CaO-SiO₂ (Reaction 2.11). This 2CaO-SiO₂ contributes to the non-reactive shell around the CaO, decreasing its desulphurisation efficiency. However, with small CaO particles (smaller than 50 µm) not enough oxygen is created via Reaction 2.3 to initiate Reaction 2.11 [21].



For the reaction between CaC₂ and sulphur (Reaction 2.4), the non-reactive shell not only consists of CaS, but also of a graphite layer. This retards the desulphurisation even further [21].

2. Sulphur removal in ironmaking and oxygen steelmaking

The kinetics of magnesium desulphurisation causes some discussion among the experts in the field. Irons and Guthrie [22] claim that 90 % of the magnesium first dissolves before it reacts with [S] and less than 10 % of the Mg-desulphurisation is heterogeneous (Mg gas at the bubble-metal interface). The formed MgS precipitates on inclusions or CaO particles. Yang et al. [20] and Lindström [21] conclude from their experiments (on lab scale) that more than 90 % of the Mg-desulphurisation is heterogeneous and that only little Mg first dissolves before it reacts. Visser [7] discussed both visions and concluded, also based on plant data, that the kinetic model of Irons and Guthrie [22] predicts the reality on plant scale best and therefore that the route via dissolved Mg is dominant.

2.5 Sulphur removal in the blast furnace

In the BF typically 2.5-3.5 kg/tHM of sulphur is introduced through the raw material input. Typically 80-90 % of the sulphur enters the process via coke. However, in steel plants that add a large amount of coal (PCI) or fuel oil, up to 45 % of the total added sulphur can be added via these fuels. Ore typically contributes to around 10 % of the sulphur input. Usually roughly 90 % of the sulphur is removed during the BF process. This happens mostly via the slag, but also about 2-3 % via dust and off-gas such as SO₂ and H₂S. Only 10-11 % of the initial sulphur in the charged material ends up in the hot metal [1, 11].

In the BF, part of the sulphur (from sulphides and sulphates) dissolves in the hot metal. The largest part of the dissolved sulphur is removed by the lime present in the slag via Reaction 2.3. The calcination of limestone (Reaction 2.12) is highly endothermic. This means that when more limestone is charged to the BF, in order to increase the basicity, also more coke should be added in order to compensate for the energy/temperature loss. A rule of thumb is that in the BF 100 kg extra limestone needs to be compensated by 25-35 kg coke. With the extra coke, also extra sulphur is added to the BF. These additions require more volume as well, decreasing the iron output. Therefore it is more efficient to remove the last 10 % sulphur later in the steelmaking process [1, 11].



An alternative for desulphurisation with lime is the use of magnesium oxide. MgO in the slag and dissolved sulphur react via Reaction 2.13 (based on Reaction 2.1). MgO however is a less effective desulphuriser than CaO, since

the affinity of Mg to sulphur is less than the affinity of Ca to sulphur. In typical BF slag there is 10 wt% MgO and 40 wt% CaO [1, 11].



Since the main desulphurisation reaction with lime (Reaction 2.3) is endothermic, better desulphurisation in the BF can be achieved by higher temperatures. Also a longer contact time between the slag and the metal is beneficial for sulphur removal. This can be achieved by tapping the BF more often or by increasing the slag volume. Furthermore several compounds have their influence on the desulphurisation process. For better desulphurisation [1, 11, 23]:

- Oxygen activity in the hot metal ($a_{[O]}$) should be as low as possible (Equation 2.2)
- Carbon concentration in the hot metal should be high (it reacts with oxygen and thus reduces $a_{[O]}$)
- Silicon concentration in the hot metal should be high (it reacts with oxygen as well and thus reduces $a_{[O]}$)
- Manganese concentration in the hot metal should be high (it reacts with sulphur to form MnS)

Although the BF is an efficient desulphuriser, a significant amount of sulphur will remain in the hot metal. Therefore sulphur removal further down the line in the steelmaking process remains inevitable.

2.6 Hot metal desulphurisation

Hot metal that leaves the BF typically contains 0.03 wt% sulphur, but the demand for the steel can be as low as 0.001 wt% sulphur (e.g. hydrogen induced cracking, HIC, resistant steel) [24-26]. Therefore most steel plants worldwide apply an HMD process, because it is more process- and cost-efficient to desulphurise before the converter [2].

2.6.1 Torpedo desulphurisation

In the 1960's and 1970's HMD took place in the torpedo cars that transported the hot metal from the BF to the steel plant (see Figure 2.6). Typical reagents were calcium carbide (Reaction 2.4), soda ash and blends of magnesium and lime. During torpedo desulphurisation the reagent is injected into the hot metal

2. Sulphur removal in ironmaking and oxygen steelmaking

via a lance; nitrogen is used as a carrier gas. The reagent reacts with the sulphur in the hot metal and the sulphides CaS or Na_2S ascend to the slag layer. This slag is then raked off by a skimmer [16, 27].

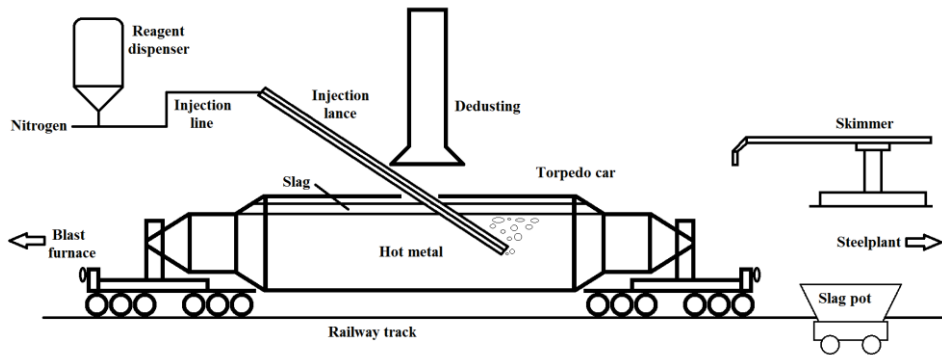


Figure 2.6: Schematic overview of torpedo desulphurisation.

The shape of the torpedo is designed for temperature preservation and not as a metallurgical reactor vessel. The hot metal bath is not very deep (1-2 m), so the reagent particles (which have a lower density than the hot metal) quickly rise to the top. Therefore, the reagents only have a short contact time with the hot metal. Reagent mixing is poor, which means that both far ends of the torpedo are not reached by the reagents. Finally a torpedo has only a small opening at the top, which makes it difficult to rake off the slag. This leads to resulphurisation via remaining slag and high iron losses. Because of these drawbacks torpedo desulphurisation was replaced by ladle desulphurisation in most steel plants [16]. Still with torpedo desulphurisation final sulphur concentrations at converter charge (including resulphurisation) as low as 0.002 wt% are reported in literature [28, 29].

2.6.2 Co-injection

Co-injection is an HMD process in which both magnesium and fluidised lime or calcium carbide are injected into the hot metal (multi-injection, that uses all three reagents, is a variation of this process). Co-injection (see Figure 7) is used worldwide and is, certainly in Europe and North America, considered as the industrial standard. Via a submerged refractory coated lance the reagents are injected at the bottom of the hot metal ladle. An inert carrier gas (usually nitrogen) transports the reagents through the injection line and creates enough turbulence in the ladle for proper mixing. The mixing of the reagents takes place

in the injection line, which makes it possible to change the ratio of the reagents during the process. When the reagents react with sulphur, the products (MgS and CaS) ascend to the slag layer, where it is removed with a skimmer.

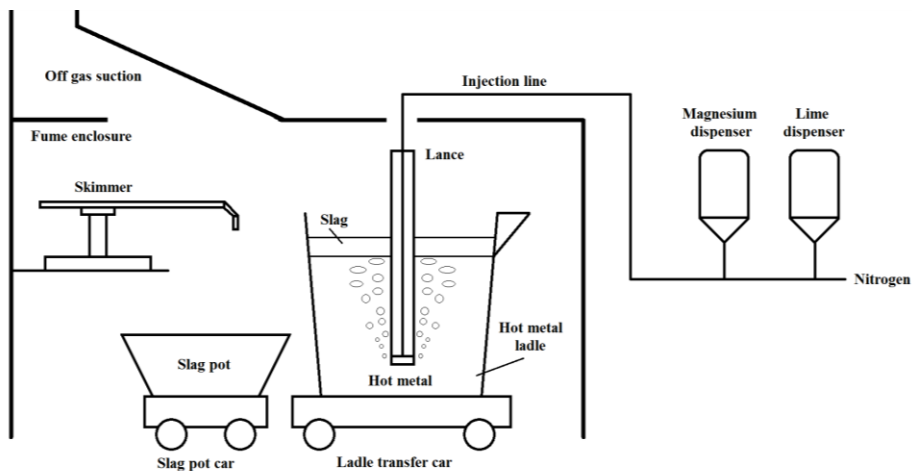


Figure 2.7: Schematic overview of co-injection desulphurisation.

Co-injection combines the advantages of magnesium (faster process) and lime/calcium carbide (deep desulphurisation). Most sulphur will initially react with magnesium to form MgS. The lime will mostly prevent the resulphurisation via Reaction 2.9.

With magnesium/lime co-injection sulphur levels below 0.001 wt% (10 ppm) have been reported in literature [29-32]. At the plants of Tata Steel in IJmuiden (NL) and Port Talbot (UK), a significant number of heats had a measured final sulphur level below 0.001 wt%, achieved with co-injection.

2.6.3 Kanbara reactor

Kanbara reactor (KR) is an HMD process developed in 1965 in Hirohata (Japan) by Nippon Steel (see Figure 2.8). The KR uses relatively cheap coarse lime (often with an additional 5-10 wt% CaF₂ as slag modifier; calcium carbide is an alternative to lime) as reagent, which is usually added on top of the hot metal ladle during the first few minutes of the process. Typically 5-15 kg/tHM of reagent is added. An immersed impellor (at one third of the bath depth) is used to mix the reagent with the hot metal. The mixing is required because the reaction between lime and sulphur (Reaction 2.3) is relatively slow, so the

2. Sulphur removal in ironmaking and oxygen steelmaking

contact time needs to be decreased. The impellor has a typical rotational speed of 60-120 rpm and an average life of about 200 heats. The stirring takes 5-15 minutes after which the impellor is lifted and the bath is allowed to rest another 5-10 minutes. This is necessary because the slag and the formed CaS need time to ascend to the top. After this the slag layer is skimmed off, which takes 10-15 minutes [2, 16, 28, 31].

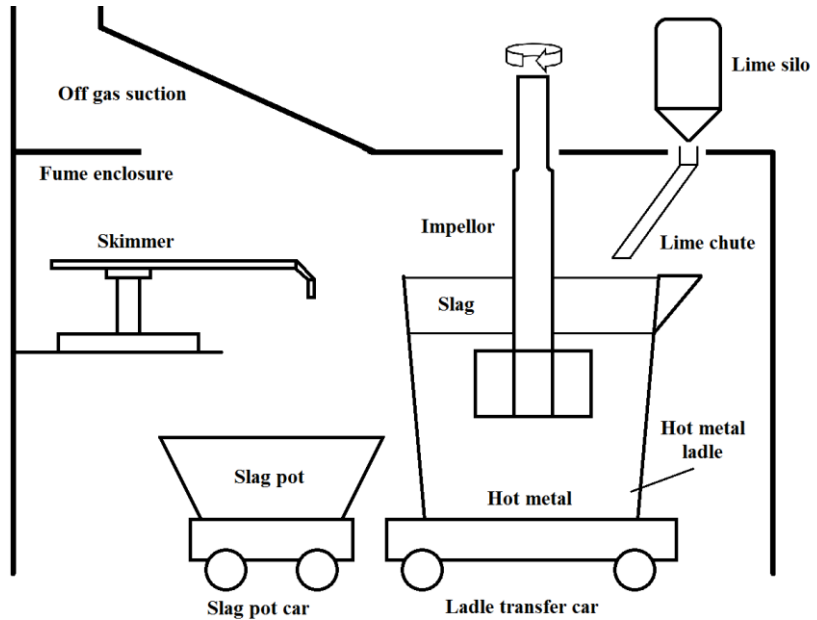


Figure 2.8: Schematic overview of a KR process.

KR is widely applied in Asia (especially Japan). With KR sulphur levels below 0.001 wt% (10 ppm) have been reported in literature [28, 31]. Around 1970 a similar process, called Rheinstahl-Rührer, was developed in Germany. It was soon abandoned due to the large slag volumes created [16].

2.6.4 Magnesium mono-injection

Magnesium mono-injection (MMI), also referred to as Ukraina-Desmag process [33], is an HMD process that uses only magnesium as a reagent (see Figure 2.9). The process was developed between 1969-1972 by the Ukrainian Academy of Sciences. In MMI the magnesium is injected in the hot metal under pressure via a submerged refractory coated lance. Nitrogen is most often used as a carrier gas. Usually a lance with an evaporation chamber at the end is used,

but also straight lances can be used. Turbulence is created by evaporation of the magnesium powder. At higher injection rates the turbulence can become a problem, increasing the iron loss by splashing. Therefore the evaporation chamber at the end of the lance is used to allow the magnesium to evaporate earlier, thus reducing the turbulence [33, 34].

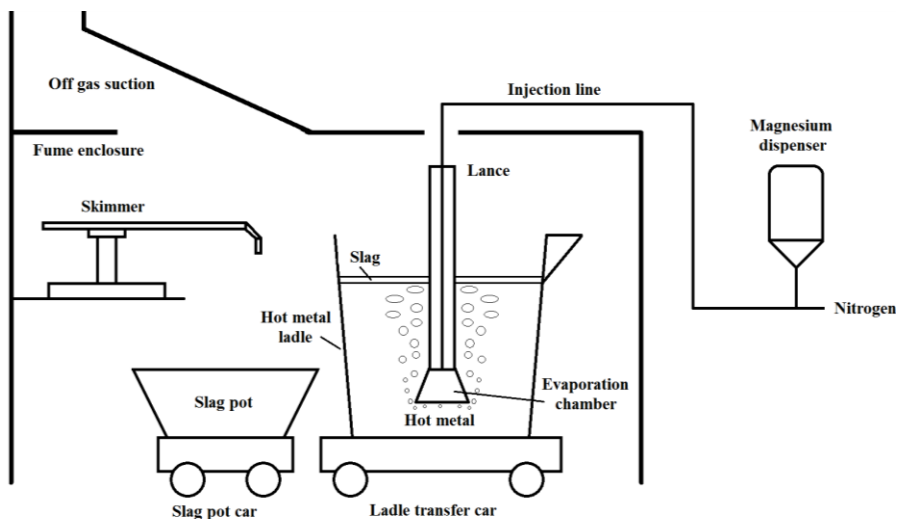


Figure 2.9: Schematic overview of MMI desulphurisation.

Because magnesium reacts with sulphur (Reaction 2.7) much faster than lime (Reaction 2.3) and calcium carbide (Reaction 2.4) [35], MMI is a very fast desulphurisation process, in which very little slag is created. A major disadvantage of MMI is the severe resulphurisation (Reaction 2.13). If no lime is used to prevent this, the sulphur concentration of the hot metal will increase significantly before converter charging. Resulphurisation can sometimes undo the desulphurisation process almost completely [20, 34, 36].

2.7 Sulphur removal in the converter

The main targets of a BOF converter are decarburisation, dephosphorisation, desiliconisation and increasing the temperature of hot metal and scrap in order to make steel with a specified composition. Sulphur removal is at best a minor target. In order to remove carbon and phosphorus, and to increase the temperature, oxygen is blown into the hot metal (which leads to an exothermic reaction with the dissolved carbon to form CO). The resulting increase of oxygen activity in the melt has a negative effect on the desulphurisation. At the

2. Sulphur removal in ironmaking and oxygen steelmaking

slag-metal interface Reaction 2.1 takes place reversed (effectively transferring sulphur from the slag back to the metal). On the other hand part of the sulphur (15-25 %) is directly oxidised via Reaction 2.14 and leaves the process [3, 10].



This reaction takes place at the metal-gas interface where oxygen is abundant. Further away from the oxygen jet the oxygen concentration is too low and the oxygen will react with silicon and carbon before it will react with sulphur [10].

Dephosphorisation is favoured by a high basicity, a low slag temperature and a high FeO content in the slag (thus a high oxygen activity). To achieve better dephosphorisation, the converter slag's basicity is increased by adding lime to the process (leading to a typical basicity of 2-4). This lime has a positive effect on the desulphurisation (Reaction 2.3). In most converters 30-45 % of the sulphur ends up via this reaction as CaS in the slag [10, 37].

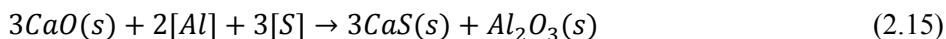
During the converter process sulphur is added to the system through scrap and additions. Between 10 and 30 wt% of the iron input in the converter comes from scrap, which contains typically 0.015-0.04 wt% sulphur [38]. From the additions most sulphur input is contributed via ore that is used to cool the steel. Ore contains 0.015-0.025 wt% sulphur.

Overall some desulphurisation takes place during the converter process. On the other hand sulphur is added via scrap and additions. This means that it differs from plant to plant (or even between steel grades) whether the sulphur concentration in the metal increases or decreases during the BOF process. Minimum sulphur levels at tapping are reported to be in the range of 0.003-0.004 wt% [29].

2.8 Steel desulphurisation

Secondary metallurgy is the last possibility to influence the steel's chemistry. For low sulphur steel grades (less than 0.002 wt% [9]) steel desulphurisation is inevitable. Liquid steel at the end of the BOF process has a high oxygen concentration (typically 200-800 ppm [4]), which is unwanted for the following process steps. Therefore most steel plants deoxidise the steel by adding Si, Mn and Al. The formed oxides end up in the slag. This slag needs to be basic for desulphurisation, therefore calcium based reagents (usually lime) are added [4, 9, 39, 40].

Lower oxygen activities in the steel enhance steel desulphurisation. After deoxidation (with aluminium) the oxygen concentration is around 2-4 ppm, which is comparable to that of hot metal. The steel temperature (~1600 °C) is higher than that of hot metal (~1300 °C). This means that magnesium is no longer an option as reagent due to its high vapour pressure, which means less magnesium will dissolve in the liquid steel. With aluminium and lime, desulphurisation takes place via Reaction 2.15, which is a variation on Reaction 2.3, but where oxygen is now bound to aluminium [9, 10, 39-41]:



Stolte [5] ranked the different secondary metallurgy processes that are used in industry with respect to their ability to desulphurise steel (see Table 2.4). These processes are further discussed in the following sections.

Table 2.4: Overview secondary metallurgy processes and their ability to desulphurise steel.

Process	Efficiency	Final sulphur	Comment
Vacuum processes (VD / VOD)	+ / +	< 0.001 wt%	Vacuum based
RH / RH-KTB	- / (+)	- / < 0.001 wt%	Vacuum based
Ladle furnace	+	< 0.002 wt%	
Stirring station	+	< 0.002 wt%	
Powder injection	+	< 0.002 wt%	Similar to HMD
Wire feeder	+	< 0.002 wt%	
CAS-OB	-	-	

2.8.1 Vacuum based processes

In a vacuum degasser (VD) or tank degasser either the ladle or a vessel that contains the ladle is put under vacuum. Argon is bubbled in the ladle via the bottom and additions are inserted from the top or via wire (also possible during the process). Optionally an oxygen lance is installed for further reducing (making it a vacuum oxygen decarburisation station, or VOD) [5, 9, 40].

Typically an argon flow of 0.2-0.5 Ndm³ per tonne of steel per minute is blown and 3-5 kg/t lime based reagent is added (most additions, typically 5-15 kg/t, are already added during converter tapping). Pressure can be reduced to 1 mbar. The total process takes typically 25 min. During the VD process a lot of turbulence is generated. This creates ideal kinetic circumstances with excellent slag-metal mixing, which can lead to final sulphur levels lower than 0.001 wt% (10 ppm) [5, 9, 10, 14, 29].

2. Sulphur removal in ironmaking and oxygen steelmaking

The recirculation degasser or RH, is in its standard version not well suited for desulphurisation because there is not enough interaction between the steel and the desulphurising slag. When a top oxygen lance (connected to a dispenser) is added (RH-KTB), a lime-based reagent is inserted in the vacuum vessel, allowing desulphurisation even to below 0.001 wt%. This is still less efficient than VD, since more reagent is required [5, 40, 42].

2.8.2 Ladle furnace

In the ladle furnace (LF) the steel is reheated by inserting three electrodes that create an electric arc inside the steel. Materials (for desulphurisation aluminium and lime, sometimes in combination with CaF_2 or silicon) are either added on top of the steel, or via injection with a lance, or by wire feeding. Argon is injected through the bottom for steel bath homogenisation [5, 9].

For desulphurisation an argon flow of up to $7 \text{ Ndm}^3 \cdot \text{tLS}^{-1} \cdot \text{min}^{-1}$ is blown (typically via the injection lance) and 5-15 kg/t of materials are added. The total process takes typically 45 min. The main limitation for desulphurisation in the LF is the high oxygen activity in the steel, making desulphurisation to a sulphur concentration below 0.005 wt% without vacuum treatment or aluminium addition difficult. For Al-deoxidised steel grades it is possible to desulphurise to below 0.002 wt%. This is impossible for Si-deoxidised steel grades, because of the low slag basicity and the higher oxygen content of the steel of 20 ppm) [5, 9, 39, 40, 43].

2.8.3 Other secondary metallurgy processes

- **Stirring station:** Argon is injected in the ladle via bottom plugs and calcium (CaO , CaSi or CaFe) is injected via a lance or added by wire feeding. By adding calcium the stirring station is suited for desulphurisation [5, 40].
- **Powder injection:** This process is similar to HMD injection processes. CaO , CaC_2 and CaSi (sometimes in combination with Al) are used as reagents. Sulphur concentrations below 0.002 wt% can be reached for Al-killed steel [5, 40].
- **Wire feeder:** This process is comparable with powder injection. The difference is that the reagents are contained in a hollow wire that is shot into the steel at a speed of 1-4 m/s (allowing the wire to penetrate the bath 1.5-2 m before the coating is completely melted and the reagents are freed). Wire feeders are typically suited for lime additions below 0.2

kg/t. Sulphur concentrations below 0.002 wt% can be reached (when the steel is Al-killed) [5, 40].

- **Chemical Heating station or CAS-OB:** Its main purpose is to reheat the steel (allowing a 15 °C lower tapping temperature at the converter). CAS-OB creates little turbulence due to its bell, which leads to poor kinetics for desulphurisation with lime. Also oxygen is blown, which further decreases the desulphurisation efficiency due to the high oxygen activity. It is possible to add an injection lance (or wire feeder) to the CAS-OB, to inject desulphurisation reagents (lime, aluminium) [5, 40].

2.9 Outlook

In the 21st century the iron- and steelmaking industry will face new challenges. The quality of the raw materials will continue to decrease, since the high quality stocks are depleting. This means that the sulphur amount added to the process will increase. On the other hand, the quality demands will continue to increase, implying that the sulphur content of the products will have to decrease. This will lead to an increased necessity for more efficient sulphur removal during ironmaking and steelmaking.

Undoubtedly one of the largest challenges for the steel industry will be reducing energy consumption and greenhouse gas emissions. The European steel industry and the European Union have committed themselves to reduce CO₂ emissions of the steel industry with 50 % by 2050. Most likely the largest changes will involve the ironmaking process (cokemaking, ore agglomeration and BF), since it is the largest producer of CO and CO₂ within the integrated steelmaking process [44-46].

Already in the 1970's and 1980's the COREX process was developed. In this process coal (to replace the majority of coke) is used to create CO and H₂ to reduce the iron ore and melt the iron. By its more efficient energy utilisation less CO₂ per tonne hot metal is produced. Worldwide a few commercial COREX plants were built, but their hot metal production remains with 0.3-2.0 Mt/y low compared to the BF process. The BF process remains more cost-effective in producing larger amounts of hot metal [1, 47].

One recent development is the HIsarna process, which was developed by a collaboration between various European steelmaking companies and universities and Rio Tinto from Australia. It is one of the outcomes of the

2. Sulphur removal in ironmaking and oxygen steelmaking

European Union ULCOS project in combination with the HIs melt technology. The pilot plant is operated at the site of Tata Steel in IJmuiden, the Netherlands. HIsarna uses coal and untreated fine iron ore as raw materials instead of coke and agglomerated iron ore. By skipping the pre-treatment of raw materials, the overall energy consumption is decreased and the net CO₂ emission is decreased by 20 % [44-46].

However, by using coal instead of coke, the sulphur concentration in the hot metal increases. At the same time, hot metal produced in HIsarna contains almost no silicon, which reduces desulphurisation efficiency. This means that hot metal desulphurisation needs to be intensified, since the sulphur aims remain the same or will even be lower in the future. Therefore part of further development will be devoted to sulphur control [46]. This topic will be addressed in more detail in Part III of this thesis.

Another possibility is to reduce the iron (partly) by another reducing agent than coal or coke. Natural gas, biomass or hydrogen gas are mentioned as alternatives [45]. This would lead to hot metal with a low sulphur range. For the heats that still require desulphurisation, magnesium-based HMD methods would become relatively more expensive.

With the ever increasing customer demand for low sulphur steel on one hand and the environmental challenges of the steel industry on the other hand, sulphur removal will remain a key issue for steelmakers. In this changing environment sulphur removal methods should continue to be developed and adapted. This will also create the necessity for a new optimisation between the different sulphur removal steps within the ironmaking and steelmaking process chain.

2.10 Concluding remarks

Sulphur removal in steelmaking becomes less efficient when it is done further down the process chain. It is therefore important from a process and economical point of view, to remove most of the sulphur from iron before it enters the oxygen steelmaking converter. Since it is not efficient to desulphurise hot metal below 0.03 % sulphur in the blast furnace, hot metal desulphurisation will be an essential part of the production of lower sulphur steel grades. However, due to additional sulphur input in the converter, desulphurisation in secondary metallurgy remains inevitable for these steel grades. A steel plant ready for 21st

century customer demands needs to be able to desulphurise by means of hot metal pre-treatment as well as by secondary metallurgy, and needs to be able to control the sulphur levels in the blast furnace and the oxygen steelmaking converter.

2.11 References

- [1] Y. Yang, K. Raipala, and L. Holappa, “Ironmaking,” in *Treatise on Process Metallurgy*, vol. 3, S. Seetharaman, Ed. Oxford (UK): Elsevier, 2014, pp. 2–88.
- [2] S. Kitamura, “Hot Metal Pretreatment,” in *Treatise on Process Metallurgy*, vol. 3, S. Seetharaman, Ed. Oxford (UK): Elsevier, 2014, pp. 177–221.
- [3] H. Jalkanen and L. Holappa, “Converter Steelmaking,” in *Treatise on Process Metallurgy*, vol. 3, S. Seetharaman, Ed. Oxford (UK): Elsevier, 2014, pp. 223-270.
- [4] L. Holappa, “Secondary Steelmaking,” in *Treatise on Process Metallurgy*, vol. 3, S. Seetharaman, Ed. Oxford (UK): Elsevier, 2014, pp. 301-345.
- [5] G. Stolte, *Secondary Metallurgy*, 1st ed. Düsseldorf (DE): Verlag Stahleisen GmbH, 2002.
- [6] H.G. Erne, “Die Entschwefelung des Roheisens mit sauren Schlacken,” (PhD thesis) Eidgenössischen Technischen Hochschule, Zürich (CH), 1952.
- [7] H.-J. Visser, “Modelling of injection processes in ladle metallurgy,” (PhD thesis) Delft University of Technology, Delft (NL), 2016.
- [8] N.N. Chatterjee, “Sulphur in coal,” *Proceedings of the Indian National Science Academy*, vol. VI, no. 3, pp. 523-534, 1940.
- [9] E.T. Turkdogan, *Fundamentals of Steelmaking*, London (UK): The Institute of Materials, 1996.
- [10] B. Deo and R. Boom, *Fundamentals of Steelmaking Metallurgy*, 1st ed. Hemel Hempstead (UK): Prentice-Hall, 1993.
- [11] M. Geerdes, R. Chaigneau, I. Kurunov, O. Lingiardi, and J. Ricketts, *Modern Blast Furnace Ironmaking*, 3rd ed. Delft (NL): IOS Press, 2015.

2. Sulphur removal in ironmaking and oxygen steelmaking

- [12] P. Hayes, "Sources of data on chemical and physical systems, " in *Process principals in minerals & materials production*, Brisbane (AUS): Hayes Publishing Co, 1993, pp. 633-646.
- [13] F.F. Grillo, et al., "Analysis of pig iron desulfurization with mixtures from the CaO-Fluorspar and CaO-Sodalite system with the use of computational thermodynamics, " *Revista Escola de Minas*, vol. 66, no. 4, 2013, pp. 461-465.
- [14] R. Tsujino, et al., "Behavior of desulfurization in ladle steel refining with powder injection at reduced pressures, " *ISIJ International*, vol. 29, no. 1, 1989, pp. 92-95.
- [15] H. Ohta and H. Suito, "Activities in CaO-MgO-Al₂O₃ slags and deoxidation equilibria of Al, Mg, and Ca, " *ISIJ International*, vol. 36, no. 8, 1996, pp. 983-990.
- [16] A. Freißmuth, "Entschwefelung von Roheisen mit Calciumcarbid - der heutige Stand und mögliche Entwicklungen, " *Stahl und Eisen*, vol. 117, no. 9, 1997. pp. 53-59.
- [17] H.-J. Visser and R. Boom, "Process Modelling of Ladle Desulphurisation by Injection of CaO/Mg and CaC₂/Mg Mixtures in 300 Ton Ladles, " in *3rd International Congress on the Science and Technology of Steelmaking*, 2005, pp. 369-379.
- [18] S.K. Saxena, "Mechanism of Sulphur Removal in Hot Metal by Using Soda, Lime, Calcium Carbide and Magnesium Based Reagents, " in *International Conference on Desulphurization and Inclusion Control*, 1997 pp. 135-150.
- [19] M. Hino and K. Ito, *Thermodynamic data for steelmaking*, Sendai (JP): Tohoku University Press, 2010.
- [20] J. Yang, et al., "Mechanism of Resulfurization in Magnesium Desulfurization Process of Molten Iron, " *ISIJ International*, vol. 45, no.11, 2005, pp. 1607-1615.
- [21] D. Lindström, "A Study on Desulfurization of Hot Metal Using Different Agents, " (PhD thesis) KTH, Stockholm (SE), 2014.
- [22] G.A. Irons and R.I.L. Guthrie, "The Kinetics of Molten Iron Desulfurization Using Magnesium Vapor, " *Metallurgical Transactions B*, vol. 12, no. 4, 1981, pp. 755-767.

Part I Introduction

- [23] R.R. Beisser, R. Boom, and W. Koen, "Trends in hot metal quality at Hoogovens IJmuiden, " in *48th Ironmaking Conference*. 1989, pp. 249-254.
- [24] Euro Inox, *Stainless Steel: Tables of Technical Properties*. 2007: Luxembourg.
- [25] Euro-Asian Council for Standardization, M.a.C.E., *GOST 5632-72*. 2007: Minsk (BY).
- [26] R. Winston Revie, *Oil and Gas Pipelines*, Hoboken (USA): John Wiley & Sons, 2015.
- [27] R. Boom, "Hot Metal Desulphurization to Control the Sulphur Balance at Hoogovens IJmuiden, " in *Development in Hot Metal Preparation for Oxygen Steelmaking*, 1983.
- [28] T. Ueki, et al., "High Productivity Operation Technologies of Wakayama Steelmaking Shop, " in *The 10th Japan-China Symposium on Science and Technology of Iron and Steel*, 2004.
- [29] M. Nadif, et al., "Desulfurization practices in ArcelorMittal Flat Carbon Western Europe, " in *Scanmet III*, 2008, pp. 569-580.
- [30] H.-J.Visser and R. Boom, "Development of a reactor model of hot metal desulphurisation on an industrial scale, " in *Scanmet III*, 2008, pp. 147-156.
- [31] T. Emi, "Steelmaking Technology for the Last 100 Years: Toward Highly Efficient Mass Production Systems for High Quality Steels, " *ISIJ International*, vol. 55, no. 1, 2015, pp. 36-66.
- [32] M. Magnelöv, "Iron losses during desulphurisation of hot metal, " (PhD thesis) Luleå University of Technology, Luleå (SE), 2014.
- [33] V.I. Bolshakov, et al., "Rational Ladle Treatment for Desulfurization of Hot Metal, " *Steel in Translation*, vol. 39, no. 4, 2009, pp. 326-333.
- [34] N.A. Voronova, *Desulfurization of Hot Metal by Magnesium*, Dayton (USA): The International Magnesium Association, 1983.
- [35] A. Ender, et al., "Metallurgical Development in Steel-plant-internal Multi-injection Hot Metal Desulphurisation, " *Steel Research International*, vol. 76, no. 8, 2005, pp. 562-572.

2. Sulphur removal in ironmaking and oxygen steelmaking

- [36] V.A. Bigeev, A.O. Nikolaev, and A.V. Brusnikova, "Production of Low-Sulfur Steel with Limited Hydrogen Content, " *Steel in Translation*, vol. 44, no. 4, 2014, pp. 272-275.
- [37] R. Boom, R.R. Beisser, and W. Van der Knoop, "Hoogovens' studies of lime and flux properties related to slag formation in oxygen steelmaking, " in *2nd International Symposium on Metallurgical Slags and Fluxes*, 1984, pp. 1041-1060.
- [38] T.W. Miller, et al., "Oxygen Steelmaking Processes, " in *The Making, Shaping and Treating of Steel*, R.J. Fruehan, Ed. Pittsburgh (USA): The AISE Steel Foundation, 1998, pp. 475-524.
- [39] E.T. Turkdogan and R.J. Fruehan, "Fundamentals of Iron and Steelmaking, " in *The Making, Shaping and Treating of Steel*, R.J. Fruehan, Ed. Pittsburgh (USA): The AISE Steel Foundation, 1998, pp. 13-157.
- [40] G.J.W. Kor and P.C. Glaws, "Ladle Refining and Vacuum Degassing, " in *The Making, Shaping and Treating of Steel*, R.J. Fruehan, Ed. Pittsburgh (USA): The AISE Steel Foundation, 1998 pp. 661-713.
- [41] M.A.T. Andersson, "Some Aspects of Oxygen and Sulphur Reactions Towards Clean Steel Production, " (PhD thesis) KTH, Stockholm (SE), 2000.
- [42] S. He, G. Zhang, and Q. Wang, "Desulphurisation Process in RH Degasser for Soft-killed Ultra-low-carbon Electrical Steels, " *ISIJ International*, vol. 52, no. 6, 2012, pp. 977-983.
- [43] S.N. Ushakov, et al., "Production of New Steel Grades in the Oxygen-Converter Shop, " *Steel in Translation*, vol. 42, no. 2, 2012, pp. 138-140.
- [44] Tata Steel Europe, "Neue Technologie zur Stahlerzeugung erhält EU-Fördergelder, " *Stahl und Eisen*, vol. 135, no. 9, 2015, pp. 10-11.
- [45] J.P. Birat, et al., "ULCOS Program: a Progress Report in the Spring of 2008, " in *Scanmet III*, 2008, pp. 61-75.
- [46] J.W.K.van Boggelen, et al., "The use of HIsarna hot metal in steelmaking, " in *Scanmet V*, 2016, 008.

Part I Introduction

- [47] A. Ziebig, K. Lampert, and M. Szega, “Energy analysis of a blast-furnace system operating with the Corex process and CO₂ removal,” *Energy*, vol. 33, 2008, pp. 199-205.

Part II
**Optimal hot metal
desulphurisation slag**

Part II Optimal hot metal desulphurisation slag

3 Optimal hot metal desulphurisation slag: fundamentals

This chapter is based on the following publication:

F.N.H. Schrama, E.M. Beunder, S.K. Panda, H.-J. Visser, J. Sietsma, R. Boom and Y. Yang, “Optimal hot metal desulphurisation slag considering iron loss and sulphur removal capacity part I: Fundamentals”, *Ironmaking and Steelmaking*, Vol. 48, No. 1, 2021, p 1-13.

In hot metal desulphurisation (HMD) the slag will hold the removed sulphur. However, the iron that is lost when the slag is skimmed off, accounts for the highest costs of the HMD process. These iron losses are lower when the slag has a lower viscosity, which can be achieved by changing the slag composition. A lower slag basicity decreases the viscosity of the slag, but also lowers its sulphur removal capacity, therefore optimisation is necessary. In this study, the optimal HMD slag composition is investigated, considering both the sulphur removal capacity and the iron losses. In this chapter the theory is discussed and in Chapter 4, the optimal slag is validated with plant data, laboratory experiments and a thermodynamic analysis.

3.1 Introduction

Since the early days of iron- and steelmaking, sulphur is considered as an unwanted impurity that needs to be removed [1]. Although there are various processes in the modern steelmaking chain where sulphur can be removed, a dedicated hot metal desulphurisation (HMD) process between the blast furnace (BF) and converter (or basic oxygen furnace, BOF) remains necessary. Essentially during the HMD process the dissolved sulphur reacts with reagents (typically magnesium and/or lime) to form sulphides that end up in the slag phase. When the slag is removed after reagent injection, the hot metal is desulphurised [2, 3].

As the sulphur is only removed by skimming off the sulphur-containing slag, it is essential for the HMD process that the slag contains all formed sulphides. The mass of removed sulphur per mass unit of a certain slag, is defined as the “sulphur removal capacity” of the slag. This sulphur removal capacity is different from the thermodynamically defined “sulphide capacity” (C_S), which was introduced by Fincham and Richardson [4]. In this chapter the sulphur removal capacity of the slag is used as the criterion for optimising slag regarding sulphur removal. Although the sulphur removal capacity is in principle a better measure to determine the desulphurisation of hot metal, it is difficult to measure, unlike C_S . Therefore, the sulphur removal capacity is considered in relation to C_S in this chapter.

The largest costs during the HMD process are the iron losses, iron that is skimmed off together with the slag. Depending on the heat size, typically 500 – 4000 kg iron (0.5 - 2.5 wt% of the total iron) is skimmed off per heat [5, 6]. By changing the apparent viscosity of the slag (η_{slag}), the iron losses can be lowered [6–11]. This means that iron losses partly depend on the slag composition.

The aim of this study is to find the optimal slag for the HMD process, which is defined as a slag with an optimal balance between maximising sulphur removal capacity and minimising iron losses. Because the slag composition changes during the process, as reagents are added, the sulphur removal capacity should be sufficient throughout the process. The slag composition that minimises the iron losses should be reached at the end of the process, so the focus here is on the final

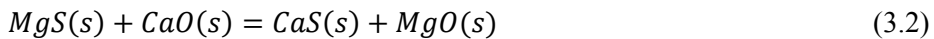
3. Optimal hot metal desulphurisation slag: fundamentals

slag composition. In order to be acceptable for industry, this optimal slag should not lead to health, safety and environmental issues and should not lead to a large increase in costs. In the present paper, part I of this study, the theory behind the sulphur removal capacity, as well as a theoretical study of HMD iron losses, are presented. This part ends with conclusions about the optimal HMD slag, based on theory. In Chapter 4 [12] the theory is examined and validated with a Monte Carlo simulation using FactSage [13], plant data analysis and laboratory viscosity and melting point experiments with the optimal slag.

3.2 Sulphur removal capacity

3.2.1 Desulphurisation process

In the magnesium-lime co-injection process, most of the desulphurisation (> 95 %) takes place by the reaction between magnesium and sulphur in the bath (Reaction 3.1). The formed MgS ascends to the slag layer and reacts with lime to form CaS (Reaction 3.2). Only a small portion of the dissolved sulphur directly reacts with lime via Reaction 3.3 [2, 14, 15].



Most of the formed sulphides and oxides eventually dissolve in the slag, although a substantial part of the CaS remains in a solid fraction [14]. All solid phases have a lower density than the hot metal and end up in the slag. The desulphurisation rate in the co-injection process is controlled by Reaction 3.1 [2, 3, 14, 15]. This leads, via Reaction 3.2, to a heterogeneous slag, which is not necessarily in equilibrium with the hot metal with respect to sulphur distribution. Other sulphur removing processes in steelmaking, including the blast furnace (BF), the Kanbara reactor (KR) HMD process and several secondary metallurgy (post BOF) processes, which include the ladle furnace and the vacuum degasser, are dominated by Reaction 3.3. The slag and metal bath are generally in equilibrium regarding the sulphur distribution. Metallic magnesium is not introduced for desulphurisation of the metal in any of the other above mentioned processes [2, 3, 15–18].

Part II Optimal hot metal desulphurisation slag

Before the HMD process starts, typically 1-3 t of BF carryover slag floats on top of the hot metal. During the reagent injection CaO, CaS and MgO are added to the slag, contributing to typically 20-40 wt% of the slag after injection. This means that the slag's composition and properties change during the process. Especially the slag's basicity increases during the injection. Table 3.1 shows how a typical HMD slag changes from the start of injection (BF carryover slag) until the end of injection (HMD final slag).

Table 3.1: Typical slag compositions for BF carryover slag and HMD slag after reagent injection [6].

	BF carryover (wt%)	HMD final (wt%)
CaO	38	37
SiO₂	37	28
Al₂O₃	14	11
MgO	8.9	13
MnO	0.14	0.11
TiO₂	0.6	0.5
K₂O	0.45	0.34
Na₂O	0.32	0.25
CaS	0.95	9.8

As slag compositions can change from plant to plant and heat to heat, Table 3.2 gives the typical range of HMD slag composition and temperature after reagent injection.

3. Optimal hot metal desulphurisation slag: fundamentals

Table 3.2: Composition and temperature range for HMD slags after reagent injection.

	Min (wt%)	Max (wt%)
CaO	30	43
SiO₂	23	33
Al₂O₃	6	15
MgO	10	17
MnO	0.03	0.25
TiO₂	0.4	1.2
K₂O	0.1	0.7
Na₂O	0.08	0.6
CaS	5	15
Temperature (°C)	1250	1425

In the slag composition the amount of FeO_x (FeO and Fe_2O_3) has been excluded, as it is difficult to measure the amount of FeO_x in the slag. With XRF (X-ray fluorescence) analysis, which is a typical method for slag analysis, all components are oxidised, so no distinction between FeO_x dissolved in the slag, and metallic Fe, captured in the slag, can be made. FeO_x does have a significant effect on the viscosity and melting point of the slag [17, 19]. Figure 3.1 illustrates the effect of adding FeO to a slag with a balanced composition of 40 wt% CaO, 30 wt% SiO₂, 15 wt% Al₂O₃ and 10 wt% MgO on the slag's liquidus temperature (T_{liq}) at thermodynamic equilibrium (determined with FactSage 7.3 [20], CON2 database). The FeO_x concentration in BF carryover slag is typically estimated around 1 wt%, but can be up to 3 wt% [15, 21, 22].

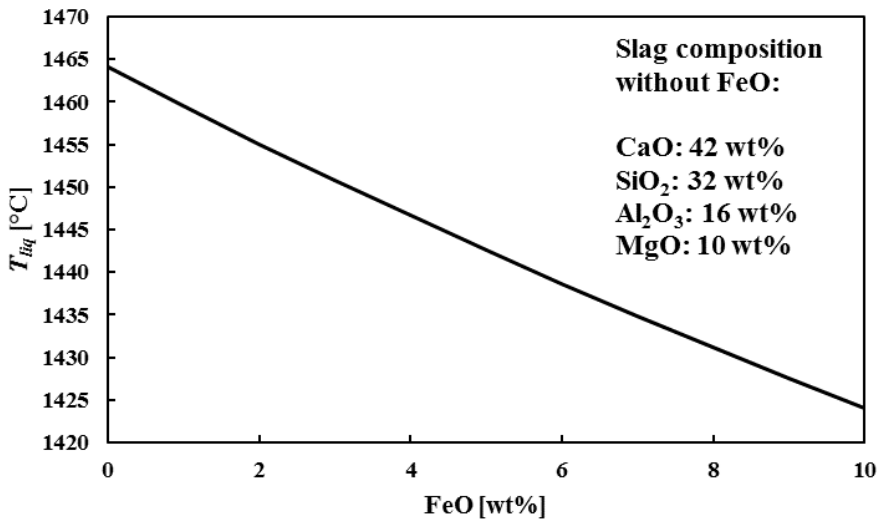


Figure 3.1: Effect of FeO concentration on T_{liq} in a slag with a balanced composition of 40 wt% CaO, 30 wt% SiO₂, 15 wt% Al₂O₃ and 10 wt% MgO. Determined with FactSage 7.3.

3.2.2 Sulphide capacity

When the oxygen partial pressure (p_{O_2}) < 1 Pa (10^{-5} atm), the only way for a sulphur atom to enter the slag is to replace an oxygen atom in an oxide (usually CaO). Under these conditions sulphur is only present in the slag as a sulphide. When $p_{O_2} > 100$ Pa (10^{-3} atm), sulphur will be present as sulphate in the slag [4]. It is generally accepted that in HMD p_{O_2} is much lower than 10^{-5} atm (in some literature a p_{O_2} of 10^{-15} atm. is mentioned [23]), so all sulphur in the slag will be present in the form of sulphides. In this study there is a clear difference between the practical “sulphur removal capacity” and the thermodynamically defined sulphide capacity (C_S), which was introduced by Fincham and Richardson [4]. Here the sulphur removal capacity is defined as the mass fraction of sulphur that can be removed with a certain slag, not necessarily in equilibrium with the hot metal. C_S is defined as “the potential capacity of a melt to hold sulphur as a sulphide” [4, 24], which is given in Equation 3.4. It should be noted that the main difference between the sulphur removal capacity and the sulphide capacity is that the sulphide capacity only takes dissolved sulphides in the liquid slag at equilibrium into account, while the sulphur removal capacity also takes solid

3. Optimal hot metal desulphurisation slag: fundamentals

sulphides, as well as dissolved sulphides that are not in equilibrium into account. Therefore, the sulphur removal capacity of a slag is a better quantity to judge sulphur removal in operational practice.

$$C_S = X_{(S)} \sqrt{\frac{p_{O_2}}{p_{S_2}}} \quad (3.4)$$

Here $X_{(S)}$ is the weight percentage of the sulphides in the slag and p_{O_2} and p_{S_2} the partial pressures of the oxygen and sulphur, respectively, in the gas phase in equilibrium with the slag. Equation 3.4 is valid when Henrian behaviour of sulphur in the slag is expected (because of the low solubility) [25]. As C_S is difficult to measure directly, often the sulphur distribution ratio (L_S) is used, which is the ratio between sulphur in the slag ($X_{(S)}$, typically as sulphides) and sulphur dissolved in the hot metal ($X_{[S]}$) [24–26]:

$$L_S = \frac{X_{(S)}}{X_{[S]}} \quad (3.5)$$

C_S can be calculated based on L_S with Equation 3.6:

$$\log(C_S) = \log(L_S) - \log(K_{S_2}^\theta) - \log(f_S) + \log(a_O) \quad (3.6)$$

Here f_S is the Henrian sulphur activity coefficient in the hot metal, which depends on hot metal composition and temperature [15], but is typically 2.5 under HMD conditions [27], a_O is the oxygen activity of the hot metal with the standard state of 1 wt% ($f_O = 1$ is chosen based on [27]) and $K_{S_2}^\theta$ is the reaction equilibrium constant for the general desulphurisation reaction between sulphur and oxygen (Reaction 3.7). $K_{S_2}^\theta$ is calculated with Equation 3.8 (T is the temperature in K) [26, 28].



$$\log(K_{S_2}^\theta) = -\frac{935}{T} + 1.375 \quad (3.8)$$

Because the BF is a reducing process, a_O of the hot metal is low. In literature different values are mentioned, between $5 \cdot 10^{-5}$ and $4 \cdot 10^{-4}$. Ender *et al.* [29] used electromagnetic force (EMF) measurements to determine a_O before and after the HMD process at the ThyssenKrupp steel plant in Duisburg, Germany. Before

Part II Optimal hot metal desulphurisation slag

HMD a_O is typically between $1.2 \cdot 10^{-4}$ and $1.6 \cdot 10^{-4}$ and after HMD it is between $7 \cdot 10^{-5}$ and $1.2 \cdot 10^{-4}$. Kitamura [15] mentions an a_O between $2 \cdot 10^{-4}$ and $4 \cdot 10^{-4}$. Zhao and Irons [30] measured an a_O between $0.5 \cdot 10^{-4}$ and $1.0 \cdot 10^{-4}$ during a laboratory experiment where CaC_2 was added to hot metal. Janke [23] measured a_O values in hot metal between $5 \cdot 10^{-5}$ and $1.0 \cdot 10^{-4}$ as well. In iron foundries a_O values between $1 \cdot 10^{-5}$ and $6 \cdot 10^{-5}$ are measured [31, 32]. These differences in a_O are caused by different process conditions, the large error for EMF measurements at low ranges and typical HMD temperatures (up to 50 % [29]) and the different measurement depth. It is expected that a_O at 50 cm below the metal-slag interface, where industrial EMF measurements are typically done, is higher than at the metal-slag interface itself, where carbon oversaturation and precipitation locally lowers a_O [14, 33]. Based on literature, it is not possible to determine the exact a_O . Therefore, in this study for hot metal after desulphurisation, an a_O of $1 \cdot 10^{-4}$ is used.

The combination of Equations 3.6 and 3.8 gives the impression that for a certain slag composition C_S only depends on temperature. Panda *et al.* [26] showed with FactSage calculations with a private database (CON2) for typical ladle furnace slags, that this is true only at high p_{O_2} values (for ladle furnace slags typically $p_{O_2} > 0.1$ Pa), or low p_{S_2} values (typically $p_{S_2} < 1$ Pa). At lower p_{O_2} or higher p_{S_2} values, p_{O_2} and p_{S_2} will influence C_S . Jung and Moosavi-Khoonsari [34] stated that the concept of C_S , where the amount of sulphides that a slag can contain only depends on its composition and temperature, is only valid if the slag contains a low fraction of sulphides. If the slag contains more sulphides, p_{O_2} and p_{S_2} play a role as well. This means that for processes where relatively low amounts of sulphur need to dissolve in the slag, like desulphurisation in secondary metallurgy, C_S is a unique temperature- and composition-dependent property of the slag. In HMD, the slag contains more sulphides (HMD slag can contain up to 15 wt% CaS), which means that C_S under HMD conditions is a function of p_{O_2} and p_{S_2} as well.

Based on literature, the influence of the different elements in the slag on C_S is known qualitatively. Table 3.3 gives the influence of different slag components and temperature on C_S based on a literature study.

3. Optimal hot metal desulphurisation slag: fundamentals

Table 3.3: Influence of slag components and temperature on C_S , ranging from ▼ (negative) to ▲▲ (very positive).

Component	Effect	Source	Comment
CaO	▲▲	[3, 10, 40, 46, 47]	
SiO ₂	▼	[3, 25, 40, 47]	
Al ₂ O ₃	▼	[3, 25, 46]	
MgO	0	[25, 40]	
MnO	▲	[26, 40]	No effect above 10 %
Na ₂ O	▲	[38]	
K ₂ O	▲	[20]	
FeO _n	▼	[20]	
CaF ₂	▼	[39]	
Temperature	▲▲	[3, 10, 25, 26, 28, 40, 46]	

It should be noted that the effect of MgO is marginal. Under industrial conditions it has a slight positive effect as it often replaces C_S -negative components like SiO₂ or Al₂O₃. Note that in this table the slag component MgO is discussed and not the metallic Mg, which is injected during the HMD process to desulphurise the hot metal. In literature, many authors made a model to predict C_S based on the slag composition, often including the optical basicity (A), which was defined by Duffy and Ingram [40] as:

$$A = X_1 A_1 + X_2 A_2 + \dots \quad (3.9)$$

Where X_n is the weight percentage of component n and A_n is the optical basicity value for component n . In this work A is determined with only the main components of the slag (normalised to 100 %): CaO ($A_{CaO} = 0.01$), MgO ($A_{MgO} = 0.0078$), SiO₂ ($A_{SiO_2} = 0.0048$) and Al₂O₃ ($A_{Al_2O_3} = 0.006$) [36, 37]. Leaving out the minor slag components does not lead to significant differences in A .

Ma *et al.* [43] made an overview of different models to predict C_S , based on the slag composition and A . Table 3.4 gives an overview of the models for $\log(C_S)$. The KTH model [44] is excluded from this list, because it gave an opposite trend when changing the MgO content. Also the model of Taniguchi *et al.* [36] is excluded, because it is developed for a steel slag composition range, which made

it too sensitive for MgO values above 10 wt%, making it not valid for the HMD slag range.

Table 3.4: Overview of different models to determine C_S , based on optical basicity (A).

Authors	Model for $\log(C_S)$	Eq.
Hao & Wang* [45]	$19.45 - \frac{11.85}{A_{corr}} + \frac{\frac{12\,410}{A_{corr}} - 27\,109}{T}$	(3.10)
Shankar <i>et al.</i> [46]	$\log\left(-9.852 \cdot 10^{-6} \cdot X_{Al_2O_3} + 0.010574A - \frac{16.2933}{T} + 0.002401\right)$	(3.11)
Sosinsky & Sommerville [47]	$\frac{22\,690 - 54\,640A}{T} + 43.6A - 25.2$	(3.12)
Young <i>et al.</i> [36, 37]	$-13.913 + 42.84A - 23.82A^2 - \frac{11\,710}{T} - 0.02223X_{SiO_2} - 0.02275X_{Al_2O_3}$	(3.13)
Zhang <i>et al.</i> [48]	$-6.08 + \frac{4.49}{A} + \frac{15\,893 - \frac{15\,864}{A}}{T}$	(3.14)

*: Hao & Wang used an alternative A : A_{corr} , which differs for HMD slag 10-13 % from A .

The two most influential factors for C_S are temperature and, via A , CaO content. Figures 3.2 and 3.3 show the influence of temperature and CaO, respectively, on the C_S determined by the models from Table 3.4. A simplified typical HMD slag composition was used (40 wt% CaO, 35 wt% SiO₂, 9 wt% MgO, 16 wt% Al₂O₃; when changing the CaO concentration the other components were changed in the same ratio).

3. Optimal hot metal desulphurisation slag: fundamentals

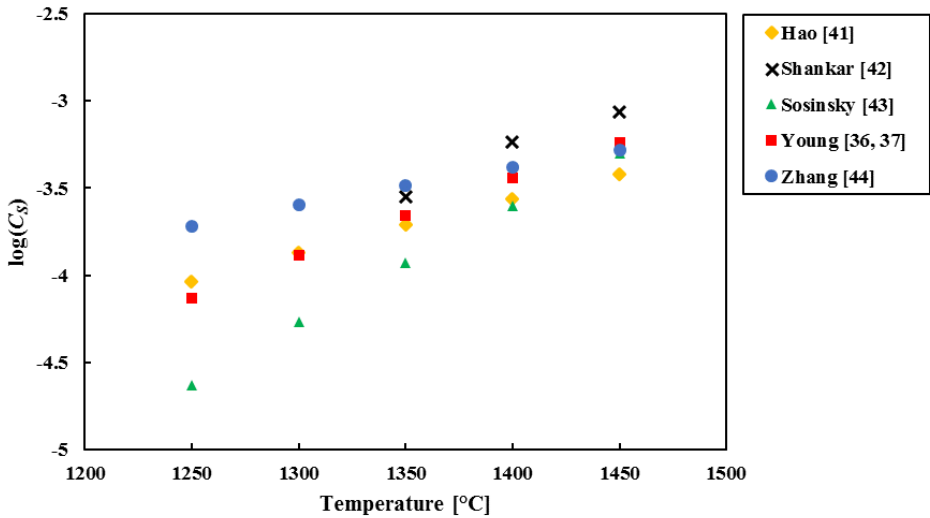


Figure 3.2: Comparison of C_S determined by the models from Table 3.3, for different temperatures.

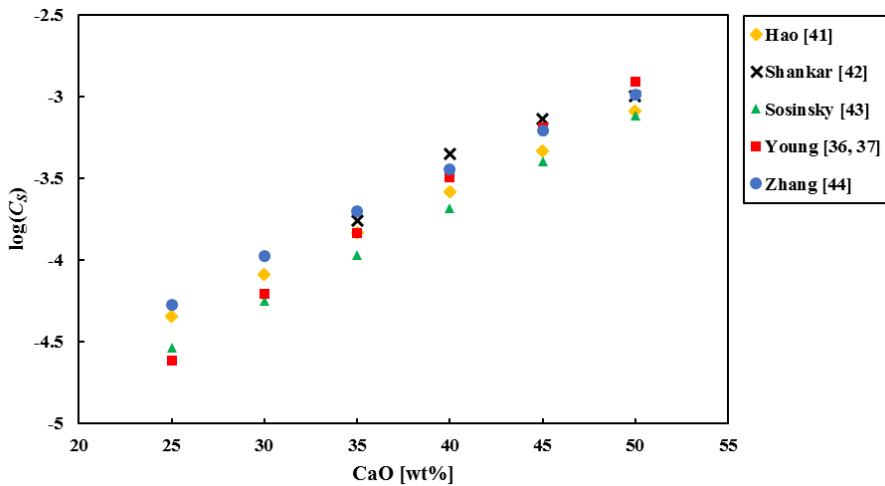


Figure 3.3: Comparison of C_S determined by the models from Table 3.3, for different CaO concentrations at 1400 °C.

Although the different models give different outcomes for a typical simplified HMD slag, the $\log(C_S)$ value ranges from -3 to -5, also when the temperature or

the CaO content is changed within relevant ranges. Condo *et al.* [49] measured C_S for synthetic typical BF slags, which are comparable to HMD slags in composition, temperature and p_{O_2} , and they also found $\log(C_S)$ values around -4.

3.2.3 C_S in an industrial HMD

To understand the significance of C_S for the HMD process, the apparent C_S is determined for industrial HMD heats. At the industrial HMD process, all sulphur that is removed from the hot metal ends up in the slag. Therefore, when the initial and final sulphur content of the hot metal at the HMD is known and an estimate for the slag weight is made (assuming 1 500 kg carryover slag from the BF for a typical heat size of 300 t), L_S can be calculated for every heat. When assuming typical values for $f_S = 2.5$ and $a_O = 1 \cdot 10^{-4}$, C_S can be calculated for every heat with Equation 3.6. Furthermore, the final composition of the slag can be estimated for every heat by assuming an average BF carryover slag composition and adding the injected reagents to that slag, assuming that all removed sulphur in the slag is CaS. Also, a homogeneous slag is assumed.

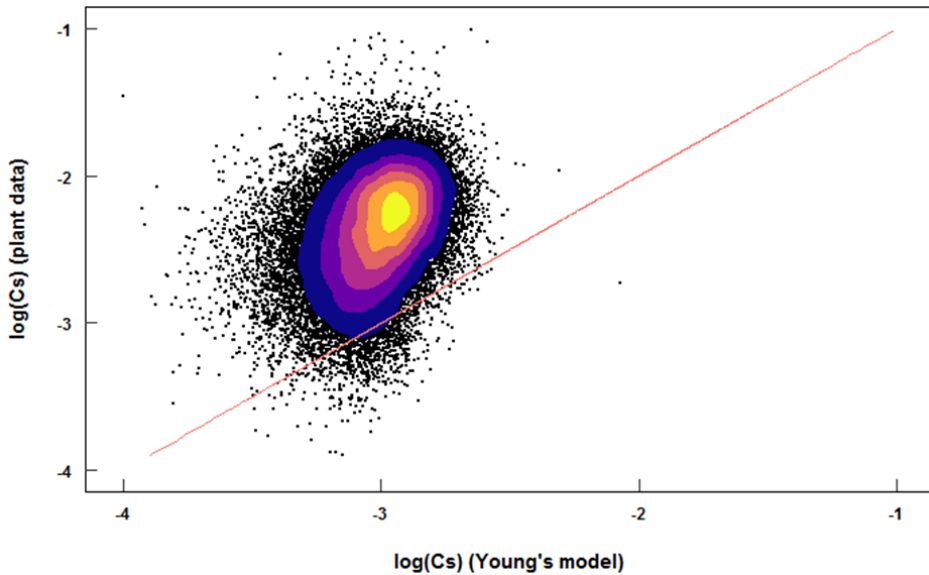


Figure 3.4: Density plot of $\log(C_S)$ values for 47 129 heats at the Tata Steel IJmuiden HMD stations, where the predicted values from Young's model are on the X-axis and the actual values based on removed sulphur are on the Y-axis.

3. Optimal hot metal desulphurisation slag: fundamentals

Figure 3.4 gives the $\log(C_S)$ values of 47 129 HMD heats from Tata Steel, IJmuiden, set against the $\log(C_S)$ values predicted by Young's model (Equation 3.13) based on the slag composition and temperature. The figure shows that C_S from Young's model is roughly a factor 10 off from C_S values based on actual industrial desulphurisation results. The actual amount of sulphides in the slag is higher than the C_S prediction with Young's model, meaning that the actual HMD slag contains almost 10 times more sulphur than the slag could contain based on the equilibrium prediction. Also, there is a large scatter for individual heats in the difference between C_S from Young's model and C_S from plant data. It should be noted that the precision of the method to determine C_S for a single industrial heat is not very high, but that cannot explain the scatter entirely. Furthermore, it should be noted that a_O was estimated at $1 \cdot 10^{-4}$, but that literature mentions typical a_O values between $5 \cdot 10^{-5}$ and $4 \cdot 10^{-4}$. However, only at $a_O = 2 \cdot 10^{-5}$, Young's model accurately predicts desulphurisation at the industrial HMD (the prediction is still not precise though, as the scatter remains). There is no reference in literature of such low a_O values at HMD, so this cannot be used to tune the results. Also by changing the f_s to 13, Young's model can be made in agreement with the plant data results. Kitamura mentions $f_s = 11$ for HMD conditions [15], which would bring Young's model more in agreement with the plant data. Finally, also when replacing Young's model for any of the other models listed in Table 3.4, the results are comparable, meaning that the actual sulphur concentration in the slag is significantly higher than C_S from the model predicts. Therefore, C_S models based on slag composition (translated to A) and temperature only, do not give an accurate or precise prediction of desulphurisation at an industrial HMD.

Most of the desulphurisation in the magnesium-lime co-injection HMD process takes place in the hot metal itself via Reaction 3.1, as this reaction is much faster than Reaction 3.3. The composition of the slag has no influence on the reaction with Mg. Only Reactions 3.2 and 3.3 take place at the hot metal-slag interface (at least for a large part). If Reaction 3.1 is significantly faster than Reaction 3.2, the slag and hot metal will not be at equilibrium. Since almost no MgS can be found in industrial HMD slag [14], all MgS that is formed via Reaction 3.1 will react to CaS via Reaction 3.2 during the HMD process. This can explain why industrial HMD slag contains more sulphur than expected based on C_S . The desulphurisation in the hot metal via Reaction 3.1 and the formation of CaS via

Part II Optimal hot metal desulphurisation slag

Reaction 3.2 are much faster than resulphurisation of the hot metal via a reversed Reaction 3.3. Both the low availability of oxygen in the hot metal and the fact that most CaS is in the solid phase will slow down resulphurisation. Resulphurisation is observed in industry, but this is in the order of magnitude of 1-10 ppm sulphur, even for heats that are delayed (allowing more time for resulphurisation). This means that in industry it takes a long time before an equilibrium between HMD slag and hot metal is established. Furthermore, Magnelöv *et al.* [7] stated that C_S calculated based on A is not applicable for the HMD process, because the HMD slag is not homogeneous and fully liquid.

Using C_S to predict the desulphurisation at an industrial HMD is based on the assumption that the slag and hot metal are at equilibrium and that the slag is fully liquid and homogeneous. However, the slag and hot metal at the end of the HMD process are not at equilibrium and the HMD slag is typically not fully liquid or homogeneous. There is a parallel desulphurisation route in industrial HMD, which is dominant: the desulphurisation by means of magnesium (Reaction 3.1). This explains the difference between model C_S values and plant data.

The plant data shows that for individual heats a C_S prediction can be almost a factor 100 off from the actual desulphurisation. This is because of practical constraints, like measurement errors, slag inhomogeneity and non-dissolved CaS. All these three factors cannot be quantified, but they all contribute in a similar magnitude to the overall variations. Therefore, a C_S prediction model is not sufficiently precise or accurate for industrial use at the HMD process.

3.2.4 Basicity

The sulphur removal capacity, as well as C_S , depend on the basicity of the slag, which depends on the slag composition. Understanding basicity as having a high concentration of free oxygen, which can be replaced by sulphur more easily, helps understanding that slags with a higher basicity will pick up more sulphur and thus help desulphurisation. This explains the large influence of a_O on C_S as well. There is no universal quantitative definition of basicity available. Therefore, different empirical definitions are used today, including optical basicity A (defined by Duffy and Ingram [40]) and the CaO/SiO₂ (known as $B2$) ratio (which can be extended with MgO, Al₂O₃ and P₂O₅), which is commonly used in steel plants [50, 51].

3. Optimal hot metal desulphurisation slag: fundamentals

Although basicity is hard to quantify from a scientific point of view, an empirical definition of the basicity, like B_2 , is sufficient for industrial practice. In a slag with a basicity (B_2) below 0.93, which is equal to a molar ratio $\text{CaO}:\text{SiO}_2$ of 1:1, the CaS formation will be retarded by the lack of free oxygen (O^{2-} ions), which are donated by basic oxides. For completeness MgO (as O^{2-} donator) and Al_2O_3 (which can act as O^{2-} acceptor) should also be taken into consideration [3, 34, 50]. Above this minimum slag basicity, there should be enough CaO, stoichiometrically, to react with the MgS, according to Reaction 3.2 (MgS reacting to CaS). Only kinetics (like undissolved lime not being in contact with the hot metal, for example the core of a lime particle [2]) will hamper this reaction. Therefore, in industry some extra lime will be needed on top of the lime required to bring the B_2 above 0.93 and the lime required for Reaction 3.2. How much extra lime is required is difficult to quantify on a theoretical basis. Li *et al.* [52] suggest a minimum B_2 of 1.1, based on industrial experience.

3.3 Iron loss

3.3.1 Types of iron loss

The definition of iron losses during the HMD process is the amount of Fe that is (unwantedly) removed during the HMD process (mostly during the skimming). Iron losses can mount up to 0.5-2.5% of the total hot metal weight. The total iron losses depend on the ladle size and geometry, larger ladles typically lead to lower iron losses, but also on the slag conditions and the skimming skills of the operator [5–10, 22, 52, 53]. It is hard though to have an accurate number for iron losses (via slag), since the iron distribution in the slag is not homogeneous, so a sample will not give an accurate value [22, 53]. Also determining the iron loss by measuring the weight difference before and after skimming is inaccurate by a few hundred kilograms (approximately 5 wt% of the slag), as the amount of BF carryover slag that was present is unknown and the weight measurements themselves are inaccurate, which makes an accurate mass balance under industrial conditions not possible. There are different types of iron losses:

- Colloid loss: iron droplets entrapped in the slag in colloidal form (like an emulsion) and removed together with the slag (see Figure 3.5).
- Entrainment loss: iron entrained with the slag during skimming (see Figure 3.5).

Part II Optimal hot metal desulphurisation slag

- Dust loss: iron that leaves the system as dust.
- Skull formation: iron that solidifies at the ladle rim or skimmer paddle and forms skull.
- Chemical loss: iron that reacts and ends up in the slag.

Of these types colloid loss and entrainment loss are the most important. Together they cover > 95 % of the total iron loss. SEM analysis of industrial HMD slag, done by Yang *et al.* [53, 54], shows both small (< 0.5 mm) round iron droplets, typical for colloid loss, and large (> 0.5 mm) irregular shaped iron, typical for entrainment loss. The total amount of iron of both droplet types is in the same order of magnitude. Although this method makes it difficult to exactly quantify the size of colloid loss and entrainment loss, it does prove that both types of iron loss are of comparable size.

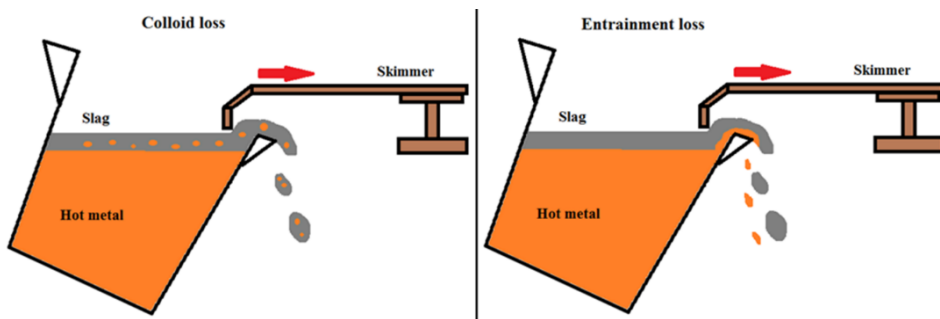


Figure 3.5: Schematic representation of colloid loss (left) and entrainment loss (right) during skimming in the HMD process [6].

Colloid loss (also referred to as emulsion loss) is the most frequently described type of iron loss in HMD. According to literature [6–10, 53–56] different factors (in terms of slag chemistry) contribute to the colloid loss:

- Viscosity of the slag: a higher viscosity leads to higher iron losses.
- Solid fraction: more solids in the slag lead to higher iron losses. A higher solid fraction also increases the slag's viscosity.
- Particle size and shape of the solids in the slag: bigger and variable sized particles lead to higher iron losses.
- Interfacial tension and wettability: a lower interfacial tension between slag and iron leads to higher iron losses.

3. Optimal hot metal desulphurisation slag: fundamentals

- Iron droplet size: smaller iron droplets lead to higher iron losses

Entrainment loss is difficult to measure. Even if the total iron loss could be measured accurately, it is difficult to distinguish clearly between entrainment loss and colloid loss afterwards. Operators claim that the more viscous and sticky a slag is, and the more solid pieces it contains, the easier it is to skim. They estimate lower entrainment losses under these conditions. However, plant data shows that iron losses increase at higher viscosities. It seems that the increased colloid losses have a larger effect on the total iron losses than the decreased entrainment losses when the slag is more viscous. In industry, entrainment loss is often minimised by mechanical improvements, like increasing the accuracy of the skimmer control or cleaning the skimmer paddle more often, or by operator training, rather than changing the slag properties.

Slag properties will not have major influence on **dust loss** and **skull formation**. Samples at the dust filters of the HMD station show that typically 0.01 % of the iron is lost via the dust (10-30 kg per heat). Skull formation is estimated to be 5-10 kg per heat. Both dust loss and skull formation contribute only little to the total iron losses.

Chemical loss is a hypothetical type of iron loss. It is possible that Fe from the hot metal reacts, most likely with oxygen, and ends up in the slag. Although most iron in the slag is in its metallic form, there is also FeO_x present. From the FeO_x in the slag it is impossible to determine when and how it was formed, as BF carryover slag already contains some FeO_x . Based on the low amount of FeO_x in the HMD slag (typically 1-3 wt%) and the small exposure of the hot metal to oxygen, it is expected that the contribution of chemical loss to the total iron loss is negligible. Besides, the only way to prevent oxygen from the air to react with the hot metal would be to keep the it constantly under inert conditions, which is not a viable solution in industry.

3.3.2 Iron droplets

Changing the slag viscosity has a larger influence on the colloid loss than on the entrainment loss. Therefore, when trying to influence the iron losses via the slag properties, which is the scope of this research, the focus should be on the colloid loss. The iron droplets, present in the slag in colloidal form, do not have a uniform

Part II Optimal hot metal desulphurisation slag

size and shape. Their size and shape depends on the way the droplets are formed. Two mechanisms of how iron droplets are formed are described in literature (see Figure 3.6). In mechanism I, droplets are formed by iron being entrained by N_2 and Mg gas into the slag, where they will get a regular round or oval shape to minimise the surface area. In mechanism II droplets are formed by iron being splashed through the open eye on top of the slag, where it solidifies in an irregular shape [9, 53, 54]. Han and Holappa [57] showed with hot metal experiments that droplets formed via mechanism I are not spherical, but irregularly shaped (in the experiments most droplets had a diameter, $d_{drop} < 10 \mu m$). The droplets do become spherical when solidifying. Besides, they define two separate mechanisms within mechanism I: film entrainment and bubble entrainment of the iron.

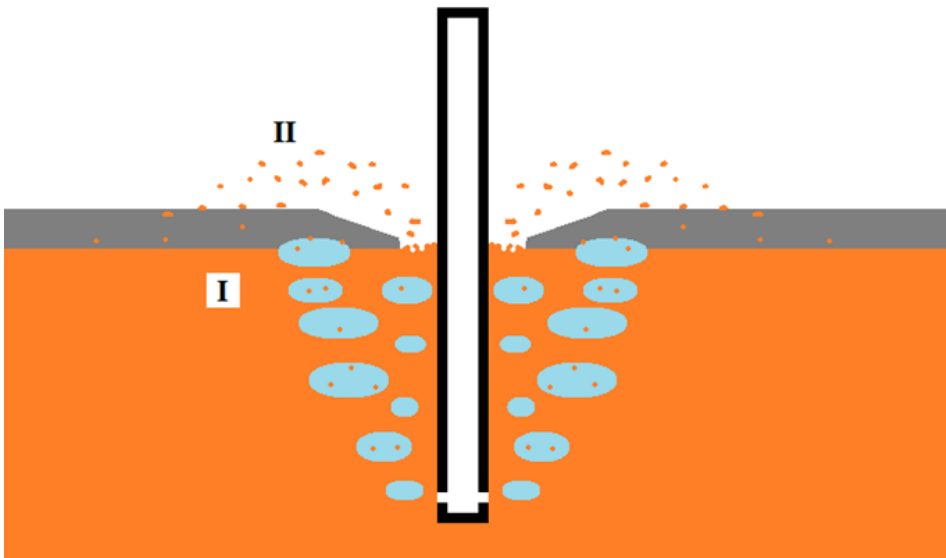


Figure 3.6: Schematic representation of iron droplet formation mechanisms at HMD. Mechanism I shows droplets entrained by gas bubbles; mechanism II shows droplets launched from the slag eye on top of the slag.

Yang *et al.* [53] found that when the injection process lasts longer, more iron ends up in the slag via mechanism I (there is an almost linear relationship), while the amount of iron in the slag via mechanism II hardly depends on the injection time at all. This is in contradiction with what Visser [14] suggested, that iron in the slag builds up over time via mechanism II. However, Visser did not consider

mechanism I as a significant source of iron and did not investigate both mechanisms. Yang and Visser agree that the total amount of iron in the slag does increase when the injection process lasts longer.

3.3.3 Viscosity of the slag

It is generally accepted that a lower apparent slag viscosity (η_{slag}) leads to lower colloid losses, which usually also leads to lower overall iron losses. Figure 3.7 shows the estimated iron loss per heat (300 t) for 47 109 heats at the HMD stations at Tata Steel, IJmuiden, for the estimated η_{slag} .

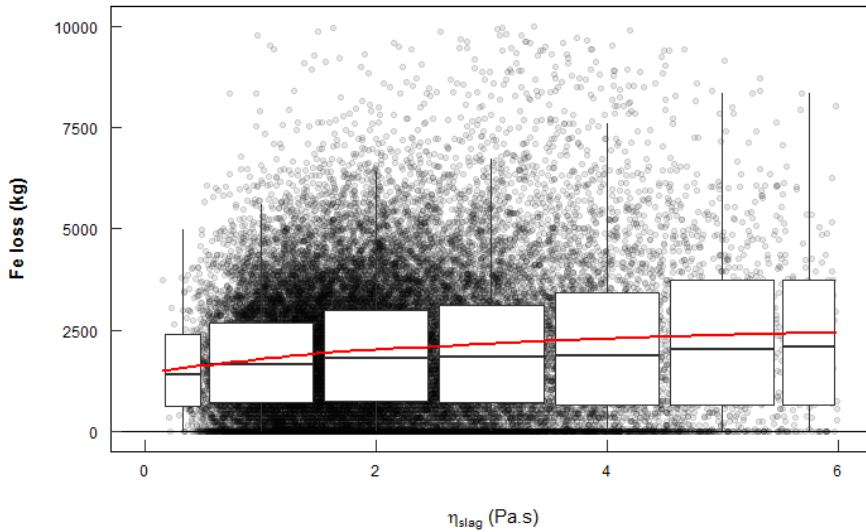


Figure 3.7: Iron loss at different η_{slag} at Tata Steel in IJmuiden. Circles show the individual heats. The boxes stretch from the 25th till the 75th percentile of the distribution. The lines (whiskers) extend to 1.5 times the interquartile range. In red a polynomial trendline.

The η_{slag} (in Pa·s) is estimated based on the Einstein-Roscoe equation [58] (Equation 3.15), which can be used to determine η_{slag} for slags.

$$\eta_{slag} = \eta_0 \cdot (1 - \varphi_{s,slag} \cdot \alpha)^{-n} \quad (3.15)$$

Here η_0 is the viscosity of the liquid part of the slag, $\varphi_{s,slag}$ is the volume fraction of solids in the slag, α and n are empirical constants. Assuming that the solid

Part II Optimal hot metal desulphurisation slag

particles are spherical and of uniform size, typically $\alpha = 0.8$ and $n = 2.5$ (these values vary with temperature).

To determine η_0 and $\varphi_{s,slag}$, simplified equations, based on FactSage calculations, were used. These equations depend on temperature and on the fractions of the major slag components (CaO, SiO₂, Al₂O₃, MgO and CaS), where the temperature has the largest influence on both η_0 and $\varphi_{s,slag}$. The slag composition is estimated by taking an average BF carryover slag composition and adding the injected reagents and removed sulphur, assuming that all sulphur becomes CaS and all Mg becomes MgO. The iron loss is estimated by doing a mass balance over every heat, measuring the ladle weight before and after the HMD process and estimating the BF carryover slag (typically 1500 kg) and the amount of slag that remains in the ladle after skimming (typically 500 kg). The method to estimate η_{slag} and iron loss is inaccurate. Estimating viscosities of industrial slags always leads to large errors, typically $> \pm 30\%$ [59]. However, the large amount of data (47 109 heats) makes the trend reliable. It is clear that a higher η_{slag} leads to higher iron losses.

With the help of Stoke's law (Equation 3.16) the influence of η_{slag} on the time an iron droplet needs to settle back from the slag into the metal bath, can be estimated [14, 55].

$$v_{drop} = \frac{g \cdot d_{drop}^2 \cdot (\rho_{HM} - \rho_{slag})}{18 \cdot \eta_{slag}} \quad (3.16)$$

Here v_{drop} is the settling speed (m/s) of the iron droplet, d_{drop} is the droplet's diameter (m), g is the gravity constant (9.81 m·s⁻²) and ρ_X is the density of hot metal (HM) or slag (kg·m⁻³). Typically, ρ_{HM} is 7000 kg·m⁻³, ρ_{slag} is around 2700 kg·m⁻³, iron droplets in the slag have diameters between 0.01-10 mm and η_{slag} can vary between 0.9-20 Pa·s [14]. For $d_{drop} > 0.1$ mm, v_{drop} can better be determined with the Hadamard–Rybczynski equation, which neglects the surface tension of the droplet [55]:

$$v_{drop} = \frac{g \cdot d_{drop}^2 \cdot (\rho_{HM} - \rho_{slag})}{12 \cdot \eta_{slag}} \quad (3.17)$$

3. Optimal hot metal desulphurisation slag: fundamentals

Figure 3.8 shows the influence of η_{slag} on the settling time (t_{settle}) of iron droplets with a d_{drop} of 0.01-10 mm in a slag with a thickness (h_{slag}) of 10 cm, which is typical for HMD slag [14, 53, 54]. Equations 3.16 and 3.17 were used to determine v_{drop} .

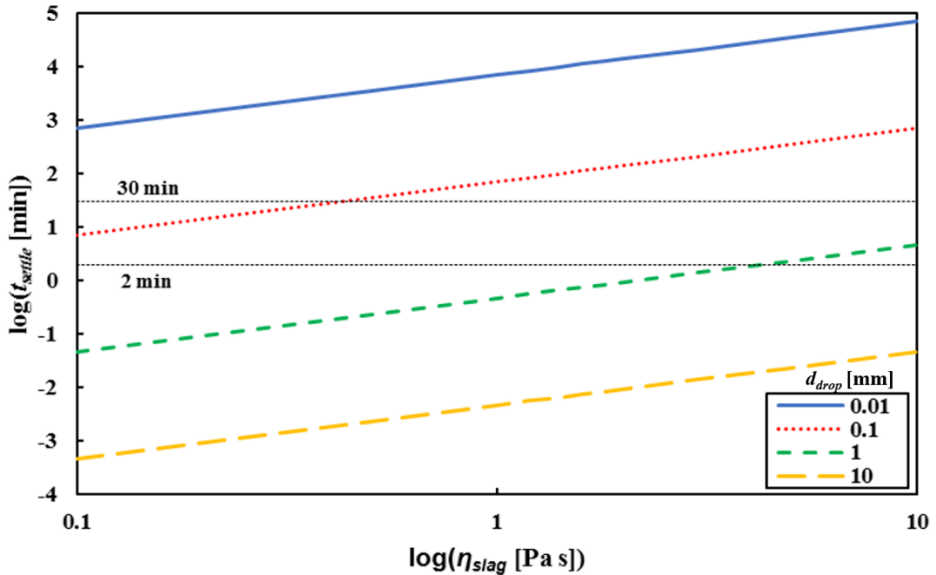


Figure 3.8: The influence of η_{slag} on t_{settle} for different d_{drop} (ranging from 0.01-10 mm) with $h_{slag} = 10$ cm.

Under industrial conditions, the minimum time between stop reagent injection and start skimming is 2 min (lance lifting, sampling and ladle tilting). Droplets that settle in less than 2 min will therefore never be skimmed off. Under normal conditions, the maximum time between the start of reagent injection and the end of skimming is 30 min. Droplets that take more than 30 min to settle will always be removed together with the slag, if they start on top of the slag. For droplets with a settling time between 2 and 30 min, it depends on the moment they ended up in the slag and on the moment when the skimming starts, whether they are skimmed off or not. Note that the mentioned settling times are valid for a droplet that starts on top of the slag; for droplets that end up in the slag via mechanism I and start at a lower point in the slag, different settling times apply. In this simplified model, the extra friction for droplets that are not spherical, as well as

the surface tension a droplet has to overcome when it lands on top of the slag, has been neglected.

Nevertheless Figure 3.8 shows that, regardless of the circumstances, droplets with $d_{drop} > 2$ mm will always settle before skimming starts. Droplets with $d_{drop} < 0.5$ mm will never settle in time. This means that by optimising η_{slag} and the allowed t_{settle} , within industrial boundaries, only the droplets between 0.5-2 mm can be retrieved.

Temperature has the largest influence on η_{slag} , but the temperature is already maximised in most steel plants, to save energy and to allow more scrap addition in the converter. Slag composition also influences η_{slag} , although the impact is lower. Different slag components will influence η_{slag} , according to Einstein-Roscoe, by changing the liquidus temperature (T_{liq}) and thus $\varphi_{s,slag}$, or by changing η_0 . The influence of many slag components on T_{liq} and η_0 has been studied by many authors before. Table 3.3 gives an overview of the influence of the most common slag components on T_{liq} and η_0 under typical HMD conditions. As the influence of slag composition on T_{liq} and η_0 is complex, the given directions in the table are not universal.

Table 3.3: Influence of different slag components on T_{liq} and η_0 , under typical HMD conditions.

Component	T_{liq}	η_0	Source	Comment
CaO	▲▲	▼	[10, 20, 60, 61]	η_{slag} will go up with CaO
SiO ₂	▼	▲	[20, 52, 60]	
Al ₂ O ₃	▼	▼	[19, 60, 62]	Below 10 % η_0 ▲ [19]
MgO	▲▲	▼	[20, 52, 60, 62]	
TiO ₂	▼	▼	[20, 48, 63]	
Na ₂ O	▼	▼	[20, 48, 52, 60]	Below 3 % T_{liq} ▲ [60]
K ₂ O	▼	▼	[20, 49, 60]	
MnO	▼	▼	[20]	
CaF ₂	▼▼	▼	[6, 20, 49, 56]	
CaCl ₂	▼	▼	[62]	
FeO _x	▼	▼	[19, 20]	
Temperature	na	▼▼	[20]	

3. Optimal hot metal desulphurisation slag: fundamentals

Although many components are able to lower T_{liq} and η_0 of the slag, some of them have disadvantages that make them unwanted or restricted for an optimal slag. Halogen-based components (CaF_2 , CaCl_2) are harmful for human health and environment. Besides, fluoride-based components lower the desulphurisation efficiency of magnesium [6]. Adding too much alkali metal oxides (Na_2O and K_2O), will make the slag less suitable for recycling at the BF, as alkali metals tend to recirculate inside the BF due to their low boiling point, which leads to an unwanted build-up of these elements [16, 17]. Furthermore, TiO_2 leads to Ti(C,N) formation. Ti(C,N) particles form a layer between the slag and hot metal and make the slag sticky, resulting in higher iron losses [14, 64]. Finally, the fact that SiO_2 lowers T_{liq} , but increases η_0 , while CaO does the opposite, explains some typical misunderstandings in steelmaking regarding the influence of basicity on η_{slag} . Einstein-Roscoe's equation (Equation 3.15) shows that for lower temperatures, where part of the slag is solid, lowering the solid fraction by lowering T_{liq} , lowers η_{slag} . At higher temperatures, where the slag is fully liquid, only lowering η_0 will lower η_{slag} . In secondary metallurgy, slag temperatures are high ($> 1500\text{ }^\circ\text{C}$) and the slags are usually liquid. Under these conditions a higher basicity decreases η_{slag} . As HMD slag has lower temperatures, typically part of the slag is solid, so a lower basicity (more SiO_2) decreases η_{slag} .

3.3.4 Solid fraction of the slag

It is generally accepted that a lower solid fraction of the slag leads to lower iron losses. Although a fully liquid slag will lead to increased entrainment losses, the decrease in colloid losses will more than make up for that. Industrial data showed that higher temperatures, resulting in a higher liquid fraction of the slag, lead to lower overall iron losses [10]. It should be noted that a substantial amount of the CaS will not dissolve in the HMD slag and, as it has a melting point of $2525\text{ }^\circ\text{C}$, will remain as a solid in the slag.

As the HMD slag is not a homogeneous single phase, the slag will not have a single melting point. Therefore, typically part of the slag is solid, while another part is liquid. The larger the liquid part of the slag is, the lower the iron losses are [11, 14, 52]. In order to better understand the influence of the slag composition on the liquid fraction of the slag, the slag can be viewed as if it is homogeneous. With the thermodynamic software FactSage, using a private database [13, 20], a

Part II Optimal hot metal desulphurisation slag

ternary diagram is made to show T_{liq} for CaO-SiO₂-Al₂O₃ slag with 10 wt% MgO (typical for HMD slags), which is shown in Figure 3.9.

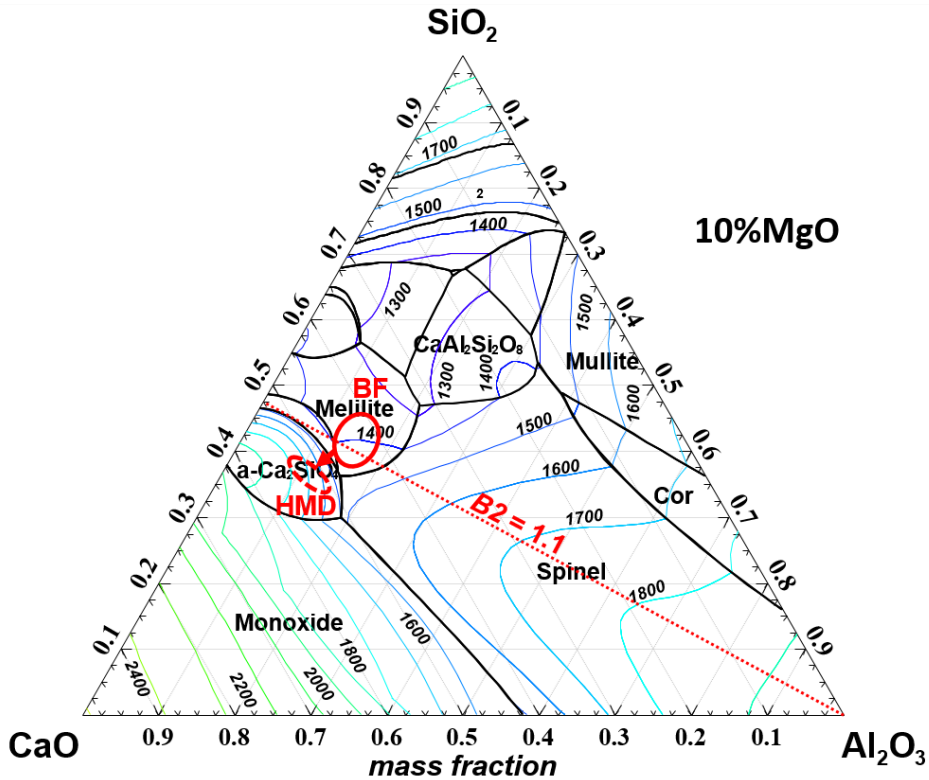


Figure 3.9: Liquidus projection of CaO-SiO₂-Al₂O₃ slag with 10 wt% MgO, determined with FactSage. The lines indicate T_{liq} (°C). Typical composition ranges for BF carryover slag (“BF” solid line) and final HMD slag (“HMD” dashed line) are encircled in the diagram. The dotted line indicates where $B2 = 1.1$.

It should be noted that the other slag components all lower T_{liq} , as can be seen in Table 3.3. Therefore at the BF and HMD the actual T_{liq} will be lower than expected based on Figure 3.9. When keeping the HMD slag composition range from Table 3.2 in mind, it is clear that lowering the slag’s basicity, so adding more SiO₂ and Al₂O₃, would lower T_{liq} of the slag. It is remarkable that the composition of BF carryover slag is closer to the ‘sweet spot’ with the lowest T_{liq} than the HMD slag composition after injection. This is due to the fact that at the BF a liquid slag is favourable and therefore a control target [16, 17]. During

3. Optimal hot metal desulphurisation slag: fundamentals

the HMD process effectively MgO (via Reactions 3.1 and 3.2) and CaO, which both increase T_{liq} , are added to the slag.

In literature MgO, CaO/SiO₂ (B_2) and Al₂O₃ (together with FeO_x) are identified as the components with the largest influence on T_{liq} of HMD slag [52, 60, 62]. Li *et al.* [60] suggest that for a mostly liquid HMD slag MgO should be < 10 wt% and Al₂O₃ should be 12-16 wt%. The composition range of a typical HMD slag (Table 3.2) shows that in practice MgO should be as low as possible, while Al₂O₃ should be increased.

Apart from the slag's solid fraction, it has been suggested that the size and shape of the solid particles themselves influence the iron losses as well. Larger and more irregularly shaped slag particles will hamper the settling of the iron droplets in the slag. Magnelöv *et al.* [7, 8, 11] showed that addition of the slag modifier nepheline syenite makes the HMD slag look more "fine-grained" during the HMD process and that this slag was easier to skim. Also cold samples from that slag, after skimming, showed a finer-grained slag compared to the reference slag, with a comparable composition. However, they could not prove that this finer-grained slag actually led to lower iron losses.

3.3.5 Interfacial tension

Interfacial tension is another factor which can influence the iron losses. When the interfacial tension between the slag and the hot metal droplet decreases, it will lead to more friction when metal droplets descend through the slag layer. Therefore, it is expected that a lower interfacial tension will lead to higher iron losses. Interfacial tensions between slag and hot metal are difficult to measure, as slag and hot metal tend to react, thus changing the initial compositions. In general the effect of dissolved elements on the interfacial tension is known [65].

The composition of the hot metal has a larger effect on the interfacial tension than the composition of the slag. Sulphur and oxygen, being surface active elements, have the largest influence on the interfacial tension. More oxygen or sulphur in the hot metal lead to lower interfacial tensions [65]. Therefore, to lower iron losses, the oxygen and sulphur concentration in hot metal should be as low as possible. Given the purpose of the HMD process, the sulphur and oxygen are always kept as low as possible, regardless their effect on the interfacial tension.

Part II Optimal hot metal desulphurisation slag

Of the elements that lower the interfacial tension of the hot metal, titanium has the largest influence. However, even though a higher titanium content of the hot metal leads to increased iron losses, the effect of the interfacial tension seems to be negligible. The increased iron losses are mostly attributed to the Ti(C,N) formation.

From all typical slag components, FeO and MnO have the largest influence on the interfacial tension. Under HMD conditions, FeO will reduce to Fe and [O], leading to an increased oxygen concentration in the hot metal, which leads to the lower interfacial tension. MnO will react with Fe to form [Mn] and FeO, which on its turn leads to Fe and [O]. Also the effect of other oxides in the slag on the interfacial tension depends on their ability to supply oxygen to the hot metal [65].

Because only little research was done about the effect of interfacial tension on iron losses, as it is difficult to measure [66], there are no reliable figures available on the influence of interfacial tension on iron losses and it is hard to isolate their effect. In general, interfacial tension is not considered as a major factor for iron losses, as iron losses can be explained without it. Furthermore, elements that have the highest influence on the interfacial tension, sulphur and oxygen, are already kept as low as possible in the HMD process. More exotic elements that increase the interfacial tension, like tungsten, are too expensive to use in industry. Therefore, to find the optimal HMD slag, interfacial tension is not taken into account in this study.

3.4 Optimal slag

The optimal HMD slag should be able to contain sufficient sulphur, while leading to the lowest possible iron losses. Under industrial conditions, the sulphur removal capacity of the slag cannot accurately be predicted by its sulphide capacity (C_S), as the HMD slag is inhomogeneous, often partly solid and not at equilibrium with the hot metal. Furthermore, the parallel desulphurisation by means of magnesium is dominant in industrial HMD, but is not described by C_S . However, C_S can be used to indicate the sulphur removal capacity of the liquid fraction of an HMD slag at equilibrium. CaO is the most important component in the slag, regarding sulphur removal capacity. There should be enough CaO to react with the sulphur and, based on industrial experience, $B2$ (CaO/SiO_2) > 1.1.

3. Optimal hot metal desulphurisation slag: fundamentals

To minimise the iron losses with an optimal HMD slag, the focus should be on minimising the colloid losses by lowering η_{slag} . As η_{slag} has an adverse effect on colloid loss and entrainment loss, the focus in industry should be on the colloid loss. At the same time, entrainment loss can be limited by taking other measures like improving skimming skills of operators, improving skimming control or by skimming automation. To lower η_{slag} , both η_0 and $\varphi_{s,slag}$ should be lowered. This can best be done by minimising the MgO content of the slag, preferably < 10 wt%, and increasing the slag's Al₂O₃ content, preferably 12-16 wt%. Furthermore, other slag components that lower the η_0 and $\varphi_{s,slag}$, like Na₂O, K₂O and MnO are desirable, keeping in mind that their use can be limited because of other process requirements. The amount of TiO₂ in the slag should be minimised and is ideally 0. For the optimal HMD slag, a $B2$ of 1.1 is required, to allow the sulphur removal.

For industry this means that the addition of reagents should be optimised, not only from a desulphurisation point of view, but also to create an optimal slag. Furthermore, a slag modifier could help to further optimise η_{slag} , and thus minimise iron losses.

3.5 Conclusions

Based on the fundamentals of hot metal desulphurisation (HMD) slag and industrial data, the following concluding remarks can be made.

- The sulphide capacity (C_S), as defined by Fincham and Richardson [4], is not applicable for direct industrial use, as the industrial slag is inhomogeneous and not at equilibrium.
- For a sufficient sulphur removal capacity of the slag, the slag should contain at least enough CaO to allow all MgS to react with CaO to form CaS. Besides, a minimal CaO:SiO₂ weight ratio ($B2$) in the slag of 1.1 is required.
- A lower apparent viscosity of the slag leads to lower overall iron losses.
- Optimising the HMD slag conditions has a higher impact on colloid losses than on entrainment losses. Therefore, in industry, the focus should be on lowering the colloid losses.

- Under industrial circumstances, MgO concentration in the HMD slag should be as low as possible and preferably < 10 wt%. Al₂O₃ should preferably be 12-16 wt%.

These remarks on the optimal HMD slag, considering sulphur removal capacity and iron losses, will be evaluated in Chapter 4.

3.6 References

- [1] G. Agricola, *De Re Metallica*. Basel (CH), 1556.
- [2] F.N.H. Schrama, E.M. Beunder, B. van den Berg, Y. Yang, and R. Boom, “Sulphur removal in ironmaking and oxygen steelmaking,” *Ironmak. Steelmak.*, vol. 44, no. 5, pp. 333–343, 2017, doi: 10.1080/03019233.2017.1303914.
- [3] B. Deo and R. Boom, *Fundamentals of Steelmaking Metallurgy*, 1st ed. Hemel Hempstead (UK): Prentice-Hall, 1993.
- [4] C.J.B. Fincham and F.D. Richardson, “The behaviour of sulphur in silicate and aluminate melts,” *Proc. R. Soc. London*, vol. 223, no. A, pp. 40–62, 1954, doi: <https://doi.org/10.1098/rspa.1954.0099>.
- [5] F.N.H. Schrama, B. van den Berg, and G. Van Hattum, “A comparison of the leading hot metal desulphurization methods,” in *Proceedings of the 6th International Congress on the Science and Technology of Steelmaking*, 2015, pp. 61–66.
- [6] F.N.H. Schrama *et al.*, “Lowering iron losses during slag removal in hot metal desulphurisation without using fluoride,” *Ironmak. Steelmak.*, vol. 47, no. 5, pp. 464–472, 2020, doi: 10.1080/03019233.2020.1747778.
- [7] M. Magnelöv, J. Eriksson, J. Drugge, J. Björkvall, and B. Björkman, “Investigation of iron losses during desulphurisation of hot metal utilising nepheline syenite,” *Ironmak. Steelmak.*, vol. 40, no. 6, pp. 436–442, 2013, doi: 10.1179/1743281212Y.0000000067.
- [8] M. Magnelöv, A. Carlsson-Dahlberg, L. Gustavsson, J. Björkvall, and B. Björkman, “Iron losses during desulphurisation of hot metal utilising co-injection of Mg and CaC₂ combined with nepheline syenite,” *Ironmak. Steelmak.*, vol. 42, no. 7, pp. 525–532, 2015, doi: 10.1179/1743281214Y.0000000257.
- [9] A.F. Yang, A. Karasev, and P.G. Jönsson, “Effect of Nepheline Syenite

3. Optimal hot metal desulphurisation slag: fundamentals

- on Iron Losses in Slags during Desulphurization of Hot Metal,” *Steel Res. Int.*, vol. 87, no. 5, pp. 599–607, 2016, doi: 10.1002/srin.201500154.
- [10] F.N.H. Schrama *et al.*, “Slag optimisation considering iron loss and sulphide capacity in hot metal desulphurisation,” in *Proceedings of the 7th International Congress on the Science and Technology of Steelmaking*, 2018, p. ICS131.
- [11] M. Magnelöv, “Iron Losses During Desulphurisation of Hot Metal,” (PhD thesis) Luleå University of Technology, Luleå (SE), 2014.
- [12] F.N.H. Schrama *et al.*, “Optimal hot metal desulphurisation slag considering iron loss and sulphur removal capacity part II: Evaluation,” *Ironmak. Steelmak.*, vol. 48, no. 1, pp. 14–24, 2021.
- [13] C.W. Bale *et al.*, “FactSage thermochemical software and databases, 2010-2016,” *Calphad Comput. Coupling Phase Diagrams Thermochem.*, vol. 54, pp. 35–53, 2016, doi: 10.1016/j.calphad.2016.05.002.
- [14] H.-J. Visser, “Modelling of injection processes in ladle metallurgy,” (PhD thesis) Delft University of Technology, Delft (NL), 2016.
- [15] S. Kitamura, “Hot Metal Pretreatment,” in *Treatise on Process Metallurgy*, vol. 3, S. Seetharaman, Ed. Oxford (UK): Elsevier, 2014, pp. 177–221.
- [16] Y. Yang, K. Raipala, and L. Holappa, “Ironmaking,” in *Treatise on Process Metallurgy*, vol. 3, S. Seetharaman, Ed. Oxford (UK): Elsevier, 2014, pp. 2–88.
- [17] M. Geerdes, R. Chaigneau, I. Kurunov, O. Lingiard, and J. Ricketts, *Modern Blast Furnace Ironmaking*, 3rd ed. Delft (NL): IOS Press, 2015.
- [18] L. Holappa, *Secondary Steelmaking*, 1st ed., vol. 3. Oxford (UK): Elsevier Ltd., 2014.
- [19] G. Zhang, N. Wang, M. Chen, and H. Li, “Viscosity and Structure of CaO–SiO₂–FeO–Al₂O₃–MgO System during Iron-Extracting Process from Nickel Slag by Aluminum Dross. Part 1: Coupling Effect of FeO and Al₂O₃,” *Steel Res. Int.*, vol. 89, p. 1800272, 2018, doi: 10.1002/srin.201800272.
- [20] CRCT (Canada) & GTT (Germany), “FactSage 7.3,” 2020. [Online]. Available: www.factsage.com.

- [21] D.J. Gavel, “Shifting the limits of nut coke use in the ironmaking blast furnace,” (PhD thesis) Delft University of Technology, Delft (NL), 2020.
- [22] A. Freißmuth, *Die Entschwefelung von Roheisen*, 1st ed. Tisnov (CZ): Almamet GmbH, 2004.
- [23] D. Janke, “Metallurgische Sensortechnik,” in *Electrochemische Sauerstoffmessung in der Metallurgie*, 1st ed., Verein Deutscher Eisenhüttenleute (VDEh), Ed. Düsseldorf (DE): Verlag Stahleisen, 1985, p. S 216-22.
- [24] E. Moosavi-Khoonsari and I.H. Jung, “Thermodynamic Modeling of Sulfide Capacity of Na₂O-Containing Oxide Melts,” *Metall. Mater. Trans. B*, vol. 47, no. 5, pp. 2875–2888, 2016, doi: 10.1007/s11663-016-0749-z.
- [25] M. Hino, S. Kitagawa, and S. Ban-ya, “Sulphide Capacities of CaO-Al₂O₃-SiO₂ and CaO-Al₂O₃-MgO Slags,” *ISIJ Int.*, vol. 33, no. 1, pp. 36–42, 1993.
- [26] S.K. Panda, E. Harbers, A. Overbosch, and R. Kooter, “Desulphurization with Ladle Furnace Slag,” in *Proceedings of METEC & 4th ESTAD*, 2019, p. P264.
- [27] X. Yang, J. Jiao, R. Ding, C. Shi, and H. Guo, “A thermodynamic model for calculating sulphur distribution ratio between CaO-SiO₂-MgO-Al₂O₃ ironmaking slags and carbon saturated hot metal based on the Ion and molecule coexistence theory,” *ISIJ Int.*, vol. 49, no. 12, pp. 1828–1837, 2009, doi: 10.2355/isijinternational.49.1828.
- [28] C.-B. Shi, X.-M. Yang, J.-S. Jiao, C. Li, and H.-J. Guo, “A sulphide capacity prediction model of CaO-SiO₂-MgO-Al₂O₃ ironmaking slags based on the ion and molecule coexistence theory,” *ISIJ Int.*, vol. 50, no. 10, pp. 1362–1372, 2010, doi: 10.2355/isijinternational.50.1362.
- [29] A. Ender, H. Van Den Boom, H. Kwast, and H.-U. Lindenberg, “Metallurgical development in steel-plant-internal multi-injection hot metal desulphurisation,” *Steel Res. Int.*, vol. 76, no. 8, pp. 562–572, 2005.
- [30] Y. Zhao and G.A. Irons, “The role of oxygen in hot metal desulphurization with calcium carbide,” in *Scaninject V - part II*, 1989, pp. 63–81.
- [31] F. Mampaey, D. Habets, J. Plessers, and F. Seutens, “On line oxygen activity measurements to determine optimal graphite form during compacted graphite iron production,” *Int. J. Met.*, vol. 4, no. 2, pp. 25–43,

3. Optimal hot metal desulphurisation slag: fundamentals

2010.

- [32] F. Mampaey, D. Habets, and F. Seutens, “The use of oxygen activity measurement to determine optimal properties of ductile iron during production,” *Int. Foundry Res.*, vol. 60, no. 1, pp. 2–19, 2008.
- [33] F.N.H. Schrama, E.M. Beunder, H.-J. Visser, J. Sietsma, R. Boom, and Y. Yang, “The Hampering Effect of Precipitated Carbon on Hot Metal Desulfurization with Magnesium,” *Steel Res. Int.*, vol. 91, no. 11, p. 1900441, 2020, doi: 10.1002/srin.201900441.
- [34] I.H. Jung and E. Moosavi-Khoonsari, “Limitation of Sulfide Capacity Concept for Molten Slags,” *Metall. Mater. Trans. B*, vol. 47, no. 2, pp. 819–823, 2016, doi: 10.1007/s11663-016-0594-0.
- [35] M.A.T. Andersson, P.G. Jönsson, and M. Hallberg, “Optimisation of ladle slag composition by application of sulphide capacity model,” *Ironmak. Steelmak.*, vol. 27, no. 4, pp. 286–293, 2000, doi: 10.1179/030192300677570.
- [36] Y. Taniguchi, N. Sano, and S. Seetharaman, “Sulphide Capacities of CaO–Al₂O₃–SiO₂–MgO–MnO Slags in the Temperature Range 1673–1773 K,” *ISIJ Int.*, vol. 49, no. 2, pp. 156–163, 2009.
- [37] M.M. Nzotta, M. Andreasson, and P. Jo, “A study on the sulphide capacities of steelmaking slags,” *Scand. J. Metall.*, vol. 29, no. 2, pp. 177–184, 2000, doi: 10.1034/j.1600-0692.2000.d01-21.x.
- [38] S. Chatterjee, B. Konar, A. Maity, and K. Chattopadhyay, “Development of Alternative Flux for Liquid Steel Desulfurization,” in *AISTech 2019 — Proceedings of the Iron & Steel Technology Conference*, 2019, pp. 1211–1224, doi: 10.33313/377/123.
- [39] F.N.H. Schrama *et al.*, “Effect of KAlF₄ on the efficiency of hot metal desulphurisation with magnesium,” in *European Oxygen Steelmaking Conference (EOSC)*, 2018, p. EOSC021.
- [40] J.A. Duffy and M.D. Ingram, “Establishment of an optical scale for Lewis basicity in inorganic oxyacids, molten salts, and glasses,” *J. Am. Chem. Soc.*, vol. 93, no. 24, pp. 6448–6454, 1971, doi: 10.1021/ja00753a019.
- [41] R.W. Young, “Use of optical basicity concept for determining phosphorus and sulphur slag–metal partitions,” (EUR 13176 EN) Luxembourg, 1991.
- [42] R.W. Young, J.A. Duffy, G.J. Hassal, and Z. Xu, “Use of the optical

- basicity concept for determining phosphorus and sulphur slag-metal partitions,” *Ironmak. Steelmak.*, vol. 19, no. 3, pp. 201–219, 1992.
- [43] X. Ma, M. Chen, H. Xu, J. Zhu, G. Wang, and B. Zhao, “Sulphide capacity of CaO-SiO₂-Al₂O₃-MgO system relevant to low MgO blast furnace slags,” *ISIJ Int.*, vol. 56, no. 12, pp. 2126–2131, 2016, doi: 10.2355/isijinternational.ISIJINT-2016-274.
- [44] A.F.T. Condo, S. Qifeng, and D. Sichen, “Sulfide Capacities in the Al₂O₃-CaO-MgO-SiO₂ System,” *Steel Res. Int.*, vol. 89, p. 1800061, 2018, doi: 10.1002/srin.201800061.
- [45] X. Hao and X. Wang, “A New Sulfide Capacity Model for CaO-Al₂O₃-SiO₂-MgO Slags Based on Corrected Optical Basicity,” *Steel Res. Int.*, vol. 87, no. 3, pp. 359–363, 2016, doi: 10.1002/srin.201500065.
- [46] A. Shankar, M. Görnerup, A.K. Lahiri, and S. Seetharaman, “Sulfide Capacity of High Alumina Blast Furnace Slags,” *Metall. Mater. Trans. B*, vol. 37B, pp. 941–947, 2006.
- [47] D.J. Sosinsky and J.A. Duffy, “The composition and temperature dependence of the sulfide capacity of metallurgical slags,” *Metall. Mater. Trans. B*, vol. 17, no. 2, pp. 331–337, 1986.
- [48] G.-H. Zhang, K.-C. Chou, and U.B. Pal, “Estimation of Sulfide Capacities of Multicomponent Slags using Optical Basicity,” *ISIJ Int.*, vol. 53, no. 5, pp. 761–767, 2013, doi: 10.2355/isijinternational.53.761.
- [49] A.F.T. Condo, C. Allertz, and D. Sichen, “Experimental determination of sulphide capacities of blast furnace slags with higher MgO contents,” *Ironmak. Steelmak.*, vol. 46, no. 3, pp. 207–210, 2019, doi: 10.1080/03019233.2017.1366089.
- [50] G.A. Brooks, M.M. Hasan, and M.A. Rhamdhani, “Slag Basicity: What Does It Mean?,” in *10th International Symposium on High-Temperature Metallurgical Processing*, 2019, pp. 297–308, doi: 10.1007/978-3-030-05955-2_28.
- [51] E.T. Turkdogan, *Fundamentals of steelmaking*. London (UK): The Institute of Materials, 1996.
- [52] Z. Li, J.W.K. van Boggelen, H. Thomson, G. Parker, and A. Ferguson, “Improved Slag Skimming Performance At Hot Metal Desulphurisation Station By Using Recycled Materials As Slag Modifying Agent,” in *Scanmet IV*, 2012, pp. 189–195.

3. Optimal hot metal desulphurisation slag: fundamentals

- [53] A.F. Yang, A. Karasev, and P.G. Jönsson, “Characterization of Metal Droplets in Slag after Desulfurization of Hot Metal,” *ISIJ Int.*, vol. 55, no. 3, pp. 570–577, 2015, doi: 10.2355/isijinternational.55.570.
- [54] A.F. Yang, A. Karasev, and P.G. Jonsson, “Behavior of metal droplets in slags during desulphurization of hot metal,” in *Proceedings of the 6th International Congress on the Science and Technology of Steelmaking, ICS 2015*, 2015, pp. 80–83.
- [55] P.K. Iwamasa and R.J. Fruehan, “Separation of Metal Droplets from Slag,” *ISIJ Int.*, vol. 36, no. 11, pp. 1319–1327, 1996.
- [56] J. Diao, B. Xie, and S.S. Wang, “Research on slag modifying agents for CaO–Mg based hot metal desulphurisation,” *Ironmak. Steelmak.*, vol. 36, no. 7, pp. 543–547, 2009, doi: 10.1179/174328109X445642.
- [57] Z. Han and L. Holappa, “Mechanisms of Iron Entrainment into Slag due to Rising Gas Bubbles,” *ISIJ Int.*, vol. 43, no. 3, pp. 292–297, 2003, doi: 10.2355/isijinternational.43.292.
- [58] R. Roscoe, “The viscosity of suspension of rigid spheres,” *Br. J. Appl. Phys.*, vol. 3, no. Aug, pp. 267–269, 1952.
- [59] K.C. Mills and S. Sridhar, “Viscosities of ironmaking and steelmaking slags,” *Ironmak. Steelmak.*, vol. 26, no. 4, pp. 262–268, 1999, doi: 10.1179/030192399677121.
- [60] Z. Li, M. Bugdol, and W. Crama, “Optimisation of hot metal desulphurisation slag in the CaO / Mg co-injection process to improve slag skimming performance,” in *Molten2012*, 2012.
- [61] L. Wu, M. Ek, M. Song, and D. Sichen, “The effect of solid particles on liquid viscosity,” *Steel Res. Int.*, vol. 82, no. 4, pp. 388–397, 2011, doi: 10.1002/srin.201000207.
- [62] C. Wang, J. Zhang, K. Jiao, and Z. Liu, “Influence of basicity and MgO/Al₂O₃ ratio on the viscosity of blast furnace slags containing chloride,” *Metall. Res. Technol.*, vol. 114, no. 2, p. 205, 2017, doi: 10.1051/metal/2016064.
- [63] H. Park, J.Y. Park, G.H. Kim, and I. Sohn, “Effect of TiO₂ on the viscosity and slag structure in blast furnace type slags,” *Steel Res. Int.*, vol. 83, no. 2, pp. 150–156, 2012, doi: 10.1002/srin.201100249.
- [64] S. Street, R.P. Stone, and P.J. Koros, “The presence of titanium in hot

Part II Optimal hot metal desulphurisation slag

- metal and its effects on desulfurization,” *Iron Steel Technol.*, vol. 2, no. 11, pp. 65–74, 2005.
- [65] K. Nakashima and K. Mori, “Interfacial Properties of Liquid Iron Alloys and Liquid Slags Relating to Iron- and Steel-making Processes.,” *ISIJ Int.*, vol. 32, no. 1, pp. 11–18, 1992, doi: 10.2355/isijinternational.32.11.
- [66] A.R. Miedema and R. Boom, “Surface Tension and Electron Density of Pure Liquid Metals,” *Zeitschrift fuer Met. Res. Adv. Tech.*, vol. 69, no. 3, pp. 183–190, 1978.

4 Optimal hot metal desulphurisation slag: evaluation

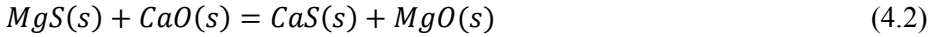
This chapter is based on the following publication:

F.N.H. Schrama, E.M. Beunder, S.K. Panda, H.-J. Visser, A. Hunt, J. Sietsma, R. Boom and Y. Yang, “Optimal hot metal desulphurisation slag considering iron loss and sulphur removal capacity part II: Evaluation”, *Ironmaking and Steelmaking*, Vol. 48, No. 1, **2021**, p 14-24.

As explained in the previous chapter, the optimal hot metal desulphurisation (HMD) slag is defined as a slag with a sufficient sulphur removal capacity and a low apparent viscosity (η_{slag}) which leads to low iron losses. In this chapter, the fundamentals as explained in Chapter 3, are explored by a Monte Carlo simulation, based on thermodynamic calculations with FactSage, plant data analysis and melting point and viscosity measurements of the optimal slag. Furthermore, the applicability of knowing the optimal slag composition for an industrial HMD is discussed.

4.1 Introduction

As discussed in Chapter 2, in the magnesium-lime co-injection hot metal desulphurisation (HMD) process, the main desulphurisation reactions (Reactions 4.1 and 4.2) take place in the hot metal, after which the sulphur is stabilised in the slag [1–3]:



Therefore, the slag and hot metal are not in equilibrium with regard to sulphur distribution, which was validated with plant data [4]. This means that an HMD slag with a sufficient sulphur removal capacity should contain enough lime to react with sulphur (Reactions 4.2 and 4.3) and should have a high enough basicity to allow Reaction 4.2 to proceed. Under industrial circumstances this is a $B2 > 1.1$ [5]. The definition of $B2$ (basicity) is given by the following equation:

$$B2 = \frac{X_{CaO}}{X_{SiO_2}} \quad (4.4)$$

Here X_{CaO} and X_{SiO_2} are the mass fractions of CaO and SiO₂, respectively. The basicity of the HMD slag should at the same time be low to minimise the iron losses, because a higher $B2$ leads to a higher solid fraction in the slag. Roughly half of the iron losses in an industrial HMD plant are caused by colloid losses (iron droplets captured in the slag in a colloid, which are removed together with the slag during skimming). These colloid losses can be reduced by decreasing the slag viscosity (η_{slag} ; in Pa·s). This η_{slag} depends on the viscosity of the liquid fraction of the slag (η_0) and the slag's solid volume fraction ($\varphi_{s,slag}$). The Einstein-Roscoe equation shows their dependency [6]:

$$\eta_{slag} = \eta_0 \cdot (1 - \varphi_{s,slag} \cdot \alpha)^{-n} \quad (4.5)$$

Here α and n are empirical constants [4].

4. Optimal hot metal desulphurisation slag: evaluation

Table 4.1: Effect of separate slag components and temperature on C_S , T_{liq} and η_0 , impact is indicated ranging from ▼▼ (very negative) to ▲▲ (very positive) [4].

Component	C_S	X_{solid}	η_0
CaO	▲▲	▲▲	▼
SiO ₂	▼	▼	▲
Al ₂ O ₃	▼	▼	▼
MgO	0	▲▲	▼
TiO ₂	▼	▼	▼
Na ₂ O	▲	▼	▼
K ₂ O	▲	▼	▼
MnO	▲	▼	▼
CaF ₂	▼	▼▼	▼
CaCl ₂	0	▼	▼
FeO _x	▼	▼	▼
Temperature	▲▲	▼▼	▼▼

As was discussed in Chapter 3, different slag components have their influence on η_{slag} , either by changing the slag's solid fraction (X_{solid}) or via η_0 , and the sulphide capacity (C_S). C_S gives the capacity of sulphides in the liquid slag when it is at equilibrium with the hot metal. Although this is not the case for the industrial HMD process, in Chapter 3 it is discussed that the slag is typically neither fully liquid nor at equilibrium with the hot metal, C_S can show the effect of a different slag composition or temperature on its sulphur removal capacity. Therefore, in this chapter C_S is used as an indication of the sulphur removal capacity. Table 4.1 summarises the effect of the separate slag components, as well as the temperature, on C_S , X_{solid} and η_0 . It shows that slag components that lead to a higher C_S , thus a better sulphur removal capacity, often also lead to a higher η_{slag} , which results in higher iron losses. The optimal slag should find the balance between a high sulphur removal capacity and low iron losses.

4.2 HMD slag thermodynamic simulation

4.2.1 Monte Carlo simulation input

To get a better picture of the thermodynamic influence of all slag components on the solid weight fraction (X_{solid}), a Monte Carlo simulation (MCS) was done with FactSage 7.3 [7] (using CON2, a consortium database), with 18 776 different HMD slag compositions. In this MCS, realistic values are used for the slag composition and its temperature, but, unlike industrial slags, these values have no interdependencies. Within the given ranges, the slag composition of the MCS is completely random. With industrial slags, the concentration of several components are correlated, because they are influenced in the same way by the

blast furnace (BF) process, or because BF operation actively aims for certain composition ratios (for example *B2*). Therefore, the MCS allows analysis of the influence of individual components on C_S and iron loss, which is not possible with analysis of industrial data. Table 4.2 gives the ranges that were used for the MCS.

Table 4.2: Composition and temperature ranges of the slags in the MCS.

Component	Min (wt%)	Max (wt%)
CaO	25	50
Al ₂ O ₃	0	20
SiO ₂	10	40
MgO	5	30
MnO	0	5
FeO	0	10
TiO ₂	0	5
P ₂ O ₅	0	3
V ₂ O ₅	0	3
Cr ₂ O ₃	0	3
Na ₂ O	0	5
K ₂ O	0	5
Temperature (°C)	1150	1500

It should be noted that the total composition is always normalised to 100 %, which leads to a skewed distribution of the weight fractions of, especially, CaO, Al₂O₃, SiO₂ and MgO. Higher weight fractions appear to be less frequent.

4.2.2 Solid fraction

For optimal HMD slag, the solid fraction (X_{solid}) should be low. To analyse which components, thermodynamically, lead to a low solid fraction, a random forest model (RFM) is created based on the MCS data. This RFM is based on 50 decision trees, each with an end node size of at least 10. With this model, it is determined how well the output, X_{solid} , can be predicted based on the parameters, in this case the slag components and temperature. Figure 4.1 shows the impact, relative to the distribution, of the parameter on X_{solid} , and whether an increase of this parameter leads to an increase (▲) or decrease (▼) of X_{solid} . The larger the impact, the more X_{solid} can be influenced by changing that parameter.

4. Optimal hot metal desulphurisation slag: evaluation

Parameter	Relative impact	X_{solid}
Temperature		▼
MgO		▲
SiO ₂		▼
CaO		▲
Al ₂ O ₃		(▼)
K ₂ O		▼
Na ₂ O		▼
FeO		▼
P ₂ O ₅		▲
TiO ₂		▼
V ₂ O ₅		▲
MnO		▼
Cr ₂ O ₃		▲

Figure 4.1: Relative impact, corrected for the distribution, of the parameters of the MCS on X_{solid} , according to the random forest model. The right column shows if X_{solid} is increased (▲) or decreased (▼) by increase of the parameter value.

The RFM shows that temperature has the largest influence on X_{solid} , which is in agreement with literature. Because CaO, SiO₂, Al₂O₃ and MgO have the largest fractions in the HMD slag, also in the MCS, their influence on X_{solid} is the most significant as well. Here MgO and, to lesser extent, CaO increase X_{solid} , while SiO₂ decreases X_{solid} . Al₂O₃ decreases X_{solid} as well, but above 12 wt% it starts to increase X_{solid} . This is all in accordance with the theory, as discussed in Chapter 3. It is remarkable that the relative impact of alkali metal oxides, K₂O and Na₂O, on X_{solid} is in the same order of magnitude as the impact of CaO and Al₂O₃. Alkali metal oxides are known to have a strong effect on T_{melt} of a slag [8]. Furthermore, FeO only has a small impact on lowering X_{solid} according to the MCS. This is remarkable, as in the previous chapter it was explained, based on FactSage calculations, that FeO lowers T_{liq} , and thus X_{solid} (see Figure 3.1). However, because the MCS was done under inert conditions, so no free oxygen, FeO itself does not shift between the solid and liquid phase. FeO does lower T_{melt} , but this only influences X_{solid} of the slag if the temperature of the slag is close to this T_{melt} . As the temperature in the MCS ranges from 1150-1500 °C, this is only the case for a small portion of the simulated slags, hence the small impact of FeO on X_{solid} in the MCS. The impact of the remaining minor elements is low, as could be expected.

Part II Optimal hot metal desulphurisation slag

Figure 4.2 gives a heat map of the influence of the two most important parameters, temperature and MgO, on X_{solid} , based on the MCS results. The yellow region of Figure 4.2 indicates that when the MgO concentration in the slag is decreased by 1 weight percent point, the slag temperature can be 3-5 °C lower to have the same X_{solid} , and thus the same iron losses.

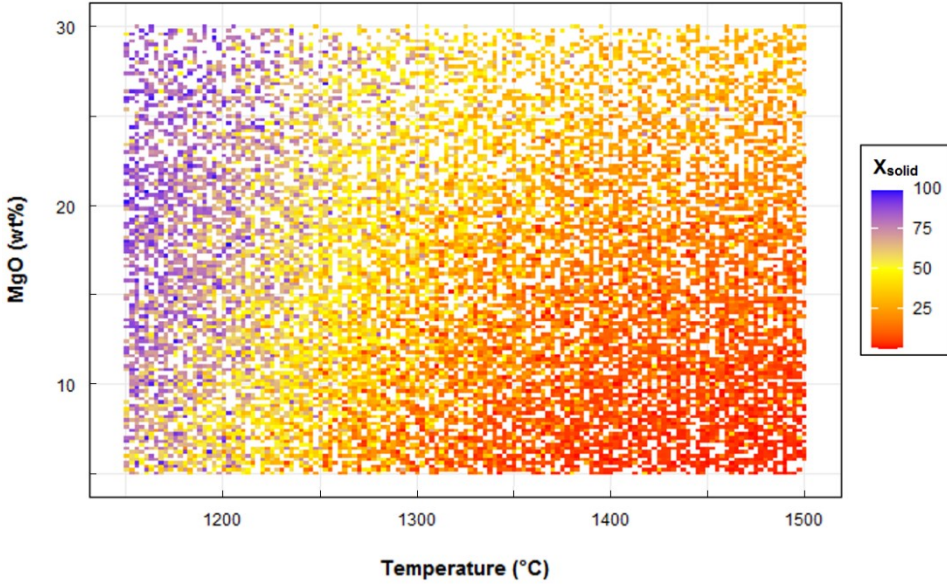


Figure 4.2: Heat map of X_{solid} as a function of temperature (x-axis) and MgO concentration (y-axis). Red indicates a low X_{solid} and blue indicates a high X_{solid} in wt%.

4.2.3 Sulphur removal capacity

As this MCS assumes a homogeneous slag at equilibrium, the sulphide capacity (C_S) is used to determine the sulphur removal capacity of the slag, as is explained in Chapter 3. C_S is calculated with Equation 4.6.

$$C_S = X_{(S)} \sqrt{\frac{p_{O_2}}{p_{S_2}}} \quad (4.6)$$

Here $X_{(S)}$ is the weight percentage of all sulphides in the slag and p_{O_2} and p_{S_2} are the partial pressures for oxygen and sulphur, respectively. The calculations were performed at a fixed $p_{O_2} = 10^{-6}$ atm and $p_{S_2} = 10^{-4}$ atm [4, 9]. The current calculations do not take into consideration the effect of p_{O_2} and p_{S_2} on C_S , which plays a part in high sulphides containing slag (~10 wt% CaS in HMD slag). The role of p_{O_2} and p_{S_2} for C_S calculations is explained by Moosavi-Khoonsari and Jung [10]. To see the thermodynamic influence of the independent slag components on C_S , a density plot is made based on the MCS results, showing the

4. Optimal hot metal desulphurisation slag: evaluation

slags with the highest 25 % C_S and with the highest 25 % X_{liquid} (see Figure 4.3). The density plot visualises the influence of an individual slag component on C_S .

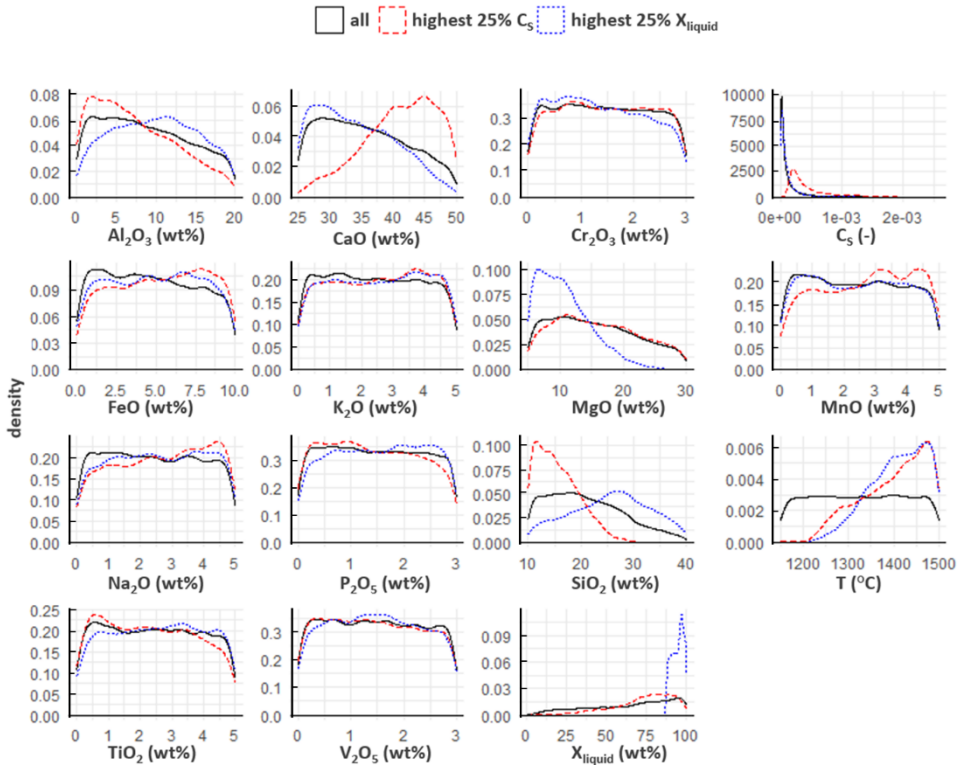


Figure 4.3: Density plot of the slag components, temperature, C_S and X_{liquid} for the complete dataset (solid black line), the 25% slags with the highest C_S value (dashed red line) and the 25% slags with the highest X_{liquid} from the MCS.

The difficulty in designing an optimal HMD slag is well illustrated by a comparison of the MCS results for X_{liquid} and the results for C_S . Oxides that are thermodynamically beneficial for a high X_{liquid} (and thus a low X_{solid}), like SiO_2 , also lead to a low C_S . CaO increases the C_S , but decreases X_{liquid} . Acidic slag components, like SiO_2 , Al_2O_3 and, to lesser extent, P_2O_5 and TiO_2 , all decrease C_S , which is in correspondence with the theory. MgO shows a small negative correlation with C_S too, which seems to be contradictory to industrial experience, where the opposite is observed. The reason is that MgO is more stable than MgS , so thermodynamically the formation of MgO is favoured over MgS . In the industrial HMD process, metallic Mg is injected, which easily reacts with the dissolved sulphur (Reaction 4.1). This Mg ends as MgO in the slag via Reaction 4.2. Therefore, industrial heats with a high sulphur removal will have more MgO

Part II Optimal hot metal desulphurisation slag

in the slag. Finally, Na_2O and MnO increase C_S , which is in correspondence with literature [10, 11].

Based on the same MCS data, a second RFM is made, to illustrate the trends of the impact of the different slag components and the temperature on C_S . Figure 4.4 shows the relative impact of all parameters on C_S , as well as the increase or decrease of C_S .

Parameter	Relative impact	C_S
Temperature		▲
CaO		▲
SiO ₂		▼
Al ₂ O ₃		▼
MgO		▲
Na ₂ O		▲
FeO		▲
MnO		▲
TiO ₂		▼
K ₂ O		0
P ₂ O ₅		▼
V ₂ O ₅		0
Cr ₂ O ₃		0

Figure 4.4: Relative impact, corrected for the distribution, of the parameters of the MCS on C_S , according to the random forest model. The right column shows if C_S is increased (▲) or decreased (▼) by increase of the parameter value.

For the largest slag fractions, CaO, SiO₂, Al₂O₃ and MgO, the RFM is in line with the findings from the density plot (Figure 4.3). It should be noted that CaO and SiO₂ have an almost equal, but opposite, influence on C_S , which shows the importance of B_2 . In the RFM, MgO shows an opposite influence on C_S than could be concluded from the density plot. MgO appears to increase C_S . The apparent increase is the result of the normalisation of the slag composition. A high MgO concentration results in lower fractions of the other components, which in majority (mainly SiO₂ and Al₂O₃) lower C_S . The actual influence of MgO itself on C_S is negligible.

4. Optimal hot metal desulphurisation slag: evaluation

4.2.4 Discussion

The MCS illustrates the effect of the individual slag components on C_S and X_{solid} at thermodynamic equilibrium. As discussed in Chapter 3, the components in the HMD slag are not at equilibrium with each other and with the hot metal, so thermodynamics alone will not predict the sulphur removal capacity of the slag. It is important to understand the thermodynamic influence of the individual slag components on X_{solid} and C_S , as it does affect the industrial situation. For example, based on industrial observations, MgO would be beneficial for the sulphur removal capacity, since a heat in which more Mg is injected, more sulphur is removed (via Reaction 4.1) and more MgO is present in the slag (via Reaction 4.2). However, MgO itself does not contribute to C_S . Therefore, adding MgO to the slag would not benefit the sulphur removal capacity of that slag. The influence of MgO is further discussed in Section 4.3.4.

4.3 Plant data analysis

4.3.1 Introduction

To identify the influencing factors on iron losses at the HMD, data analysis was done on 47 129 heats from the HMD stations at Tata Steel in IJmuiden, the Netherlands. The iron loss per heat is indirectly determined by a mass balance over the ladle weight before and after the HMD process, taking into account the injected reagents and removed sulphur, and using the operator's estimates of the BF carryover slag (typically 1500 kg) and the remaining slag after skimming (typically 500 kg). It should be noted that this iron loss estimate is inaccurate for a single heat, but for a large data set the trend is very reliable.

Plant data analysis is complicated, as, unlike with controlled laboratory experiments or simulations, different parameters have interdependencies. In this study, the presented correlations have been checked for interdependencies with other parameters. Relevant interdependencies are mentioned in this section.

4.3.2 Temperature

Of all measured parameters at the HMD, temperature has the largest influence on iron loss. This is mainly because a higher temperature leads to a lower η_{slag} , which leads to lower iron losses, as discussed in Chapter 3. Figure 4.5 shows the iron loss for different hot metal temperatures, which are assumed to be an accurate indicator of the slag temperatures.

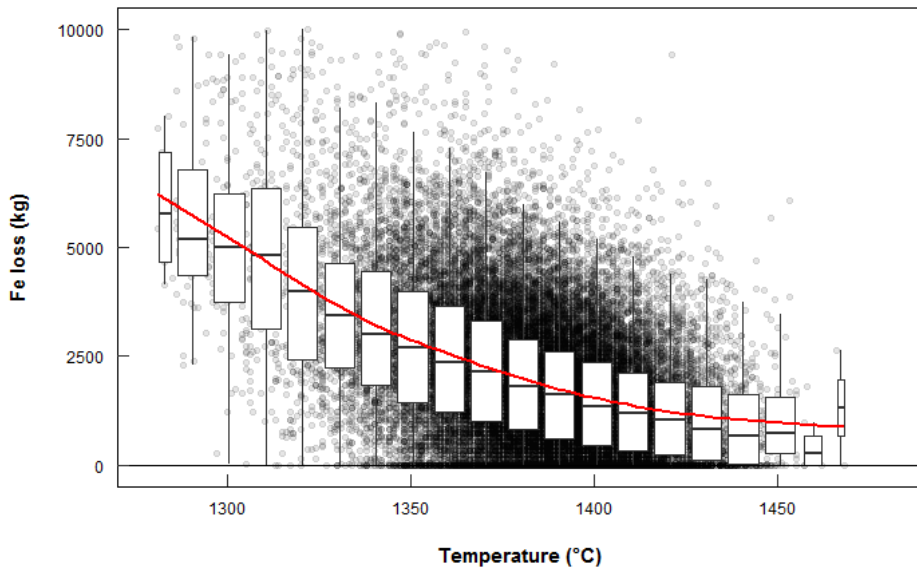


Figure 4.5: Iron loss (in kg) at different hot metal temperatures at the HMD stations of Tata Steel in IJmuiden, the Netherlands. Boxes stretch from the 25th till the 75th percentile of the distribution. The lines (whiskers) extend to 1.5 times the interquartile range. In red a polynomial trendline. The circles represent individual heats.

Figure 4.5 shows that higher temperatures lead to lower iron losses until, around 1430 °C, the iron losses stabilise at roughly 1000 kg/heat. According to FactSage [7] calculations, the slag is fully liquid around 1430 °C, so a further increase in temperature will not have a significant effect on η_{slag} (albeit higher temperatures decrease η_0 , the effect on η_{slag} is insignificant).

4.3.3 Slag weight

Since colloid losses are caused by iron droplets being entrapped in the slag, a higher slag volume should lead to more iron losses. This effect can be seen in the plant data (see Figure 4.6).

4. Optimal hot metal desulphurisation slag: evaluation

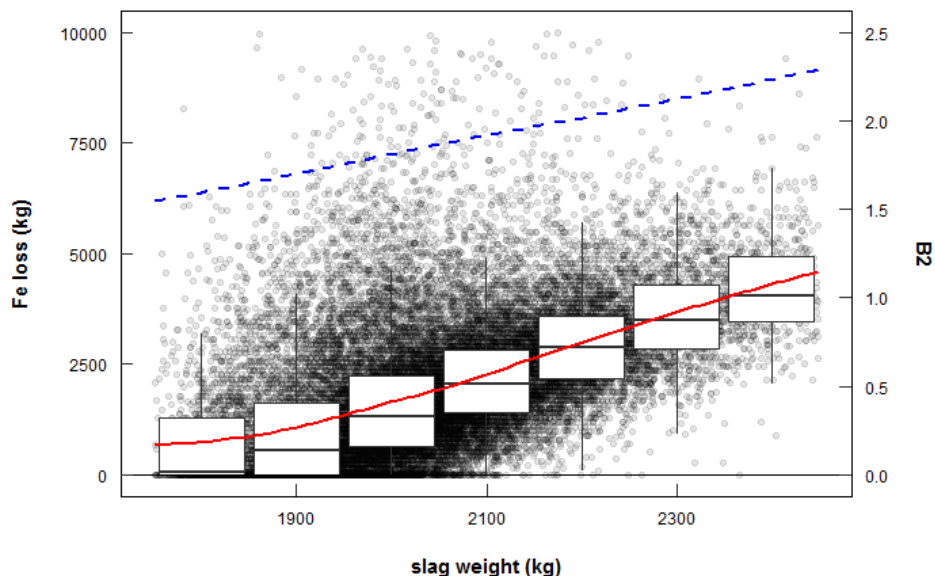


Figure 4.6: Iron loss (red solid line) and B2 (blue dashed line) at different slag weights at the HMD stations of Tata Steel in IJmuiden, the Netherlands. Boxes stretch from the 25th till the 75th percentile of the distribution. The lines (whiskers) extend to 1.5 times the interquartile range. The circles represent individual heats.

In most cases a standard BF carryover slag weight of 1500 kg is used to calculate the slag weight. Therefore, an increased slag weight is the result of a higher reagent injection, which leads to a more basic slag. In industry a common definition of basicity is B_2 , which is CaO/SiO_2 [4]. As slag basicity influences η_{slag} , and thus the iron losses, it is difficult to quantify, based on Figure 4.6, which part of the increased iron losses can be attributed to the slag weight itself and which part is caused by an increased η_{slag} . However, when selecting the heats that have a higher reported BF carryover slag, the iron losses are higher than for heats with an average BF carryover slag of 1500 kg, so slag weight has an influence on iron losses.

4.3.4 Slag composition

Based on the theory, explained in Chapter 3, the slag components that influence η_{slag} the most are CaO, SiO₂ (together as B_2), Al₂O₃ and MgO. The SiO₂ and Al₂O₃ concentration depend on the BF carryover slag composition only, which is quite constant during stable BF operation. For this study, an average BF carryover slag composition is used. Therefore, the effect of Al₂O₃ and SiO₂ cannot be studied on a heat basis. As the amount of injected CaO and Mg (which ends up

as MgO in the slag, see Reaction 4.2) are known, their effect on the iron losses can be analysed with plant data (see Figure 4.7).

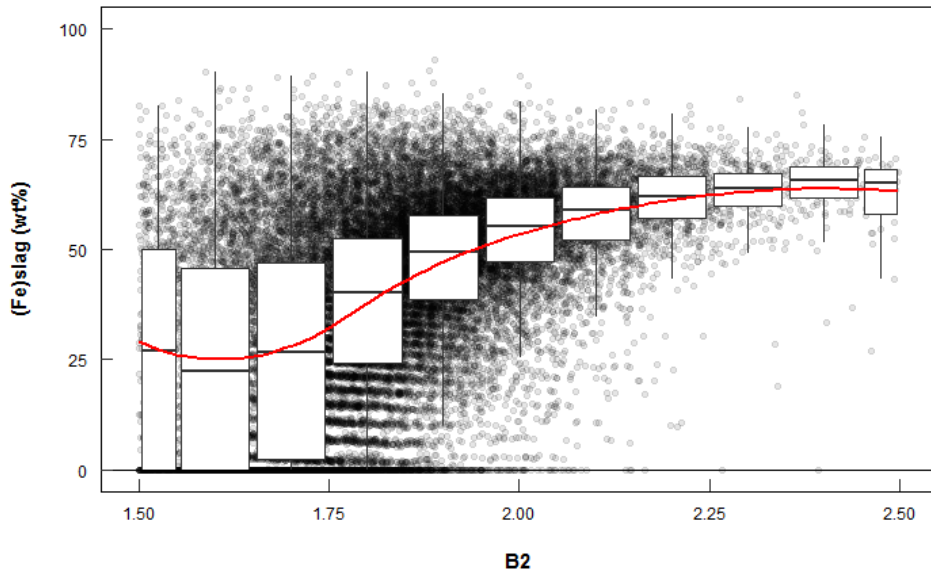


Figure 4.7: Iron concentration in skimmed off slag at different $B2$ values at the HMD stations of Tata Steel in IJmuiden, the Netherlands. Boxes stretch from the 25th till the 75th percentile of the distribution. The lines (whiskers) extend to 1.5 times the interquartile range. The circles represent individual heats.

Figure 4.7 shows the iron concentration in skimmed off slag, calculated by dividing total iron loss by total skimmed off slag weight, at different $B2$ values. The influence of $B2$ can be analysed independent of the total slag weight. As is expected, based on the thermodynamics [4], a higher $B2$, which means more CaO, leads to higher iron losses. However, below a $B2$ of 1.7 there seems to be no correlation between basicity and iron losses. As explained in Chapter 3, $B2$ influences η_{slag} mostly by influencing the solid fraction, as a higher $B2$ leads to a higher T_{melt} under HMD conditions. Possibly, at the typical HMD temperatures (mean hot metal temperature in this data set is 1390 °C) the slag has a liquid fraction above 90 wt% at $B2 < 1.7$. This would mean that lowering the $B2$ would hardly influence η_{slag} . The thermodynamic calculations in Chapter 3 indicate that a lower $B2$ is required to reach a liquid slag, but in that calculation the influence of minor slag elements, like FeO_x or alkali metal oxides, which lower η_{slag} , was neglected.

4. Optimal hot metal desulphurisation slag: evaluation

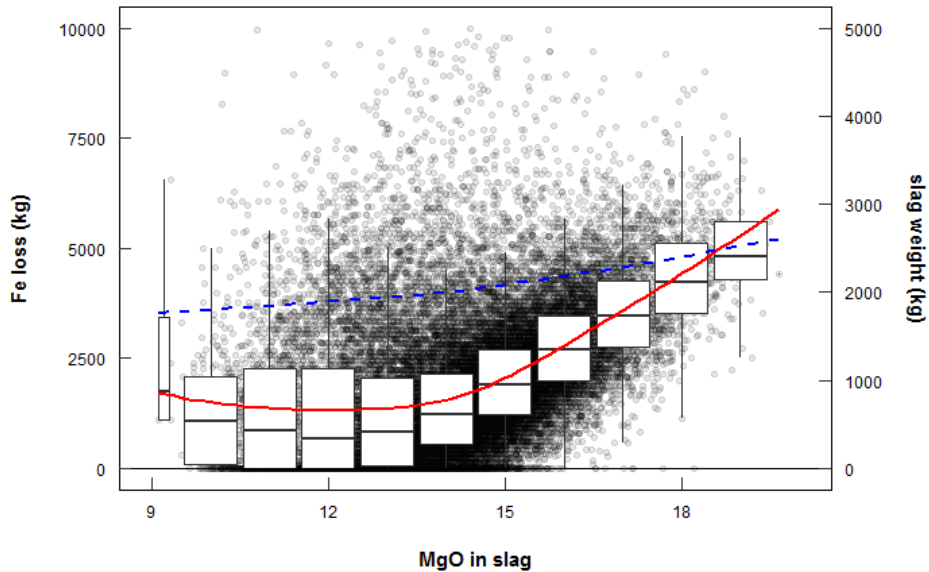


Figure 4.8: Iron loss (red solid line) and slag weight (blue dashed line) at different MgO concentrations in the slag at the HMD stations of Tata Steel in IJmuiden, the Netherlands. Boxes stretch from the 25th till the 75th percentile of the distribution. The lines (whiskers) extend to 1.5 times the interquartile range. The circles represent individual heats.

Figure 4.8 shows the correlation between MgO fraction in the slag and iron losses. The plant data clearly show that for MgO concentrations above 14 wt%, the iron losses increase. Although total slag weight increases with the MgO concentration in the slag, the slag weight has only little effect on the correlation between MgO concentration and iron losses. It is in line with the theory, that a higher MgO concentration in the slag leads to a higher solid fraction, and thus to a higher η_{slag} , which finally leads to higher iron losses [4]. It should be noted that for MgO concentrations below 14 wt%, the iron losses do not further decrease, although that would be expected based on the theory. As at $B2 < 1.7 \eta_{slag}$ is not affected significantly because the slag is already liquid, also MgO fractions below 14 wt% probably do not lead to lower iron losses anymore, as the slag is liquid at MgO < 14 wt% under the HMD conditions in the data set.

4.3.5 Silicon and titanium

TiO₂ is identified as a component that influences η_{slag} . However, in an industrial blast furnace, TiO₂ is correlated with SiO₂ in the slag, as are Ti and Si in the hot metal. This means that industrial slags with a high SiO₂ concentration will be high in TiO₂ as well [12]. Therefore, it is not possible to identify an independent correlation between TiO₂ in the slag and iron losses with this plant data analysis.

Part II Optimal hot metal desulphurisation slag

To understand the effect of silicon concentration in the hot metal on iron losses, independent from $B2$, the correlation between silicon in hot metal and iron losses is investigated. Besides the correlation between silicon and titanium in hot metal, there is a strong reverse correlation between silicon and sulphur in the hot metal, which leads to a correlation with the slag weight as higher sulphur removal requires more reagents being injected. In general, a higher oxygen activity, a_o , in the hot metal at the BF leads to less silicon in the hot metal and more SiO_2 in the slag. SiO_2 decreases the $B2$, so less desulphurisation takes place in the BF, leading to more sulphur in the hot metal [12, 13]. The plant data confirm the correlation between silicon and sulphur at a silicon concentration below 0.5 wt%. However, for a silicon concentration above 0.5 wt%, the reversed correlation between silicon in the metal and SiO_2 in the slag becomes weaker. This is because high silicon concentrations (above 0.5 wt%) are typically caused by more silicon in the BF in total ($[\text{Si}]$ in hot metal + (SiO_2) in slag). Therefore, at silicon concentrations above 0.5 wt%, the correlation between silicon in the hot metal and $B2$, and thus between silicon and sulphur in the hot metal, decreases.

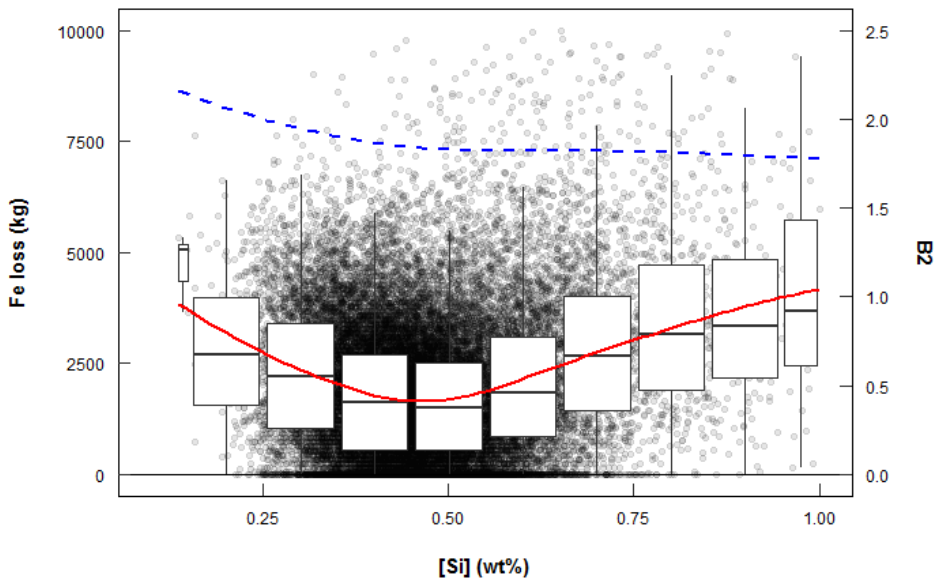


Figure 4.9: Iron losses (solid red line) and mean $B2$ (dashed blue line) at different silicon concentrations in hot metal, $[\text{Si}]$ (in wt%) at the HMD stations of Tata Steel in IJmuiden, the Netherlands. Boxes stretch from the 25th till the 75th percentile of the distribution. The lines (whiskers) extend to 1.5 times the interquartile range. The circles represent individual heats.

Figure 4.9 shows the correlation between silicon in the hot metal and the iron losses (solid red line). For $[\text{Si}] < 0.5$ wt%, an increasing silicon fraction correlates

4. Optimal hot metal desulphurisation slag: evaluation

with a decreasing sulphur concentration, thus with less reagents being injected, which ultimately leads to lower iron losses. For $[\text{Si}] > 0.5$ wt%, this phenomenon no longer dictates the iron losses, as the iron losses are now increasing with an increasing silicon concentration. It should be noted that the highest silicon concentrations (above 0.8 wt%) are often the result of starting up the BF, when higher slag amounts, more sulphur and lower temperatures occur. However, there is an increase in iron losses at 0.5-0.7 wt% $[\text{Si}]$ as well, which cannot be explained by non-standard circumstances. The $B2$ of the slag (dashed blue line) does not change significantly at higher silicon concentrations, so it cannot explain the increasing iron losses. The increase cannot be explained by a different mean temperature, as high silicon concentrations correlate with higher hot metal temperatures [12, 13], so a decrease of iron losses would be expected. One possible explanation is the titanium concentration, which correlates strongly with the silicon concentration in hot metal. A high titanium concentration in the hot metal will lead to a high TiO_2 concentration in the slag and a high concentration of $\text{Ti}(\text{C},\text{N})$ particles, which leads to a sticky, viscous slag [2, 14]. Because the slag composition is not directly measured and the titanium and silicon in hot metal are too much correlated, this hypothesis cannot be proven with the current plant data. Another possible explanation is the a_{O} , as a low a_{O} in the BF hearth would lead to a higher silicon concentration in the hot metal. At a low a_{O} , it is expected that the FeO_x concentration in the slag will be low. FeO_x has a large influence on η_{slag} , so a slag with a low FeO_x concentration will have a high η_{slag} and, thus, high iron losses. As FeO_x and a_{O} are not measured, this hypothesis cannot be proven either with the current plant data.

4.3.6 Discussion

Analysis of plant data identifies several factors that influence the iron losses during the HMD process. This analysis confirms the theory, that η_{slag} governs the iron losses, which is illustrated by the strong correlations of temperature, $B2$ and MgO concentration with the iron losses. It should be noted that both $B2$ and MgO increase when more CaO and Mg are injected to desulphurise the hot metal. According to the theory, iron losses are also influenced by TiO_2 and FeO_x concentration in the slag, as both oxides influence η_{slag} , but this cannot be confirmed by the plant data analysis.

The total slag weight also plays a role, albeit minor compared to MgO and $B2$. Figure 4.7 shows that the basicity of the slag, and thus the η_{slag} , contributes more to the iron losses than the slag weight, which is correlated with $B2$.

Although it was expected that less basic oxides in the slag would lead to a lower melting point, thus lower iron losses, there seems to be an optimal $B2$ and MgO

concentration. Lowering the $B2$ below 1.7 or lowering MgO below 14 wt% does not seem to significantly influence the iron losses. This is explained by the slag temperature. If a certain $B2$ or MgO concentration leads to a T_{melt} below the slag temperature, a further decrease of T_{melt} by changing the slag composition will not influence the iron losses. Therefore, the optimal $B2$ and MgO concentration in the slag depends on the slag temperature. It should be noted that for plants with an average hot metal temperature below 1390 °C, the optimal $B2$ and MgO concentration will be lower.

4.4 Viscosity and melting range experiments

4.4.1 Introduction

To validate if optimal HMD slag, as described in this work, actually has a low apparent viscosity (η_{slag}), experiments with a synthetic optimal HMD slag were done, where the viscosity and melting temperature were measured. The synthetic optimal HMD slags were prepared by mixing the necessary chemical components and prefusing them in a graphite crucible in a muffle furnace at 1600 °C for 10 minutes. The prefused slags were then quenched on a steel plate and milled in a Tema mill for 30 seconds. The milled samples were decarburised at 650 °C for 16 hours to remove any residual carbon that had been absorbed from the graphite crucible during prefusing. The composition of the tested slags is given in Table 4.3. The main difference between Slag #1 and #2 is the MgO:Al₂O₃ ratio. Slag #2 is considered the optimal HMD slag, according to the theory, in terms of its main components CaO, SiO₂, Al₂O₃ and MgO.

Table 4.3: X-ray fluorescence (XRF) analysis of synthetic slags #1 and #2 for viscosity and melting range measurements. For comparison, composition of an industrial HMD slag (HMD) and of another synthetic slag, both from another study [15], are added. Compositions are in wt%.

	Slag #1	Slag #2	HMD slag	Slag 2.1
CaO	38.83	40.47	34.24	43.63
SiO ₂	29.98	29.54	17.30	26.79
Al ₂ O ₃	10.66	15.27	6.33	9.81
MgO	15.80	10.55	10.06	14.80
Na ₂ O	0.27	0.73	0.21	0.19
CaS	4.06	3.10	4.51	2.83
Fe ₂ O ₃	0.24	0.18	24.26	0.32
P ₂ O ₅	0.05	0.07	0.12	-
TiO ₂	0.05	0.05	0.84	-
Cr ₂ O ₃	0.05	0.04	-	-

4. Optimal hot metal desulphurisation slag: evaluation

It should be noted that the CaS value is low compared to industrial HMD slag, which typically contains around 13.5 wt% CaS. When the synthetic slags were prepared, 13.5 wt% of CaS was added to the slag. However, when the slag was heated to 1600 °C to homogenise the slag components, the CaS reacted with oxygen to form CaO. The XRF analysis of the slags was done prior to the viscosity and melting point experiments.

For comparison, an industrial HMD slag sample and a synthetic HMD slag sample, both from the study discussed in Chapter 5, have been added to Table 4.3. Note that the industrial HMD sample contains a high amount of Fe₂O₃, which is mostly entrapped iron that oxidised during preparation for XRF analysis. During the melting point and viscosity measurements, part of the entrapped iron was already oxidised. The FeO_x concentration in the slag during the HMD process is in the order of 1-3 wt%. Slag 2.1 showed the closest resemblance to slag #1.

4.4.2 Melting point measurements

For the melting point measurements, a Misura HM2-1600 heating microscope was used. Samples were prepared using a steel die to manually compress prefused powdered slag into cylinders of 3 mm in height and 2 mm in diameter. The samples were then placed onto an alumina plate and inserted into the horizontal tube furnace of the heating microscope. The samples were heated to 1100 °C at 50 °C/min under inert conditions, after which they were heated to the melting point at 6 °C/min. The device is able to acquire and store images of the sample at 2 °C intervals during the heating cycle. During the heating cycle, all the dimensional parameters of the sample were measured automatically in order to identify phase transitions of the material. The DIN 51730 standard was used to calculate T_{melt} of the sample.

To put the measured T_{melt} of Slag #1 and #2 into perspective, the T_{melt} of an industrial HMD slag sample and of a synthetic HMD slag sample (master Slag 2.1) [15], are added for comparison. All four samples were analysed with the same equipment and procedure.

Table 4.4: Measured T_{melt} for Slag #1 and #2, compared with an industrial and synthetic HMD slag.

Sample	T_{melt} (°C)
Slag #1	1438
Slag #2	1416
Industrial HMD slag [15]	1334
Synthetic HMD slag 2.1 [15]	1424

Part II Optimal hot metal desulphurisation slag

As expected, based on the theory, the slag with the highest MgO concentration (Slag #1) has the highest T_{melt} . It is observed that Slag 2.1, with a similar MgO and Al_2O_3 concentration as slag #1, has a lower T_{melt} than Slag #1. This is because Slag 2.1 contains less CaS (which increases T_{melt}) and also contains 0.10 wt% B_2O_3 , which lowers T_{melt} . The much lower T_{melt} of the industrial HMD slag sample is caused by the high FeO_x concentration. According to literature, an increase from 0 wt% to 20 wt% of FeO_x in typical BF carryover slag can lower T_{melt} by 150 °C [12].

The melting point measurements show that Slag #2, which has an optimal CaO-SiO₂-Al₂O₃-MgO distribution for HMD slag according to the theory from Part I, has a lower T_{melt} than a synthetic HMD slag. However, when comparing Slag #2 with (synthetic) slags with an added slag modifier (containing fluorides or alkali oxides), a lower T_{melt} can be achieved. Under industrial conditions, the T_{melt} of a slag with the same relative CaO, SiO₂, Al₂O₃ and MgO concentration as Slag #2 will be lower than 1416 °C, as a result of FeO_x and other minor oxides. This is illustrated by the comparison of the industrial HMD slag and synthetic Slag 2.1.

It should be noted that industrial HMD slag does not have a specific T_{melt} , but rather a melting temperature trajectory. However, for understanding of the correlations between temperature, slag composition, viscosity and iron losses, a single T_{melt} is sufficient.

4.4.3 Apparent viscosity

A Bahr VIS-403 HF rotational viscometer (see Figure 4.10) was used to measure the viscosity of the synthetic slags continuously under inert conditions. This machine measures the torque applied to a constant speed rotating bob submerged in a known volume of slag. The viscosity is calculated by the ratio of shear stress (τ , in Pa) to shear rate ($\dot{\gamma}$, in s⁻¹). For a Newtonian fluid contained within two concentric cylinders (Taylor-Couette flow), the shear rate is set according to Equation 4.7 and the resulting shear stress is measured by Equation 4.8:

$$\dot{\gamma} = \omega_s \cdot \frac{2R_c^2}{R_c^2 - R_s^2} \quad (4.7)$$

$$\tau = \frac{Tor}{2\pi \cdot R_s^2 \cdot h_s} \quad (4.8)$$

Where ω_s is the rotational speed of the spindle (rad/s), R_c and R_s are the radius of the crucible and the spindle respectively (m), Tor is the measured torque (N·m) and h_s is the height of the spindle head (m).

4. Optimal hot metal desulphurisation slag: evaluation

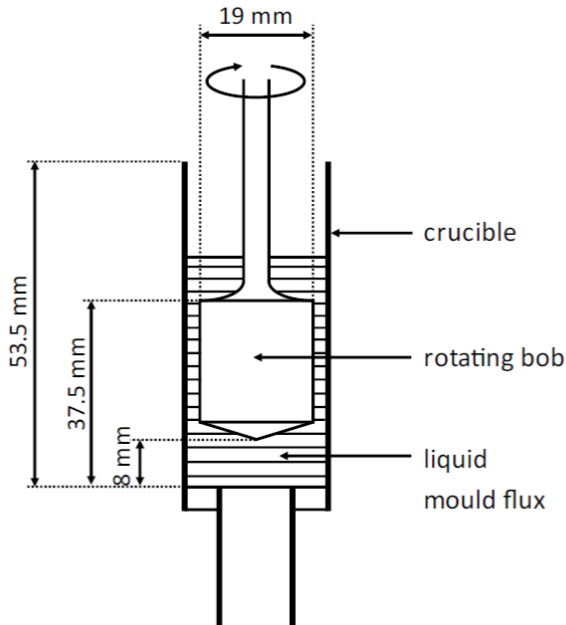


Figure 4.10: Schematic of the viscometer (courtesy of Materials Processing Institute).

Torque measurements were calibrated at room temperature using three certified silicon oils between 0.1 and 1.0 Pa·s. Regression analysis was used to determine the calibration curve. The calibration was specific to the rotation speed selected for the tests. A temperature calibration was determined by measuring the sample temperature at various steps up to 1600 °C. The sample temperatures were measured with an R-type thermocouple fed into the crucible inside the viscometer furnace. Regression analysis was applied to the slag temperature measurements in conjunction with the furnace temperature measurements to determine the calibration curve.

For every test, 24 g of prefused powdered slag was put into the crucible and inserted into the rotational viscometer. The oxygen level in the furnace chamber was lowered with an argon purge at 200 ml/min, to protect the molybdenum crucible and spindle from oxidation. The sample was heated to 1600 °C whereby the rotating spindle was submerged into the liquid sample. A constant rotation speed of 280 rpm was used for the test. The sample was cooled at 10 °C/min until the sample reached a maximum torque of 25 mNm.

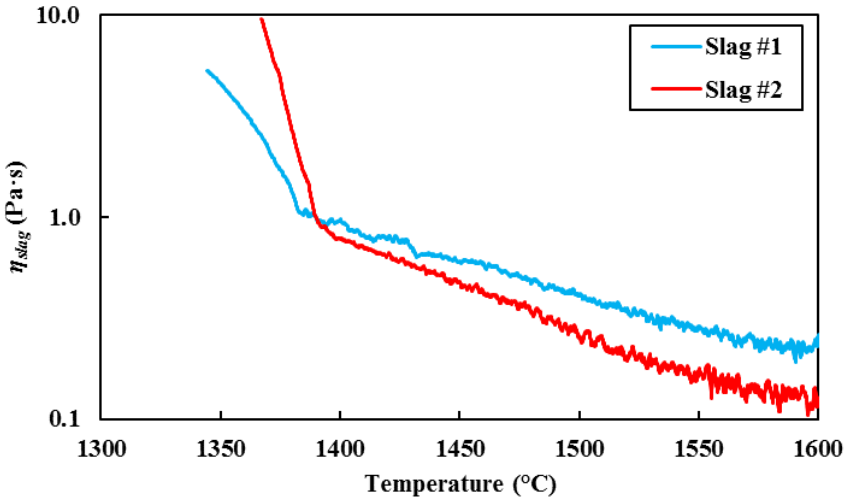


Figure 4.11: Viscosity measurements for Slag #1 and #2 at different temperatures.

Figure 4.11 shows that both slags have a low η_{slag} ($< 1 \text{ Pa}\cdot\text{s}$) at temperatures above $1390 \text{ }^\circ\text{C}$. At these temperatures, MgO and Al_2O_3 have an effect on η_{slag} : a lower MgO concentration leads to a lower η_{slag} . However, at $\eta_{slag} < 1 \text{ Pa}\cdot\text{s}$, its effect on iron losses in industry will be negligible. At some point below $1390 \text{ }^\circ\text{C}$, there is a marked increase in the viscosity of both slags. This is due to the growth of solid particles causing a dramatic resistance to liquid flow. Below $1390 \text{ }^\circ\text{C}$, η_{slag} is higher for Slag #2 (with less MgO) than for Slag #1, while based on theory it was expected that MgO leads to a higher solid fraction. Furthermore, the viscosity measurement suggests that Slag #1 has a lower solidification temperature than Slag #2, while the melting temperature experiments show that Slag #2 has the lowest T_{melt} . A possible explanation for this is that when the slag is cooled down from $1600 \text{ }^\circ\text{C}$ during the experiment, the cooling goes faster than in industrial practice, producing a super-cooled liquid, so the slag is not at equilibrium, which leads to the formation of MgAl_2O_4 -rich spinel, melilite, CaS, Ca-Mg-orthosilicate ($\text{Ca}_3\text{MgSi}_2\text{O}_8$) compound formation at low temperature which increases η_{slag} . Due to the cooling rate of $10 \text{ }^\circ\text{C}/\text{min}$ and the composition of Slag #1, it is possible that more super-cooled liquids were present [16].

4. Optimal hot metal desulphurisation slag: evaluation

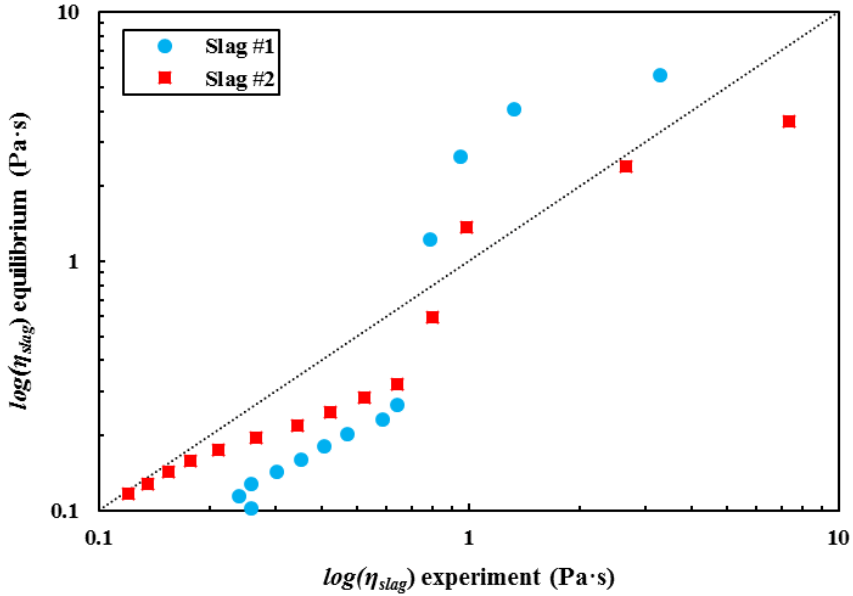


Figure 4.12: Measured viscosity versus equilibrium viscosity at the same temperature (range: 1370-1600 °C), according to FactSage for Slag #1 and #2 on a logarithmic scale.

To validate if the quick cooling of the slag during the experiment caused the higher viscosity, the viscosity of Slag #1 and #2 at the temperature range of 1370-1600 °C are modelled with FactSage 7.3 (CON2 database) [7] to determine both η_0 and $\varphi_{s,slag}$ (including CaS). Here η_{slag} is determined via the Einstein-Roscoe equation (Equation 4.5). Figure 4.12 shows the experimental η_{slag} versus the thermodynamic η_{slag} under the same conditions. The comparison shows that at $\eta_{slag} < 0.7$ Pa·s, the experiments give a greater η_{slag} than the equilibrium calculations. When comparing Slag #1 and #2, at $\eta_{slag} > 2$ Pa·s, experiments give a lower η_{slag} for Slag #1, while the experiments almost always predict a higher η_{slag} than the equilibrium calculations for Slag #2. The equilibrium calculations in FactSage show the formation of the η_{slag} -increasing solids.

Under industrial HMD conditions, the temperature of the slag changes very slowly (typically the temperature decreases with 0.5 °C/min). Therefore, it is likely that the slag conditions are closer to the equilibrium situation than to the fast cooling experimental conditions. This means that the experiments overestimate η_{slag} at temperatures below 1390 °C for Slag #2 when compared to the industrial HMD process. Note that, despite the small changes in temperature, the industrial HMD slag is constantly changing composition during the process, so it is not necessarily at equilibrium.

4.5 Discussion

4.5.1 Validation

In Chapter 3, claims were made about the composition of the optimal HMD slag, regarding sulphur removal capacity and iron losses, based on a theoretical study. In this chapter, these claims are put to the test with a thermodynamic MCS study, industrial plant data analysis and laboratory experiments with synthetic HMD slag.

The sulphur removal capacity, in the thermodynamic MCS study represented with the C_S , indeed depends on the CaO concentration of the slag. It is noteworthy that, although the injected magnesium mostly determines the desulphurisation, the final form of magnesium, MgO, does not contribute to the C_S of the slag. The claim that the $B2 > 1.1$ is required for the HMD process could not be validated with the plant data, as no heats were found were $B2 < 1.3$. The penalty for having a too low sulphur removal capacity is much higher than the penalty for increased iron losses as a result of a higher $B2$. So, since iron losses are more or less constant for $B2 < 1.7$, it is not strange that no heats were found with a too low $B2$; the steel plant will always try to be on the safe side.

With respect to the iron losses, the trends predicted by the theory regarding the influence of the different components in the slag on the iron losses, are confirmed by the thermodynamic MCS study, the plant data and the laboratory experiments. However, the importance of this influence seems to be different. Based on the theory and the thermodynamics, the MgO concentration of the slag should be as low as possible and preferably $\text{MgO} < 10 \text{ wt}\%$. However, the plant data show no significant influence of MgO on the iron losses for $\text{MgO} < 14 \text{ wt}\%$. The reason for this is the slag's temperature. As MgO lowers T_{melt} of the slag, it will only significantly influence the iron losses if it decreases T_{melt} to below the temperature of the slag. This is confirmed by the melting point and viscosity experiments, where MgO hardly influences η_{slag} above T_{melt} . This means that it depends on the slag and hot metal temperatures at a specific HMD station which MgO concentration in the slag is still acceptable. It should be noted that the temperatures at the HMD stations of Tata Steel IJmuiden are relatively high compared to most other steel plants. Therefore, in most other plants the maximum allowed MgO will be lower than 14 wt%.

The influence of CaO on the iron losses is comparable to that of the influence of MgO, as CaO also increases η_{slag} , and thus the iron losses, mostly by increasing T_{melt} . Plant data show that higher CaO concentrations (or $B2$ values) are more acceptable than expected based on the theory and thermodynamics. In practice,

4. Optimal hot metal desulphurisation slag: evaluation

for $B2 > 1.1$ iron losses do not immediately increase. Only when the $B2$ reaches a certain threshold, 1.7 for the given plant conditions, a further increase in $B2$ will lead to higher iron losses. As with MgO, the maximum allowed $B2$ depends particularly on the slag temperature. Higher slag temperatures mean higher $B2$ values can be reached without increasing the iron losses.

In this part of the study, there is less focus on the influence of the other slag elements on the iron losses. The thermodynamic MCS study gives comparable results as the theory. According to the MCS, Na₂O and K₂O have a relatively large impact on T_{melt} , despite their low concentrations. This explains why these alkali metal oxides are suited as slag modifiers, as they lower η_0 [15].

The melting range experiments showed that FeO_x significantly lowers T_{melt} . This confirmed the FactSage calculations about the addition of FeO to the slag from Chapter 3. In the MCS the influence of FeO on X_{solid} was small, because the MCS was done under inert conditions, with a wide range of temperatures, which meant the influence of FeO on T_{melt} had only a small effect on X_{solid} . However, under industrial conditions, FeO_x will lower X_{solid} and, thus, the iron losses.

4.5.2 Industrial implications

Based on the theory and plant trials at the former Tata Steel plant in Scunthorpe, UK, around 2010 [5], the minimal $B2$ of the slag for sufficient sulphur removal is 1.1. Besides, enough magnesium should be injected to remove the sulphur. Stoichiometrically a magnesium to sulphur weight ratio of 0.76:1 is sufficient, but due to magnesium dissolution in hot metal and kinetic constraints, a minimal magnesium to sulphur weight ratio of 1:1 is required. However, in most steel plants typically more Mg and CaO are injected than necessary, to be on the safe side, as the costs for not achieving the final sulphur aim is supposed to be higher than the costs of extra reagents. The resulting increased iron losses are usually not monitored accurately, so their costs are often overlooked. Therefore, in general HMD slags typically have higher CaO and MgO concentrations than necessary, which increases the slag's T_{melt} .

Although the slag's viscosity, its solid fraction and the size and shape of solids all influence the colloidal iron losses during the HMD process, in practice the solid fraction, which heavily influences η_{slag} , determines these colloidal iron losses. This means that, in order to keep the iron losses as low as possible, the slag should have a low T_{melt} . Under industrial HMD conditions this means CaO and MgO concentrations should be kept as low as possible. Steel plants where the hot metal (and slag) temperatures are typically high will have more freedom to inject extra CaO and magnesium than steel plants where the hot metal

temperatures are typically lower, as high slag temperatures allow for a higher T_{melt} . This also means that if a change in the BF process or the hot metal transport time lead to lower temperatures, adjustments in the HMD process might be required to avoid an increase in iron losses.

At the HMD, the temperature of the slag is difficult to increase. In general, steel plants already try to keep the temperature of the hot metal (and slag) as high as possible. However, other adjustments, to lower the iron losses are more practical:

- At the BF, the MgO concentration in the carryover slag can be decreased, to lower T_{melt} . Decreasing the total amount of carryover slag would be beneficial as well, but this is in practice harder to achieve.
- During the HMD process, the amount of injected CaO and magnesium can be lowered, if the desulphurisation requirements allow. This decreases T_{melt} and also slightly lowers the total slag amount.
- Slag modifiers, which lower T_{melt} and/or η_{slag} , like Na₂O and K₂O, can be added.
- Increase the time between reagent injection and slag skimming, to give entrapped iron more time to drip back into the metal bath (see Chapter 3, Figure 3.8). However, this increases the process time, which could lead to a lower productivity if the HMD is the bottleneck in the steel plant.

4.6 Conclusions

The validation of the fundamentals of the optimal HMD slag, considering sulphur removal capacity and iron losses, using a thermodynamic MCS, a plant data analysis and viscosity and melting point measurements in a laboratory, confirmed the initial conclusions from Chapter 3. However, some additional remarks can be made based on this study:

- To achieve the desired sulphur removal capacity, the slag should contain at least enough CaO to allow all MgS to react with CaO to form CaS. Besides, a minimal CaO:SiO₂ weight ratio ($B2$) in the slag of 1.1 is required.
- A lower CaO and MgO concentration in the slag does lead to a lower η_{slag} and thus to lower iron losses, but as soon as T_{melt} of the slag is lower than the slag temperature, the optimal CaO and MgO concentration is reached. A further decrease in CaO would be even unwanted as it would lower the sulphur removal capacity of the slag.
- The slag weight contributes much less to the iron losses than η_{slag} .

4.7 References

- [1] F.N.H. Schrama, E.M. Beunder, B. van den Berg, Y. Yang, and R. Boom, “Sulphur removal in ironmaking and oxygen steelmaking,” *Ironmak. Steelmak.*, vol. 44, no. 5, pp. 333–343, 2017, doi: 10.1080/03019233.2017.1303914.
- [2] H.-J. Visser, “Modelling of injection processes in ladle metallurgy,” (PhD thesis) Delft University of Technology, Delft (NL), 2016.
- [3] S. Kitamura, “Hot Metal Pretreatment,” in *Treatise on Process Metallurgy*, vol. 3, S. Seetharaman, Ed. Oxford (UK): Elsevier, 2014, pp. 177–221.
- [4] F.N.H. Schrama *et al.*, “Optimal hot metal desulphurisation slag considering iron loss and sulphur removal capacity part I: Fundamentals,” *Ironmak. Steelmak.*, vol. 48, no. 1, pp. 1–13, 2021, doi: 10.1080/03019233.2021.1882647.
- [5] Z. Li, J.W.K. van Boggelen, H. Thomson, G. Parker, and A. Ferguson, “Improved Slag Skimming Performance At Hot Metal Desulphurisation Station By Using Recycled Materials As Slag Modifying Agent,” in *Scanmet IV*, 2012, pp. 189–195.
- [6] R. Roscoe, “The viscosity of suspension of rigid spheres,” *Br. J. Appl. Phys.*, vol. 3, no. Aug, pp. 267–269, 1952.
- [7] CRCT (Canada) & GTT (Germany), “FactSage 7.3,” 2020. [Online]. Available: www.factsage.com.
- [8] Z. Li, M. Bugdol, and W. Crama, “Optimisation of hot metal desulphurisation slag in the CaO / Mg co-injection process to improve slag skimming performance,” in *Molten2012*, 2012.
- [9] S.K. Panda, E. Harbers, A. Overbosch, and R. Kooter, “Desulphurization with Ladle Furnace Slag,” in *Proceedings of METEC & 4th ESTAD*, 2019, p. P264.
- [10] E. Moosavi-Khoonsari and I.H. Jung, “Thermodynamic Modeling of Sulfide Capacity of Na₂O-Containing Oxide Melts,” *Metall. Mater. Trans. B*, vol. 47, no. 5, pp. 2875–2888, 2016, doi: 10.1007/s11663-016-0749-z.
- [11] S. Chatterjee, B. Konar, A. Maity, and K. Chattopadhyay, “Development of Alternative Flux for Liquid Steel Desulfurization,” in *AISTech 2019 — Proceedings of the Iron & Steel Technology Conference*, 2019, pp. 1211–1224, doi: 10.33313/377/123.

Part II Optimal hot metal desulphurisation slag

- [12] M. Geerdes, R. Chaigneau, I. Kurunov, O. Lingiardi, and J. Ricketts, *Modern Blast Furnace Ironmaking*, 3rd ed. Delft (NL): IOS Press, 2015.
- [13] Y. Yang, K. Raipala, and L. Holappa, “Ironmaking,” in *Treatise on Process Metallurgy*, vol. 3, S. Seetharaman, Ed. Oxford (UK): Elsevier, 2014, pp. 2–88.
- [14] S. Street, R.P. Stone, and P.J. Koros, “The presence of titanium in hot metal and its effects on desulfurization,” *Iron Steel Technol.*, vol. 2, no. 11, pp. 65–74, 2005.
- [15] F.N.H. Schrama *et al.*, “Lowering iron losses during slag removal in hot metal desulphurisation without using fluoride,” *Ironmak. Steelmak.*, vol. 47, no. 5, pp. 464–472, 2020, doi: 10.1080/03019233.2020.1747778.
- [16] Y. Sun, Z. Zhang, L. Liu, and X. Wang, “Multi-Stage control of waste heat recovery from high temperature slags based on time temperature transformation curves,” *Energies*, vol. 7, no. 3, pp. 1673–1684, 2014, doi: 10.3390/en7031673.

5 Slag modifiers without fluoride

This chapter is based on the following publication:

F.N.H. Schrama, F. Ji, A. Hunt, E.M. Beunder, R. Woolf, A. Tuling, P. Warren, J. Sietsma, R. Boom, Y. Yang, “Lowering iron losses during slag removal in hot metal desulphurisation without using fluoride”, *Ironmaking and Steelmaking*, Vol. 47, No. 5, **2020**, p 464-472

To lower the iron losses of the hot metal desulphurisation (HMD) process, slag modifiers can be added to the slag. These slag modifiers decrease the apparent viscosity of the HMD slag, thus allowing entrapped iron droplets to drip back into the metal bath. Most common slag modifiers in industry contain fluoride as a fluidiser, as this effectively lowers the melting point of the slag. However, fluoride leads to a higher magnesium consumption and has health, safety and environment issues. Fluoride-free alternatives like nepheline syenite (NS) and fly ash (or pulverised fuel ash, PFA) can decrease the slag’s viscosity by decreasing its basicity, and thus its solid fraction, and by addition of alkali metal oxides, which break the SiO₂ networks without increasing the slag’s solid fraction.

Experiments with HMD slags containing CaF₂, NS and PFA and without any slag modifier were performed for slags with a high and an average basicity. The melting points of the slags were measured with a heating microscope and their viscosities at a temperature range between 1250-1600 °C were measured with a viscometer. The experimental results are compared with FactSage calculations.

It can be concluded that both PFA and NS can be used as alternative slag modifiers for the industrial HMD process, as reasonable amounts of both are sufficient to reach the same lower apparent viscosities and melting points as with CaF₂.

5.1 Introduction

As discussed in Chapters 3 and 4, iron losses during the slag removal are the largest costs of the hot metal desulphurisation (HMD) process. Typically, during the slag skimming, more than half of the removed material is iron rather than slag. This means that, depending on the process scale, 500-3000 kg of iron is removed per heat. On an annual basis, millions of euros worth of iron is skimmed off in the HMD process and only part of that can be recovered during slag processing. Furthermore, in the previous chapters it was explained that most of the iron losses can be categorised as entrainment losses and colloidal losses, both being of comparable size [1–6].

Colloidal iron losses can be reduced by having a less viscous slag, so the entrapped iron will sink back more easily into the metal bath. The liquidity and viscosity of the slag can be made more beneficial by increasing the slag temperature or by changing the slag composition. As it is not economically viable to heat up the slag, many steel plants all over the world use slag modifiers to change the slag composition in order to decrease its apparent viscosity, which depends on the solid fraction and the viscosity of the liquid fraction. Often, fluoride-containing slag modifiers like fluorspar (CaF_2), sodium cryolite (Na_3AlF_6) or potassium cryolite (KAlF_4) are used [7]. A problem with fluoride is that it is environmentally unfriendly and in the magnesium-lime co-injection HMD process, fluoride can decrease the magnesium efficiency, because the fluoride reacts with the magnesium to form MgF_2 [1]. A fluoride-free slag modifier that would decrease the apparent viscosity of the slag just as effectively would therefore be beneficial for the industrial HMD process. In literature nepheline syenite (NS) [4–6] and fly ash (or pulverised fuel ash, PFA) [8] are reported as successful fluoride-free slag modifiers for the HMD process.

5.2 Theory

5.2.1 HMD slag

Hot metal from the blast furnace typically contains 0.03-0.06 wt% sulphur, therefore the hot metal needs to be desulphurised before it is charged into the converter. In the HMD process, reagents (usually Mg, CaO and/or CaC_2) are injected or added to the hot metal, where they react with the dissolved sulphur. The formed sulphides (CaS and MgS) end up in the slag layer that floats on top of the hot metal. This slag is then skimmed off to permanently remove the sulphur. The amount of the formed slag is typically 0.2-0.5 wt% of the hot metal. Typically, the hot metal arrives at the steel plant together with 0.5-1 wt% carryover slag from the blast furnace, so the HMD slag prior to skimming consists for roughly one third of slag formed at HMD and two third of blast furnace (BF)

carryover slag [9, 10]. Table 5.1 shows typical slag compositions at the HMD process before injection (BF carryover slag) and after injection.

Table 5.1: Typical slag compositions for BF carryover slag and HMD slag after injection (without slag modifier). Composition in wt%, excluding iron.

	BF carryover	HMD final
CaO	38	37
SiO ₂	37	28
Al ₂ O ₃	14	11
MgO	8.9	13
TiO ₂	0.6	0.5
MnO	0.14	0.11
K ₂ O	0.45	0.34
Na ₂ O	0.32	0.25
CaS	0.95	9.8

Figure 5.1 shows that the HMD final slag has a high solid fraction at typical HMD temperatures (1300-1450 °C) and that the slag's solid fraction increases during the HMD process. Note that the exact composition of Table 5.1 is used for the FactSage calculations that will be presented in this paper, so no slag modifier or FeO, which would decrease the solid fraction, is considered.

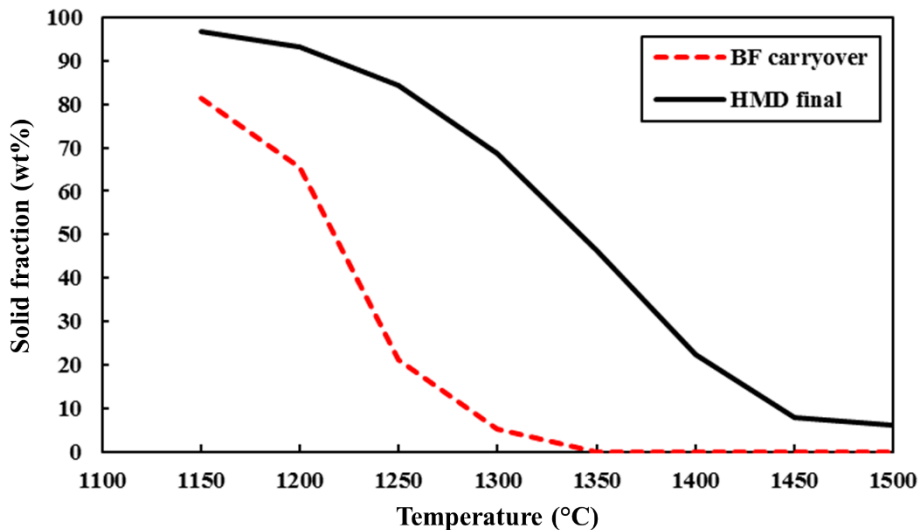


Figure 5.1: Solid fraction of the BF carryover slag and the HMD final slag (see Table 5.1) at different slag temperatures (FactSage 7.3 [11]).

5.2.2 Iron loss

HMD slags with a higher apparent viscosity (η_{slag} , in Pa·s) have higher colloidal iron losses, as entrapped iron droplets cannot easily drip back into the bath. Slags with a very low η_{slag} will have higher entrainment iron losses, because it will be harder to skim off a very liquid slag. Therefore, the most ideal slag would have a low η_{slag} during injection but would be solid during skimming (after all the iron dripped out of the slag). However, such a large physical change of the slag in such a short time will be difficult to accomplish in practice, even with the use of slag modifiers. Since typically the overall iron losses increase at an increasing η_{slag} , a slag with a low η_{slag} is desired. The η_{slag} depends on the volume fraction of the solids ($\varphi_{s,slag}$) and the viscosity of the liquid fraction (η_0). For slags with $\varphi_{s,slag} < 5$ vol%, η_{slag} can be determined with the Einstein-Roscoe equation [2, 12, 13]:

$$\eta_{slag} = \eta_0 (1 - \alpha \cdot \varphi_{s,slag})^{-n} \quad (5.1)$$

Here α and n are empirical constants. Roscoe [12] proposes $\alpha = 1.35$ and $n = 2.5$ when assuming all solid particles are spherical and of uniform size. The values of these constants vary with temperature and composition [14]. For $\varphi_{s,slag} > 10$ vol%, the apparent viscosity of the slag solely depends on the solid fraction and the particles' size, shape and distribution.

5.2.3 Basicity

The viscosity of the slag is influenced by its basicity. In industry, basicity of the slag is typically determined via $B2$ (Equation 5.2) or $B4$ (Equation 5.3) [15]:

$$B2 = \frac{m_{CaO}}{m_{SiO_2}} \quad (5.2)$$

$$B4 = \frac{m_{CaO} + 1.4m_{MgO}}{m_{SiO_2} + 0.6m_{Al_2O_3}} \quad (5.3)$$

Here m_x is the mass of component x in the slag. Although $B4$ is more accurate, $B2$ is used more often in industry, as it is simpler and unambiguous, therefore in this chapter $B2$ is used. Both empirical definitions are practical for industrial use, but to better understand basicity, the concept of network formers and network modifiers is to be introduced. In basic slags, the slag structure is based on ionic bonding, rather than covalent bonding. Ionic bonds are weaker than covalent bonds, therefore basic oxides, like CaO and MgO, act as network modifiers or network breakers, while acid oxides, like SiO₂ and Al₂O₃, act as network formers. A slag with a high fraction of network formers, so with a low basicity, will be more polymerised and thus have a higher viscosity. Adding network modifiers to this slag will reduce the polymerisation of the slag and reduce the viscosity of the

liquid fraction (η_0). A slag with mostly network modifiers, so with a high basicity, has a higher crystallised fraction. When adding network formers to such a basic slag, the activation energy for crystallisation is increased. For very basic slags this means that the solid fraction ($\varphi_{s,slag}$) will be lowered when network formers are added [15, 16]. Equation 5.1 shows that both η_0 and $\varphi_{s,slag}$ influence η_{slag} and there will be an optimal basicity for the lowest η_{slag} .

As can be seen in Table 5.1, a typical HMD slag is basic (for this example $B4 = 1.6$ and $B2 = 1.3$). The FactSage calculations for the typical HMD slag from Table 5.1 at 1350 °C, only changing $B2$, show that the solid fraction (including solid CaS) is lowered by lowering $B2$ (see Figure 5.2). Furthermore, since $\varphi_{s,slag} > 10$ vol%, lowering the solid fraction is the only way to lower η_{slag} .

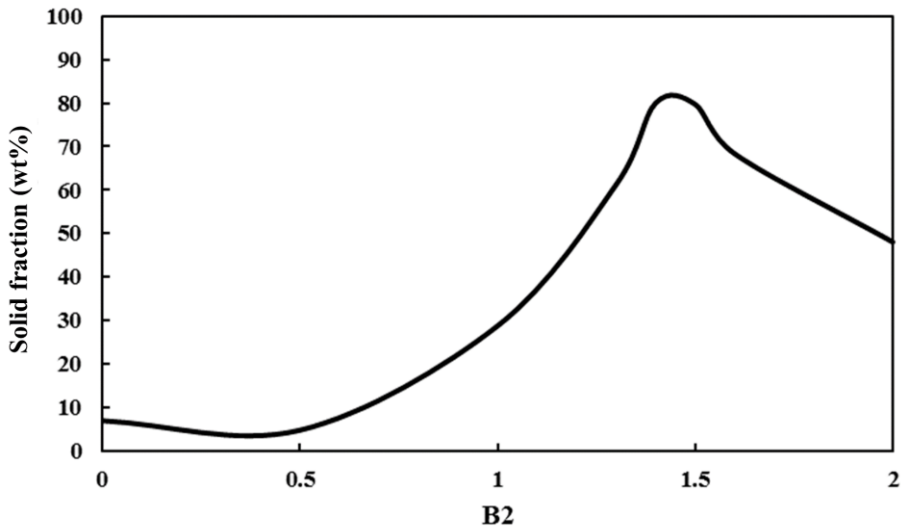


Figure 5.2: Solid fraction (in wt%) of typical HMD slag for different $B2$ values at 1350° C. Determined with FactSage [11].

5.2.4 Slag modifiers

Adding acid network formers, like SiO_2 or Al_2O_3 , decreases the apparent viscosity of HMD slag because they lower its melting temperature. However, they increase the viscosity of the liquid fraction of the slag. Adding alkali metal oxides, like Na_2O or K_2O , which are strong basic network modifiers, will decrease the apparent viscosity of HMD slag as well. Because alkali metal oxides are network modifiers, they decrease η_0 , just like CaO does. Unlike CaO, alkali metal oxides decrease the solid fraction of the slag. Alkali metal oxides are

therefore excellent HMD slag modifiers. In addition, they increase the sulphur capacity of the slag [17].

Fly ash, or pulverised fuel ash (PFA) is the light fraction of the ash from coal fired power plants or waste incineration plants. Although PFA compositions vary strongly, it is typically rich in SiO_2 and Al_2O_3 , but contains only low fractions of Na_2O and K_2O (Table 5.2). PFA decreases the HMD slag viscosity by decreasing its basicity and thus its solid fraction. Nephelene syenite (NS) is a natural mineral which is mined on all continents. Like PFA it consists for a large part of SiO_2 and Al_2O_3 , but in addition it is rich in K_2O and Na_2O . NS therefore does not only decrease η_{slag} of HMD slag by decreasing its B_2 , and thus its solid fraction, but it also lowers the η_0 thanks to the alkali metal oxides.

Table 5.2: Typical compositions (in wt%) of NS and PFA.

	NS	PFA
Fe	0.1	6.1
CaO	1.1	3.1
SiO_2	58	62
Al_2O_3	25	22
MgO	0.2	2.3
P_2O_5	0.02	0.4
K_2O	8.9	2.3
Na_2O	8.5	1.0
TiO_2	0.1	1.1
Cr_2O_3	0.04	0.06
CaS	-	0.07
ZnO	0.06	0.09

Fluoride-containing slag modifiers have been widely used for decades in industry. Fluoride decreases the slag's liquidus temperature and its viscosity. However, fluoride does not act as a network modifier in the sense that it breaks down the SiO_2 polymeric network. Instead fluoride tends to be calcium driven in an HMD slag and forms CaF^+ ion pairs, which break up divalent calcium ions that bind silicate anions (thus forming bridges between two silicate structures). This effectively lowers the slag's viscosity [18, 19]. This means that fluoride is more effective as a slag modifier for slags with a higher basicity, as these have more calcium-silicate bridges.

The disadvantage of fluoride-containing slag modifiers is that they decrease the desulphurisation efficiency of magnesium. The fluoride reacts with the injected

magnesium to form MgF_2 , thus preventing it from reacting with the dissolved sulphur. This phenomenon has been described in more detail in an earlier publication [1]. In addition to that, fluoride can have a negative influence on human health and the environment. Therefore, the use of fluoride-containing slag modifiers is restricted in several countries.

5.3 Experiments

5.3.1 Slag preparation

To study the process of nepheline syenite or fly ash affecting the slag's viscosity and melting point, experiments with synthetic HMD slag, without slag modifier, with CaF_2 , with NS and with PFA were done at different basicity. The compositions of the tested materials are given in Table 5.3. Slags 1.1-1.4 have a B_2 of 1.8 and Slags 2.1-2.4 have a B_2 of 1.6.

Table 5.3: Compositions (in wt%) of the synthetic HMD slags with different modifiers used for the experiments, determined by XRF.

Slag	1.1	1.2	1.3	1.4	2.1a	2.1	2.2	2.3	2.4
CaO	46.24	44.82	45.27	44.89	43.06	43.63	43.16	42.94	43.04
SiO ₂	24.95	24.64	25.06	25.16	27.72	26.79	26.62	27.36	27.35
Al ₂ O ₃	9.17	9.08	9.26	9.47	9.66	9.81	9.64	9.96	9.84
MgO	14.50	14.41	14.45	14.47	14.85	14.80	14.73	14.48	14.54
MnO	1.34	1.35	1.35	1.34	1.44	1.39	1.38	1.38	1.37
K ₂ O	0.00	0.00	0.07	0.02	0.00	0.01	0.01	0.10	0.03
Na ₂ O	0.06	0.05	0.11	0.07	0.11	0.19	0.17	0.24	0.16
CaS	3.51	4.64	4.09	4.12	2.71	2.83	3.09	2.99	3.03
CaF ₂	0.00	0.66	0.00	0.00	0.00	0.00	0.62	0.00	0.00
Fe ₂ O ₃	0.24	0.25	0.24	0.32	0.26	0.32	0.35	0.32	0.42
B ₂ O ₃	0.00	0.10	0.10	0.14	0.10	0.10	0.10	0.10	0.10
Modifier	none	CaF ₂	NS	PFA	none	none	CaF ₂	NS	PFA

The composition of the slags without slag modifiers (master slags) are based on slag composition measurements at Tata Steel in Port Talbot (UK). To prepare the master slags, reagents of CaCO_3 , SiO_2 , Al_2O_3 , MgO , MnO , K_2CO_3 , Na_2CO_3 and CaS were weighed and mixed in a Tema mill for 20 seconds. The mixed reagents were then put into a graphite crucible and heated to 1600 °C in an induction furnace to prefuse. After 10 minutes at 1600 °C, the furnace was cooled to room temperature with the crucible and slag inside. Once cooled, the prefused slag was pulverised in a Tema mill for 60 seconds. The prefused powdered slag was then decarburised in an alumina crucible inside a muffle furnace at 700 °C for 18 hours

Part II Optimal hot metal desulphurisation slag

to remove any residual carbon that had been absorbed from the graphite crucible during prefusing.

For the synthetic slag with CaF_2 a concentration typical for industry was added. For the synthetic slags with high basicity (1.3 and 1.4), an equivalent of 20 kg per heat of NS or PFA, respectively, was added. For the lower basicity slags (Slags 2.3 and 2.4), an equivalent of 25 kg per heat of NS or PFA, respectively, was added. For the modified slags, the actual slag modifiers were added to the master slags and prefused again. For Slags 2.2-2.4, Slag 2.1 was used as the master slag. Slag 2.1a was only used for reference.

5.3.2 Viscosity measurements

For the slag viscosity measurements, a Bähr VIS-403 HF rotational viscometer was used (a schematic of the setup was presented in Chapter 4, Figure 4.10). In this setup the torque applied to a spindle that is rotating at a constant speed, while being submerged in a known volume of the melted slag, is measured. The viscosity is calculated as the ratio of shear stress (τ , in Pa) to shear rate ($\dot{\gamma}$; in s^{-1}). For a Newtonian fluid contained within two concentric cylinders (Taylor-Couette flow), the shear rate is set according to:

$$\dot{\gamma} = \omega_s \cdot \frac{2R_c^2}{R_c^2 - R_s^2} \quad (5.4)$$

The resulting shear stress is calculated by:

$$\tau = \frac{Tor}{2\pi \cdot R_s^2 \cdot h_s} \quad (5.5)$$

Where ω_s is the rotational speed of the spindle (rad/s), R_c and R_s are the radius of the crucible and the spindle respectively (m), Tor is the measured torque (N·m) and h_s is the height of the spindle head (m).

The Bähr VIS-403 HF viscometer was calibrated at room temperature using three certified silicon oils with viscosities between 0.1 and 1.0 Pa.s. Regression analysis was used to determine the calibration curve. The calibration was specific to the rotation speed selected for the tests. The viscosity measurement has a typical error of 10 %.

Crucibles made from different materials were tested for the viscosity measurements. A zirconia crucible was not suited, because when the slag inside the crucible was melted, the crucible started to leak at the point where the bottom is glued to the wall. A molybdenum crucible was better suited, although the crucibles initially broke when cooling them down after the experiment due to slag expansion for slag 1.1. This was caused by the phase transformation of dicalcium

silicate (C2S) from β to γ during cooling. By doping the other slags with 0.1 wt% B_2O_3 (0.14 wt% for slag 1.4), the crucibles survived cooling down. Lowering the CaO content for Slags 2.1-2.4 also helped preventing the $\beta \rightarrow \gamma$ phase transformation of C2S during cooling.

For every experiment, 24 g of prefused powdered slag was put into the crucible and inserted into the rotational viscometer. The oxygen level in the chamber was lowered by an argon purge at 200 ml/min, to protect the crucible and spindle from oxidation. The temperature inside the furnace was increased to 1600 °C after which the rotating spindle was submerged into the molten sample. A constant rotation speed of 400 rpm was maintained throughout the experiment. The sample was then cooled at 10 °C/min until the sample reached a maximum torque of 25 mNm.

5.3.3 Melting point measurements

For the melting point measurements, a Misura HM2-1600 heating microscope was used. Samples were prepared using a steel die to manually compress prefused powdered slag into cylinders of 3 mm in height and 2 mm in diameter. The samples were then placed onto an alumina plate and inserted into the horizontal tube furnace. The samples were heated to 1100 °C at 50 °C/min, after which they were heated to the melting point at 6 °C/min. The device acquires and stores images of the sample at 2 °C intervals during the heating cycle. During the heating cycle, all the dimensional parameters were measured automatically in order to identify phase transitions of the material. The sintering temperature of the sample is defined as the temperature where the sample height is less than 95 % of the original height. The softening temperature is defined as the temperature where the corners of the sample soften. This is a subjective measure, but it is automatically done by the device's software, so it is reproducible. The melting temperature of the sample is defined as the temperature where the base of the sample is three times larger than the sample height, which is according to the DIN 51730 standard. The melting point measurement has a typical error of ± 4 °C.

5.4 Results

5.4.1 Viscosity measurements

As a reference, a slag sample from the Tata Steel HMD station in Port Talbot (UK), where $KAlF_4$ is used as slag modifier (the fluoride content is proportional to 0.6 wt% CaF_2 in the post HMD slag), was analysed with the viscometer. Figure 5.3 gives the apparent viscosity as a function of temperature. It should be noted that, unlike the synthetic slags, the measured slag also contains FeO , which lowers the slag viscosity.

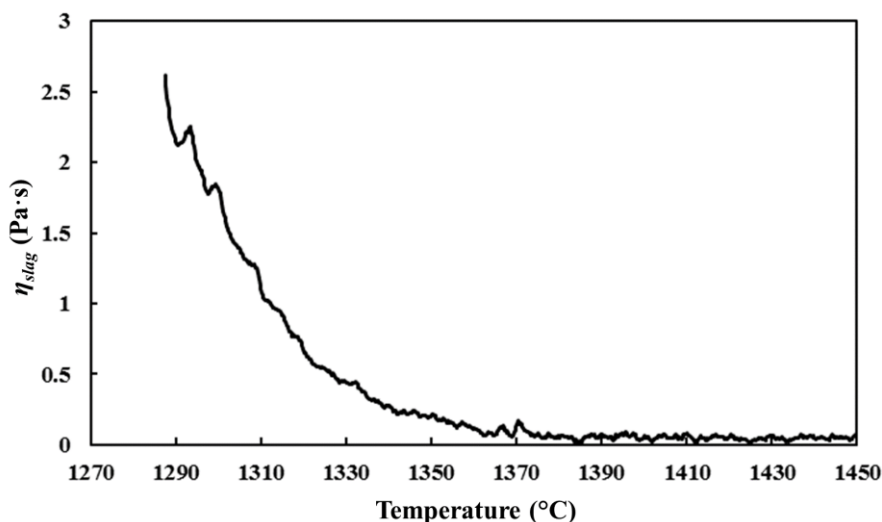


Figure 5.3: Viscosity measurement of HMD slag from Tata Steel Port Talbot (UK) at different slag temperatures (October 2018).

Figure 5.4 gives the apparent viscosity of Slags 1.1-1.4 as a function of temperature. Compared to the real HMD slag from Figure 5.3, the viscosities of the synthetic slags are much higher at similar temperatures. This is partly because no FeO is added to the slag, but also because of a higher basicity of the synthetic slags (Slags 1.1-1.4) compared to the reference slag sample. The measurements clearly show that at lower temperatures PFA and CaF₂ significantly lower the slag's viscosity, whereas NS has no significant effect on the viscosity. At higher temperatures, all slags are liquid, so their viscosities are all around 0.1 Pa·s.

Figure 5.5 gives the measured viscosities of Slags 2.1-2.4, in which more slag modifier is added than in Slags 1.1-1.4, at different temperatures. Although the viscosities are lower than for Slags 1.1-1.4, they are still higher than for the reference industrial HMD slag sample. The basicity is now comparable, but still no FeO was added to the synthetic slags, which explains the difference with the HMD slag. This measurement clearly shows an effect of all slag modifiers on the slag's viscosity at lower temperatures (below 1400 °C), where PFA has the largest influence and CaF₂ the smallest.

5. Slag modifiers without fluoride

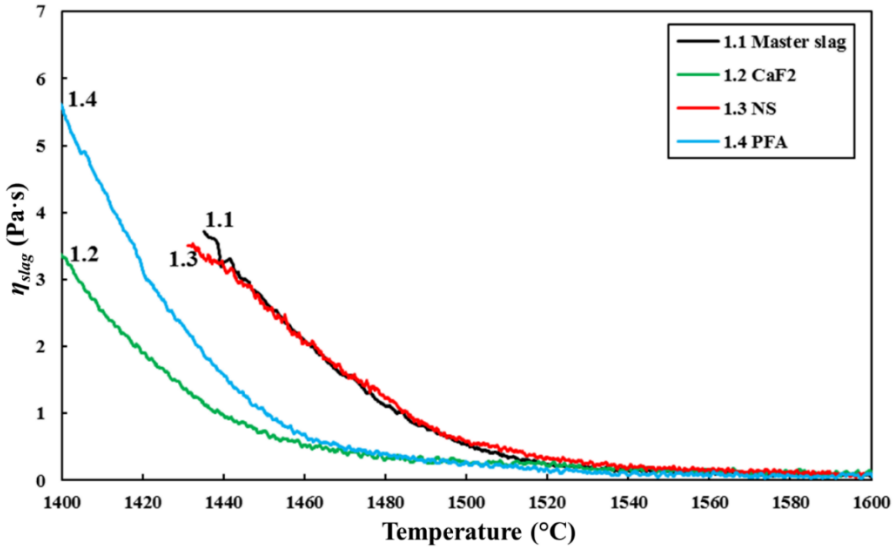


Figure 5.4: Viscosity measurements for Slags 1.1 (master; black), 1.2 (with CaF_2 ; green), 1.3 (with NS; red) and 1.4 (with PFA; blue) at different temperatures.

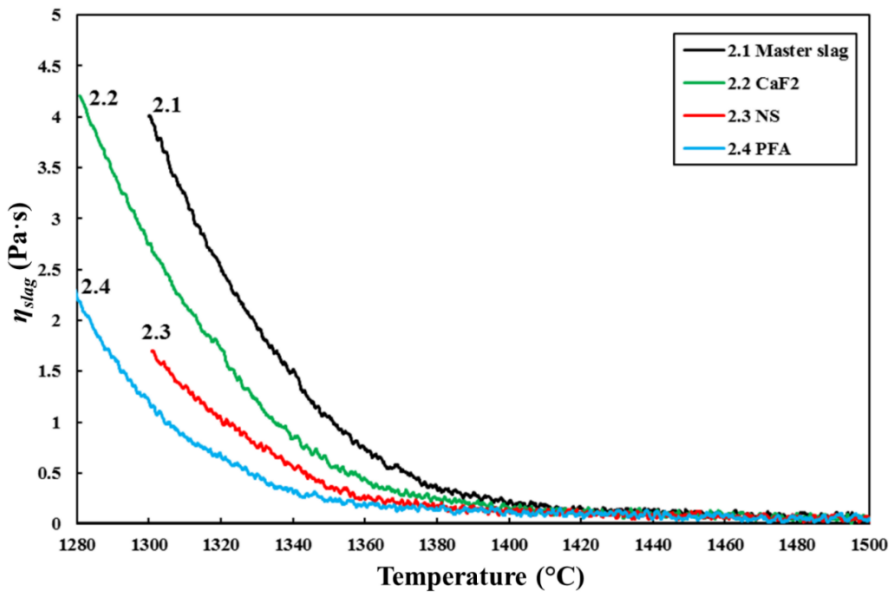


Figure 5.5: Viscosity measurements for Slags 2.1 (master slag; black), 2.2 (CaF_2 ; green), 2.3 (NS; red) and 2.4 (PFA; blue) at different temperatures.

5.4.2 Melting point measurements

The reference HMD slag sample from the Tata Steel HMD station in Port Talbot was analysed with the heating microscope as well, to determine its melting point. Figure 5.6 shows that the slag starts to soften at 1326 °C and melts at 1334 °C.

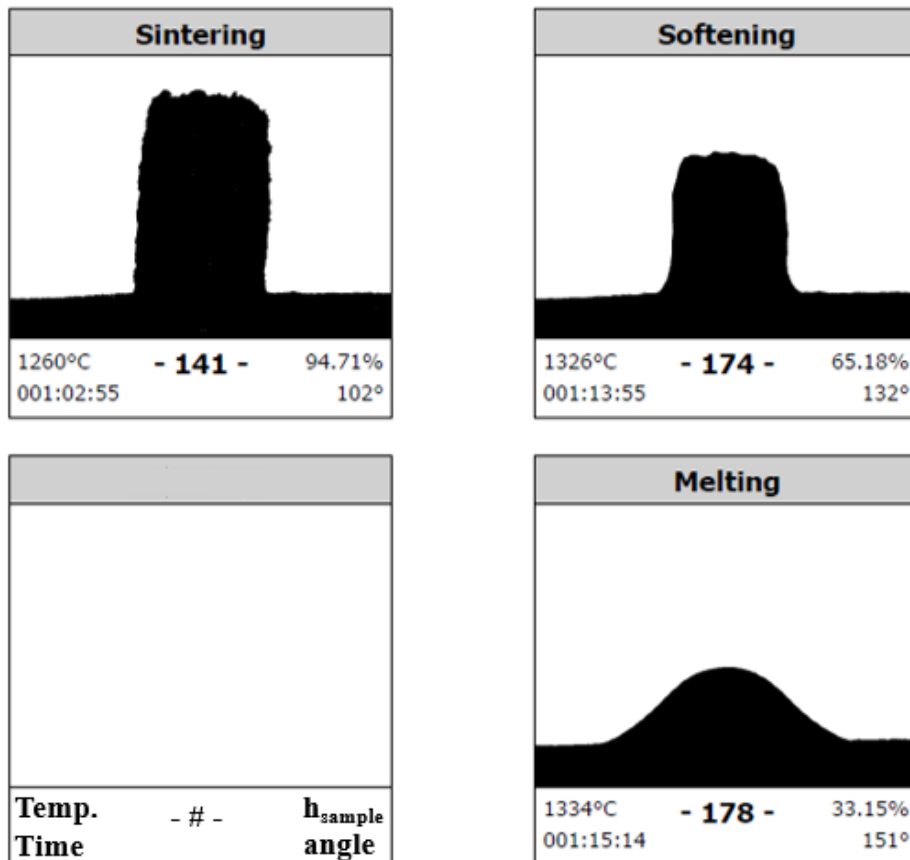


Figure 5.6: Melting point measurement of HMD slag from Tata Steel Port Talbot.

The melting temperature (T_{melt}) of all synthetic slags was also determined with the heating microscope. For reference the equilibrium liquidus temperature (T_{liq}) is calculated with FactSage (consortium database CON2) [11].

Table 5.4 gives the calculated T_{liq} and measured T_{melt} values for all slags, including their difference with the relevant master slag (ΔT).

Table 5.4: T_{liq} for all synthetic slags, determined with FactSage and their measured T_{melt} , determined with the heating microscope. ΔT gives the difference with the relevant master slag.

Slag	T_{liq} (°C), equilibrium	ΔT (°C)	T_{melt} (°C), measured	ΔT (°C)	Comment
0			1334		Industrial slag
1.1	1591	-	1445	-	Master
1.2	1533	58	1394	51	CaF ₂
1.3	1559	32	1418	27	NS
1.4	1543	48	1426	19	PFA
2.1b	1465	-	1424	-	Master
2.2	1433	32	1414	10	CaF ₂
2.3	1443	22	1406	18	NS
2.4	1446	19	1412	12	PFA

5.5 Discussion

5.5.1 Experimental results

The large difference between the industrial HMD slag sample and the synthetic slags, both for the apparent viscosity and for the melting temperature, shows that the results with the synthetic slags cannot be used to quantitatively predict the effect of the tested slag modifiers in an industrial HMD slag. This is because the slag sample contains FeO_x and has a different basicity from the synthetic slags. Finally a HMD slag under industrial conditions is never homogeneous, both in composition and temperature, as is discussed in Chapter 3. This means that the laboratory results should be discussed semi-quantitatively.

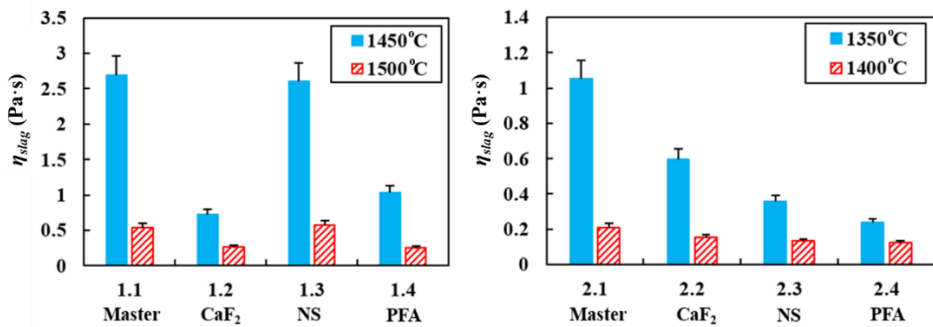


Figure 5.7: Measured viscosities for Slags 1.1-1.4 at 1450 °C and 1500 °C (left) and for Slags 2.1-2.4 at 1350 °C and 1400 °C (right).

The viscosity measurements show that for a high-basicity slag and high temperatures (see Figure 5.7, left), NS does not decrease the slag viscosity. At a

Part II Optimal hot metal desulphurisation slag

high basicity, η_0 will already be low, while the high η_{slag} is mainly caused by the high solid fraction. Adding alkali oxides, which lower η_0 , will not lead to a significantly lower η_{slag} under these conditions. PFA and CaF_2 significantly lower the slag viscosity. At a high basicity, fluoride has a larger effect on η_{slag} , as it breaks down the divalent calcium bridges (see Section 5.2.4). Adding SiO_2 and Al_2O_3 via PFA will lower the basicity, so this is also an effective way to lower the slag viscosity under the given conditions. However, NS also adds SiO_2 and Al_2O_3 to the slag, albeit less than PFA does, so it is an unexpected result that NS does not seem to have any effect at all on η_{slag} at high basicity. FactSage calculations predict that NS (under the same circumstances as Slag 1.3) does lower the solid fraction of the slag compared to Slag 1.1, so it should have a significantly lower η_{slag} than Slag 1.1. Possibly something went wrong with the composition of Slag 1.3 (NS), as the NS did not seem to influence the break temperature (T_{break}) of the high basicity slag either (see Figure 5.8, left), whereas it did influence T_{break} for the medium basicity slag.

The viscosity measurement results for lower basicity slags and lower temperatures (see Figure 5.7, right) give another picture. Due to the lower basicity, most of the slag, with or without slag modifier is already liquid at 1400 °C. As discussed in Chapter 3, the solid fraction of the slag has the highest influence on η_{slag} . At 1350 °C there are clear differences, as part of the slag is solid. All slag modifiers lower the viscosity, but PFA does that most successfully. The difference between CaF_2 and PFA can be explained by the fact that at a lower basicity, the divalent calcium bridge breaking by fluoride has less effect on the viscosity, as there are fewer calcium bridges to break.

The lower viscosity for slags with PFA compared to slags with NS is more remarkable, as the network-modifying effect of the surplus of alkali metal oxides in NS seems less successful in lowering the viscosity than the surplus of FeO_x in PFA. The small difference in basicity between Slag 2.3 (NS) and Slag 2.4 (PFA), cannot explain the difference in measured viscosity. Besides as Slag 2.3 has a lower B_2 than Slag 2.4, it would be expected that Slag 2.3 has the lowest viscosity, which is not the case.

Figure 5.8 shows the effect of the different slag modifiers on T_{melt} compared to the master slag without slag modifier. As a reference, the break temperature (T_{break}) from the viscosity measurements is added in the left figure. T_{break} is the temperature at which η_{slag} increases at a faster rate due to crystallisation and the formation of a two phase melt. Under ideal conditions with a single substance, T_{break} is equal to T_{melt} . T_{break} can be used as an alternative way to look at T_{melt} .

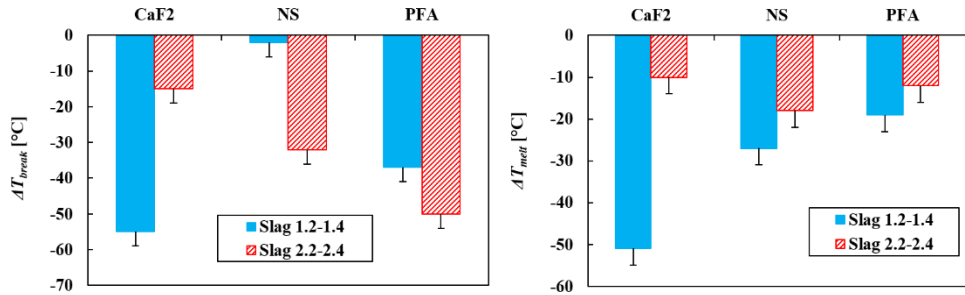


Figure 5.8: Difference in break temperature (ΔT_{break} ; left) and melting point (ΔT_{melt} ; right) between the master slag and slag with a slag modifier.

When looking at the effect of the slag modifiers on the slag's melting point (Figure 5.8), a similar image as with the viscosity is observed. At high basicity slags CaF_2 decreases the slag melting point the most, whereas at a lower slag basicity NS and PFA are more effective in lowering T_{melt} , albeit that the differences are smaller. This suggests that T_{melt} is influenced in a similar way as the viscosity by the different slag modifiers. Note that the measured T_{break} of Slag 1.3 (NS) is doubtful. As was discussed earlier, its viscosity measurements gave unexpected results. As PFA has the highest influence on the slag basicity compared to NS, it consequently has the largest effect on T_{melt} . This is in line with the theory.

The results for slags with different basicity show similar trends and are in accordance with the theory, apart from the measurements of Slag 1.3 (NS). Also, the results from the viscosity measurements and the melting point measurements are in agreement with each other. It is therefore concluded that the observed trends for the different slag modifiers are reliable.

5.5.2 Industrial use of slag modifiers

The slag compositions that were measured in this research are representative of adding realistic amounts of slag modifier in an industrial HMD. For a heat size of around 300 t, the synthetic slags represent roughly the addition of 15 kg CaF_2 , 20 kg of NS and 25 kg of PFA, respectively. The experimental results show that adding a relatively small amount of slag modifier, compared to a total slag weight of around 2500 kg, has a large influence on the slag's viscosity. This implies that in an industrial HMD process, iron losses can be lowered by a relatively small addition to the slag. When looking purely at the slag modifying aspect, all three slag modifiers can be used effectively in an industrial HMD process.

For an industrial use of slag modifiers, more considerations need to be taken into account. As mentioned in Section 5.2.4, the use of fluoride-containing slag modifiers is restricted due to health, safety and environmental reasons. Besides fluoride addition leads to a higher magnesium consumption. NS and PFA are fluoride-free. Of these two, PFA has the lower cost to achieve the same low viscosity. However, as PFA is a by-product from coal fired power plants or waste incinerators, its composition and size can in practice be less consistent. Furthermore, the ash could contain unwanted components, like heavy metals, which could make the resulting slag difficult to recycle or even hazardous for health, safety and environmental reasons. NS has, as it is a mined mineral, fewer problems with unwanted or unexpected impurities. Also, as it is mined on all continents, it is widely available. However, the alkali metal oxides in NS, which have the desired effect on the slag's viscosity, also make the slag less suitable for recycling. One of the few options to recycle HMD slag is to recharge it to the BF. Thus the iron in the slag is recovered and the composition of HMD slag is quite close to that of blast furnace (BF) slag. The high sulphur content of the HMD slag is not problematic, as the BF is an excellent desulphuriser [9]. Alkali metals are problematic for the BF, as they can accumulate inside, due to their low melting point. This can lead to skull formation on the BF walls [20]. The addition of alkali metals, also in the form of oxides, is therefore restricted.

5.6 Conclusions

In this research slag modifiers were investigated and compared, the objective being to lower the apparent viscosity of slag in the hot metal desulphurisation process in order to decrease iron loss to the slag. Because of the restrictions of fluoride-containing slag modifiers, two fluoride-free slag modifiers, nepheline syenite and pulverised fuel ash, were compared with CaF_2 and with a slag without any slag modifier. The main conclusions of this research on synthetic HMD slags are as follows:

- Both PFA and NS are viable alternatives for fluoride-containing slag modifiers, lowering the apparent viscosity like CaF_2 , to reduce iron losses at the HMD.
- At higher basicity and temperature, fluoride-based slag modifiers are more effective. Under these conditions, alkali metal oxides will not have a significant effect on the slag's apparent viscosity. Lowering the slag's basicity by adding SiO_2 and Al_2O_3 does lower the apparent viscosity of the HMD slag.
- At higher temperatures (typically above $1350\text{ }^\circ\text{C}$), the apparent viscosity of the HMD slag is already low enough without slag modifiers, as a result

of the low solid fraction. Slag modifiers will not significantly contribute to lower iron losses above these temperatures.

- Relatively small changes in the HMD slag composition can lead to large effects on the slag's apparent viscosity, and thus iron loss to the slag. This makes the use of slag modifiers for an industrial HMD viable.

5.7 References

- [1] F.N.H. Schrama *et al.*, “Effect of KAIF₄ on the efficiency of hot metal desulphurisation with magnesium,” in *European Oxygen Steelmaking Conference (EOSC)*, 2018, p. EOSC021.
- [2] F.N.H. Schrama *et al.*, “Slag optimisation considering iron loss and sulphide capacity in hot metal desulphurisation,” in *Proceedings of the 7th International Congress on the Science and Technology of Steelmaking*, 2018, p. ICS131.
- [3] F.N.H. Schrama, B. van den Berg, and G. Van Hattum, “A comparison of the leading hot metal desulphurization methods,” in *Proceedings of the 6th International Congress on the Science and Technology of Steelmaking*, 2015, pp. 61–66.
- [4] M. Magnelöv, J. Eriksson, J. Drugge, J. Björkvall, and B. Björkman, “Investigation of iron losses during desulphurisation of hot metal utilising nepheline syenite,” *Ironmak. Steelmak.*, vol. 40, no. 6, pp. 436–442, 2013, doi: 10.1179/1743281212Y.0000000067.
- [5] M. Magnelöv, A. Carlsson-Dahlberg, L. Gustavsson, J. Björkvall, and B. Björkman, “Iron losses during desulphurisation of hot metal utilising co-injection of Mg and CaC₂ combined with nepheline syenite,” *Ironmak. Steelmak.*, vol. 42, no. 7, pp. 525–532, 2015, doi: 10.1179/1743281214Y.0000000257.
- [6] A.F. Yang, A. Karasev, and P.G. Jönsson, “Effect of Nepheline Syenite on Iron Losses in Slags during Desulphurization of Hot Metal,” *Steel Res. Int.*, vol. 87, no. 5, pp. 599–607, 2016, doi: 10.1002/srin.201500154.
- [7] S. Kitamura, “Hot Metal Pretreatment,” in *Treatise on Process Metallurgy*, vol. 3, S. Seetharaman, Ed. Oxford (UK): Elsevier, 2014, pp. 177–221.
- [8] J. Zhang, Y.-W. Cong, and S.-H. Whang, “Research and Development on Slag Conglomeration Agent Used for Desulphurization of Hot Metal (in Chinese),” *Shandong Metall.*, vol. 27, no. 2, pp. 31–32, 2005.
- [9] F.N.H. Schrama, E.M. Beunder, B. van den Berg, Y. Yang, and R. Boom,

- “Sulphur removal in ironmaking and oxygen steelmaking,” *Ironmak. Steelmak.*, vol. 44, no. 5, pp. 333–343, 2017, doi: 10.1080/03019233.2017.1303914.
- [10] H.-J. Visser, “Modelling of injection processes in ladle metallurgy,” (PhD thesis) Delft University of Technology, Delft (NL), 2016.
- [11] CRCT (Canada) & GTT (Germany), “FactSage 7.3,” 2020. [Online]. Available: www.factsage.com.
- [12] R. Roscoe, “The viscosity of suspension of rigid spheres,” *Br. J. Appl. Phys.*, vol. 3, no. Aug, pp. 267–269, 1952.
- [13] S.-H. Seok, S.-M. Jung, Y.-S. Lee, and D.-J. Min, “Viscosity of Highly Basic Slags,” *ISIJ Int.*, vol. 47, no. 8, pp. 1090–1096, 2007, doi: 10.2355/isijinternational.47.1090.
- [14] S. Wright, L. Zhang, S. Sun, and S. Jahanshahi, “Viscosity of a CaO-MgO-Al₂O₃-SiO₂ melt containing spinel particles at 1646K,” *Metall. Mater. Trans. B*, vol. 31, no. 1, pp. 97–104, 2000, doi: 10.1007/s11663-000-0134-8.
- [15] E.T. Turkdogan, *Fundamentals of steelmaking*. London (UK): The Institute of Materials, 1996.
- [16] G.A. Brooks, M.M. Hasan, and M.A. Rhamdhani, “Slag Basicity: What Does It Mean?,” in *10th International Symposium on High-Temperature Metallurgical Processing*, 2019, pp. 297–308, doi: 10.1007/978-3-030-05955-2_28.
- [17] E. Moosavi-Khoonsari and I.H. Jung, “Thermodynamic Modeling of Sulfide Capacity of Na₂O-Containing Oxide Melts,” *Metall. Mater. Trans. B*, vol. 47, no. 5, pp. 2875–2888, 2016, doi: 10.1007/s11663-016-0749-z.
- [18] M. Hayashi, N. Nabeshima, H. Fukuyama, and K. Nagata, “Effect of fluorine on silicate network for CaO-CaF₂-SiO₂ and CaO-CaF₂-SiO₂-FeOx glasses,” *ISIJ Int.*, vol. 42, no. 4, pp. 352–358, 2002, doi: 10.2355/isijinternational.42.352.
- [19] K.C. Mills and S. Sridhar, “Viscosities of ironmaking and steelmaking slags,” *Ironmak. Steelmak.*, vol. 26, no. 4, pp. 262–268, 1999, doi: 10.1179/030192399677121.
- [20] Y. Yang, K. Raipala, and L. Holappa, “Ironmaking,” in *Treatise on Process Metallurgy*, vol. 3, S. Seetharaman, Ed. Oxford (UK): Elsevier, 2014, pp. 2–88.

Part III

**Desulphurisation of
Hisarna hot metal**

Part III Desulphurisation of Hisarna hot metal

6 The hampering effect of precipitated carbon on hot metal desulphurisation

This chapter is based on the following publication:

F.N.H. Schrama, E.M. Beunder, H.-J. Visser, J. Sietsma, R. Boom, Y. Yang, “The hampering effect of precipitated carbon on hot metal desulfurization with magnesium”, *Steel Research International*, Vol. 91, No. 11, **2020**, 1900441.

Carbon may precipitate during the hot metal desulphurisation (HMD) process as a result of carbon oversaturation because of temperature decrease during transport from the blast furnace to the HMD station. The precipitated carbon flakes will form a layer between the hot metal and the slag. It was postulated that this carbon layer hampers the desulphurisation with magnesium by preventing the MgS particles from reaching the slag phase. As HISarna hot metal contains less carbon than blast furnace hot metal, the absence of the hampering effect of precipitated carbon on the HMD process could be an advantage for the HISarna process.

At Tata Steel in IJmuiden, the Netherlands, carbon in hot metal has been measured in 657 heats after reagent injection. With this data it could be validated whether the hampering effect of precipitated carbon on the MgS flotation has a significant effect on the performance of the industrial HMD process. After filtering out the effect of other parameters, the plant data show that there is a correlation between the precipitated carbon and the specific magnesium consumption for hot metal with a low sulphur concentration (below 225 ppm) prior to HMD. This correlation cannot be found for hot metal with a higher initial sulphur concentration (above 325 ppm). In addition, a sulphur mass balance was made over the converter process, that shows no effect of carbon precipitation during HMD on resulphurisation in the converter.

The scatter and measurement errors of the plant data are too large to describe the hampering effect of precipitated carbon on the HMD efficiency quantitatively. The measurement results do suggest that the postulated effect is small. This implies that the lower carbon concentration in HISarna hot metal, compared to hot metal from the blast furnace, will not have the advantage of avoiding this hampering effect.

6.1 Introduction

In the modern blast furnace process, hot metal is typically not saturated with carbon when it is tapped [1], as in the blast furnace the carbon concentration in the hot metal is determined by kinetics, rather than thermodynamics. During transport from the blast furnace to the steel plant and during tapping into the ladle, the hot metal temperature will decrease, which enhances carbon saturation of the hot metal, because a lower temperature leads to a lower carbon solubility. Dust of precipitated carbon, called kish, is often observed during filling of the hot metal ladle. Studying samples taken from the top layer of the hot metal bath, Visser [2] found that during the hot metal desulphurisation (HMD) process graphite flakes, probably formed due to (local) oversaturation of carbon in the hot metal, accumulate in the top layer of the hot metal, just below the hot metal-slag interface. Visser postulated that these graphite flakes could possibly obstruct the rising MgS particles, which are formed during the desulphurisation reaction between the injected magnesium and the dissolved sulphur, to be absorbed in the slag. By remaining in the metal, the MgS is not removed during the slag skimming, so the desulphurisation efficiency decreases due to this phenomenon. This leads to higher reagent consumptions and a lower reliability of the HMD process.

Hot metal from the HIsarna contains less carbon than hot metal from the blast furnace. Although hot metal from the HIsarna will cool down during transport as well, it can be expected that carbon saturation of the hot metal is less likely. The above described phenomenon of precipitated carbon blocking rising MgS particles during the HMD process, will, therefore, appear less frequent for HIsarna hot metal compared to blast furnace hot metal as well. Replacing a blast furnace by a HIsarna could then lead to less kish formation and an improved magnesium efficiency (it should be noted that other aspects of HIsarna hot metal, like a lower temperature, a higher sulphur concentration and oxygen concentration, and a different hot metal composition will all influence the HMD process too).

The proposed effect of carbon oversaturation of the hot metal on the desulphurisation efficiency was not validated before in an industrial process, as in steel plants the carbon content is typically not measured but calculated, assuming carbon saturation. With this assumption the effect of carbon saturation on HMD cannot be studied. In the steel plant of Tata Steel in IJmuiden, the Netherlands, a trial was conducted in which the carbon content of the hot metal was measured in 657 heats. Wavelength dispersive X-ray fluorescence spectroscopy (WD-XRF) was used to analyse the samples. For the heats in which

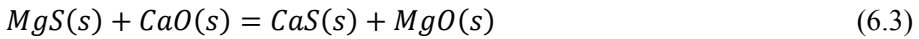
6. The hampering effect of precipitated carbon on hot metal desulphurisation

carbon was measured, the effect of carbon (over)saturation on HMD can be studied. The first results of this study have shown a correlation between graphite precipitation and desulphurisation efficiency [3]. However, this correlation was weak and further investigation was required to determine if the correlation can confirm the postulated effect of carbon precipitation on HMD efficiency.

6.2 Theoretical evaluation

6.2.1 HMD reactions

When injecting magnesium and lime into hot metal, the main desulphurisation reaction takes place between dissolved magnesium and dissolved sulphur (Reaction 6.1). The solid MgS that is formed then floats to the slag layer. Since MgS in the slag will react with oxygen from the air, thereby leading to resulphurisation of the hot metal (Reaction 6.2), lime is added to form the more stable CaS via Reaction 6.3. The injected lime can also directly desulphurise the hot metal via Reaction 6.4, but due to kinetic constraints this reaction only contributes for roughly 5% to the total desulphurisation [2, 4–7].



MgS formed through Reaction 6.1 coalesces and, as these MgS particles grow, their buoyancy increases, so they rise to the slag layer. There the MgS reacts with the lime present in the slag by means of Reaction 6.3. MgS particles that remain in the hot metal will not be removed during the skimming and thus do not contribute to the desulphurisation [5, 8, 9].

6.2.2 Specific magnesium consumption

In HMD through co-injection of magnesium and lime, the desulphurisation via magnesium (Reaction 6.1) is most important and this determines the performance of the process. Therefore, one way to measure the desulphurisation efficiency is by determining the specific magnesium consumption (\dot{m}_{Mg}) of the process [10]:

$$\dot{m}_{Mg} = \frac{m_{Mg}}{m_{\Delta S}} \quad (6.5)$$

Here m_{Mg} and $m_{\Delta S}$ are the mass of the injected magnesium and the mass of the removed sulphur respectively. Equation 6.5 neglects the effect of lime (via Reaction 6.4). This equation does not show the effect of the initial sulphur content

either (if the hot metal has a higher initial sulphur content, desulphurisation is more efficient in terms of specific reagent use [10]). Neither does it include the final sulphur concentration (desulphurising to lower sulphur concentrations is less efficient [4]). This means that Equation 6.5 is not useful if there is a large variation in initial or final sulphur concentrations. Furthermore, when magnesium is injected, an equilibrium has to be established in the hot metal, meaning that a certain amount of magnesium has to dissolve in the hot metal before MgS is formed. This magnesium capacity (C_{Mg}) of the hot metal depends on the temperature and the sulphur concentration: for low final sulphur concentrations, more magnesium has to dissolve before MgS is formed. Ender [11], Turkdogan [12] and Yang [13] came up with slightly different equations for C_{Mg} . All equations are based on the principle that there is a temperature-dependent solubility product of MgS (P_{MgS}) for Reaction 6.1:

$$P_{MgS} = [Mg] \cdot [S] \quad (6.6)$$

Here the concentrations are in ppm. Ender's equation [11] is based on calculations with plant conditions. Under HMD conditions, the difference between Ender's equation and the equations of Turkdogan and Yang are minimal [2]. In this study C_{Mg} is calculated with Ender's equation:

$$C_{Mg} = \frac{10^{-14.3+0.00679T}}{[S]} \quad (6.7)$$

Here T is the temperature of hot metal in °C. Equation 6.7 can then be corrected for the amount of magnesium that has to dissolve in the hot metal before desulphurisation takes place, via the following equation:

$$\dot{m}'_{Mg} = \frac{m_{Mg} - C_{Mg} \cdot m_{HM}}{m_{\Delta S} \cdot 100} \quad (6.8)$$

Where \dot{m}'_{Mg} is the adjusted specific magnesium consumption and m_{HM} is the total mass of the hot metal in kg.

6.2.3 Carbon saturation of hot metal

The carbon solubility and concentration in the hot metal depends on the composition and temperature of the hot metal. The carbon concentration increases when the hot metal sulphur, silicon and phosphorus concentrations are low, or when the manganese concentration is high. Furthermore, a high temperature enhances carbon dissolution in the hot metal. Sulphur delays the reaching of an equilibrium for carbon dissolution in the hot metal during the BF process which, in practice, leads to lower carbon concentrations at higher sulphur concentrations [1, 14]. This also works vice versa, so if the carbon concentration

6. The hampering effect of precipitated carbon on hot metal desulphurisation

in hot metal is higher, the sulphur concentration and its solubility will be lower [1, 15]. Based on earlier research, Neumann et al. [16] established an empirical equation that predicts the carbon concentration of hot metal at saturation (at thermodynamic equilibrium), which is the carbon capacity of the hot metal (C_C) in wt%:

$$C_C = 1.3 + 0.00257T - 0.31[Si] - 0.33[P] + 0.27[Mn] - 0.4[S] \quad (6.9)$$

Here the concentrations of elements are in wt% and T is in °C. Equation 6.9 ignores the influence of other elements dissolved in the hot metal, so for industrial use of this equation a plant-dependent correction factor is needed. For typical HMD conditions the temperature factor in Equation 6.9 has the strongest effect, thus C_C is highly temperature dependent.

6.2.4 Graphite formation in hot metal

Visser [2] explains that the temperature in the ladle is not uniform. Close to the slag layer the hot metal has a lower temperature than in the bulk, leading to a local decrease in carbon capacity which results in graphite precipitation. The graphite precipitates in the form of flakes due to the presence of the anti-spheroidising element sulphur [17]. Because the density of graphite (2200 kg/m³) is much lower than the density of hot metal (7000 kg/m³), it will rise to the slag. As graphite cannot break through the viscous slag, which has a density of ~2700 kg/m³ [18], the graphite flakes will accumulate horizontally at the interface between the slag and hot metal. Carbon-saturated hot metal with a low oxygen concentration (1 ppm) does not wet the graphite flakes. Graphite is not wetted by FeO-MnO-SiO₂-CaO-Al₂O₃ systems, components of which are typically present in HMD slag (besides, HMD slag also contains significant amounts of MgO). This means that graphite flakes, once formed, are likely to stay between the hot metal and the slag or leave the system as kish through the slag eye, which is the gap in the slag created by escaping injection gasses [2, 17]. These graphite flakes were observed by Visser in the slag-hot metal interface when he took samples from hot metal ladle at the HMD station of Tata Steel in IJmuiden. The graphite flakes clearly differed from small graphite segregates that are formed during solidification of the sample. The samples retrieved by Visser did not only show graphite flakes, but also a high concentration of MgS precipitates. This indicates that the graphite blocks the MgS particles, preventing them from reaching the slag, which hampers the desulphurisation efficiency [2, 3].

It is possible that the formation of graphite in the top layer of the hot metal bath is further enhanced by the sudden availability of nucleation sites when the reagent injection starts. In the preceding period, the top layer of the bath has little

turbulence, which could lead to local carbon oversaturation as a result of the decreasing temperature and the lack of nucleation sites. When injection starts, solid lime and MgS particles quickly rise to the top layer, which creates a sudden abundance of nucleation sites. This could lead to instant graphite layer formation, which means that graphite can influence the HMD process from the start. However, there are no observations that support this theory.

6.2.5 The hampering effect of graphite on HMD

Neumann's Equation 6.9 shows that at HMD temperatures (1250-1450 °C), temperature has the strongest influence on C_C . As higher temperatures lead to a higher \dot{m}_{Mg} [4] and a higher C_C , and as hot metal is usually close to carbon saturation, thus $[C]$ is close to C_C , typically heats with a high carbon concentration will show a lower desulphurisation efficiency (a higher \dot{m}_{Mg}). This is also observed in steel plants [10]. To distinguish between the effect of precipitated graphite and the effect of temperature on HMD, which is correlated with the C_C , ΔC should be studied, where:

$$\Delta C = C_{C,0} - \gamma_{[C],meas} \quad (6.10)$$

Here $C_{C,0}$ is the carbon capacity of the hot metal prior to HMD, calculated via Neumann's Equation 6.9, and $\gamma_{[C],meas}$ is the measured carbon content of the hot metal after HMD. A large ΔC means that the hot metal is far from carbon saturation, thus little graphite precipitation is expected. The smaller ΔC gets, the closer the hot metal is to carbon saturation, so a smaller (local) decrease in temperature or change in composition can cause graphite precipitation. In this study ΔC is used as an indication for the amount of expected precipitated graphite in the hot metal, without quantifying the amount of graphite.

Figure 6.1 gives an overview of the different processes inside the ladle that play a role in HMD. 1) The injected magnesium dissolves in the hot metal. 2) The dissolved magnesium reacts with sulphur via Reaction 6.1 and then further reacts with lime via Reaction 6.3. 3) Alternatively, the sulphur directly reacts with lime via Reaction 6.4. 4) Because of the lower temperature at the slag-hot metal interface (the top layer), dissolved carbon precipitates as graphite. The effect of a lower sulphur concentration at the interface is not strong enough to avoid graphite precipitation, as the effect of sulphur on C_C is smaller than the effect of temperature, according to Neumann's Equation 6.9. 5) It is expected that these precipitated graphite flakes block the MgS, thus preventing it from reaching the slag layer. MgS staying in the hot metal means a lower desulphurisation efficiency (and thus a higher \dot{m}_{Mg}). It is expected that the hampering effect of

6. The hampering effect of precipitated carbon on hot metal desulphurisation

graphite on \dot{m}_{Mg} becomes relatively stronger when more graphite is present. The expected relation is therefore not linear.

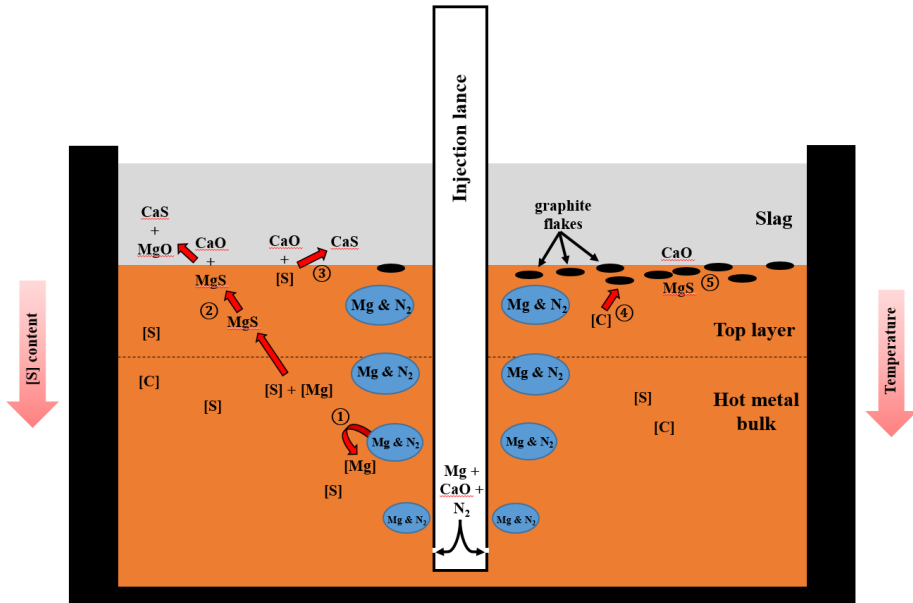


Figure 6.1: Schematic overview of the top part of the ladle in the co-injection HMD process. Where 1) Mg dissolving in hot metal, 2) desulphurisation with Mg via Reactions 6.1 and 6.3, 3) desulphurisation with CaO via Reaction 6.4, 4) graphite formation, 5) graphite flakes blocking MgS particles.

The graphite blocking the MgS to reach the slag layer is comparable with the mechanism proposed by Street *et al.* [19] for Ti(C,N) particles that can form a layer between the hot metal and the slag, which blocks MgS during HMD.

6.3 Measurements and discussion

6.3.1 Plant measurements

In 2018 at Tata Steel's plant in IJmuiden, the Netherlands, a trial was executed to measure the carbon content of the hot metal at the magnesium-lime co-injection HMD station, immediately after reagent injection. Besides the standard sample and temperature measurements, hot metal samples of 657 heats were taken for this trial. The sample was taken with an automatic sampling lance at a fixed height: 60 cm below the slag surface. It is assumed that when the sampling lance breaks through the slag layer and the graphite-MgS layer below, some MgS will be dragged down with it and ends up in the sample, leading to a higher sulphur concentration in the sample. Retrieved samples were air cooled before they were sent to the laboratory. At the laboratory, the samples were milled and then

Part III Desulphurisation of HIsarna hot metal

analysed by wavelength dispersive X-ray fluorescence spectroscopy (WD-XRF). The analysis of the 657 samples for carbon measurement was validated by using the combustion method with infra-red detection. Each sample was analysed once. The total standard deviation for the carbon measurement (the sum of all deviations) is 0.1 wt%.

The dataset of the 657 HMD heats where carbon was measured, including the standard data that is retrieved for every heat and the carbon measurement, were filtered for outliers. Heats where data is missing, where $C_{Mg} > 0.01$ wt%, or with temperatures below 1350 °C or above 1450 °C, were excluded. Filtering on C_{Mg} was done because high C_{Mg} values are caused by very low sulphur concentrations, but at very low sulphur concentrations the measurement error has a too large influence on C_{Mg} . Filtering on temperature was done because temperature has a large effect on HMD efficiency, so extreme temperatures could have a disproportionate effect on the trends. After filtering 546 heats remained for further analysis [3].

Figure 6.2 shows a plot of $\dot{m}_{Mg,cor}$ against ΔC for the 546 HMD heats. Measured hot metal temperature (in °C) of a heat is indicated via the colour of the data points, as temperature is known to have a strong effect on desulphurisation efficiency. With the software package R [20], the best fitted linear function (black line) and logarithmic function (red line) for this data set is calculated.

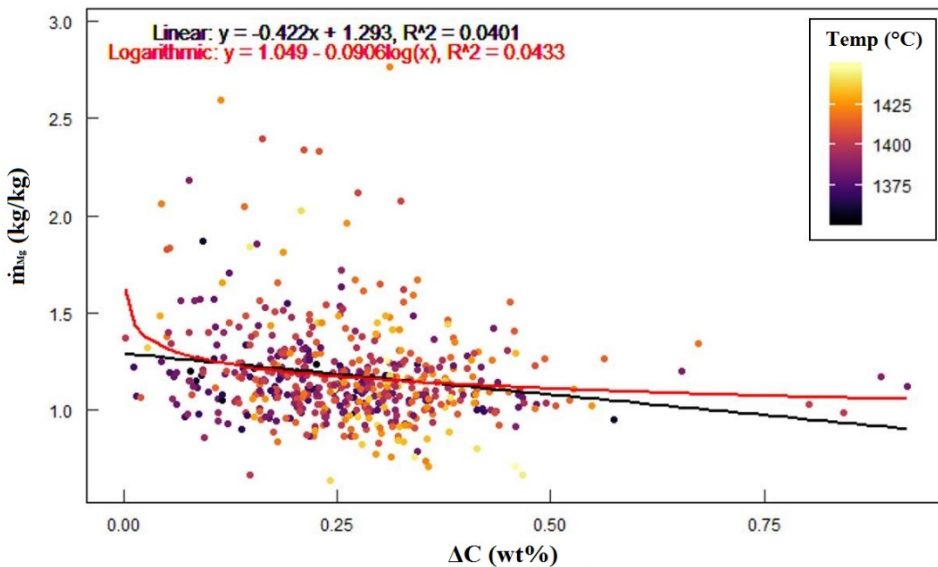


Figure 6.2: \dot{m}'_{Mg} against ΔC . The colours of dots indicate the hot metal temperature. The black line is the linear best fit and the red line is the logarithmic best fit.

6. The hampering effect of precipitated carbon on hot metal desulphurisation

Figure 6.2 shows a weak correlation between \dot{m}'_{Mg} and ΔC . The slope of the best fitted linear line has a standard deviation of 0.088 for the gradient, indicating a high probability that the correlation between \dot{m}'_{Mg} and ΔC is negative, as is expected. As the hot metal temperature seems to be scattered randomly, the data is well corrected for the temperature effect, so the observed trend cannot be attributed to temperature. A low R^2 value is expected when looking at plant data, but an R^2 of 0.04 indicates that other factors play a role in this correlation as well.

To make the trend better visible, the data is grouped for ΔC , per 0.05 wt%, and for every group the average \dot{m}'_{Mg} is taken and plotted in Figure 6.3. The error bars indicate the 1σ standard deviation per group and the plotted red line is the same logarithmic best fit as in Figure 6.2.

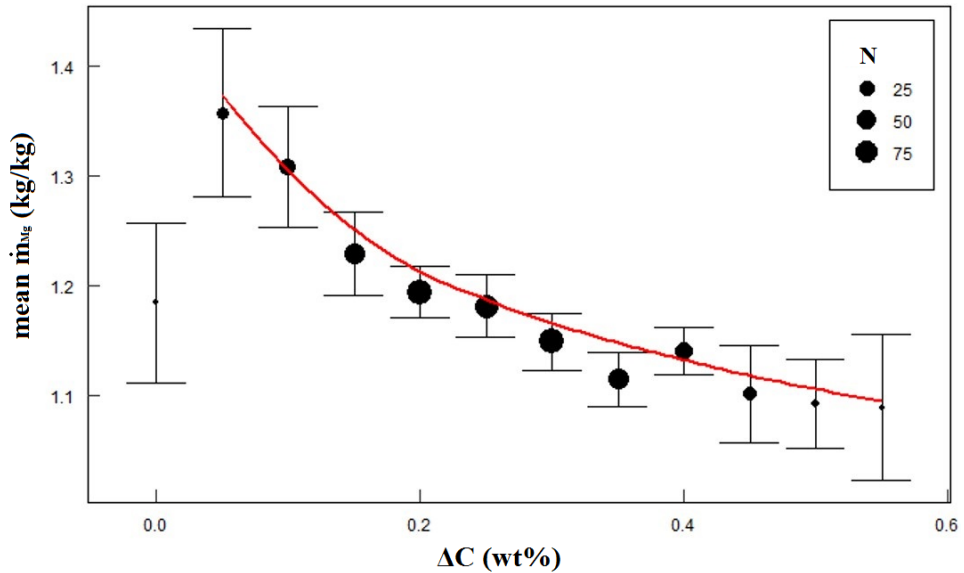


Figure 6.3: \dot{m}'_{Mg} versus grouped ΔC (per 0.05 wt%). The dot size indicates the number of measurements per group. The red line is the best fitted logarithmic function from Figure 6.2. The error bars show the 1σ standard deviation per group.

6.3.2 Influence of the hot metal composition

Figures 6.2 and 6.3 show that there is a correlation, albeit weak, between \dot{m}'_{Mg} and ΔC that is independent of temperature. However, in the HMD process other elements in the hot metal have their influence on the desulphurisation efficiency as well. In Figure 6.4 the concentration of manganese, phosphorus, silicon and titanium are plotted against ΔC .

Part III Desulphurisation of HIsarna hot metal

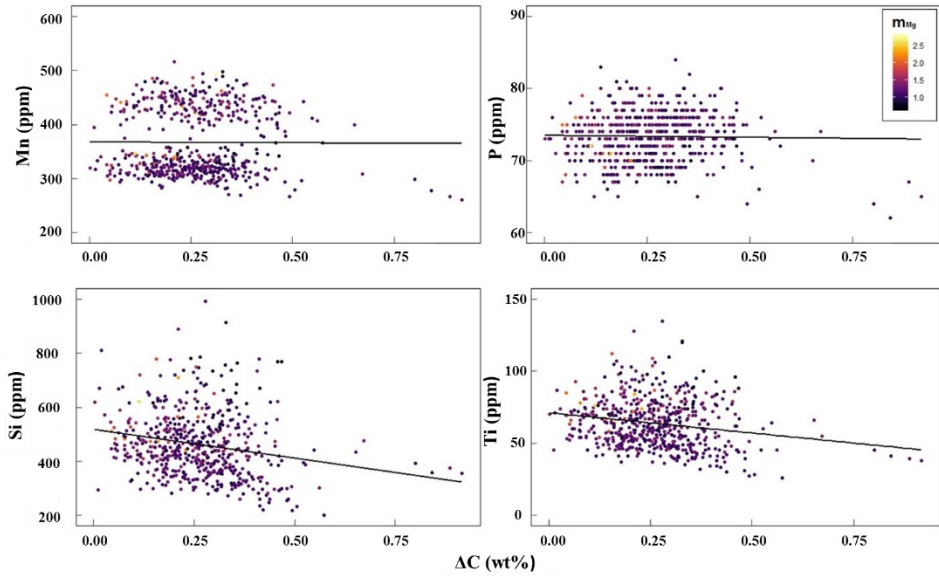


Figure 6.4: Correlation between ΔC and main other elements in the hot metal (Mn, P, Si and Ti). The black line is the linear trend line. The colours of the data points indicate \dot{m}_{Mg} .

Figure 6.4 clearly shows there is no correlation between ΔC and the elements phosphorus and manganese concentration in the hot metal. Both silicon and titanium do show a negative correlation with ΔC , but this could be expected, as the concentrations of silicon, titanium and carbon in hot metal are known to be correlated. However, silicon and titanium do not have an independent influence on \dot{m}_{Mg} [1, 10]. The reason for the apparent two groups for the manganese concentration in Figure 6.4 has not been investigated, as it has no influence on the graphite formation or desulphurisation.

The data is not corrected for the initial sulphur concentration (S_{in}), even though S_{in} has an impact on \dot{m}_{Mg} . The initial carbon and sulphur concentrations are correlated, as Equation 6.9 shows, so the apparent effect of ΔC , and thus graphite precipitation, could also be caused by a different S_{in} . Figure 6.5 shows the correlation of S_{in} with ΔC (a) and $\dot{m}_{Mg,cor}$ (b) respectively.

6. The hampering effect of precipitated carbon on hot metal desulphurisation

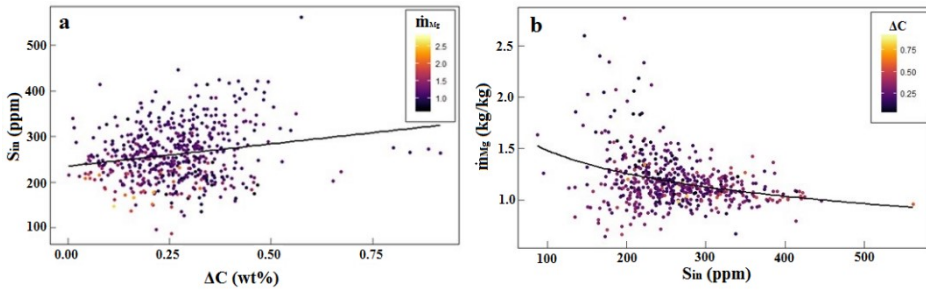


Figure 6.5: The correlation of S_{in} with \dot{m}'_{Mg} and ΔC . a) S_{in} versus ΔC , where the colours of the dots indicate \dot{m}'_{Mg} and where the black line is the linear trend line. b) \dot{m}'_{Mg} versus S_{in} , where the colours of the dots indicate ΔC and where the black line is the logarithmic best fit.

From Figure 6.5 it can be concluded that the correlation between \dot{m}'_{Mg} and ΔC can as well be attributed to the effect of S_{in} on \dot{m}'_{Mg} . Because this research is based on plant data, it is difficult to isolate the effect of a certain parameter, like in a laboratory experiment, where all parameters can be controlled. It is possible to make a selection from the available heats, grouping them based on the initial sulphur concentration. Table 6.1 shows the number of heats in every S_{in} group.

Table 6.1: Number of heats per S_{in} group.

S_{in} range [ppm]	Count
<125	2
125-175	25
175-225	144
225-275	172
275-325	122
325-375	56
375-425	23
>425	2

Figure 6.6 shows the correlation between \dot{m}'_{Mg} and ΔC for S_{in} groups. For heats with a lower S_{in} (below 225 ppm), there is a correlation between \dot{m}'_{Mg} and ΔC , as expected. For higher initial sulphur concentrations (above 325 ppm) there is no significant correlation. A possible explanation for this is that at higher initial sulphur concentration, more sulphur is removed. Based on Neumann's equation, desulphurisation leads to a higher C_c (Equation 6.9). The higher the degree of desulphurisation, which is strongly correlated with S_{in} , the more strongly S_{in} and C_c , and thus ΔC , are correlated. This could result in no detectable separate correlation between ΔC and \dot{m}'_{Mg} .

Part III Desulphurisation of Hisarna hot metal

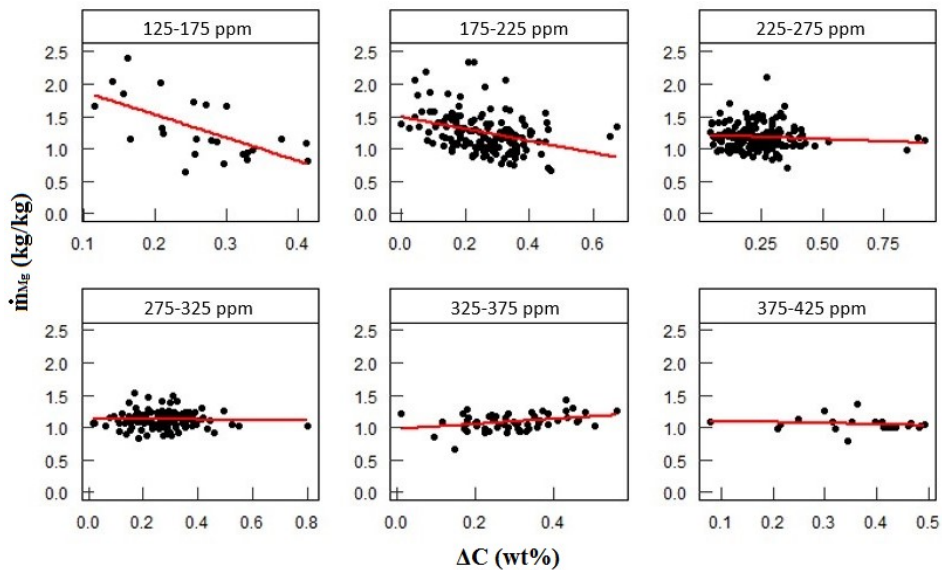


Figure 6.6: \dot{m}'_{Mg} against ΔC for S_{in} groups (steps of 50 ppm). The S_{in} group is in the title of every mini figure. The red line is the linear trend line.

To investigate if the observed correlation can still be attributed to S_{in} , \dot{m}'_{Mg} is plotted against S_{in} in Figure 6.7. It can be seen that there is no correlation between S_{in} and \dot{m}'_{Mg} .

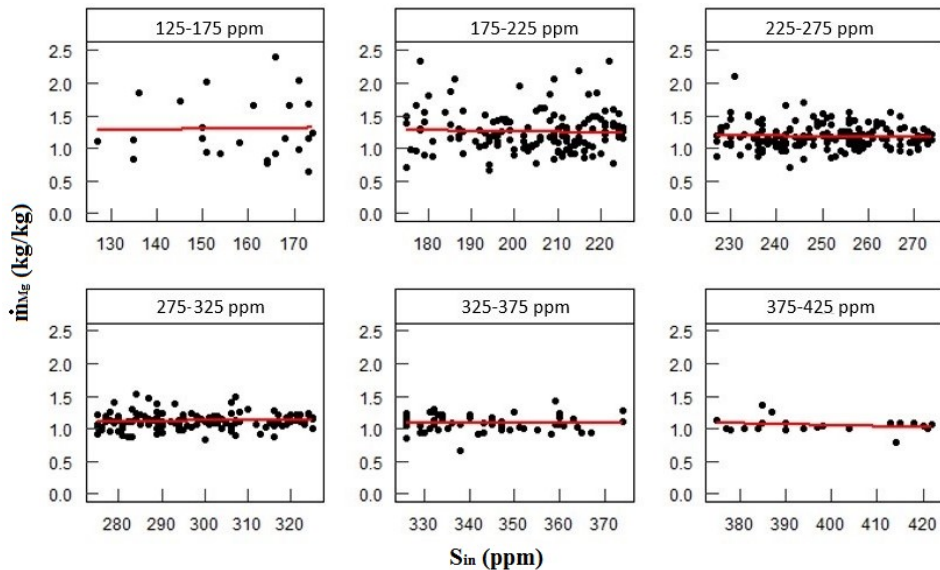


Figure 6.7: Correlation between S_{in} and \dot{m}'_{Mg} for S_{in} groups (steps of 50 ppm). The S_{in} group is in the title of every mini figure. The red line is the linear trend line.

6. The hampering effect of precipitated carbon on hot metal desulphurisation

6.3.3 The magnitude of the effect

Because the effect of graphite precipitation on the desulphurisation efficiency could not be clearly isolated from the HMD data, the converter data was studied for the same 546 heats. A sulphur mass balance was made, taking into account the measured sulphur input via the hot metal, as well as the estimated sulphur input via scrap and additions, and the measured sulphur output via the liquid steel and the estimated sulphur output via the slag. Based on the theory, a significant hampering effect of graphite precipitation on the HMD efficiency, should lead to a sulphur concentration in the hot metal that is higher than expected, and that is possibly missed by the sulphur measurement at the end of the HMD process. This should then lead to a higher resulphurisation in the converter for heats that had more graphite precipitation during the HMD process. However, the sulphur mass balance over the converter did not show any correlation between ΔC at the HMD and resulphurisation. This excludes the possibility that the effect of graphite on HMD efficiency is missed because of a systematic measurement error when measuring the sulphur concentration at the end of the HMD process. The lack of any significant correlation in the converter data shows that the postulated effect is too small to have any detectable consequences in the converter. This could be either because only a small amount of MgS is blocked by the graphite, or because the graphite-MgS layer is skimmed off together with the slag in the HMD, effectively leading to successful desulphurisation.

In the HMD process data there only is a significant correlation between graphite formation and desulphurisation efficiency at low initial sulphur concentrations. However, as there are many other factors that have a stronger influence on the desulphurisation efficiency, it is difficult to isolate this effect. This suggests that the postulated effect is small. The fact that there are hundreds of HMD stations worldwide, but that no correlation between graphite formation and the specific magnesium consumption has as yet been found, invigorates the suggestion that the effect is small.

Nevertheless, the high number of plant measurements, also in the low S_{in} range, make the correlation between ΔC and \dot{m}'_{Mg} significant, despite of the standard deviation of 0.1 wt% per single measurement and the assumption that sulphur from the MgS-graphite layer is captured in the sample. Furthermore, it has been proven that the graphite layer between the slag and the hot metal is formed when the metal gets oversaturated with carbon [2, 3]. In theory the observed correlation between ΔC and \dot{m}'_{Mg} can also be caused by carbon itself. Carbon can help to decrease the oxygen concentration of the hot metal, which will decrease \dot{m}_{Mg} . However, the oxygen concentration in the hot metal is already low (typically 1

ppm) and even at low carbon concentrations still enough carbon remains to decrease the oxygen concentration. Furthermore, carbon has an influence on the sulphur concentration. In the blast furnace more dissolved carbon leads to a lower sulphur dissolution. However, in the HMD process, the sulphur concentration is by definition below the sulphur dissolution limit. Thus, carbon itself will not have a significant effect on HMD.

6.4 Conclusions and recommendations

6.4.1 Conclusions

Based on the theoretical studies and the data analysis from the industrial samples, the following conclusions can be drawn:

- The measurements show that there is a correlation between ΔC and \dot{m}'_{Mg} for lower initial sulphur concentrations (below 225 ppm), which cannot only be contributed to the other elements than carbon in the hot metal or to the hot metal temperature. However, this effect of ΔC , thus of graphite formation, on the specific magnesium consumption is small. For higher initial sulphur concentrations (above 325 ppm) the effect is invisible or non-existing.
- The postulated effect of graphite formation on the desulphurisation efficiency has no significant influence on resulphurisation in the converter. The possible increase in sulphur concentration is so small that the uncertainties of sulphur content of the scrap and the additions make it insignificant.
- An effect of precipitated graphite on the HMD efficiency is only visible at lower initial sulphur concentrations. Possibly a larger difference between initial and final sulphur concentrations counters the effect of graphite on \dot{m}_{Mg} .
- The size and impact of graphite on the HMD process cannot be quantified from this data, because in plant data the parameter of graphite formation (or ΔC) cannot be isolated from other parameters.
- Since the graphite formation does not significantly hamper the HMD efficiency at sulphur concentrations above 325 ppm, the lower carbon concentration in HIsarna hot metal, compared to blast furnace hot metal, will not lead to a significantly better desulphurisation efficiency.

6.4.2 Recommendations

- As the effect of graphite formation on the desulphurisation efficiency is difficult to isolate from plant data, better controlled laboratory experiments should be done to confirm the existence of this effect.

6. The hampering effect of precipitated carbon on hot metal desulphurisation

- Possibly graphite formation in the top layer of the hot metal bath is enhanced by the availability of nucleation sites for the carbon as a result of the reagent injection. As this could lead to instant graphite formation at the start of the HMD process (assuming there is local carbon oversaturation in the top layer resulting from unavailability of nucleation sites prior to injection), the graphite could influence the process from the beginning. Further investigations are required to confirm this.

6.5 References

- [1] K. Raipala, “On hearth phenomena and hot metal carbon content in blast furnace,” (PhD thesis) Helsinki University of Technology, Helsinki (FIN), 2003.
- [2] H.-J. Visser, “Modelling of injection processes in ladle metallurgy,” (PhD thesis) Delft University of Technology, Delft (NL), 2016.
- [3] F.N.H. Schrama, E.M. Beunder, H.-J. Visser, R. Boom, J. Sietsma, and Y. Yang, “Effect of graphite on hot metal desulphurisation,” in *Proceedings of METEC & 4th ESTAD*, 2019, p. P308.
- [4] F.N.H. Schrama, E.M. Beunder, B. van den Berg, Y. Yang, and R. Boom, “Sulphur removal in ironmaking and oxygen steelmaking,” *Ironmak. Steelmak.*, vol. 44, no. 5, pp. 333–343, 2017, doi: 10.1080/03019233.2017.1303914.
- [5] H.-J. Visser and R. Boom, “Advanced Process Modelling of Hot Metal Desulphurisation by Injection of Mg and CaO,” *ISIJ Int.*, vol. 46, no. 12, pp. 1771–1777, 2006, doi: 10.2355/isijinternational.46.1771.
- [6] H. Sun, Y.-C. Liu, and M.-J. Lu, “Behaviour of Ar-1%Mg Bubbles in Desulfurization of Hot Metal by Magnesium Injection,” *Steel Res. Int.*, vol. 80, no. 3, pp. 209–217, 2009, doi: 10.2374/SRI08SP129.
- [7] A. Freißmuth, *Die Entschwefelung von Roheisen*, 1st ed. Tisnov (CZ): Almamet GmbH, 2004.
- [8] D. Lindström, P. Nortier, and D. Sichen, “Functions of Mg and Mg-CaO mixtures in hot metal desulfurization,” *Steel Res. Int.*, vol. 85, no. 1, pp. 76–88, 2014, doi: 10.1002/srin.201300071.
- [9] G.A. Irons and R.I.L. Guthrie, “The kinetics of molten iron desulfurization using magnesium vapor,” *Metall. Trans. B*, vol. 12, no. 4, pp. 755–767, 1981, doi: 10.1007/BF02654145.
- [10] F.N.H. Schrama, E.M. Beunder, J.W.K. van Boggelen, R. Boom, and Y. Yang, “Desulphurisation of HIsarna hot metal - a comparison study based

- on plant data,” in *Science and Technology of Ironmaking and Steelmaking*, 2017, pp. 419–422.
- [11] A. Ender, H. Van Den Boom, H. Kwast, and H.-U. Lindenberg, “Metallurgical development in steel-plant-internal multi-injection hot metal desulphurisation,” *Steel Res. Int.*, vol. 76, no. 8, pp. 562–572, 2005.
- [12] E.T. Turkdogan, “Physicochemical aspects of reactions in ironmaking and steelmaking processes.,” *Trans. Iron Steel Inst. Japan*, vol. 24, no. 8, pp. 591–611, 1984, doi: 10.2355/isijinternational1966.24.591.
- [13] J. Yang, M. Kuwabara, T. Teshigawara, and M. Sano, “Mechanism of Resulfurization in Magnesium Desulfurization Process of Molten Iron,” *ISIJ Int.*, vol. 45, no. 11, pp. 1607–1615, 2005, doi: 10.2355/isijinternational.45.1607.
- [14] J.A. Kitchener, O.M. Bockris, and D.A. Spratt, “Solutions in liquid iron. Part 2.—The influence of sulphur on the solubility and activity coefficient of carbon,” *Trans. Faraday Soc.*, vol. 48, pp. 608–617, 1952.
- [15] V. Sahajwalla and R. Khanna, “Influence of sulfur on the solubility of graphite in Fe-C-S melts: Optimization of interaction parameters,” *Acta Mater.*, vol. 50, no. 4, pp. 663–671, 2002, doi: 10.1016/S1359-6454(01)00398-6.
- [16] F. Neumann, H. Schenck, and W. Patterson, “Einfluß der Eisenbegleiter auf Kohlenstofflöslichkeit, Kohlenstoffaktivität und Sättigungsgrad im Gußeisen,” *Giesserei*, vol. 47, no. 2, pp. 25–32, 1960.
- [17] Y. Yin *et al.*, “Molecular dynamics simulations of iron/graphite interfacial behaviors: Influence of oxygen,” *ISIJ Int.*, vol. 58, no. 6, pp. 1022–1027, 2018, doi: 10.2355/isijinternational.ISIJINT-2017-667.
- [18] Verein Deutscher Eisenhüttenleute, Ed., *Slag atlas*, 1st ed. Düsseldorf (DE): Verlag Stahleisen mbH, 1981.
- [19] S. Street, R.P. Stone, and P.J. Koros, “The presence of titanium in hot metal and its effects on desulfurization,” *Iron Steel Technol.*, vol. 2, no. 11, pp. 65–74, 2005.
- [20] R Core Team, *R: A language and environment for statistical computing*. Vienna (AUT): R Foundation for Statistical Computing, 2018.

7 Desulphurisation of high-sulphur HISarna hot metal

This chapter is based on the following prepared manuscript for publication in a peer-reviewed international journal:

F.N.H. Schrama, E.M. Beunder, A. Emami, C.M. Barnes, J.W.K. van Boggelen, J. Sietsma, R. Boom, Y. Yang, “Desulfurization of high-sulfur HISarna hot metal”.

HISarna hot metal contains 3-4 times more sulphur than hot metal from blast furnaces (BF), so when replacing a blast furnace for the HISarna process, more sulphur needs to be removed from the hot metal. This will have consequences for the hot metal desulphurisation (HMD) process. In this chapter, the effects of HISarna hot metal on the magnesium-lime co-injection HMD process, in comparison with HMD of typical BF hot metal, are investigated. A literature study, a thermodynamic analysis and plant data analysis from Tata Steel, in IJmuiden, are used to investigate the consequences of HISarna hot metal for the current HMD process.

Although the high sulphur concentration and low temperature of HISarna hot metal will lead to a higher total reagent consumption, compared to desulphurisation of BF hot metal, the specific magnesium consumption will decrease. The higher oxygen concentration in HISarna hot metal will only lead to a small increase in reagent consumption. This means that desulphurisation of HISarna hot metal is possible with the current state-of-the-art co-injection HMD, and that, compared to BF hot metal, HISarna hot metal will lead to longer process times and higher reagent consumptions at the HMD, but that the efficiency of the HMD process will increase.

7.1 Introduction

The current concern on global climate change is leading to numerous new ironmaking processes with a lower CO₂ footprint than the current blast furnace (BF) process, or even CO₂-neutral processes, being developed by industry and academia [1, 2]. One new ironmaking process that is in an advanced development stage is HIsarna. HIsarna is a smelting reduction ironmaking process, which uses coal and lower grade iron ore instead of coke and pellets as raw materials. This lowers the CO₂ footprint of the produced hot metal by 20 %, compared to the BF. Furthermore, the HIsarna off gas is better suited for carbon capture and storage (CCS) or carbon capture and usage (CCU), which could lead to a total CO₂ reduction of 80 % [2–5].

The HIsarna process consists of two parts (see Figure 7.1). In the upper part, the smelting cyclone, also called “cyclone converter furnace” (CCF), the iron ore is pre-reduced (10-20 % reduction), pre-heated and melted by combustion of the CO gas from the lower part with injected oxygen. This results in the oxidising environment in the upper part of the furnace. In the lower part, the “smelting reduction vessel” (SRV), the pre-reduced molten ore is further reduced by the carbon from the injected powdered coal. Due to the strongly reducing environment in the SRV, oxygen is injected to partly oxidise the coal to form CO gas.

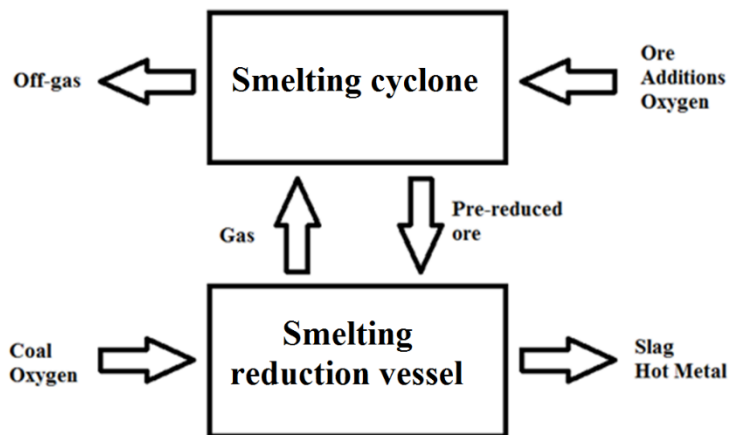


Figure 7.1: Process scheme of the HIsarna process [6].

The pre-reduced and molten ore from the cyclone will dissolve entirely in the slag, which leads to a high metal-slag interface area in the emulsion. The turbulence created by the formation of CO gas further increases the metal slag contact, which leads to a higher FeO content (~6 %) in the emulsion than in BF

7. Desulphurisation of high-sulphur HISarna hot metal

slag. Because the strongly endothermic reduction of FeO takes place in the SRV, while part of the exothermic carbon oxidation takes place at the CCF, the tapping temperature from the SRV is 1400-1450 °C, which is lower than at a BF. This means that during tapping, HISarna hot metal is typically 40-80 °C colder than hot metal from the BF. The hot metal is tapped separately from the slag, which implies that no hot metal-slag reactions will take place after the tapping [2–7].

Due to the less reducing environment in the SRV, compared to the BF, the HISarna hot metal typically contains very little silicon, low phosphorus and manganese and slightly less carbon. On the other hand the sulphur and oxygen concentrations are higher [5, 6]. Table 7.1 gives a typical composition of the hot metal from HISarna and the BF.

Table 7.1: Typical hot metal composition for HISarna and BF.

Composition (wt%)	HISarna	BF [7]
C	4.0	4.5
Si	0.007	0.4
S	0.1	0.03
Mn	0.03	0.3
P	0.04	0.07
Ti	0.001	0.04
V	0.01	-
O	6 ppm	0.5 ppm

Trials at the pilot HISarna at Tata Steel in IJmuiden, the Netherlands, show sulphur concentrations between 0.03 and 0.2 wt%. High sulphur concentrations are caused by both a higher sulphur input via the coal, and a higher oxygen activity (a_O) in the SRV, which hampers the desulphurisation of the hot metal. Trials with low-sulphur coal led to hot metal with a sulphur concentration of 0.03-0.05 wt%, which is similar to BF hot metal. However, when the sulphur input via coal and coke is equal, HISarna hot metal will have a higher sulphur concentration than BF hot metal [3, 5, 6]. This means that at an integrated steelmaking site, where a BF is replaced by the HISarna process, more sulphur needs to be removed by hot metal desulphurisation (HMD), prior to the converter process. This could lead to a longer processing time at the HMD station.

Desulphurised HISarna hot metal is expected to be lower in all major dissolved elements, compared to BF hot metal. This leads to a shorter converter process, as smaller amounts of these elements need to be removed by oxidation. Therefore, the converter process with desulphurised HISarna hot metal is comparable to the

second converter process in the Japanese de-P de-C double converter practice, in which carbon and phosphorus concentrations are low and the silicon concentration is nearly zero at the start of the process. Blowing times in this de-P de-C double converter process typically take 10-12 minutes [8, 9], a reduction of some 40 % with respect to the typical converter process blowing time of 16-20 minutes [10, 11]. The shorter converter process with desulphurised HISarna hot metal would have a big impact on the steel plant logistics and would increase the time pressure on the HMD process step.

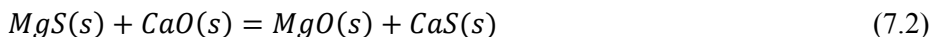
The time pressure on the HMD process will come from two sides, when HISarna hot metal would replace BF hot metal in the steel plant. On one hand the HMD process could take longer due to the higher sulphur concentration in the hot metal, while on the other hand the converter process becomes faster, requesting a shorter process time from the HMD. HISarna hot metal will lead to different reagent consumption and processing time at the HMD, but the impact is yet unknown.

In 2025, Tata Steel plans to have an industrial-size test HISarna in operation in Jamshedpur, India. As the hot metal will be used for commercial steelmaking, it has to be desulphurised at the HMD. Therefore, it is important to understand the impact of the composition and temperature of HISarna hot metal on the HMD process. In this chapter, the effect of the lower temperature and different composition of HISarna hot metal on the processing time and reagent consumption of the Mg-CaO co-injection HMD process is investigated.

7.2 Theoretical evaluations

7.2.1 HMD process

As was discussed in the previous chapters, globally the most widely used HMD process is the magnesium-lime co-injection process. In this process, the reagents magnesium and lime are injected in the hot metal via a refractory-coated lance. The magnesium dissolves and reacts with the dissolved sulphur (Reaction 7.1). The formed MgS reacts with lime to form the stable CaS (Reaction 7.2) [12–15].



Although a small degree of desulphurisation takes place via a direct reaction between lime and dissolved sulphur, typically > 95% of the desulphurisation takes place via Reactions 7.1 and 7.2. This means that for an industrial HMD process, the desulphurisation efficiency can be expressed by the specific magnesium consumption (\dot{m}_{Mg}) [16]:

7. Desulphurisation of high-sulphur HIsarna hot metal

$$\dot{m}_{Mg} = \frac{m_{Mg}}{m_{\Delta S}} \quad (7.3)$$

Here m_{Mg} and $m_{\Delta S}$ are the mass of consumed metallic magnesium and removed sulphur, respectively. In industrial HMD stations, \dot{m}_{Mg} values between 1.0 and 2.5 are observed [12, 13, 16, 17]. This wide range is caused by differences in process conditions and reagent quality. However, to have a fair measure for desulphurisation efficiency of industrial HMD stations, \dot{m}_{Mg} needs to be adjusted for part of the magnesium remaining dissolved in the hot metal without reacting with the dissolved sulphur. According to Ender [18], based on plant data, the concentration of magnesium in the hot metal at equilibrium ($X_{[Mg]}$) can be estimated via:

$$X_{[Mg]} = \frac{10^{-18.3+0.00679T}}{X_{[S]}} \quad (7.4)$$

Here $X_{[S]}$ is the concentration of dissolved sulphur in the hot metal (in wt%) and T is the temperature in °C. In this equation, carbon saturation of the hot metal is assumed. It should be noted that actual equilibrium in the hot metal is not reached during the HMD process, but according to Visser [13] the estimated $X_{[Mg]}$ from Equation 7.4 is in agreement with industrial observations. This leads to the following adjusted specific magnesium consumption (\dot{m}'_{Mg}) [16]:

$$\dot{m}'_{Mg} = \frac{m_{Mg} - X_{[Mg]} \cdot m_{HM}}{m_{\Delta S}} \quad (7.5)$$

Here m_{HM} is the mass of the hot metal.

7.2.2 Oxygen

Oxygen activity (a_O) in the hot metal and the slag is important for the HMD process. A higher a_O in the hot metal causes less sulphur to go to the slag and more sulphur to remain dissolved in the hot metal, at equilibrium. The following general equilibrium exists between sulphur and oxygen in hot metal and slag [12, 19]:



This implies that the amount of dissolved sulphur in the hot metal can be lowered by either lowering the concentration of dissolved oxygen in the hot metal (lowering a_O) or by increasing the concentration of oxygen in the slag phase (increasing the slag basicity). Therefore, \dot{m}_{Mg} will decrease with decreasing a_O .

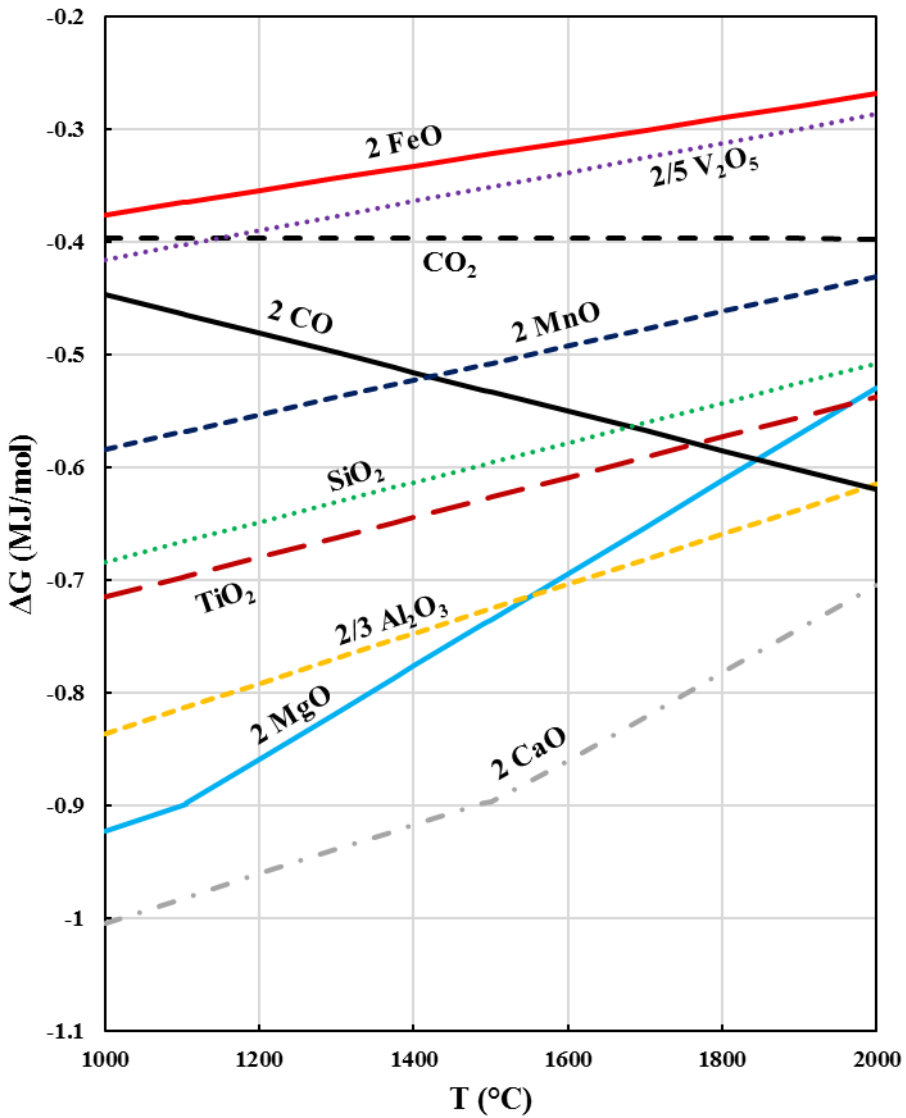


Figure 7.2: Ellingham diagram (based on data from Hayes [20]).

In industry, the oxygen concentration is typically not measured in hot metal. Based on different industrial measurements in different plants, the typical oxygen concentration in hot metal prior to the HMD process is 0.5-1 ppm [18, 20]. However, the oxygen concentration fluctuates from heat to heat. The composition of the hot metal gives an indication of the oxygen concentration and, thus, a_{O} . The lower an element is on the Ellingham diagram (see Figure 7.2), the

7. Desulphurisation of high-sulphur HIsarna hot metal

stronger its affinity with oxygen [22]. So, silicon and titanium concentrations in the hot metal are most strongly influenced by a_O , (a high a_O leads to low silicon and titanium concentrations in the hot metal). Elements that are lower in the Ellingham diagram (like aluminium) are typically fully oxidised and moved to the slag phase in the BF and, therefore, not present in hot metal. This means that a_O can best be predicted based on the concentrations of silicon and titanium in hot metal.

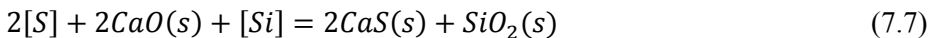
In secondary steelmaking, a_O is lowered by adding silicon or aluminium to the liquid steel. With the addition of aluminium oxygen concentrations of 2-3 ppm can be reached in liquid steel. At temperatures of 1300-1400 °C, magnesium is slightly below aluminium in the Ellingham diagram, indicating that magnesium could be used to deoxidise the hot metal as well. Since magnesium is already injected during the HMD process, there is no need to inject a separate component to reduce a_O . To lower the oxygen concentration from 6 ppm to 0.5 ppm, stoichiometrically 8.35 gram magnesium per tonne hot metal would be required, Which amounts to an extra 2.5 kg of pure magnesium at the HMD for a 300 t ladle. Therefore, even when taking reagent purity and efficiency into account, the increased oxygen concentration would lead to an increase of \dot{m}_{Mg} of 1-2 %.

7.2.3 Influence of hot metal composition on HMD

In HMD, several elements in the hot metal are correlated with the desulphurisation efficiency. Most correlations can be explained by the effect of oxygen on the hot metal composition. As explained in the previous section, a_O influences \dot{m}_{Mg} , but it also influences the amount of silicon, titanium and manganese in hot metal. In the following section, the individual influence of the concentration of the most important elements on the HMD process is discussed.

7.2.3.1 Silicon

Apart from the correlation between silicon and a_O , silicon has a direct influence on the desulphurisation process as well. Silicon enhances the direct desulphurisation with lime, via the following reaction [13, 23]:



Typically, in the co-injection process, the direct desulphurisation via lime only contributes for only a fraction of less than 5 % of the total sulphur removal. Therefore, the influence of silicon on the HMD process is limited. However, in some steel plants the HMD process depends more on Reaction 7.7, if the Mg to CaO ratio is low, e.g. 1:5. For HMD processes which fully depend on lime, like the Kanbara reactor (KR) process, silicon in hot metal is even more important [12]. The KR process is an alternative HMD process that uses only lime (or CaC_2

or CaF_2) as reagents to desulphurise the hot metal [12, 14, 24]. As a result, the co-injection HMD process is better suited to desulphurise HIsarna hot metal, which contains almost no silicon, than the KR process. For the co-injection HMD process, the absence of silicon in hot metal will lead to an even lower contribution of the direct desulphurisation via lime, but this will have only a small influence on \dot{m}_{Mg} .

7.2.3.2 Titanium

Titanium, similar to silicon, acts as an indicator of a_{O} in the hot metal, which partly explains the correlation with \dot{m}_{Mg} . Furthermore, a high concentration of titanium in hot metal (more than 0.1 wt%) leads to the formation of $\text{Ti}(\text{C},\text{N})$ during the HMD process. $\text{Ti}(\text{C},\text{N})$ particles lead to a ‘sticky slag’, which can result in high iron losses. It was also reported that this ‘sticky slag’ could hamper MgS particles that formed to reach the slag, thus reducing the desulphurisation efficiency [13, 25]. However, for typical titanium concentrations (lower than 0.05 wt%), no effect on \dot{m}_{Mg} could be observed [16]. Therefore, the absence of titanium in HIsarna hot metal will not significantly affect \dot{m}_{Mg} compared to typical BF hot metal. The low titanium in HIsarna hot metal could lead to lower iron losses during the HMD process.

7.2.3.3 Carbon

Carbon concentration in the hot metal correlates with a_{O} , albeit less than silicon and titanium concentrations do. Apart from that, carbon can influence the HMD process by influencing the solubility of magnesium. A lower carbon concentration increases the solubility of Mg in the hot metal [13, 26]. However, the effect of carbon on the magnesium solubility is very small, compared to the effect of temperature. The theoretical increase of \dot{m}_{Mg} as a result of the lower carbon concentration in HIsarna hot metal, will probably not be observed in an industrial HMD.

During the HMD process with carbon-saturated hot metal, carbon precipitates and forms flakes. In theory, these carbon flakes prevent the MgS particles from reaching the slag layer, thus hampering the desulphurisation process. The lower carbon concentration, which is below the saturation point, in HIsarna hot metal implies that less carbon precipitation takes place. However, in an earlier study it was shown that the hampering effect of precipitated carbon on the HMD efficiency is negligible under industrial conditions [16]. Furthermore, the amount of kish (airborne precipitated carbon) will decrease with HIsarna hot metal.

7. Desulphurisation of high-sulphur HIsarna hot metal

The lower carbon concentration in HIsarna hot metal will, in itself, not lead to a significant change in HMD efficiency, in comparison with the desulphurisation of BF hot metal.

7.2.3.4 Manganese

Although manganese reacts with sulphur and it helps desulphurisation at the ironmaking unit (BF or HIsarna), it is observed in steel plants that manganese and sulphur are at equilibrium with each other upon arrival at the HMD. Therefore, manganese will not contribute directly to desulphurisation at the HMD [12, 21]. However, manganese helps increasing the sulphide capacity of the slag [13, 27]. Therefore, it is expected that manganese has a small positive effect on the HMD efficiency.

7.2.3.5 Sulphur

Since HIsarna hot metal has a higher sulphur concentration than BF hot metal, the HMD process will take longer and the total reagent consumption will be higher. Consequently, the costs for the HMD process will increase when HIsarna hot metal is introduced. However, the specific magnesium consumption (\dot{m}_{Mg}) will decrease as a result of the higher sulphur concentration, as it is easier to remove sulphur when sulphur is present at a higher concentration. Although the total reagent consumption will be higher as a result of more sulphur that needs to be removed, the efficiency of the HMD process increases with a higher initial sulphur concentration [6, 28].

7.2.4 Temperature

Temperature has a significant effect on the magnesium-based HMD process. The desulphurisation reaction with magnesium is enhanced at lower temperatures. Lower \dot{m}_{Mg} values are observed in industrial HMD stations when the hot metal temperature is lower [12]. Magnesium solubility in hot metal decreases at increasing hot metal temperatures. This is because the increasing temperature increases the vapour pressure of magnesium gas, making it thermodynamically favourable for magnesium to be in the gas phase, rather than being dissolved in hot metal [14, 24, 29–31]. Although desulphurisation of hot metal with magnesium gas is possible under HMD conditions, the homogeneous reaction between dissolved magnesium and dissolved sulphur (Reaction 7.1) is kinetically favourable. Irons and Guthrie [32] found that more than 90 % of the magnesium-based desulphurisation is via dissolved magnesium rather than via magnesium gas. Thermodynamically, Reaction 7.1 is favoured at lower temperatures [12, 33].

It should be noted that the desulphurisation efficiency increases with increasing temperature, when the reagents are calcium-based (CaO or CaC₂). The reaction

between dissolved sulphur and lime or calcium carbide is thermodynamically favoured at higher temperatures [12, 33]. This is also supported by industrial observations [28] and this is a reason why no magnesium-based desulphurisation is done in liquid steel, which is typically 200 °C warmer than hot metal. However, since in the magnesium-lime co-injection HMD process is governed by the desulphurisation reaction via magnesium, the beneficial effect of a higher temperature on calcium-based desulphurisation does not balance its negative effect on desulphurisation via magnesium. Therefore, the overall HMD process is more efficient and faster at low hot metal temperatures, which is also observed in industry [12, 24].

7.2.5 Slag

Since HIsarna hot metal is tapped without any carryover slag, the slag composition at the HMD depends only on the HMD process itself. When Mg and CaO are injected, the slag will consist of the formed sulphides and oxides: CaS, MgO and CaO. Such a slag would be solid at HMD temperatures, which is undesired. Besides, compared to desulphurisation of BF hot metal, more sulphides and oxides are formed (more sulphur needs to be removed) and the temperature is lower, which further enhances the slag's solid fraction. A slag with a low liquid fraction has a high apparent viscosity, which leads to high iron losses [20, 34, 35]. Furthermore, a high solid fraction decreases the reaction surface, and therefore the reactivity, of the slag, hampering the reaction between MgS and CaO (Reaction 7.2). As MgS, in contact with oxygen from the air, thermodynamically favours the formation of MgO, the sulphur would return to the hot metal; a process called resulphurisation [12, 26]. Therefore, the addition of a synthetic slag is required. In order to make the slag liquid, its melting temperature should be lowered by adding acidic oxides such as SiO₂ and Al₂O₃. Also the addition of small quantities of alkali metal oxides, like Na₂O and K₂O, could lower the slag's melting point and viscosity [21].

It would require specific equipment to add the synthetic slag, but such a procedure would lead to lower iron losses and less slag that needs to be treated after the HMD process, eventually leading to lower costs. Alternatively, BF slag (if available) could be used instead of synthetic slag, which would lead to roughly the same slag composition as is common today at the HMD. Also basic low-sulphur slag from another steelmaking process (e.g. from secondary metallurgy) could be used to make a liquid slag, but it depends on the composition of that slag if it is suitable for that. This needs further investigation.

Although the same composition of current HMD slag could be achieved, desulphurisation of HIsarna hot metal will lead to a colder slag, because of the

7. Desulphurisation of high-sulphur HIsarna hot metal

lower temperature of the hot metal. This leads to a higher solid fraction of the slag. It is not certain that a slag modifier could completely compensate for this, as its use is limited by slag basicity (a too acidic slag would not desulphurise) and alkali metal oxide concentration (slag that is recycled at the BF cannot contain too much alkali metal oxides, because these will build up inside a BF) [21]. Furthermore, the total slag volume will increase, because more reagents are added to remove the higher amount of sulphur in HIsarna hot metal. This will, despite slag modifiers, lead to higher iron losses [20, 34]. Apart from the iron losses, the slag skimming time will increase when there is more slag to remove, leading to a longer total process time and higher temperature losses.

7.2.6 Summary

The theoretical influence of the different hot metal composition and temperature of HIsarna hot metal on the HMD process is summarised in Table 7.2. The column $\dot{m}_{Mg, HsHM}$ shows how the \dot{m}_{Mg} changes for HIsarna hot metal compared to BF hot metal for the given variable.

Table 7.2: Influence of different hot metal composition and temperature on \dot{m}_{Mg} by changing from BF hot metal to HIsarna hot metal. Influence ranges from a large increase (▲▲) to a large decrease(▼▼) for \dot{m}_{Mg} of HIsarna hot metal.

Factor	BF	HIsarna	$\dot{m}_{Mg, HsHM}$	Remarks
[O]	0.5 ppm	6 ppm	▲▲	
[Si]	0.4 wt%	0.007 wt%	▲	Excluding a_O
[Ti]	0.04 wt%	0.001 wt%	0	Excluding a_O
[C]	4.5 wt%	4.0 wt%	0	Excluding a_O
[Mn]	0.3 wt%	0.03 wt%	(▼)	Excluding a_O
[S]	0.03 wt%	0.1 wt%	▼▼	
T	1375 °C	1325 °C	▼▼	Temperature at HMD

Based on this analysis, a lower \dot{m}_{Mg} can be expected at the HMD for HIsarna hot metal compared to BF hot metal. However, due to the higher sulphur concentration, the total reagent consumption would increase.

The \dot{m}_{Mg} of an HMD supplied with BF hot metal varies from plant to plant, due to reagent purity, Mg:CaO ratio, initial sulphur concentration and local process conditions. Typically, \dot{m}_{Mg} varies from 1.0 to 2.5 (occasionally \dot{m}_{Mg} can be higher than 4). Stoichiometrically, \dot{m}_{Mg} can never be lower than 0.76 [6, 12]. As a result of the high sulphur concentration and low temperature of HIsarna hot metal, it is reasonable to assume that the lowest \dot{m}_{Mg} achieved in industry today for BF hot metal (1.0) would be a good estimate for desulphurisation of HIsarna hot metal. This implies that desulphurising HIsarna hot metal requires more magnesium

than desulphurising hot metal from the BF. However, as the final sulphur concentration ($[S]_{\text{final}}$) aim becomes lower, the difference between desulphurisation of HIsarna hot metal and BF hot metal becomes smaller, as is illustrated by Figure 7.3. This is mainly the result of the lower temperature of HIsarna hot metal, which decreases \dot{m}_{Mg} .

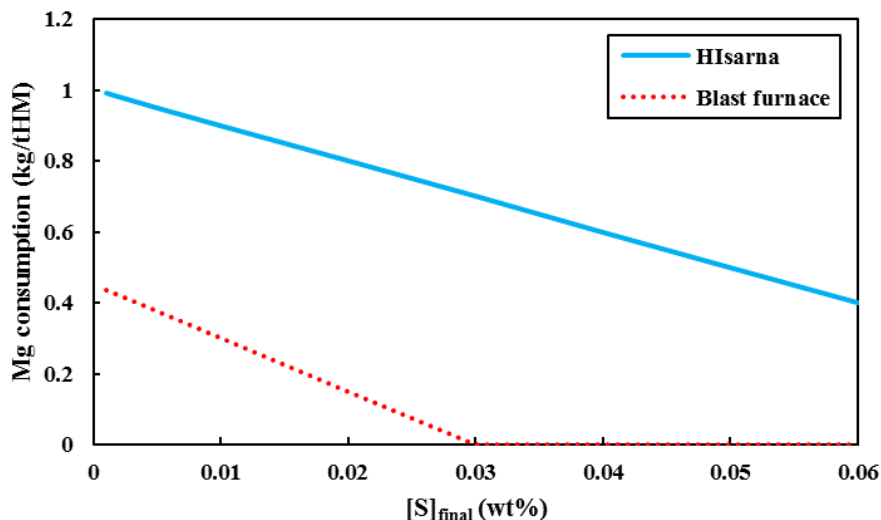


Figure 7.3: Estimated Mg consumption (kg/tHM) for hot metal from HIsarna and BF for different final sulphur concentrations, based on expected \dot{m}_{Mg} (1 for HIsarna hot metal and 1.5 for BF hot metal).

As the difference in Mg consumption between hot metal from HIsarna and BF is roughly 0.6 kg/tHM, a heat of 300 t would lead to an extra magnesium consumption of 180 kg. Depending on the injection speed that means an extra processing time of 7-10 minutes (excluding extra skimming time). This extra processing time will increase the probability that the HMD becomes the bottleneck in the steelmaking process chain. Also the extra processing time will lead to an extra temperature loss of 3-5 °C.

7.3 Thermodynamic simulations

In order to better understand the thermodynamic consequences of desulphurising HIsarna hot metal, compared to typical BF hot metal, FactSage calculations were conducted. FactSage 7.3 was used for simulation of HMD with different hot metal conditions, using the FSstel-Liqu and CON3 SLAG base phases [36]. The hot metal compositions from Table 7.1 were assumed and a surplus of Mg was added (1.0 wt% of the hot metal; depending on the initial sulphur concentration,

7. Desulphurisation of high-sulphur HIsarna hot metal

stoichiometrically 0.023-0.076 wt% Mg is required to remove all sulphur). In the simulation, reactions with slag, air and lime were not considered, so only desulphurisation via Reaction 7.1 was taken into account. Since 1375 °C is a common hot metal temperature at the HMD and HIsarna hot metal is typically 50 °C colder than BF hot metal, the temperature was varied from 1325 °C to 1375 °C.

The FactSage calculations showed no significant difference between the desulphurisation of HIsarna hot metal and of BF hot metal. At equilibrium, the surplus of magnesium is large enough to remove nearly all sulphur, regardless of the initial sulphur concentration and oxygen concentration. A higher temperature does lead to a higher equilibrium sulphur concentration in the hot metal. Also, the higher carbon concentration in blast furnace hot metal slightly increases the equilibrium sulphur concentration, compared to that of HIsarna hot metal.

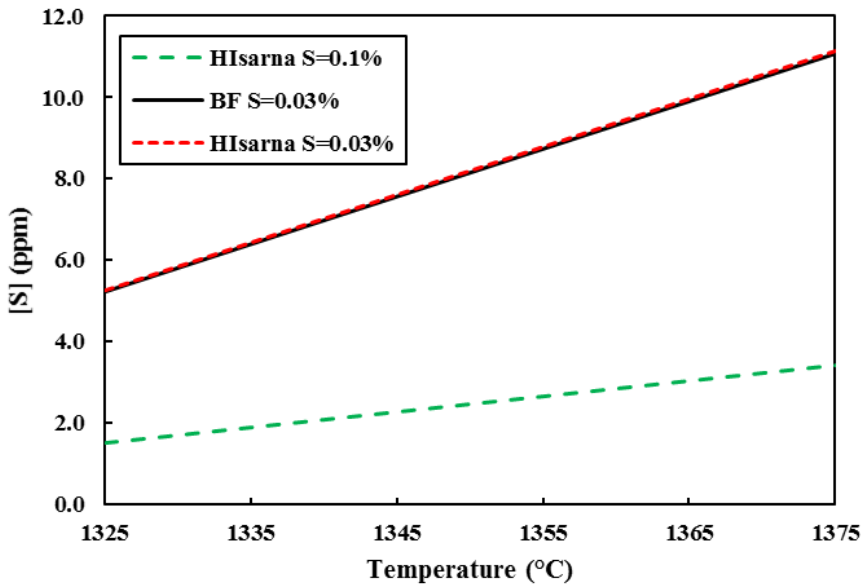


Figure 7.4: Sulphur concentration in hot metal equilibrium after HMD, calculated with FactSage 7.3, for BF hot metal (black solid line), HIsarna hot metal with 0.1 wt% [S] (green dashed line) and HIsarna hot metal with 0.03 wt% [S] (red small-dashed line).

When instead of a surplus of magnesium, only enough magnesium for an \dot{m}_{Mg} of 1.0 is added (so 1 kg magnesium is added per kg of sulphur present), there is a difference between HIsarna hot metal and BF hot metal. Figure 7.4 shows the

equilibrium sulphur concentration in the hot metal after HMD for the different initial hot metal compositions.

As was expected based on the theory, the final sulphur concentration in the HIsarna hot metal is lower than that of the BF hot metal. The reason is that more magnesium is added, as HIsarna hot metal initially also contains more sulphur (so \dot{m}_{Mg} remains the same). Since, thermodynamically, desulphurisation becomes harder at lower sulphur concentrations, the overall efficiency of desulphurising HIsarna hot metal is higher than that of BF hot metal. However, when leaving the desulphurisation of HIsarna hot metal until a sulphur concentration of 0.03 wt% (the initial sulphur concentration of BF hot metal) out of the comparison, so taking the composition of HIsarna hot metal, but with an initial sulphur concentration of 0.03 wt% (red small-dashed line), the differences between desulphurisation of HIsarna hot metal and BF hot metal become negligible for the same temperatures. The difference in oxygen concentration or other elements do not significantly change the equilibrium of the final sulphur concentration in the hot metal.

For desulphurisation of HIsarna hot metal, extra magnesium is required to remove the surplus of sulphur, compared to BF hot metal. This sulphur is removed at a high efficiency. The real thermodynamic advantage of desulphurisation of HIsarna hot metal over desulphurisation of BF hot metal only lies in the lower hot metal temperature of HIsarna hot metal.

It should be noted that the sulphur concentrations in the hot metal at equilibrium are lower than the sulphur concentrations after HMD observed in industry. This is because kinetics play an important role in the HMD process, impeding reaching equilibrium with an economically viable amount of reagents and within a feasible time [12–14]. This will be discussed in association with plant data analysis in the following section.

7.4 Plant data analysis

To be able to include the kinetics in the overview of the effect of hot metal composition and temperature on the HMD process, a plant data analysis was conducted with 31 663 heats from the HMD stations for BF hot metal at Tata Steel, the Netherlands. The BF does not produce hot metal that is similar to HIsarna hot metal, so analysis of this plant data, with hot metal coming from the BF, will not directly answer the question of how HIsarna hot metal would behave. However, this plant data does give an indication of the effect of different components on the HMD efficiency. In the analysis, \dot{m}'_{Mg} (Equation 7.5) is used to indicate the HMD efficiency. When analysing plant data, it should be noted

7. Desulphurisation of high-sulphur HIsarna hot metal

that a correlation does not necessarily mean causality. Furthermore, it should be noted that several parameters correlate with each other as well, like the silicon and titanium concentration of hot metal, which are heavily correlated with each other, resulting in correlations between silicon and any other parameter will be similar to the correlation between titanium and that same parameter.

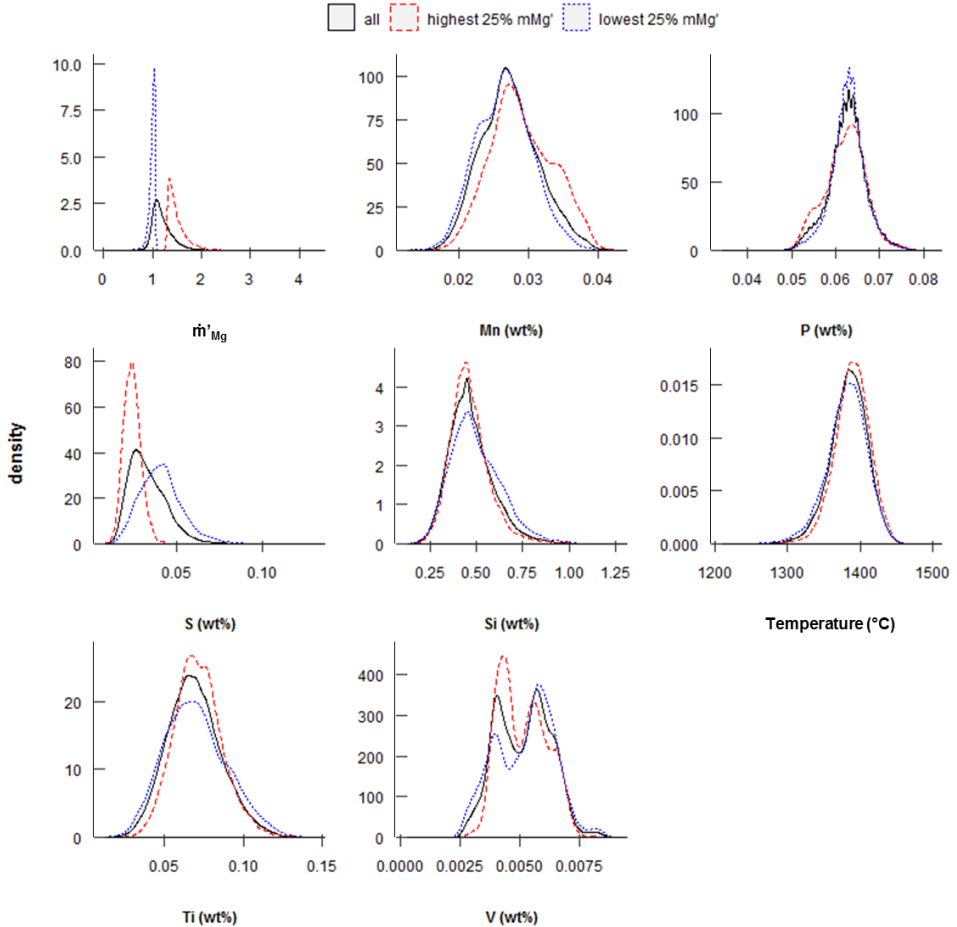


Figure 7.5: Distribution of the plant data from Tata Steel, IJmuiden, for the key parameters. Black solid lines show all data, the red dashed lines include only the data with the highest 25% \dot{m}'_{Mg} and the blue dotted lines include only the data with the lowest 25% \dot{m}'_{Mg} .

A distribution plot of the plant data, which is given in Figure 7.5, reveals the correlation between \dot{m}'_{Mg} and the composition and temperature of the hot metal. The plot shows the distribution of concentration of certain elements in the hot metal, temperature and \dot{m}'_{Mg} for the whole dataset (black solid lines) and also the

distribution for the same parameters for the data with the highest 25 % (red dashed lines) and lowest 25 % (blue dotted lines) of \dot{m}'_{Mg} . The initial sulphur concentration clearly shows the highest correlation with \dot{m}'_{Mg} . Temperature and silicon (and titanium and vanadium) are in correspondence with the predictions from Section 7.2 as well. It is remarkable that manganese shows a clear negative correlation with \dot{m}'_{Mg} . Low manganese concentrations correlate with a high desulphurisation efficiency (low \dot{m}'_{Mg}). Based on the theory, a small positive effect of manganese on the desulphurisation efficiency is expected. The correlation cannot be explained by a_O , since a low manganese concentration would indicate a high a_O , but a high a_O would lead to a high \dot{m}'_{Mg} . However, the opposite is found here. At the BF manganese helps desulphurising the hot metal [12, 21], which leads to an inverse correlation between the manganese and sulphur concentrations in the hot metal. Upon arrival at the HMD station, the manganese and sulphur concentrations are already at equilibrium, so manganese will not influence the desulphurisation at the HMD. However, since a lower sulphur concentration leads to a higher \dot{m}'_{Mg} , a high manganese concentration is correlated with a low \dot{m}'_{Mg} as well.

In order to better understand the relative impact of the different components in the hot metal and the temperature on \dot{m}_{Mg} , a random forest model (RFM) is made for the plant data. With a RFM the predicting value of the different parameters to predict \dot{m}'_{Mg} in the data set (impact) is determined [37]. In this study, the package “randomForest” within the software R is used. The RFM used 50 trees and a minimal node size of 20. Figure 7.6 gives the overview of the impact of the different parameters on \dot{m}'_{Mg} .

Parameter	Impact	\dot{m}'_{Mg}
Sulphur		▼
Temperature		▲
Silicon		▼
Titanium		▼
Phosphorus		▼
Vanadium		▲
Manganese		▲

Figure 7.6: Relative impact of parameters on \dot{m}'_{Mg} , according to the RFM.

The RFM shows that \dot{m}'_{Mg} can best be predicted by the initial sulphur concentration of the hot metal, followed by temperature, silicon and titanium

7. Desulphurisation of high-sulphur HIsarna hot metal

concentrations. Despite the seemingly strong correlation between manganese concentration and \dot{m}'_{Mg} based on the distribution plot, manganese shows to be a poor parameter to predict \dot{m}'_{Mg} . This supports the explanation that the correlation between manganese and \dot{m}'_{Mg} is caused by the correlation between manganese and sulphur, rather than by an independent effect of manganese on \dot{m}'_{Mg} . The correlation between the silicon (and titanium) concentration and \dot{m}'_{Mg} , cannot be fully attributed to the effect of a_O on the HMD process. The hot metal composition depends on the BF process. A high hot metal silicon concentration correlates with a lower slag basicity at the BF [7], which lowers the sulphur removal capacity of the slag, thus the desulphurisation efficiency. A high silicon concentration in the hot metal correlates with a high sulphur concentration prior to HMD. Furthermore, a high silicon concentration at the BF indicates a low hot metal temperature, which leads to a lower \dot{m}'_{Mg} . Therefore, based on this plant data it is not possible to quantify the effect of a_O on \dot{m}'_{Mg} , but it is clear that, in practice, the effect of a_O is smaller than the effect of sulphur concentration and temperature on \dot{m}'_{Mg} .

The influence of the hot metal composition and temperature on \dot{m}'_{Mg} is not linear. The most important factor, the initial sulphur concentration ($[S]_{in}$), has only a significant impact up to ~ 0.04 wt%. At higher sulphur concentrations, sulphur is abundant compared to dissolved magnesium anyway, so a higher sulphur concentration does not increase the desulphurisation efficiency much further.

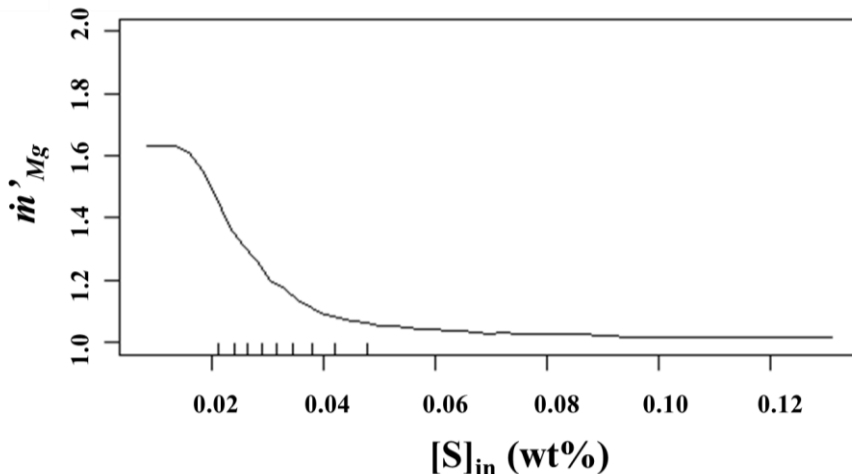


Figure 7.7: Partial dependency of \dot{m}'_{Mg} on initial sulphur concentration, based on the RFM.

This is illustrated by Figure 7.7, based on the RFM, showing the partial dependency of \dot{m}'_{Mg} on the initial sulphur concentration. It should be noted that the number of datapoints at initial sulphur concentrations above 0.05 wt% are limited. However, an asymptote at $\dot{m}'_{Mg} \approx 1.0$ is in accordance with the expectations discussed in Section 7.2.6.

The plant data analysis shows that the higher sulphur concentration and lower temperature of HIsarna hot metal, compared to BF hot metal, will lead to a typical \dot{m}'_{Mg} of 1.0. The plant data analysis supports the theory that a_O has a significant effect on \dot{m}'_{Mg} , but that this effect is smaller than the effect of the initial sulphur concentration and temperature.

7.5 Discussion

Given the much higher sulphur concentration in HIsarna hot metal, compared to hot metal from state-of-the-art blast furnaces, desulphurisation will take longer and cost more reagent. However, the high sulphur concentration and the low hot metal temperature will lead to a low \dot{m}'_{Mg} , in the order of 1.0. The high a_O , compared to BF hot metal, will influence the magnesium consumption, but it will only lead to a minor increase in magnesium consumption (in the order of a few kilograms per heat of ~300 tonnes, which is negligible compared to the overall increase of typically 180 kg Mg per heat, due to the higher initial sulphur concentration). All other investigated factors seem to have a much smaller influence on \dot{m}'_{Mg} .

The fact that HIsarna hot metal has virtually no silicon will hardly influence the magnesium-lime co-injection HMD process. Silicon plays an advantageous role in the HMD process via lime (Reaction 7.7), but direct desulphurisation via lime plays only a minor role in the magnesium-lime co-injection process. The absence of silicon in hot metal is problematic for lime-based HMD processes like the KR. Additional research would be required to determine how the KR process could be made suitable for desulphurisation of HIsarna hot metal.

Temperature loss could become an issue for HIsarna hot metal, as a lower hot metal temperature increases the risk of skull formation and lowers the amount of scrap that can be charged at the converter. HIsarna hot metal has already a lower temperature than BF hot metal and it contains less silicon, which acts as a fuel in the converter process. The longer processing time at the HMD will lead to a higher temperature loss as well. However, the extra processing time will only be roughly 10 minutes, which would lead to an estimated extra temperature loss of ~5 °C. This is a small amount, compared to the initial difference in hot metal temperature between HIsarna and the BF (~50 °C).

7. Desulphurisation of high-sulphur HIsarna hot metal

It should be noted that the predictions for HIsarna hot metal in both the theory and the plant data analysis are based on extrapolation of current BF hot metal data and experience. This means that certain effects of the HIsarna hot metal composition on the HMD process might be missed by this analysis. Plant trials with HIsarna hot metal would be required to rule out that certain aspects of the HIsarna hot metal composition have not been taken into account. Currently only the pilot scale HIsarna, at Tata Steel in IJmuiden, exists, which is too small to create enough hot metal for an entire heat to be processed at the steel plant. In order to verify whether the HMD station can effectively desulphurise HIsarna hot metal, a trial with synthetic HIsarna hot metal should be organised. Synthetic HIsarna hot metal can be produced by tapping “semi-steel” from the converter after only ~5 min blowing. This semi-steel does not contain silicon and titanium, has low phosphorus and manganese concentrations and contains ~2.5 wt% carbon. Extra carbon and sulphur can be added to the semi-steel, to create synthetic HIsarna hot metal, which has a comparable composition, at least for the main elements (being carbon, sulphur, phosphorus, silicon, titanium and manganese), to HIsarna hot metal. After cooling down the synthetic HIsarna hot metal, it can be desulphurised at the HMD station and further processed at the converter and the following processes. Since for this trial no actual HIsarna hot metal is required, it can be performed at any steel plant. For steelmaking companies that consider installing a HIsarna installation, this trial is a cost-effective way to investigate the consequences of HIsarna hot metal for their steel plant.

Nevertheless, the HMD process cannot only be rated on \dot{m}_{Mg} . The fact that more sulphur needs to be removed means that the HMD process will take longer. This can lead to the HMD becoming the bottleneck in the steel plant, resulting in a lower plant capacity. Furthermore, more slag will be produced as a result of more sulphur being removed, leading to higher iron losses. Because hot metal from the HIsarna does not come with any carryover slag, slag, or slag components, should be added in order to keep the slag liquid during the HMD process. A synthetic slag (containing SiO_2 and Al_2O_3 and some K_2O or Na_2O) can be added, but since that could have too high costs, recycling slag from another process in the steelmaking route (containing high concentrations of SiO_2 and Al_2O_3) seems more likely. Given the current experience with BF carryover slag, slag from the BF would be a good candidate. However, it should be noted that due to the lower temperature of HIsarna hot metal and the longer HMD process time, the slag will be 50 °C, or more, colder than typical HMD slag. This means that despite of a slag modifier, the slag could be partly solid, resulting in a higher slag viscosity

Part III Desulphurisation of HIsarna hot metal

and, therefore, higher iron losses than at the current HMD process with BF hot metal.

To lower the impact of the above described effects of HIsarna hot metal on the HMD process, the initial sulphur concentration in the hot metal could be lowered prior to the HMD process. One option is to decrease the sulphur input in the HIsarna, by using low-sulphur coal, which can lead to hot metal with 50 % lower sulphur concentrations. Another option would be to mix the HIsarna hot metal with hot metal from a BF or another ironmaking unit that produces hot metal with a lower sulphur concentration. Diluting the HIsarna hot metal in this way would lead to shorter process times and less slag at the HMD, but it would also decrease the advantages of HIsarna hot metal. As discussed already, desulphurisation of HIsarna hot metal is more efficient than desulphurisation of BF hot metal when looking at the reagent costs per amount of removed sulphur. Diluting the HIsarna hot metal would not lower the total amount of sulphur that needs to be removed. However, diluted HIsarna hot metal with a lower sulphur concentration will lead to shorter process times at the HMD, which limits the temperature loss and lowers the chance of production loss due to delays at the HMD. Furthermore, the variation in HMD process times for mixed hot metal heats will be smaller than the variation in HMD process times for pure HIsarna hot metal heats and heats containing only hot metal from the other ironmaking unit. The smaller variation in HMD process time is beneficial for the plant's logistic flexibility. Mixing hot metal streams after the HMD process would make use of the efficiency advantage, but mixing hot metal after the HMD has too many practical problems. Since mixing two streams of hot metal by pouring it from one ladle into another has safety issues and would require at least two different ladle sizes, either a separate mixing vessel or mixing in the converter would be required. Both solutions mean extra handling time, leading to more delays and a higher chance of production loss, and would decrease the process flexibility. Besides, diluting HIsarna hot metal can only be considered when another ironmaking unit is available.

Another way to limit the consequences of desulphurisation of HIsarna hot metal is to increase the aim for the final sulphur concentration. This implies that the pressure on the secondary metallurgy desulphurisation increases. Besides, sulphur removal at secondary metallurgy is more expensive than desulphurisation of hot metal [12].

Given the disadvantages of the alternatives, the most promising solution for desulphurisation of HIsarna hot metal is investing in the capacity of the HMD process, preferably the magnesium-lime co-injection HMD process. This can be done by either solving the bottleneck at the HMD or by building an extra HMD

7. Desulphurisation of high-sulphur HIsarna hot metal

station. Alternatively, desulphurisation of HIsarna hot metal can already start at the tap of the HIsarna, by installing a continuous hot metal desulphurisation (CHMD) process [38]. This CHMD process, which will be discussed in more detail in the next chapter, is in an early stage of development.

7.6 Conclusions and outlook

7.6.1 Conclusions

Based on the theory, a thermodynamic evaluation and plant data analysis, it can be concluded that the magnesium-lime co-injection HMD process is capable of desulphurising HIsarna hot metal to final sulphur concentrations as low as current practice with BF hot metal (that is below 10 ppm). The following conclusions can be drawn:

- Desulphurising HIsarna hot metal will take longer and consumes more reagents than desulphurisation of BF hot metal, as a result of the higher initial sulphur concentration.
- Desulphurisation of HIsarna hot metal will have a lower \dot{m}_{Mg} than BF hot metal desulphurisation, because of the higher initial sulphur concentration and lower temperature.
- The higher oxygen concentration of HIsarna hot metal will lead to a higher reagent consumption at the HMD, but this will be in the order of a 10-50 gram magnesium per tonne hot metal
- As a result of the very low silicon concentration in HIsarna hot metal, the lime-based KR process will be less efficient in desulphurising HIsarna hot metal.
- Other elements dissolved in the hot metal do not have a significant influence on the HMD process efficiency.

7.6.2 Outlook

Given the current climate change mitigation, steelmakers worldwide will need to change the way they produce hot metal. Since HIsarna is in a mature phase of its development, it is expected that the HIsarna process will contribute to the worldwide hot metal production around the year 2035. Whether the HIsarna hot metal will be mixed with hot metal from other sources or used in its pure form, the desulphurisation of the hot metal is more challenging and requires special attention.

The current study shows that desulphurisation of hot metal to the required low sulphur concentrations is possible, but that it can lead to capacity problems in maladjusted steel plants. This means that in the coming years the steel industry

should not only focus on new ways to produce hot metal with less or no CO₂ emission, but also on the potential consequences on efficiency and quality for the subsequent processes in the steel plant. It is expected that with relatively easy adaptations, the magnesium-lime co-injection HMD process will be ready for desulphurisation of Hisarna hot metal. However, more innovative, new HMD processes, like the CHMD [38], could prove to be more efficient in desulphurising Hisarna hot metal.

7.7 References

- [1] J. Zhao, H. Zuo, Y. Wang, J. Wang, and Q. Xue, “Review of green and low-carbon ironmaking technology,” *Ironmak. Steelmak.*, vol. 47, no. 3, pp. 296–306, 2020, doi: 10.1080/03019233.2019.1639029.
- [2] M. Abdul Quader, S. Ahmed, S.Z. Dawal, and Y. Nukman, “Present needs, recent progress and future trends of energy-efficient Ultra-Low Carbon Dioxide (CO₂) Steelmaking (ULCOS) program,” *Renew. Sustain. Energy Rev.*, vol. 55, pp. 537–549, 2016, doi: 10.1016/j.rser.2015.10.101.
- [3] H.K.A. Meijer *et al.*, *Hisarna Experimental Campaigns B and C*, vol. EUR-27515. Luxembourg: Publications Office of the European Union, 2015.
- [4] H.K.A. Meijer, C. Guenther, and R.J. Dry, “Hisarna Pilot Plant Project,” *InSteelCon*, no. July, pp. 1–5, 2011.
- [5] J.W.K. van Boggelen, H.K.A. Meijer, C. Zeilstra, and Z. Li, “The Use of Hisarna Hot Metal in Steelmaking,” in *Scanmet V*, 2016, p. 008.pdf.
- [6] F.N.H. Schrama, E.M. Beunder, J.W.K. van Boggelen, R. Boom, and Y. Yang, “Desulphurisation of Hisarna hot metal - a comparison study based on plant data,” in *Science and Technology of Ironmaking and Steelmaking*, 2017, pp. 419–422.
- [7] M. Geerdes, R. Chaigneau, I. Kurunov, O. Lingiardi, and J. Ricketts, *Modern Blast Furnace Ironmaking*, 3rd ed. Delft (NL): IOS Press, 2015.
- [8] T. Tamura, M. Miyata, Y. Higuchi, and T. Matsuo, “Development of Hot Metal Dephosphorization with Powder CaO Top Blowing,” in *EOSC 2011*, 2011, pp. 6–04, doi: 10.2320/materia.51.16.
- [9] “private communication with Prof. Dr. Yasuyuki Tozaki.” 2019.
- [10] B.K. Rout, G.A. Brooks, M.A. Rhamdhani, Z. Li, F.N.H. Schrama, and J. Sun, “Dynamic Model of Basic Oxygen Steelmaking Process Based on Multi-zone Reaction Kinetics: Model Derivation and Validation,” *Metall. Mater. Trans. B*, vol. 49, no. 2, pp. 537–557, 2018, doi: 10.1007/s11663-

7. Desulphurisation of high-sulphur HIsarna hot metal

017-1166-7.

- [11] H. Jalkanen and L. Holappa, *Converter Steelmaking*, vol. 3. Oxford (UK): Elsevier Ltd., 2014.
- [12] F.N.H. Schrama, E.M. Beunder, B. van den Berg, Y. Yang, and R. Boom, “Sulphur removal in ironmaking and oxygen steelmaking,” *Ironmak. Steelmak.*, vol. 44, no. 5, pp. 333–343, 2017, doi: 10.1080/03019233.2017.1303914.
- [13] H.-J. Visser, “Modelling of injection processes in ladle metallurgy,” (PhD thesis) Delft University of Technology, Delft (NL), 2016.
- [14] S. Kitamura, “Hot Metal Pretreatment,” in *Treatise on Process Metallurgy*, vol. 3, S. Seetharaman, Ed. Oxford (UK): Elsevier, 2014, pp. 177–221.
- [15] H.-J. Visser and R. Boom, “Advanced Process Modelling of Hot Metal Desulphurisation by Injection of Mg and CaO,” *ISIJ Int.*, vol. 46, no. 12, pp. 1771–1777, 2006, doi: 10.2355/isijinternational.46.1771.
- [16] F.N.H. Schrama, E.M. Beunder, H.-J. Visser, J. Sietsma, R. Boom, and Y. Yang, “The Hampering Effect of Precipitated Carbon on Hot Metal Desulfurization with Magnesium,” *Steel Res. Int.*, vol. 91, no. 11, p. 1900441, 2020, doi: 10.1002/srin.201900441.
- [17] W. Ma, H. Li, Y. Cui, B. Chen, G. Liu, and J. Ji, “Optimization of Desulphurization Process using Lance Injection in Molten Iron,” *ISIJ Int.*, vol. 57, no. 2, pp. 214–219, 2017, doi: 10.2355/isijinternational.55.570.
- [18] A. Ender, H. Van Den Boom, H. Kwast, and H.-U. Lindenberg, “Metallurgical development in steel-plant-internal multi-injection hot metal desulphurisation,” *Steel Res. Int.*, vol. 76, no. 8, pp. 562–572, 2005.
- [19] U.B. Pal and B.V. Patil, “Role of dissolved oxygen in hot metal desulphurization,” *Ironmak. Steelmak. Steelmak.*, vol. 13, no. 6, pp. 294–300, 1986.
- [20] P. Hayes, “Sources of data on chemical and physical systems,” *Process principals in minerals & materials production*. Hayes Publishing Co., Brisbane (AUS), pp. 633–646, 1993.
- [21] F.N.H. Schrama *et al.*, “Optimal hot metal desulphurisation slag considering iron loss and sulphur removal capacity part I: Fundamentals,” *Ironmak. Steelmak.*, vol. 48, no. 1, pp. 1–13, 2021, doi: 10.1080/03019233.2021.1882647.

Part III Desulphurisation of Hisarna hot metal

- [22] Y. Yang, K. Raipala, and L. Holappa, "Ironmaking," in *Treatise on Process Metallurgy*, vol. 3, S. Seetharaman, Ed. Oxford (UK): Elsevier, 2014, pp. 2–88.
- [23] P.K. Iwamasa and R.J. Fruehan, "Effect of FeO in the Slag and Silicon in the Metal on the Desulfurization of Hot Metal," *Metall. Mater. Trans. B*, vol. 28, no. February, pp. 47–57, 1997, doi: 10.1007/s11663-997-0126-z.
- [24] P.J. Koros, "Pre-Treatment of Hot Metal," in *The Making, Shaping and Treating of steel*, 11th ed., R. J. Fruehan, Ed. Pittsburgh (USA): AISE Steel Foundation, 1998, pp. 413–429.
- [25] S. Street, R.P. Stone, and P.J. Koros, "The presence of titanium in hot metal and its effects on desulfurization," *Iron Steel Technol.*, vol. 2, no. 11, pp. 65–74, 2005.
- [26] J. Yang, M. Kuwabara, T. Teshigawara, and M. Sano, "Mechanism of Resulfurization in Magnesium Desulfurization Process of Molten Iron," *ISIJ Int.*, vol. 45, no. 11, pp. 1607–1615, 2005, doi: 10.2355/isijinternational.45.1607.
- [27] R.W. Young, "Use of optical basicity concept for determining phosphorus and sulphur slag–metal partitions," (EUR 13176 EN) Luxembourg, 1991.
- [28] R. Samanta, A. Ganguly, A. Kumar, and S. Pathak, "Impact of Hot Metal Properties on Steel Making Process and Its Pretreatment," in *Proceedings of the 6th International Congress on the Science and Technology of Steelmaking, ICS 2015*, 2015, pp. 67–71.
- [29] P.J. Guichelaar, P.K. Trojan, T. McCluhan, and R.A. Flinn, "A new technique for vapor pressure measurement applied to the Fe-Si-Mg system," *Metall. Mater. Trans. B*, vol. 2, no. 12, pp. 3305–3313, 1971, doi: 10.1007/BF02811611.
- [30] G.A. Irons, "Metallurgical aspects of desulphurization," in *International Magnesium Association Meeting*, 1999.
- [31] N.A. Voronova, *Desulfurization of hot metal by magnesium*. Dayton (USA): The International Magnesium Association, 1983.
- [32] G.A. Irons and R.I.L. Guthrie, "The kinetics of molten iron desulfurization using magnesium vapor," *Metall. Trans. B*, vol. 12, no. 4, pp. 755–767, 1981, doi: 10.1007/BF02654145.
- [33] E.T. Turkdogan, *Fundamentals of steelmaking*. London (UK): The Institute of Materials, 1996.

7. Desulphurisation of high-sulphur HIsarna hot metal

- [34] F.N.H. Schrama *et al.*, “Optimal hot metal desulphurisation slag considering iron loss and sulphur removal capacity part II: Evaluation,” *Ironmak. Steelmak.*, vol. 48, no. 1, pp. 14–24, 2021.
- [35] M. Magnelöv, “Iron Losses During Desulphurisation of Hot Metal,” (PhD thesis) Luleå University of Technology, Luleå (SE), 2014.
- [36] CRCT (Canada) & GTT (Germany), “FactSage 7.3,” 2020. [Online]. Available: www.factsage.com.
- [37] K. Fawagreh, M.M. Gaber, and E. Elyan, “Random forests: From early developments to recent advancements,” *Syst. Sci. Control Eng.*, vol. 2, no. 1, pp. 602–609, 2014, doi: 10.1080/21642583.2014.956265.
- [38] A. Emami, F.N.H. Schrama, and J.W.K. van Boggelen, “Device and method for continuous desulphurisation of liquid hot metal,” WO2020/239554A1, 2020.

8 A novel process for continuous hot metal desulphurisation

This chapter is based on the following prepared manuscript for publication in a peer-reviewed international journal:

F.N.H. Schrama, A. Emami, E.M. Beunder, J.W.K. van Boggelen, K.A. Buist, J.A.M. Kuipers, J. Sietsma, Y. Yang, “A novel process for continuous hot metal desulphurisation”.

A new continuous hot metal desulphurisation (CHMD) process is developed at Tata Steel IJmuiden, the Netherlands. The process is based on the magnesium-lime co-injection process, but the efficiency is greatly improved by employing several (typically three) reactors in series, using an optimised reactor shape for desulphurisation. The CHMD process is designed to desulphurise hot metal from continuous ironmaking processes like HIsarna, but it can also replace the conventional batch hot metal desulphurisation (HMD) process for blast furnaces (BF) that produce hot metal (nearly) continuously. Since the HIsarna process produces high-sulphur hot metal compared to the BF, combining this CHMD process with the HIsarna process will avoid a higher time pressure on the HMD process in the steel plant. In fact, the CHMD process can even make the batch HMD process redundant. A simulation study shows that the CHMD process will reduce reagent costs by ~20 % and iron loss by 40-60 %, compared to the batch HMD. Furthermore, it is estimated that its dust emissions are ~40 % lower than for the batch HMD.

In this chapter the CHMD process is introduced and its characteristics, key benefits and drawbacks are discussed.

8.1 Introduction

As a result of the worldwide energy transition and an increased awareness of the human impact on the environment, the steel industry stands at the dawn of its biggest transformation since the industrial revolution. The current focus lies at the front end of the steelmaking chain, the coke- and ironmaking, which contributes the most to the emissions of the steel industry. New ironmaking processes and routes in different stages of development are emerging all over the world. Reduction by hydrogen (directly reduced iron or hybrid blast furnaces), smelting-reduction ironmaking units (HIsarna or FINEX), or electrical steelmaking (electric arc furnaces) are all seen as successful methods to make the steel industry more sustainable [1, 2].

As a consequence of these new ironmaking processes, the whole subsequent steelmaking route will have to adapt to the new situation. The current global state of the art in steelmaking is the blast furnace (BF) – basic oxygen furnace (BOF) route. In this BF-BOF route the hot metal desulphurisation (HMD) is the first process after the ironmaking in the BF. New ironmaking units will make hot metal at a different rate and with either a higher (HIsarna, FINEX) or lower (hydrogen- or electricity-based processes) sulphur concentration. This makes it evident that the hot metal desulphurisation process will change in the future.

At Tata Steel in IJmuiden, the Netherlands, the HIsarna process is developed as the environmental friendly alternative for the BF. HIsarna produces hot metal in a constant flow, which leaves the process without any slag. The HIsarna hot metal also has a much higher sulphur concentration than BF hot metal (typically 1200 ppm, against 350 ppm at the BF) [3, 4]. This creates both the opportunity and the necessity to develop a new continuous hot metal desulphurisation (CHMD) process [5].

The CHMD process that is being developed at Tata Steel is designed to desulphurise any continuous stream of hot metal. This means that the process is not only designed for HIsarna hot metal, but it is compatible with a BF as well, provided that the BF is able to continuously supply hot metal (this will require a change in BF operation, as typically there is a period of 30 min without production between closing one taphole and opening the next [6]; some kind of buffer would be required). In this chapter, the general concept of the CHMD process is introduced. Furthermore, the benefits and downsides of this process will be discussed, together with a business case. Finally, an outlook will be given towards the further development of the CHMD process.

8.2 Process overview

8.2.1 CHMD process

In this new CHMD process [5], hot metal from a BF or HIsarna (or any other continuous hot metal source) flows through several reactor vessels in series, as can be seen in Figure 8.1.

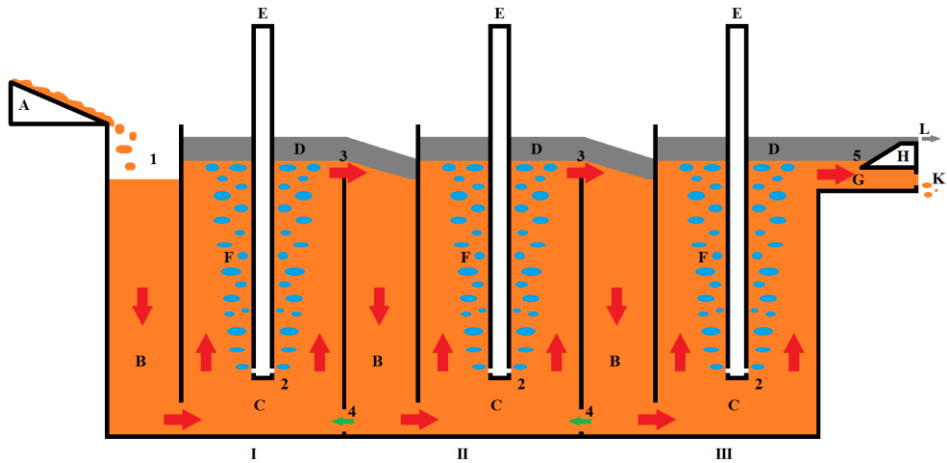


Figure 8.1: Schematic representation of the CHMD, with three reactors in series (I, II and III). Here A is the hot metal source, B the entry vessel, C the reaction vessel, D the slag layer, E the reagent injection lance, F the Mg and N₂ gas bubbles, G the shallow vessel, H the slag skimmer, K the hot metal outflow and L the slag outflow. Furthermore, 1 is the inflow of hot metal, 2 the entry of reagents, 3 the difference in bath height between vessels B and C, 4 the optional recycle stream and 5 the slag skimming. The arrows indicate the dominant direction of the hot metal flow.

The hot metal enters the system from its source (A), where it flows down into the entry vessel (B). Via an opening at the bottom, the hot metal enters the first reaction vessel (C), where magnesium and lime are injected, together with a carrier gas, into the hot metal, via an injection lance (E), similar to the co-injection HMD process. The magnesium instantly evaporates and forms gas bubbles (F). As the reaction vessel height is 6-8 m, with a diameter of 1.2-1.6 m, magnesium has a sufficiently long residence time (~5 seconds) to dissolve in the hot metal. Part of the sulphur will react with the reagents to form sulphides, which will end up in the slag phase on top of the hot metal (D). The hot metal enters the second entry vessel (II), where the process will be repeated. Process simulations reveal that both for a HIsarna and a BF typically three reactor vessels in series (I, II and III) are required, but it is possible to add a fourth reactor vessel or to operate with just two reactor vessels. At every reactor vessel (only depicted at the last vessel), a shallow vessel (G) allows sulphides in the hot metal to ascend to the slag layer

and iron droplets in the slag to flow back into the hot metal. Slag is removed separately from every reaction vessel. After that, the slag is separated from the hot metal with a foxhole-type skimmer (H) and the desulphurised, deslagged hot metal leaves the CHMD near the top of the last reactor vessel (K), while the slag leaves the CHMD separately (L).

As a result of the gas injection in reaction vessel C, the density of the mixture is lower there than in entry vessel B, causing a difference in bath height (1 and 3). This so called ‘gaslift’ phenomenon enhances the hot metal flow into the right direction. Optionally, recycle streams can be introduced, by allowing hot metal to flow back from entry vessel B into the previous reaction vessel (4). This recycle stream could increase the desulphurisation efficiency of a reaction vessel, which could lead to smaller reaction vessels or fewer reactors in the process. When a recycle stream is introduced, the gaslift phenomenon prevents hot metal to bypass the reaction vessels.

The desulphurisation rate in the CHMD is controlled by adjusting the reagent injection in the different reactor vessels. The reagent injection in the different vessels can be controlled independently from each other. Depending on the hot metal source, also the hot metal flow through the system can be used to control the desulphurisation rate. Regular temperature measurements and sampling can be done in all reactor vessels in order to monitor the process.

After the CHMD process, the desulphurised, slag-free hot metal can directly be charged to the converter, thus avoiding any time- and energy-consuming process steps in between. The CHMD process will greatly simplify the process logistics and decrease transport times at the front end of the steel plant.

8.2.2 Earlier continuous HMD processes

In the past, several attempts have been made to develop a continuous HMD process. The most successful attempt was the Rheinstahl Rührer (Rheinstahlstirrer) process, developed in 1967 in Germany at Thyssen-Heinrichshütte AG. The Rheinstahl Rührer (see Figure 8.2) was installed at the BF runner, where CaC_2 (comparable to lime, but reacting three times faster [7]) was added to the flowing hot metal and an impeller was used to mix the CaC_2 and hot metal. Note that a batch version of this process, with the same name, was developed as well [8, 9]. Although the continuous Rheinstahl Rührer was introduced in industry, the process eventually disappeared. One possible reason for this was that it could not reach lower sulphur levels than 0.008 wt% in hot metal. Given the industrial demands for ever lower sulphur concentrations, the continuous Rheinstahl Rührer would always require a batch HMD process as a next step prior to the converter.

8. A novel process for continuous hot metal desulphurisation

Another reason why the process disappeared could be the large amount of produced slag [9].

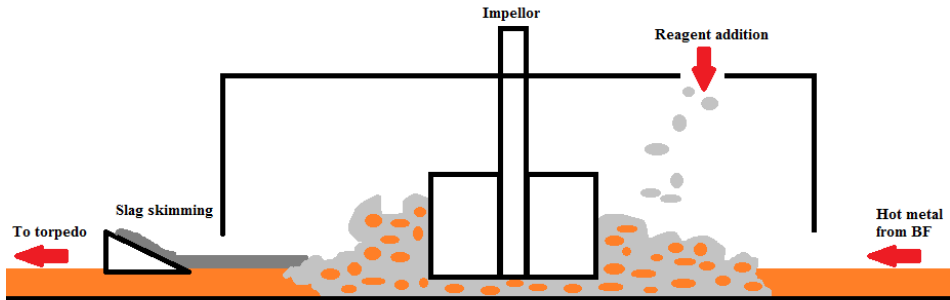


Figure 8.2: Schematic representation of the continuous Rheinstahl Rührer process.

Other continuous HMD processes never made it to industrial application. Like the Rheinstahl Rührer, the continuous HMD processes designed by Kawasaki Steel [10] and by Derge and Goldman [11], performed the desulphurisation in a single vessel. Having different reactors in series is what distinguishes the novel CHMD process from earlier attempts to develop a continuous HMD process. As will be explained in more detail in Section 8.4.1, having a single reactor means that either the process cannot reach sufficiently low sulphur concentrations, or the process requires a very large reactor size and a very long residence time. With several reactors operating in series, low sulphur concentrations (below 10 ppm) are achievable within a reasonable total reactor volume and residence time. This is a reason why the new CHMD process can be economically viable, unlike earlier attempts to develop a continuous HMD process.

8.3 Theory

8.3.1 Desulphurisation reactions

The CHMD process is based on the magnesium-lime co-injection HMD batch process, as it desulphurises the hot metal by injection of the reagents magnesium and lime. This leads to the following reactions in the hot metal:



Note that Reaction 8.2 is necessary to prevent the sulphur to be re-absorbed by the hot metal because of the reaction of MgS with oxygen. Although the reagents

are injected in a solid form, most of the magnesium will quickly dissolve in the hot metal. Because the desulphurisation reaction via magnesium (Reaction 8.1) is roughly 20 times faster than the direct desulphurisation via lime (Reaction 8.3) [12, 13], it is expected that more than 95% of the sulphur will be removed via Reaction 8.1. Since MgS is less stable in the slag than CaS, the MgS will react to CaS via Reaction 8.2. With co-injection of magnesium and lime, sulphur concentrations below 10 ppm can be achieved in hot metal [7, 14–17].

Magnesium is a faster reagent than lime, which means that a Mg-based HMD process requires a shorter residence time and, consequently, a lower reagent volume than a CaO-based HMD process, to achieve the same sulphur concentration. For a continuous HMD process, a shorter residence time and a lower reagent volume both translate to a smaller reactor volume. Furthermore, the necessity of an impeller to create agitation for a CaO-based HMD process, similar to the KR HMD process [7, 15, 18], is a disadvantage. Therefore, a CaO-based CHMD process was considered to be unviable.

Besides magnesium and lime other reagents, such as CaC_2 , CaF_2 and NaSiO_4 , are being used in the HMD processes. However, these alternative reagents are all less efficient than magnesium, albeit sometimes more efficient than CaO. Furthermore, these reagents have environmental or safety issues [7]. Therefore, these alternative reagents will not be applied as reagents for the new CHMD process.

8.3.2 Slag chemistry

The slag chemistry for the batch HMD process depends on the BF carryover slag (typically 75-80 % of the slag mass) and the products from the injected reagents: CaO, MgO and CaS (typically 20-25 wt%). Sometimes a slag modifier is added, which influences the slag composition [19].

If the hot metal comes from a BF, it is expected that the amount of BF carryover slag present in the CHMD will be comparable to the amount of BF carryover slag in the typical batch HMD process, as the CHMD will have a volume and top surface comparable to that of a hot metal ladle. The reagent efficiency of the CHMD will be higher than the batch HMD (this will be explained in more detail in Section 8.4.2), so the amount of MgO and CaO in the slag is expected to be lower on average, which is beneficial as this leads to a less viscous slag. Still, for a CHMD reactor connected to a BF, it can be assumed that the slag composition will be comparable to the current HMD slag.

If the hot metal is produced at the HIsarna, all slag will be produced in the CHMD, as HIsarna does not produce carryover slag [3]. Part of the slag will be the

8. A novel process for continuous hot metal desulphurisation

products of the injected reagents, being CaO, MgO and CaS. As HIsarna produces hot metal with a 3-4 times higher sulphur concentration than a BF [4], more CaO, MgO and CaS will end up in the slag. Because a slag purely based on these components would be solid at the operating temperatures (1350-1450 °C), adding other components is required. The addition of SiO₂, Al₂O₃ and some Na₂O or K₂O would lead to a liquid slag with a sufficient sulphur removal capacity, with a low viscosity to limit the colloidal iron loss during slag removal [19].

8.3.3 Ideal reactors

In process engineering, when designing a continuous process, there are two basic models to start with: a continuously stirred tank reactor (CSTR) and a plug-flow reactor (PFR), which are both schematically represented in Figure 8.3. In a CSTR, under stable conditions where the inlet and outlet streams are equal in magnitude, the composition (e.g. sulphur concentration) in the vessel is equal to the composition of the outlet stream, as the reactor vessel is ideally mixed. In a PFR, under stable conditions with an equal inlet and outlet stream, the composition changes gradually from equal to the inlet concentration at the inlet to equal to the outlet concentration at the outlet [20, 21].

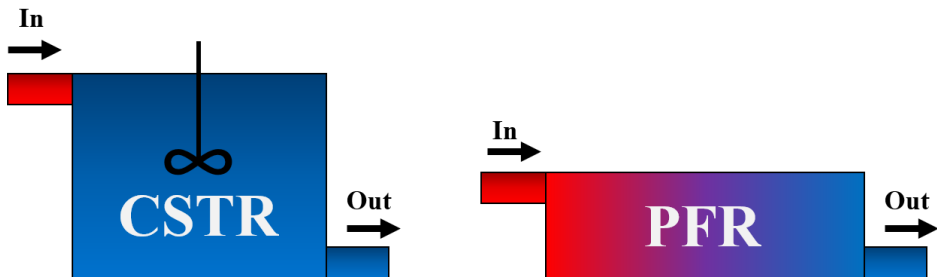


Figure 8.3: Schematic representations of a CSTR (left) and PFR (right), where the colours indicate the assumed change in concentration from initial (red) to final (blue).

A real reactor behaves like something in between an ideal CSTR and PFR. Depending on the reactor characteristics, CSTR- or PFR-behaviour can be assumed. By modelling a single reactor as several ideal reactors in series and/or parallel, the reactor model can be made more realistic, resulting in more reliable predictions [20, 21].

8.4 Process design and characteristics

8.4.1 Reactor volume

A continuous desulphurisation process requires a certain residence time of the hot metal inside the reactor vessel to allow the reagents to bring the sulphur level

down to the desired concentration. In a continuous process with a given inlet flow rate, which is equal to the outlet flow rate under stationary process conditions, this means that the trajectory of the liquid in the reactor determines the residence time. The larger the reactor trajectory is, the longer the hot metal residence time is, which means that a lower final sulphur concentration can be achieved.

A continuous reactor can be assumed to follow a well-mixed, uniform behaviour due to intense agitation induced by the gas injection. Therefore, the performance equation for the continuous reactor can be expressed in the form of a performance equation for a CSTR [22]:

$$r_A^{app} = -\frac{F_{A0} \cdot (M_{A0} - M_{Af})}{V_R} \quad (8.4)$$

In which r_A^{app} is the apparent reaction rate (in $\text{mol} \cdot \text{s}^{-1} \cdot \text{m}^{-3}$), F_{A0} the volumetric hot metal flow rate ($\text{m}^3 \cdot \text{s}^{-1}$), V_R the reactor volume (m^3), and M_{A0} and M_{Af} the inlet and final molar concentration in $\text{mol} \cdot \text{m}^{-3}$ respectively. Based on this governing equation for the reactor performance, the apparent reaction rate versus final sulphur concentration in the hot metal can be obtained for each reactor.

r_A^{app} depends on the process conditions, especially hot metal temperature and aimed sulphur concentration, and the height to diameter aspect ratio of the reactor. When developing the CHMD process, the authors developed a simulation flow model, based on the bubble column reactor principles by Deckwer [23], to estimate r_A^{app} . In the model, CSTR behaviour is assumed for the hot metal and PFR behaviour for the Mg gas. The details of this model will be published separately. Table 8.1 gives the model's main assumptions. In this model no internal recycle stream was added. The model was validated with plant data from a batch HMD process.

Table 8.1: CHMD flow model assumptions.

Parameter	Value
Hot metal temperature	1380 °C
Hot metal flow rate	1.0 Mt/y ($\sim 4.7 \cdot 10^{-3} \text{ m}^3/\text{s}$)
Height to diameter aspect ratio	5:1

In chemical engineering applications, a method to reduce the total reactor volume, for a reaction following a first- or higher-order kinetic behaviour, is to have several reactors in series [22]. In order to determine the desulphurisation capacity of several reactors in series, Equation 8.4 is used for every reactor separately, where C_{Af} of the previous reactor becomes C_{A0} in the next. F_{A0} ,

8. A novel process for continuous hot metal desulphurisation

depends on the continuous flow of the hot metal source and is taken here as $4.7 \cdot 10^{-3} \text{ m}^3/\text{s}$. Figure 8.4 shows the final sulphur concentration in the CHMD as a function of the total reactor volume, i.e. the sum of the individual reactors in series, for 1, 2, 3 and 4 reactors in series.

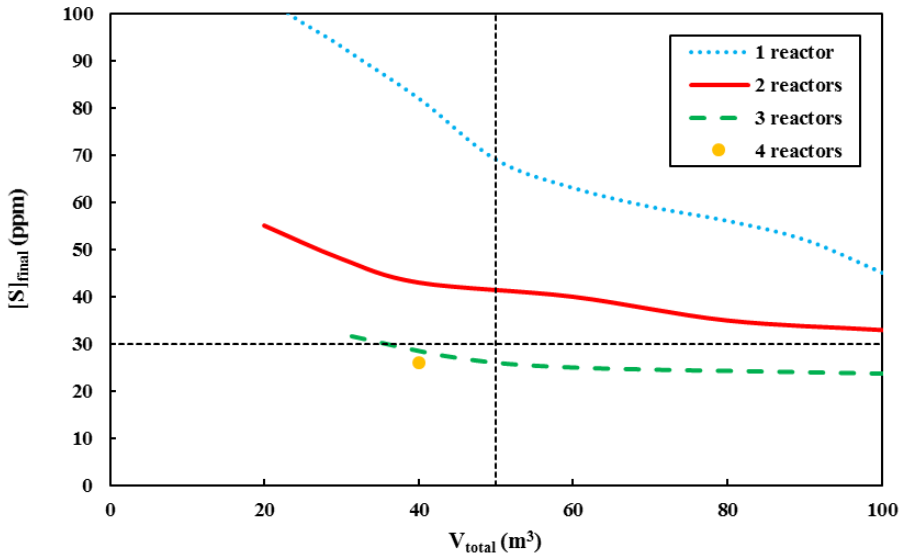


Figure 8.4: Final sulphur concentration in the CHMD as a function of the total reactor volume, for 1-4 reactors in series. Horizontal and vertical dashed lines indicate the design requirements for V_{total} and $[S]_{\text{final}}$.

For a CHMD process that is able to desulphurise the hot metal from a concentration of 1000 ppm to below 30 ppm (without optimisation) and with a reasonable total reactor volume of 50 m^3 (the volume of a large hot metal ladle), Figure 8.4 shows that three reactors in series are required. Having four or more reactors in series would, in theory, lead to even lower final sulphur concentrations and total reactor volumes. However, having four reactors in series with a total volume of 40 m^3 , would mean that each reactor has a volume of 10 m^3 , which may lead to practical problems like excessive refractory wear, temperature loss or a too small surface area for the slag.

It should be noted that the used method to estimate r_A^{app} becomes unreliable at sulphur levels below 20-25 ppm, as at these low sulphur concentrations, the magnesium solubility product rapidly increases [14]. The magnesium solubility is considered constant in the model calculations. Sulphur concentrations below 10 ppm can be achieved with a CHMD, at the cost of a higher magnesium consumption, just like in the batch HMD process [7].

8.4.2 Reagent consumption

Visser [14] showed that in an industrial HMD, the magnesium consumption is not optimal, as part of the injected magnesium will not dissolve in the hot metal, but leaves the system as a gas, after which it burns in the air. This causes the white flashes often observed in industrial HMD stations. The magnesium consumption can be decreased by increasing the residence time of the magnesium in the hot metal, which is typically 2-3 seconds for current industrial HMD stations (for a 300 t ladle, based on equations from Sahai and Guthrie [24] and Visser [14]). This can be done by either decreasing the rising velocity of the magnesium gas in the plume (which mainly depends on the ladle dimensions and the total gas flow rate), or by increasing the immersion depth of the lance or height of the bath.

Therefore, instead of the typical 3-4 m bath height that can be achieved in a hot metal ladle, the CHMD process will have a bath height of 6-8 m. To increase the mixing effect of the bubble plume, decreasing the reactor diameter would further enhance the magnesium dissolution rate, which leads to a lower magnesium consumption. The CHMD process has a height to diameter aspect ratio of 5, where a hot metal ladle, the reactor at the HMD batch process, has a typical aspect ratio of 1-1.5. Furthermore, as the reagent injection is distributed over the three reaction vessels, the flow rate per reaction vessel will be one third of the typical reagent flow rate in the batch HMD process, assuming a similar total reagent consumption. In practice, the flow rate per reactor will be even lower because of the increased efficiency. Based on these design parameters, the residence time of the magnesium in the hot metal will roughly double, compared to the batch process, to 5 seconds.

Because the residence time of the magnesium gas in the hot metal doubles, it is assumed that all injected magnesium will dissolve in the hot metal. This means that the total magnesium consumption is the sum of the amount of magnesium required to form MgS and the magnesium capacity (C_{Mg}), which is the amount of magnesium that stays dissolved in the hot metal at equilibrium at the final temperature and final sulphur concentration of the hot metal, $[S]_f$ (in wt%). Stoichiometrically 0.76 kg magnesium is required to remove 1 kg of sulphur [7]. Various authors [12, 25–27] have attempted to describe C_{Mg} depending on hot metal composition (mainly sulphur) and temperature based on thermodynamics via the MgS solubility product (assuming carbon saturation). They assumed that an equilibrium between sulphur and magnesium in the hot metal is reached after injection is stopped. Visser [14] showed that the different equations from these authors are roughly in agreement with his measurements of magnesium in hot

8. A novel process for continuous hot metal desulphurisation

metal samples from an industrial HMD station at end of injection. This means that C_{Mg} can be estimated via the following equation [26, 28]:

$$C_{Mg} = \frac{10^{(-14.3+0.00679T)}}{[S]_f} \quad (8.5)$$

Here temperature T is in °C. A way to measure the desulphurisation efficiency in an industrial HMD is by the specific magnesium consumption \dot{m}_{Mg} , the amount of magnesium required to remove 1 kg of sulphur [28]:

$$\dot{m}_{Mg} = \frac{m_{Mg}}{m_{\Delta S}} \quad (8.6)$$

Here m_{Mg} and $m_{\Delta S}$ are the mass of injected magnesium and the mass of removed sulphur, respectively. In the industrial HMD process, \dot{m}_{Mg} is influenced by temperature and the sulphur aim. A lower temperature leads to a lower magnesium consumption, thus a lower \dot{m}_{Mg} [7]. As C_{Mg} increases at lower sulphur concentrations, \dot{m}_{Mg} increases for lower sulphur aims. As \dot{m}_{Mg} does not take the desulphurising capacity of CaO into account, \dot{m}_{Mg} can be lowered by adding more CaO. In most steel plants a Mg to CaO ratio of 1:2.3-4 is used, but when comparing with \dot{m}_{Mg} in a steel plant with a higher Mg to CaO ratio, the effect of CaO should be taken into account. Finally, the industrial magnesium reagent is not 100% pure magnesium, but contains 2-15% other materials (often CaO or a slag modifier). m_{Mg} is corrected for this. Typically, \dot{m}_{Mg} is 1.25-2.0 for industrial HMD stations.

Figure 8.5 shows a comparison between the expected \dot{m}_{Mg} for the CHMD and the typical \dot{m}_{Mg} for an industrial HMD station. Where desulphurising a typical HMD heat at 1380 °C from 0.04 wt% sulphur to 0.003 wt% sulphur has an \dot{m}_{Mg} value around 1.5, whereas desulphurising exactly the same heat with the CHMD process has an expected \dot{m}_{Mg} value of only 0.9. This is a reduction in magnesium consumption of 40%. Of course, comparing an industrial value with an ideal theoretical value is debatable, assuming that only half of this reduction can be achieved in practice would give a more realistic value. Therefore, a reduction of ~20 % in magnesium consumption can be expected when desulphurising hot metal with the CHMD process, instead of the typical batch HMD process.

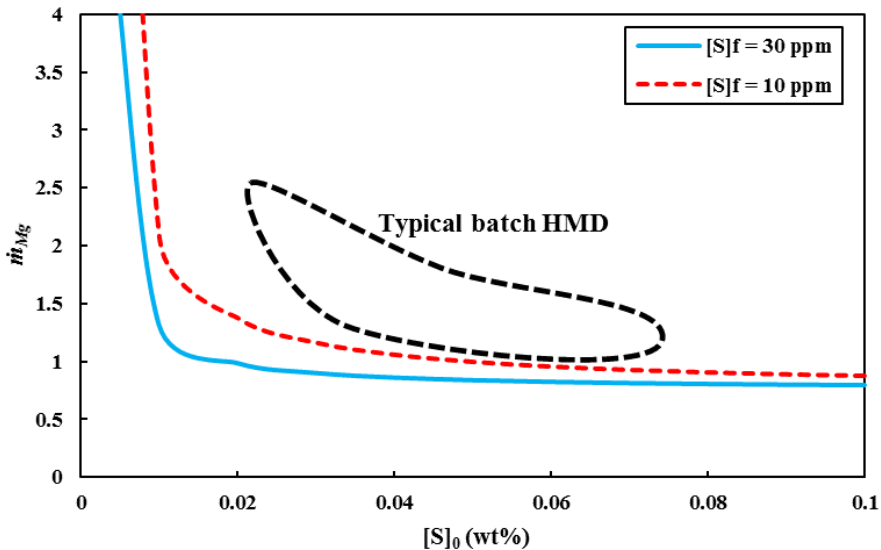


Figure 8.5: Expected m_{Mg} for the CHMD process as a function of the initial sulphur concentration $[S]_0$, for a final sulphur concentration of 30 ppm (blue solid line) and 10 ppm (red dashed line), respectively. The ‘banana’ indicates the typical range for the industrial batch HMD. Temperature = 1380 °C.

8.4.3 Residence time and temperature loss

As the desulphurisation reaction with magnesium is fast (in the order of seconds), the residence time of the hot metal in the CHMD is the result of the required reactor volume and the hot metal flow rate. The model calculations for the CHMD (see Section 8.4.1) assumed a hot metal flow rate of 1 Mt/y ($\sim 4.7 \cdot 10^{-3} \text{ m}^3/\text{s}$). With a total reactor volume of 50 m^3 , this leads to a residence time of 2 hours and 45 minutes.

The residence time of the hot metal in the CHMD has no influence on the logistics. There will be a constant flow of desulphurised hot metal at the CHMD outflow. The only parameter that is influenced by the residence time is the temperature loss of the hot metal during the CHMD process. Irrespective of the residence time of the hot metal, temperature loss during the CHMD process should be minimised. The batch HMD process has a typical average (injection, skimming, idle) temperature loss of $0.5 \text{ }^\circ\text{C}/\text{min}$. Since the batch HMD has a higher gas and reagent injection rate than the CHMD, the temperature loss of the CHMD cannot be higher than $0.5 \text{ }^\circ\text{C}/\text{min}$. With a suitable refractory selection, the CHMD can be better isolated than the batch HMD, leading to a lower temperature loss per unit time, compared to the batch HMD. Since the torpedo is

8. A novel process for continuous hot metal desulphurisation

especially designed to minimise temperature loss and no injection or stirring takes place, the temperature loss in the CHMD cannot be lower than 0.1 °C/min, which is the average temperature loss of a well-isolated torpedo. The temperature loss of the CHMD process is somewhere in between the temperature loss of the batch HMD and the torpedo. Therefore, a temperature loss of ~0.3 °C/min is assumed, resulting in almost 50 °C temperature loss for the CHMD process. In a batch HMD process, which typically takes 40 min, the temperature drop amounts only 20 °C.

In the model calculations for the CHMD, the liquid phase in the reactors was simulated as a CSTR, which means that ideal mixing in the entire reaction vessel is assumed. This assumption leads to a lower desulphurisation efficiency per reaction vessel, as the final sulphur concentration, which is the lowest, is considered for the entire vessel. This leads to an underestimation of the desulphurisation efficiency. Furthermore, the model was made for 1 Mt/y (~0.3 m³/min) HISarna hot metal with an initial sulphur concentration of 1000 ppm. Both the relatively small metal flow and the high sulphur concentration, for the given volume, lead to a longer residence time. Because of this, the residence time of 2 hours and 45 minutes from the model is inaccurate and the actual residence time in the CHMD is likely to be significantly lower than that, without increasing \dot{m}_{Mg} .

8.4.4 Slag removal and iron loss

An important aspect of any HMD process is the slag removal. The removed sulphur remains as sulphides in the slag and could resulphurise the hot metal unless the slag is removed. Furthermore, the slag removal has a significant influence on the total operational costs of the process because of the iron loss. Iron loss in the batch HMD can be 0.5-2.5 wt% of the total hot metal. Two types of iron loss can be distinguished: entrainment loss (iron being entrained with the slag when the slag is skimmed) and colloidal loss (iron being entrapped in the slag in colloidal form and being removed with it). Plant data analysis of the batch HMD process suggests that the entrainment loss is on average 0.5 wt% and that the colloidal loss can fluctuate between 0 and 2.0 wt%, depending on the slag conditions. Typically colloidal loss is around 0.5 wt% of the total hot metal weight as well. A slag with a low apparent viscosity will have a low colloidal loss [19, 29].

The CHMD process enables slag removal without a moving skimmer arm, common for the batch HMD process. Instead, a foxhole-type skimmer is used, similar to the one used at the BF. The foxhole-type skimmer will lead to virtually no entrainment loss. Although the foxhole-type skimming at the CHMD is

comparable to that of the blast furnace, the separation of slag and hot metal is expected to work even better at the CHMD, as the flow of hot metal there will be constant. At the blast furnace, typically the hot metal to slag ratio will change during tapping [6]. Furthermore, the colloidal loss can be reduced in the CHMD process by allowing the iron droplets in the slag extra time to flow back into the metal at the shallow vessel at the end of the process [19]. Due to the lower reagent injection per reaction vessel and the condition that virtually no magnesium reaches the bath surface for its violent reaction with oxygen, less ‘spitting’ is expected [19, 30], meaning that less iron will enter the slag. Furthermore, the colloidal iron loss can be further reduced by changing the slag composition to a low viscosity slag [19, 29]. Assuming that the colloidal loss can thus be reduced by at least 20 %, a conservative estimate for the total iron loss would be 0.4 wt% of the hot metal. This is 60 % less than in a state-of-the-art batch HMD process.

The different reaction vessels of the CHMD process allow for slag recycling. Since most sulphur will be removed in the first vessel, the slag in the first vessel will also receive more CaS. It is possible to recycle slag from vessels further down the process, which contains less CaS, at earlier vessels. However, recycling of slag is only beneficial if the slag from the later vessels is not saturated with CaS and if only little or no slag would enter the CHMD as carryover slag from the ironmaking unit. The HIsarna process produces hot metal without slag [4]. Slag recycling would lead to a lower slag production, which leads to a lower environmental footprint of the process.

8.4.5 Environmental consequences

During the CHMD process, like the batch HMD process, the only CO₂ that is emitted directly is kish (precipitated carbon) oxidising in contact with air. For a typical 300 t HMD batch process, the total CO₂ emission as a result of oxidised kish is estimated at 250 kg/heat. More important are the indirect CO₂ emissions, as a consequence of the CHMD process.

The CHMD process does influence the CO₂ emissions indirectly, by its temperature loss. Hot metal arriving with a higher temperature at the BOF means that more scrap can be added. Since hot metal typically contains 4.5 wt% carbon, which needs to be oxidised in the converter, increasing the scrap to hot metal ratio immediately lowers the CO₂ footprint per tonne of steel. According to Díaz and Fernández [31], typical CO₂ emissions increase by 0.6 kg/°C·tLS (kg CO₂ per degree Celsius per tonne liquid steel).

Replacing a batch HMD by a CHMD will reduce the transport time, as the hot metal can be transferred directly to the converter, instead of traveling via the

8. A novel process for continuous hot metal desulphurisation

HMD station first. Temperature loss in a ladle during transport inside the steel plant is typically 1 °C/min [32]. As a batch HMD is usually placed inside the steel plant, the transport time in a torpedo car does not change when replacing a batch HMD by a CHMD. It is estimated that by skipping the batch HMD station, on average 10 minutes of transport time, so 10 °C temperature loss, can be avoided. However, as discussed in Section 8.4.3, the residence time of the hot metal in the CHMD is expected to be longer than in a batch HMD, resulting in an estimated extra temperature loss of 30 °C. Therefore, the estimated net difference between the batch HMD and the CHMD process is 20 °C. This means that the CO₂ footprint of the CHMD would be 12 kg/tLS higher than for the batch process. It should be noted that, alternatively, FeSi could be added to the converter to generate heat, which would allow more scrap to be added. Although FeSi is an expensive addition, it could help lowering the CO₂ emission as a result of the lower hot metal temperature.

The dust emissions will be lower for the CHMD process, compared to the batch HMD. Based on plant experience, roughly 60 % of the dust created at the batch HMD station is emitted during skimming. For dust created during injection, it is difficult to estimate the amount. Injection in the CHMD will be less turbulent, but will also take longer. Furthermore, some dust is created when the hot metal cools down and some carbon in the hot metal precipitates as kish. Based on this, it is estimated that the total dust emissions for the CHMD process will be 40-60 % lower than for the batch HMD process.

8.4.6 Steel plant logistics

When replacing a batch HMD process with a CHMD process under normal operating conditions, which is directly connected to the blast furnace (or other ironmaking unit), logistics in the hot metal bay of the steel plant are greatly improved (see Figure 8.6). Hot metal entering the steel plant at the hot metal pit (HMP), can be charged directly into the converter, instead of sending it to the HMD station first. This leads to one crane movement less per heat. Furthermore, it decreases the risk of delays by eliminating a process step. As a result, the improved logistics will, on average, lead to a lower transport time and, thus, a lower temperature loss. Buffering of hot metal in the CHMD is not possible, but the overall process flexibility is not hampered by this, as buffering in the torpedo transport cars, which is already common practice at many plants, will compensate.

Typical BF-BOF route:



New BF-BOF route:

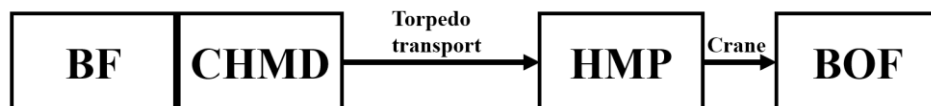


Figure 8.6: Process steps and movements for hot metal between the BF and BOF, both for the typical BF-BOF route and the new route including a CHMD attached to the BF.

8.5 Business case

To provide insight into the viability of the CHMD process, a business case is worked out for the following situation:

- One CHMD station is compared to one state-of-the art Mg-CaO co-injection HMD station.
- The total annual hot metal output of a 3 Mt blast furnace is considered.
- Initial sulphur concentration is 0.05 wt% and the post-treatment concentration is 0.005 wt% sulphur.

8.5.1 Financial comparison

The most important costs at the HMD process are iron loss and reagent costs. Heat loss (including CO₂ penalty and scrap consumption) is expected to contribute more significantly to the total costs in the near future, if CO₂ costs and scrap costs will increase. However, due to the large uncertainty, these costs are excluded in the present financial comparison. Other costs, including wear and maintenance, power consumption and consumables are either in a comparable range for both CHMD and the batch HMD, or are relatively small [13]. In order to compare a continuous process with a batch process properly, the costs are presented in €/tHM (euro per tonne hot metal).

The iron loss is the highest cost for the HMD process. Typically 0.5-2.5 wt% of the hot metal is lost during the desulphurisation step. The costs for iron loss are estimated at 300 €/t lost iron. At the batch HMD on average 1 wt% iron is lost, which equals 3 €/tHM. At the CHMD only 0.4 wt% iron, so 1.2 €/tHM, is lost under similar circumstances.

Both the CHMD and the batch HMD process use magnesium and lime as reagents. In this business case it is assumed that the Mg to CaO ratio is 1:3 and

8. A novel process for continuous hot metal desulphurisation

that it is similar for both processes. The estimated reagent costs are typically 2 €/kg for Mg (based on a 2-year average [33]) and 0.2 €/kg for CaO. Under typical HMD conditions in a state-of-the-art batch station (1380 °C), it requires 0.6 kg/tHM Mg to desulphurise from 0.04 wt% to 0.003 wt% sulphur. As a consequence, typically 1.8 kg/tHM CaO is injected with it. Total reagent costs for the batch process are 1.6 €/tHM. As explained in Section 8.4.2, a realistic estimate for CHMD reagent consumption is 20% lower than the reagent consumption of the batch HMD process (for an equal Mg to CaO ratio). Therefore, reagent costs for the CHMD process are estimated at 1.3 €/tHM.

Under the current market conditions (March 2021), scrap is roughly 50 €/t more expensive than hot metal. Typically, a 6.5 °C higher hot metal temperature, enables the replacement of 1 tonne hot metal by 1 tonne scrap. Typical CO₂ emissions increase by 0.6 kg/°C·tLS [31] and the costs for CO₂ emissions in the European Union are 40 €/t (March 2021) [34]. Under these conditions, charging less scrap and paying the penalty for higher CO₂ emissions is economically beneficial, which means that the typical temperature loss during HMD has no significant economic impact. It is likely that the costs for CO₂ emissions will increase significantly in the near future, which will probably lead to a higher demand and price for scrap as well. Because of this uncertainty, the financial impact of temperature loss cannot be included in this comparison.

Table 8.2: Comparison of main costs CHMD and batch HMD process.

	CHMD	Batch HMD
Iron loss	1.2 €/tHM	3.0 €/tHM
Reagent consumption	1.3 €/tHM	1.6 €/tHM
Total	2.5 €/tHM	4.6 €/tHM

As the size of the CHMD process is comparable to the size of a hot metal ladle and the injection system similar to that of the batch HMD process, it is expected that the CAPEX of the CHMD process will be similar to that of a batch HMD process as well. The extra costs involved for the developing a new process are then excluded.

Based on the comparison of the two major costs in hot metal desulphurisation, it becomes clear that the development of the CHMD process would be financially viable in industry. Although these figures are based on assumptions and estimates, and a comparison between an industrial process and a novel design is inaccurate, it does show that further development of this process is economically justified.

8.5.2 Qualitative comparison

It should be noted that some differences between the CHMD and the batch HMD cannot simply be translated into financial consequences. The steel plant logistics will benefit, as less crane movements are required by eliminating a process step there. The improved logistics will lead to less delays at the primary metallurgy side of the steel plant. Furthermore, the product quality will benefit from the continuous process, as a continuous process will have a more stable product quality.

The hot metal in the CHMD has a long residence time, 120 minutes, compared to the batch HMD process, which typically takes 40 minutes. Despite the better isolation of the CHMD process, its temperature loss will be higher than for a batch HMD process, resulting in a lower amount of scrap that can be charged at the converter, which can be directly translated in higher CO₂ emissions.. According to Díaz and Fernández [31], typical CO₂ emissions increase by 0.6 kg/°C·tLS (kg CO₂ per degree Celsius per tonne liquid steel). A temperature difference of 20 °C therefore leads to an increased CO₂ emission of 3600 kg for a 300 t converter.

As mentioned in Section 8.4.5, the CHMD process is expected to have 40-60 % lower dust emissions than the batch HMD per tonne hot metal, as a result of a different slag skimming method and a less turbulent process. When slag recycling is possible, CHMD will produce less slag than the batch HMD process.

Table 8.3: Qualitative comparison of CHMD and batch HMD.

	CHMD	Batch HMD
Production		
Plant logistics	+	-
Product stability	+	-
Environment		
CO ₂ emissions	-	+
Dust	+	-
Waste	+	-

The CHMD process has, besides an economical advantage, several other advantages over the batch HMD process. The CHMD process leads to simpler plant logistics and a more stable product. Also, less dust and waste can be expected per tonne desulphurised hot metal. However, due to the higher temperature loss, a higher CO₂ footprint is expected for the CHMD process, compared to the batch HMD process. Therefore, the development of the CHMD

8. A novel process for continuous hot metal desulphurisation

process should focus on minimising the temperature loss, in order to have a CHMD temperature loss equal to or even lower than the temperature loss of the batch HMD.

8.6 Conclusions and outlook

The CHMD process is still in the design phase and, therefore, this study is based on model calculations. Nevertheless, the comparison with the batch HMD process does reveal the benefits and drawbacks of the CHMD process.

- The CHMD process has significantly lower operation costs than the batch HMD process, under equal realistic conditions.
- Iron loss and reagent consumption will be significantly reduced in a CHMD process.
- Residence time and, as a consequence, temperature loss remain an issue that needs to be resolved for an industrial CHMD. The current design has not yet been optimised for residence time and it is expected that significant improvements can be made.
- Steel plant logistics will greatly benefit when changing from a batch HMD process to a CHMD process.
- Because of the concept of different reactor vessels in series, the CHMD process overcomes the problem that earlier attempts of designing a continuous HMD process had: desulphurising hot metal below 10 ppm.

In addition to further reducing the residence time and temperature loss, more detailed modelling of the flow, the heat transfer and the chemical reactions needs to be done. Also practical design considerations, such as refractory wear or redundancy, need to be investigated, as well as the procedures around starting up and shutting down the process. Furthermore, other aspects of the process should be investigated and could be optimised, like the effect of wear on the recycle openings between the vessels or the effect of the reactor dimensions on the turbulence.

The CHMD process needs to be tested at pilot plant scale. The concept of desulphurising continuously flowing hot metal with magnesium injection has not been investigated before. A pilot plant trial would not only be a proof of concept, but it would also reveal unforeseen consequences of a continuous hot metal desulphurisation process.

Based on the current state of the development, it is expected that an industrial CHMD will be realised in about 10 years, around 2030.

8.7 References

- [1] J. Zhao, H. Zuo, Y. Wang, J. Wang, and Q. Xue, “Review of green and low-carbon ironmaking technology,” *Ironmak. Steelmak.*, vol. 47, no. 3, pp. 296–306, 2020, doi: 10.1080/03019233.2019.1639029.
- [2] Y. Yang, K. Raipala, and L. Holappa, “Ironmaking,” in *Treatise on Process Metallurgy*, vol. 3, S. Seetharaman, Ed. Oxford (UK): Elsevier, 2014, pp. 2–88.
- [3] H.K.A. Meijer *et al.*, *Hisarna Experimental Campaigns B and C*, vol. EUR-27515. Luxembourg: Publications Office of the European Union, 2015.
- [4] J.W.K. van Boggelen, H.K.A. Meijer, C. Zeilstra, and Z. Li, “The Use of Hisarna Hot Metal in Steelmaking,” in *Scanmet V*, 2016, p. 008.pdf.
- [5] A. Emami, F.N.H. Schrama, and J.W.K. van Boggelen, “Device and method for continuous desulphurisation of liquid hot metal,” WO2020/239554A1, 2020.
- [6] M. Geerdes, R. Chaigneau, I. Kurunov, O. Lingiardi, and J. Ricketts, *Modern Blast Furnace Ironmaking*, 3rd ed. Delft (NL): IOS Press, 2015.
- [7] F.N.H. Schrama, E.M. Beunder, B. van den Berg, Y. Yang, and R. Boom, “Sulphur removal in ironmaking and oxygen steelmaking,” *Ironmak. Steelmak.*, vol. 44, no. 5, pp. 333–343, 2017, doi: 10.1080/03019233.2017.1303914.
- [8] K.D. Haverkamp, H.P. Schulz, and J. Mandel, “The desulfurization of pig iron using the Rheinstahl-stirrer for the production of BOF-steel grades low in sulphur,” in *External Desulphurization of Hot Metal*, 1975, pp. 14 (1–7).
- [9] A. Freißmuth, “Entschwefelung von Roheisen mit Calciumcarbid - der heutige Stand und mögliche Entwicklungen,” *Stahl und Eisen*, vol. 117, no. 9, pp. 53–59, 1997.
- [10] S. Tachuchi, “Method and apparatus for continuously pre-treating molten iron,” Japan patent 05171239, 1993.
- [11] G. Derge and K.M. Goldman, “Method of sulphur removing from pig iron,” US Patent 2706152, 1955.
- [12] N.A. Voronova, *Desulfurization of hot metal by magnesium*. Dayton (USA): The International Magnesium Association, 1983.
- [13] F.N.H. Schrama, B. van den Berg, and G. Van Hattum, “A comparison of

8. A novel process for continuous hot metal desulphurisation

the leading hot metal desulphurization methods,” in *Proceedings of the 6th International Congress on the Science and Technology of Steelmaking*, 2015, pp. 61–66.

- [14] H.-J. Visser, “Modelling of injection processes in ladle metallurgy,” (PhD thesis) Delft University of Technology, Delft (NL), 2016.
- [15] S. Kitamura, “Hot Metal Pretreatment,” in *Treatise on Process Metallurgy*, vol. 3, S. Seetharaman, Ed. Oxford (UK): Elsevier, 2014, pp. 177–221.
- [16] P.J. Koros, “Pre-Treatment of Hot Metal,” in *The Making, Shaping and Treating of steel*, 11th ed., R. J. Fruehan, Ed. Pittsburgh (USA): AISE Steel Foundation, 1998, pp. 413–429.
- [17] H.-J. Visser and R. Boom, “Advanced Process Modelling of Hot Metal Desulphurisation by Injection of Mg and CaO,” *ISIJ Int.*, vol. 46, no. 12, pp. 1771–1777, 2006, doi: 10.2355/isijinternational.46.1771.
- [18] T. Emi, “Steelmaking Technology for the Last 100 Years : Toward Highly Efficient Mass Production Systems for High Quality Steels,” *ISIJ Int.*, vol. 55, no. 1, pp. 36–66, 2015, doi: 10.2355/isijinternational.55.36.
- [19] F.N.H. Schrama *et al.*, “Optimal hot metal desulphurisation slag considering iron loss and sulphur removal capacity part I: Fundamentals,” *Ironmak. Steelmak.*, vol. 48, no. 1, pp. 1–13, 2021, doi: 10.1080/03019233.2021.1882647.
- [20] J.A.M. Kuipers and M. van Sint Annaland, “Fysische Transport Verschijnselen (lecture notes).” University of Twente, 2003.
- [21] M. van Sint Annaland, “Reactor and micro-reactor Engineering (lecture notes).” University of Twente, 2007.
- [22] O. Levenspiel, *Chemical reaction engineering*, 2nd ed. New York (USA): Wiley, 1972.
- [23] W.-D. Deckwer and R.W. Field, *Bubble column reactors*. New York (USA): Wiley, 1992.
- [24] Y. Sahai and R.I.L. Guthrie, “Hydrodynamics of Gas Stirred Melts: Part I. Gas/Liquid Coupling,” *Metall. Trans. B*, vol. 13B, no. June, pp. 193–202, 1982.
- [25] J. Yang, M. Kuwabara, T. Teshigawara, and M. Sano, “Mechanism of Resulfurization in Magnesium Desulfurization Process of Molten Iron,” *ISIJ Int.*, vol. 45, no. 11, pp. 1607–1615, 2005, doi:

10.2355/isijinternational.45.1607.

- [26] A. Ender, H. Van Den Boom, H. Kwast, and H.-U. Lindenberg, “Metallurgical development in steel-plant-internal multi-injection hot metal desulphurisation,” *Steel Res. Int.*, vol. 76, no. 8, pp. 562–572, 2005.
- [27] E.T. Turkdogan, *Fundamentals of steelmaking*. London (UK): The Institute of Materials, 1996.
- [28] F.N.H. Schrama, E.M. Beunder, H.-J. Visser, J. Sietsma, R. Boom, and Y. Yang, “The Hampering Effect of Precipitated Carbon on Hot Metal Desulfurization with Magnesium,” *Steel Res. Int.*, vol. 91, no. 11, p. 1900441, 2020, doi: 10.1002/srin.201900441.
- [29] F.N.H. Schrama *et al.*, “Optimal hot metal desulphurisation slag considering iron loss and sulphur removal capacity part II: Evaluation,” *Ironmak. Steelmak.*, vol. 48, no. 1, pp. 14–24, 2021.
- [30] A.F. Yang, A. Karasev, and P.G. Jönsson, “Characterization of Metal Droplets in Slag after Desulfurization of Hot Metal,” *ISIJ Int.*, vol. 55, no. 3, pp. 570–577, 2015, doi: 10.2355/isijinternational.55.570.
- [31] J. Díaz and F.J. Fernández, “The impact of hot metal temperature on CO₂ emissions from basic oxygen converter,” *Environ. Sci. Pollut. Res.*, vol. 27, no. 1, pp. 33–42, 2020, doi: 10.1007/s11356-019-06474-3.
- [32] R.C. Urquhart, R.I.L. Guthrie, and D.D. Howat, “Heat Losses From Ladles During Teeming,” *J. South African Inst. Min. Metall.*, vol. 74, no. 4, pp. 132–139, 1973.
- [33] “China Magnesium Ingot 99.9% FOB MACNRDAY Index.” 2020.
- [34] “Ember Carbon price viewer.” [Online]. Available: <https://ember-climate.org/data/carbon-price-viewer/>. [Accessed: 29-Mar-2021].

Part IV

Conclusions and outlook

Part IV Conclusions and outlook

9 Conclusions and recommendations

In this study, desulphurisation in 21st century iron- and steelmaking is investigated. The current state-of-the-art hot metal desulphurisation (HMD) methods are discussed and reviewed in future perspective. Optimisation of the slag composition and condition, regarding iron loss and sulphur removal capacity, is one of the key challenges of the magnesium-lime co-injection HMD process. Furthermore, as a result of the current global climate change, ironmaking processes will have to adapt or have to be replaced within 10 years. This will have consequences for the hot metal composition and conditions and, therefore, for the HMD process. One of the promising new ironmaking processes is HIsarna. It is important to understand the consequences of HIsarna hot metal for the HMD process.

Based on this study, recommendations regarding further research are given in this chapter as well. An industrial perspective is chosen for these recommendations, in order to stimulate process improvements in industry.

9.1 Conclusions

9.1.1 Optimal HMD slag

The slag composition and condition can be optimised for the magnesium-lime co-injection HMD process, aiming for low iron losses and a sufficient sulphur removal capacity of the slag. Based on the study presented in this thesis, the following conclusions can be drawn:

- The sulphur removal capacity of the HMD slag should be sufficient to contain all the removed sulphur, as sulphides, in the slag. To achieve this, the $B2$ basicity (CaO/SiO_2 mass ratio) should be higher than 1.1. In addition, enough lime should be present to convert all the sulphur to CaS .
- In the industrial HMD process, a lower apparent viscosity of the slag leads to lower total iron losses. A fully liquid slag is considered optimal regarding iron losses. Even though a slag with a very low apparent viscosity could be more difficult to skim off, leading to higher entrainment losses, the beneficial effect of lower colloidal losses as a result of the low viscosity leads to lower overall iron losses.
- Increasing the liquid fraction of the slag has the strongest influence on lowering the apparent viscosity of the slag. Therefore, a higher slag temperature leads to considerable lower iron losses in the industrial HMD.
- Changing the slag composition is, after the slag temperature, the second-most important factor to influence the apparent viscosity of the slag. For industrial HMD slag, the desired low viscosity can be achieved by having the MgO concentration as low as possible, preferably below 10 wt%, and the Al_2O_3 concentration between 12-16 wt%.
- A lower $B2$ basicity (implying either a lower CaO concentration or a higher SiO_2 concentration), decreases the apparent viscosity of the HMD slag as well. However, if the temperature of the HMD slag leads to a fully liquid slag, the $B2$ should be as high as possible without increasing the solid fraction of the slag. This is because a higher $B2$ increases the slag's sulphur removal capacity.
- Slag modifiers enable an effective way to influence the slag's composition in order to lower its apparent viscosity.
- Fluorine-containing slag modifiers (like CaF_2 and KAlF_4) are effective in lowering the iron losses during the HMD process, but are undesired, since they hamper the desulphurisation efficiency of magnesium and they are detrimental for health and environment.

- Alternative fluorine-free slag modifiers exist: pulverised fuel ash (PFA or fly ash) and nepheline syenite (NS) can be used as slag modifiers in an industrial HMD to lower the apparent viscosity of the slag and, thus, lowering the iron losses of the HMD process.
- PFA lowers the apparent viscosity of the HMD slag by decreasing the basicity of the slag and, thus, shifting the slag composition closer to the ‘sweet spot’ with the lowest melting point for the CaO-SiO₂-Al₂O₃-MgO system.
- NS lowers the apparent viscosity of the HMD slag not only by decreasing the melting temperature of the slag, but also by adding alkali metal oxides (Na₂O and K₂O) to the slag, thus breaking the polymeric SiO₂ structures in the slag without increasing the slag’s melting temperature.
- Because in the current situation, PFA has lower costs and a higher availability than NS, PFA is a better alternative to replace fluorine-containing slag modifiers than NS on the short term.
- As a result of the entrainment losses, which can never be fully avoided, iron losses during the industrial HMD process will always exist. Albeit, these iron losses can be minimised.

9.1.2 Desulphurisation of HIsarna hot metal

HIsarna hot metal, which contains more sulphur and less carbon than conventional blast furnace (BF) hot metal, contains virtually no silicon and has a lower temperature than BF hot metal, can effectively be desulphurised. Based on this study, the following conclusions can be drawn:

- Desulphurising HIsarna hot metal will take more time and consumes more reagents than desulphurisation of BF hot metal, as a result of the higher initial sulphur concentration.
- Because of the higher initial sulphur concentration and the lower temperature of HIsarna hot metal, compared to BF hot metal, desulphurisation will have a lower specific magnesium consumption (amount of magnesium required to remove a certain amount of sulphur).
- The higher oxygen concentration of HIsarna hot metal, compared to BF hot metal, will only lead to a small increase in reagent consumption (in the order of 10-50 g/tHM Mg).
- Lime-based HMD processes (like the Kanbara reactor, KR), are less efficient for desulphurisation of HIsarna hot metal, due to the extremely low silicon concentration.
- A higher carbon concentration in the hot metal and a lower temperature lead to carbon precipitation. During the HMD process, the precipitated

graphite flakes form a layer between the slag and the hot metal. Although this layer potentially blocks the formed MgS to reach the slag phase, this effect does not significantly decrease the desulphurisation efficiency. Therefore, the lower carbon concentration in the HIsarna hot metal does not lead to a higher desulphurisation efficiency.

- A continuous hot metal desulphurisation (CHMD) process will have major benefits in terms of cost, efficiency and logistics for the future HIsarna-converter steelmaking route.
- A CHMD will result in lower iron losses and reagent consumptions, compared to the state-of-the-art batch HMD process.
- A CHMD will, as a result of the longer residence time, lead to hot metal that arrives at the converter at a lower temperature than hot metal that was treated in the conventional batch HMD process. As a result, the overall CO₂ emission of the steelmaking route will increase, since less scrap can be charged in the converter. More research is required to solve this drawback of the CHMD process.
- The CHMD process is compatible with a conventional blast furnace as well, if the blast furnace is large enough to produce hot metal semi-continuously (no more than 30 min between two taps).

9.2 Recommendations

In order to utilise the findings of the research regarding optimal hot metal desulphurisation slag, a model that determines the desired B_2 basicity of the slag should be developed. Lab experiments are needed to determine the minimal sulphur removal capacity of HMD slag at different B_2 levels. Furthermore, a model should be developed to determine the slag's melting temperature at different B_2 levels, possibly based on calculations with thermodynamic software like FactSage. Such a model could be used as a basis for an industrial hot metal desulphurisation model, which advises on the amount of lime required, depending on the slag's composition and temperature, and the amount of sulphur that has to be removed.

To determine the impact of HIsarna hot metal on the hot metal desulphurisation process, as well as the converter process, plant trials are required. Since currently no industrially sized HIsarna installation exists, synthetic HIsarna hot metal could be used for the trial instead. In a converter, after a short blowing process, semi-steel with low phosphorus and manganese and no silicon and titanium can be produced. When carbon (which is removed during the converter process as well) and sulphur are added to this semi-steel afterwards, hot metal is created with a composition similar to what is expected for an industrial HIsarna. Due to the

9. Conclusions and recommendations

lower temperature expected for HIsarna hot metal, the synthetic HIsarna hot metal then needs to cool down to the desired temperature. This heat can then be desulphurised at the hot metal desulphurisation station and, afterwards, treated at the converter, as if it was an actual HIsarna heat. With this trial the performance and the overall desulphurisation efficiency could be evaluated.

The development of the continuous hot metal desulphurisation process, as described in Chapter 8, requires more research before the process can be used in industry. The long residence time inside the vessels, resulting in temperature loss, is the main design issue that needs to be solved. Extra research regarding process optimisation, leading to a shorter residence time of the hot metal in the process, is required. At the same time, a study for the optimal refractory to minimise temperature losses should be done. When the issue with temperature loss of the process has been solved, trials with a pilot set-up are required, to prove the concept design of continuous desulphurisation of flowing hot metal.

Part IV Conclusions and outlook

10 Outlook

As a result of the current global climate change, ironmaking processes will have to adapt or have to be replaced within 10 years. The HIsarna process is one of the possible new processes that can contribute to achieve the climate change mitigation goals of the steel industry before 2030. Even more fundamental changes in the industry are expected and required within 30 years. By 2050, the steel industry should be carbon neutral. These changes will have an impact on the composition and condition of hot metal and liquid steel, and, therefore, on the desulphurisation processes.

In this chapter, the consequences for sulphur removal in iron- and steelmaking on the longer term (30 years) are discussed. The desulphurisation processes in iron- and steelmaking will have to change as a consequence of changes in steelmaking. When the share of coal and coke in iron- and steelmaking will decrease, the sulphur input to the steelmaking process chain will decrease with it. However, the presence of sulphur in scrap and other additions, the remaining share of coal in some form and the demand for a low sulphur concentration in the steel product, will make desulphurisation processes in iron- and steelmaking still necessary in 2050.

10.1 Climate change and the steelmaking industry

When it comes to the outlook for sulphur removal in iron- and steelmaking for the coming decades (2025, 2030 and 2050), it can be assumed that the future of desulphurisation will mostly depend on the consequences of the climate change mitigation for the steelmaking industry. Although it is likely that customers will also continue to demand steel with ever decreasing sulphur concentrations in the coming decades, this would most likely only lead to further optimisation of the existing desulphurisation processes. However, the climate change mitigation demands from the steel industry to completely reinvent the iron- and steelmaking processes. This will have major implications for the desulphurisation processes as well.

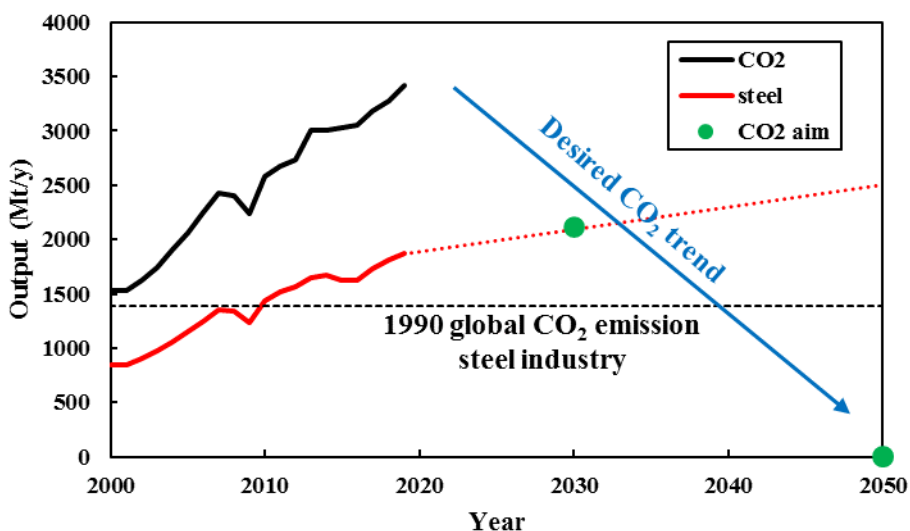


Figure 10.1: Global CO₂ emission (black) and steel production (red) since 2000 (after 2020 dotted red line indicates prediction global steel production) [1]. The green dots are the CO₂ emission targets for the global steel industry based on extrapolation of the national climate promises made in the Paris agreement for the 16 largest CO₂-emitting countries plus the European Union (including UK) [2].

When looking back to the first two decades of the 21st century, it becomes clear that, even though people are aware of the global climate change and the resulting necessity of the energy transition, the CO₂ emission of the global steel industry is only increasing. As can be seen in Figure 10.1, the global trend in CO₂ emission of the steel industry is upwards; the total CO₂ emission of the global steel industry has more than doubled in the first two decades of this century. This massive

increase in CO₂ emission can mostly be attributed to the global increase in steel production over the same period, mostly caused by China's steelmaking boom [1].

It is remarkable though that the net CO₂ emission per tonne produced crude steel did not notably change; since the year 2000 about 1.8 kg CO₂ per kg produced crude steel is emitted [1]. When assuming that the steel industry will contribute proportionally to national promises regarding CO₂ emission reduction per 2030, as made in the Paris agreement [2], the CO₂ emission targets for 2030 seems challenging. It should be noted that the fact that China, responsible for nearly 24 % of the global CO₂ emission in 2012 [2], did not make a hard promise for 2030, is taken into account here (0 % change for China in 2030 is used in the calculations for Figure 10.1). However, China is making work of climate change mitigation. In 2030, China should reach its peak CO₂ emission and the aim is that China is CO₂ neutral in 2060 [3]. Furthermore, China's biggest steel producer Baowu Steel Group plans to reduce its CO₂ emission by 30 % in 2030 and be CO₂ neutral in 2050 [4]. For the 2030 global prediction, it is assumed that the USA will live up to their promise (28 % decrease compared to 2005) made in the Paris agreement.

Table 10.1: Overview of all countries/unions with more than 5 % of the global CO₂ emission in 2012 and their promises for CO₂ reduction in 2030, based on the Paris agreement [2].

Country/union	share global CO₂ 2012 (%)	Promise CO₂ 2030 (%)	Reference year
China	23.8	0*	-
United States	12.1	-28	2005
European Union**	9.0	-55	1990
India	5.7	-35	2005
Brazil	5.7	-43	2005
Russia	5.4	-30	1990

*: China did not promise any CO₂ reduction for 2030, but promises to lower CO₂ emission after 2030 [2, 3].

** : European Union including United Kingdom (agreement signed prior to Brexit).

In 2019, 73 countries signed a climate ambition alliance under the flag of the United Nations aiming for the global net CO₂ emission in 2050 to be zero [5]. Although no hard political promises were made for 2050, the impact of climate change as a result of the CO₂ emission will force the entire world to aim for zero net CO₂ emission in 2050 [6]. Therefore, in this work the aim of zero net CO₂ emission for the global steel industry is used.

The fact that every continent on the world has a different level of development and a different growth perspective for population and steel demand, makes it difficult to have one global outlook. Therefore, a variety of solutions and their consequences for desulphurisation, for the short, middle and long term will be discussed in this outlook.

10.2 The year 2025

Given the demands to the global steelmaking industry to heavily reduce their CO₂ emissions by the year 2030 [2, 7, 8], it is likely that steelmakers worldwide will focus on investing either in upgrading current processes or in entirely new processes that help meeting the targets of low-carbon steelmaking. Furthermore, the current worldwide overcapacity in steel production [9–11] forces steelmakers to reduce their profit margins on their products. The combination of an unprecedented demand for investments within 10 years and decreasing profit margins [8], will lead to a focus on (financial) optimisation on the short term which does not require major investments.

For sulphur removal in iron- and steelmaking this means that optimisation of the current hot metal desulphurisation process is the most likely route for steelmaking companies for the coming 3-5 years. As a result of the low temperature and low oxygen activity of the hot metal, removing one gram of sulphur at the hot metal desulphurisation (HMD) process is more cost efficient than removing that same gram of sulphur at a secondary steelmaking process. At the HMD process, be it co-injection or Kanbara reactor (KR), the iron losses form the largest costs. It is, therefore, likely that the optimisation of the HMD process will result in lowering the iron losses. As is discussed in Part II of this study, lowering the iron losses, without sacrificing the slag's sulphur removal capacity, is possible by changing the slag's composition. A slag modifier, a change at the blast furnace (BF) to alter the BF carryover slag or a different reagent injection ratio, can all lead to a more optimised HMD slag composition, without the necessity of major capital investments.

The easiest solution to improve the HMD slag composition is to inject less Mg and CaO during the process, as MgO and CaO increase the apparent viscosity of the HMD slag. Improving the reagent efficiency (e.g. by lowering the hot metal temperature or improving the reagent quality) leads directly to smaller amounts of reagents being injected and therefore less MgO and CaO in the slag. Also injecting more CaO, and consequently injecting less Mg, could be considered (MgO influences the slag's viscosity more than CaO does). Lower reagent consumptions can lead to lower reagent costs and do not require capital

investment. However, most industrial HMD processes have already been optimised regarding reagent consumption. For example, a lower hot metal temperature leads to a higher magnesium efficiency, but this lower temperature also leads to a higher iron loss, which costs more than the savings made by a lower reagent consumption. This means that for many steel plants no further significant improvement of the slag composition by only changing the reagent injection can be expected.

Roughly 75 % of the HMD slag is BF carryover slag. A change in slag composition, like less MgO and CaO or more Na₂O and K₂O, would lead to lower iron losses. The slag composition at the BF is primarily the result of the BF process, which focusses on the reduction of the iron ore. Furthermore, BF slag is used as a raw material in the cement industry and in road construction. Therefore, changing the blast furnace slag composition requires a thorough analysis of the consequences for the BF process and the value of the slag as by-product. The outcome of this analysis strongly depends on the local circumstances, but if the analysis reveals that the BF slag can be improved from a HMD perspective, this is a very cost-efficient way to lower the iron losses at the HMD.

Also a higher slag temperature at the HMD leads to lower iron losses. Since there are no efficient slag heating methods available (slag and hot metal temperatures at the HMD are above 1300 °C), the only way to achieve this is producing hot metal at a higher temperature at the BF or taking measures to lower the temperature loss during the transport from the BF to the steel plant. However, since a high hot metal temperature is beneficial for the converter process (basic oxygen furnace, or BOF) as well, the hot metal temperature is already optimised at most integrated steelmaking sites.

Changing the slag composition by adding a slag modifier is also a viable way to lower iron losses. A slag modifier can be added separately or be mixed with one of the reagents. A separate addition of slag modifiers requires a small capital investment (a small silo that can release the slag modifier in a controlled way into the hot metal ladle), but has the advantage that the amount of slag modifier added per heat can be optimised (as far as possible, given that the amount of BF carryover slag is only known approximately). Injecting the slag modifier together with the reagents would not need any capital investment and only requires an extra preparation step at the reagent supplier. Regardless of the type of slag modifier (fluorine-based, alkali metal oxides or basicity reducing), the costs of the material are far less than the cost savings by lowering the iron losses. It is, therefore, expected that most steel plants that want to lower their iron losses at the HMD will find a slag modifier to be their best option. Given the increasing

attention for consequences for human health and environment, fluorine-free slag modifiers will turn out to be the preferred option.

As steel plants can at relatively low costs lower their iron losses at the HMD, this will have consequences for the slag processing as well. HMD slag is usually sent to a slag recycling process (which, sometimes, is at an external company), where part of the iron from the slag is recovered and brought back into the steelmaking process. If the iron loss at the HMD decreases, the slag will contain less iron, which increases the slag recycling costs per kg slag, since less valuable iron can be retrieved from it. This results in part of the cost reduction because of less iron being lost, is again lost due to the higher costs per tonne at the slag recycling. However, since avoiding iron loss is always more efficient than gaining back the lost iron, a successful decrease in iron losses at the HMD will save costs for the entire steelmaking process chain.

10.3 The year 2030

10.3.1 Lowering the CO₂ emission

The European Union promised to produce 55 % less CO₂ than in 1990 by the year 2030 [12]. Also in the Paris agreement, all 191 countries that signed the agreement, promised to significantly lower their CO₂ emission by 2030 [2]. Regardless of the world achieving the set goals by 2030, it is beyond a doubt that the world is aware of the necessity to massively reduce its CO₂ emission as fast as possible. The global steel industry, responsible for roughly 5 % of the world's CO₂ emission, will be forced by governments, customers and the public opinion to significantly reduce its CO₂ emission.

Given that the global steel industry aims for a total CO₂ emission of 2000 Mt/y by 2030 (this is 40 % less than in 2019) and that the global demand for steel continues to increase at the current pace, resulting in a demand of 2000 Mt/y crude steel (see Figure 10.1), the steel industry should reduce its CO₂ emission per kg produced steel from 1.8 kg today to ~1.0 kg in 2030.

Eventually, the steelmaking industry will move towards steelmaking with zero net CO₂ emission. Given that recycling of scrap alone will not satisfy the world's demand for steel the coming years and the reduction of iron ore with hydrogen will not be mature enough in 2030 to cover the production of virgin iron (iron gained by iron ore reduction), carbon will still play a significant role in steelmaking in 2030.

In order to achieve, or at least approach, the CO₂ emission targets for 2030, a combination of process changes is required. In this analysis, the focus will be on

integrated steelmaking sites, where iron ore is the main source of iron, and the influence on desulphurisation. The three required process changes are:

- Optimising scrap usage in steelmaking
- Improved or new ironmaking processes with lower CO₂ emission (like HIsarna)
- Carbon capture and storage (CCS) or usage (CCU)

10.3.2 Optimising scrap

Optimising the amount of scrap in the steelmaking process alone will not be enough to fulfil the world's steel demand in a sustainable way, as said before. However, on a single plant level, optimal scrap usage will be seen as the easiest and fastest way to lower the plant's CO₂ emission. This will have consequences for sulphur removal at the different steelmaking process steps. First of all, if the annual steel production of a steelmaking site remains the same, but more scrap is used to make the steel, consequently less hot metal is required per year. Given that, without major changes in the existing processes, the optimisation of scrap usage will be in the order of a maximum of 10 % decrease in hot metal demand, the optimised scrap usage will typically not lead to the shutdown of a blast furnace. The lower hot metal demand will result in less pressure on the BF and, consequently, on the HMD station. The longer time available at the HMD could be used to take more time to skim the slag, resulting in lower iron losses and/or less carryover slag that is charged to the converter, so less resulphurisation.

Adding an electric arc furnace (EAF) to an integrated steelmaking site, will allow for a further increase of the scrap to hot metal ratio. This scenario is very realistic for the year 2030, since this allows a single steelmaking site to achieve its CO₂ targets and could lead to the shutdown of a BF. Provided that the electricity is generated in a CO₂-free way. It is possible to have a separate steelmaking route for the EAF steel, which de facto means that the desulphurisation of the BF hot metal will not be influenced. The desulphurisation of the EAF steel will be similar to current EAF steel desulphurisation with a ladle furnace (LF; desulphurisation of EAF-produced steel is not in the scope of this work). However, an integration of the EAF in the BF-BOF route is possible as well. Mixing EAF steel (raw steel from scrap without much refining) with BF hot metal will lead to hot metal that is low in sulphur and carbon, but high in nitrogen, oxygen and tramp elements [13]. The temperature of the mixed hot metal will be higher than conventional BF hot metal. The consequences for this specific mixed hot metal for the HMD process will have to be further investigated, but a lower desulphurisation efficiency (with higher reagent consumptions) can be expected, because of the lower sulphur concentration and higher temperature. However, the higher

temperature is beneficial for a low-viscosity slag, which leads to low iron losses. Mixing the EAF steel with BF hot metal after the HMD process, or even after the BOF process, will only have consequences for secondary steelmaking desulphurisation.

At the secondary steelmaking desulphurisation, more flexibility will be demanded. The higher scrap consumption (both with and without an integrated EAF) requires the use of external scrap. It can be expected that the global demand for scrap will increase, resulting in higher prices for scrap, so steel plants will have to accept lower quality scrap or higher costs. Due to the difficulty in analysing the scrap composition (especially sulphur), heats with unexpectedly high sulphur concentrations at the converter will appear more frequent. This demands a higher flexibility at the steel desulphurisation station at the secondary metallurgy. Besides taking this extra uncertainty into account at the planning of the casting machine, an increased desulphurisation capacity at secondary steelmaking is an option. Installing extra calcium wire shooters or calcium injection lances at existing secondary steelmaking stations can be ways to increase the desulphurisation capacity at relatively low capital costs.

10.3.3 Alternative ironmaking processes

Optimising the scrap recycling is not sufficient to meet the global 2030 CO₂ emission targets. Alternative low-CO₂ ironmaking processes are required to achieve the set targets, since zero-CO₂ steelmaking processes are not mature enough. Low-CO₂ ironmaking processes replace (part of) the coke for another reductant and energy source that leads to a lower CO₂ emission, like coal, natural gas or hydrogen. These new processes can be an adapted BF, a shaft furnace producing DRI with natural gas or syngas (CO and H₂), or an entirely new process [14].

Replacing part of the coke for coal, natural gas or hydrogen in a BF requires relatively small adaptations of the existing installation. However, since coke in a BF is not only used as reductant and energy source, but also to support the ferrous burden and to allow gas to flow counter-current to the burden [15, 16], the amount of coke that can be replaced is limited. Replacing coke by natural gas or hydrogen decreases the sulphur input in the BF, resulting in a lower sulphur concentration in the hot metal. However, this decrease in sulphur concentration will be in the order of 10 % (that is also the amount of coke that can be replaced), so the HMD process remains required for this hot metal. As described in the previous section, this will lead to a lower pressure on the HMD station but also to a lower desulphurisation efficiency.

HIsarna depends (partly) on the energy efficiency improvements when using coal instead of coke as a carbon source [17]. Coke is essentially pyrolysed coal and by pyrolysing the coal, part of its energy is lost and is not used in the steelmaking process. However, during the coke making, a large part (50-80 wt%) of the sulphur present in coal is removed as well. This results in a higher sulphur input to the new ironmaking process and, consequently, a higher sulphur concentration in the hot metal. It should be noted that the higher sulphur concentration in HIsarna hot metal is also caused by the less reducing environment of the HIsarna process compared to the blast furnace process. On the other hand, increasing the amount of coal at the blast furnace, replacing coke, will lead to hot metal with a higher sulphur concentration as well. Other smelting reduction processes, like Corex or FINEX, also replace coke with coal and have a less oxidising environment compared to the BF, resulting in high-sulphur hot metal [18]. Although both Corex and FINEX are not designed to lower the carbon footprint of steelmaking, they can be more easily adapted to produce hot metal with a lower CO₂ emission [14]. Based on the expected increase in the share of smelting reduction processes in the global steel production, it is expected that hot metal in the year 2030 will typically contain more sulphur than in the year 2021.

The surplus of sulphur in the hot metal will be removed at the HMD with a high efficiency. However, it will increase the pressure on the HMD process step, since more sulphur needs to be removed, which requires more time and a higher reagent consumption. Depending on the capacity of the existing HMD equipment, the increased demand for hot metal desulphurisation will lead to either less flexibility at the existing HMD stations (less idle time, less time left to desulphurise heats with exceptionally high sulphur concentrations) or the necessity to increase the capacity of the existing HMD equipment (either upgrading of existing stations or adding an HMD station).

DRI comes from iron ore that is reduced at a lower temperature (typically around 900 °C) with coal, natural gas or syngas. In the future it is expected that pure hydrogen can be used to produce DRI [19], but since this is still in the development phase, it is expected that in 2030 most DRI will come from ore reduction with natural gas or syngas. An example of DRI production with gas is the MIDREX process. As a result of the lower temperatures, DRI remains as a solid, so an EAF is required to melt it and refine it. DRI has roughly the same composition as hot metal, regarding iron and carbon, but it typically has a lower sulphur concentration [18]. Since it is expected that DRI in 2030 will be produced mostly via gas, it will contain little or no sulphur. However, because the iron ore contains some sulphur and some sulphur is added in the EAF as well via coal,

desulphurisation of the steel, e.g. in an LF, remains required. An HMD process will not be required in this route.

10.3.4 CCS and CCU

The BF-BOF route, which has been used and optimised by steelmakers for decades, will not easily be replaced. New processes will require some time to optimise and develop further. Using an EAF results in more nitrogen (via the process) and metallic impurities (via the scrap) in the steel, which are difficult to remove. Using DRI instead of scrap partly overcomes these problems, but DRI has a larger carbon footprint than scrap [19]. In both cases a steelmaker runs the risk of not being able to produce all steel grades that could be made via the BF-BOF route. This makes keeping the BF-BOF route also after 2030 a tempting alternative, besides the lower investment costs. When keeping the BF-BOF route (at least partly), its CO₂ emission must be lowered somehow. The easiest solution is to buy CO₂ certificates. Although this solution is not desirable from an environmental point of view, it is likely that steelmakers will choose for this option on the short term. However, it is expected that, on the longer term, governments and public opinion will make this solution not viable.

A technical solution is carbon capture and storage (CCS) or usage (CCU). CO-rich gas from BF, BOF and coke and sinter plants can be collected. The energy from the gas can be gained by oxidising it in a power plant (like what happens today), creating CO₂. This CO₂ can be stored in empty gas or oil fields (CCS), or could be used to produce chemicals (CCU). In order to make the gas suitable for CCS or CCU, it should be purified. The original BF gas contains roughly 60 % nitrogen [15], which should be removed before CCS and CCU.

The advantage of CCS and CCU is that it is a mature technology and that the capital investments are lower than the costs for installing a new ironmaking process. The disadvantage of CCS is that it is not sustainable, as suitable storage locations (like empty oil and gas fields) are limited. Furthermore, there is always a risk of the CO₂ escaping again, for example due to an earthquake (with devastating effects for the local sea life if large quantities of stored CO₂ would be released at once) or by small leakages. This will also lead to a permanent public opinion against CCS. Finally, CCS requires a suitable storage place nearby the CO₂ source, which makes CCS not suitable for all BF-BOF steelmaking sites. CCU does not have these disadvantages, but if CCU will become a major solution in decreasing the CO₂ emission, most CO₂ will have to be converted to other chemicals, which costs energy (the demand for CO₂ from the greenhouses and soda industry is limited). The required energy should be green in order to have a net decrease in CO₂ emission.

Due to the BF-BOF being optimised for decades, it is likely that many steelmaking companies would combine the CCS/CCU with their current BF (and possibly BOF). This means that not much would change for the desulphurisation processes at these sites. However, since new smelting-based ironmaking processes, like HISarna, Corex or FINEX, have more concentrated CO₂ as off gas, these ironmaking processes are better suitable for CCS/CCU, as this would simplify or obsolete the gas purification step [14, 18]. Therefore, CCS/CCU could lead to an increase in the use of smelting-based ironmaking processes. This, in turn, would lead to hot metal with a higher sulphur concentration and to more pressure on the HMD process, as was discussed in Section 10.3.3.

10.3.5 Conclusion

Since in 2030 a mix of the discussed solutions for CO₂ reduction can be expected, it is likely that the global average sulphur concentration in hot metal will not change dramatically, but that locally, depending on the chosen solution, the hot metal sulphur concentration will be significantly higher or lower. For most steelmaking sites, optimisation of their current HMD stations by small improvements will be sufficient to deal with the new situation. Only for some steelmaking sites, where new ironmaking processes are installed leading to a significantly higher sulphur concentration in the hot metal, there is an incentive to invest in their HMD capacity. For these specific cases, new HMD processes could be the most viable solution. It can therefore be expected that in 2030, various new HMD processes will emerge globally, but most hot metal will still be desulphurised with the conventional co-injection or Kanbara reactor HMD processes.

10.4 The year 2050

10.4.1 Zero CO₂

The aim for 2050 is that the steel industry is carbon neutral (zero net CO₂ emission). There are different ways to achieve a carbon neutral steel industry and it is likely that a combination of these solutions is required to achieve the global aim. In general three types of solutions are possible:

- Recycling of scrap (using green energy)
- CO₂ compensation and capture
- Hydrogen steelmaking

These three possible solutions and their consequences for desulphurisation are discussed in this section.

10.4.2 Scrap recycling

One of the advantages of steel is that it is practically 100 % recyclable. Therefore, recycling of scrap to create new steel will be an important source of steel in 2050. However, since always some steel will be lost for recycling and since in 2050 a still growing demand for steel can be expected based on a growing world population and growing welfare, recycling of scrap will not be sufficient to fulfil the full global demand for steel. With an average lifespan of 35 years for steel products [20], the expected global steel demand of 2050 (2500 Mt) can be covered for about 65 % by the global steel production of 2015 (1622 Mt) [1]. This 65 % is a good estimate of the share of scrap recycling in 2050.

As discussed in Section 10.3.2, scrap recycling can be done in an EAF or by adding scrap to hot metal (in a converter, Hisarna or other process). Desulphurisation of EAF steel, which will be the largest share of scrap recycling, is not in the scope of this work. When adding scrap to hot metal, the effect on the desulphurisation processes will depend on the sulphur concentration of the hot metal and scrap. Hot metal produced with the help of coal (like in a BF or smelting reduction process) is high in sulphur, thus adding scrap (typically containing 0.005 wt% sulphur) would dilute the sulphur in the hot metal, leading to less pressure on the HMD process. When the scrap to hot metal ratio would be high, the sulphur concentration in the resulting hot metal would be diluted so much that a separate HMD process would no longer be required. A single CaO-based desulphurisation step just before casting the steel (like the current steel desulphurisation) would be sufficient.

10.4.3 CO₂ compensation and capture

In 2050, the aim is to have zero net CO₂ emission globally. This means that the steel industry could still emit CO₂ in 2050, but this has to be compensated. CO₂ is best removed from the atmosphere by biomass (plants, algae). For this solution, no new techniques are required, only space where the biomass can grow and absorb CO₂. Since the world population is expected to still grow in 2050, land will be scarce in 2050, which limits the solution of using biomass for CO₂ capture.

CCS and CCU will also be an option to achieve the net CO₂ emissions of the steelmaking industry to be zero, while still producing CO₂ during the iron- and steelmaking process. Compared to 2030 (as was discussed in Section 10.3.4), the political and social pressure against CCS might have increased in 2050 and the techniques and possibilities for CCU might have improved. Still, good usage of CCS/CCU would allow remaining integrated BF-BOF steelmaking sites to produce steel at zero CO₂ emission. For these sites, the HMD process and the steel desulphurisation processes will be comparable to the current state of the art.

However, when a BF reaches the end of its lifetime, it would probably be replaced by an alternative ironmaking process. This could be a smelting reduction process, which produces hot metal comparable to the BF hot metal (no major investments required for the rest of the site) and emits a high purity CO₂ off-gas, making CCS/CCU easier, as the gas purification becomes obsolete. Alternatively, the BF is replaced with hydrogen steelmaking, which emits no CO₂ (obsoleting the entire CCS/CCU process chain), but this will require new steelmaking processes.

In 2050, it is likely that some integrated BF-BOF steelmaking sites still exist thanks to CO₂ compensation or capture, but they will be phased out and replaced by cleaner alternatives. Therefore, smelting reduction processes, using CCS/CCU and/or CO₂ compensation will play a more important role than in 2030. The total share of carbon-based steelmaking in 2050 will be much lower than in 2030 though. The advantages of carbon-base steelmaking, being the capability of producing certain steelgrades and a 200-year head start in experience, will only ensure a niche market. This means that the HMD process becomes necessary for just a niche market as well.

10.4.4 Hydrogen steelmaking

In theory, hydrogen can be used instead of carbon to reduce iron ore. Although the technology for this is just emerging, the technology will be mature in 2050. The HYBRIT process, developed by SSAB in Sweden, is expected to replace all SSAB's BFs by 2045. In 2026 the first hydrogen-based steel is expected from the pilot process [21]. Although other parties are working on hydrogen-based steelmaking processes as well, this means that in 2050, hydrogen-based steelmaking only just starts to play a significant role in the global steel production. Besides, hydrogen production has a high energy requirement. It will take 10-20 years before enough green hydrogen can be produced in a cost-efficient way to fulfil the demand from the steelmaking industry [22]. It can therefore be expected that the share of hydrogen-based steelmaking will further increase after 2050. Certainly because the processes will be further developed and optimised based on built-up experience.

For hydrogen-based steelmaking, the only source of sulphur is the ore (and the scrap, if scrap is used). Iron ore contains 0.3 gram sulphur per kg iron. This would lead to metal with 0.03 wt% sulphur if no desulphurisation is done. During the process in which iron ore is reduced with hydrogen, some hydrogen might react with the sulphur to form the gas H₂S. If the amount of H₂S gas created during the hydrogen-based process is comparable (per ratio) to H₂S in the BF, only 10 % of the sulphur would be removed. If the metal leaves the hydrogen-based process as a solid (like in the HYBRIT process), the metal needs to be molten and treated in

an EAF afterwards, resulting in liquid steel with a high oxygen activity and still around 0.03 wt% sulphur (when not diluted with scrap). LF-type desulphurisation of the steel would then be required, to a degree that is comparable to the current steel desulphurisation after the EAF. If a hydrogen-based process would produce liquid metal with a low oxygen activity (like the BF), a desulphurisation process similar to the current HMD processes would be the optimal solution to lower the sulphur levels to an acceptable level.

10.5 Conclusion

It is difficult to predict the future, but it is safe to assume that 2050 will be very different from 2021 regarding steelmaking worldwide. Lowering the carbon footprint of the steelmaking industry will be the most important reason for this change. Figure 10.2 shows the qualitative prediction of the share of the different steelmaking routes until the year 2060. The prediction is purely based on the discussion in this outlook chapter. Therefore, the trends rather than the depicted percentages should be taken from this figure.

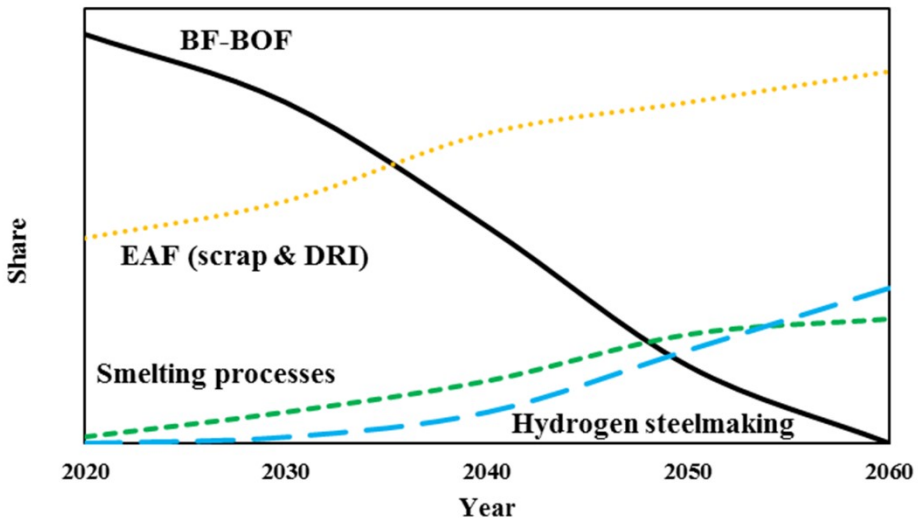


Figure 10.2: Qualitative prediction of the share of different steelmaking routes worldwide between 2020 and 2060.

Based on the qualitative prediction depicted in Figure 10.2 and the discussion above, a qualitative prediction of the share of the types of HMD processes can be made, which is depicted in Figure 10.3. In this prediction LF desulphurisation (and similar) of EAF steel is added to the figure, but steel desulphurisation after

the converter in the BF-BOF route is not (as in this route there is an HMD process). Also for this qualitative prediction, the trends rather than the depicted share should be taken from the figure. Apart from continuous hot metal desulphurisation, all other possible new HMD processes are categorised under the presently known HMD types, being injection, KR and LF.

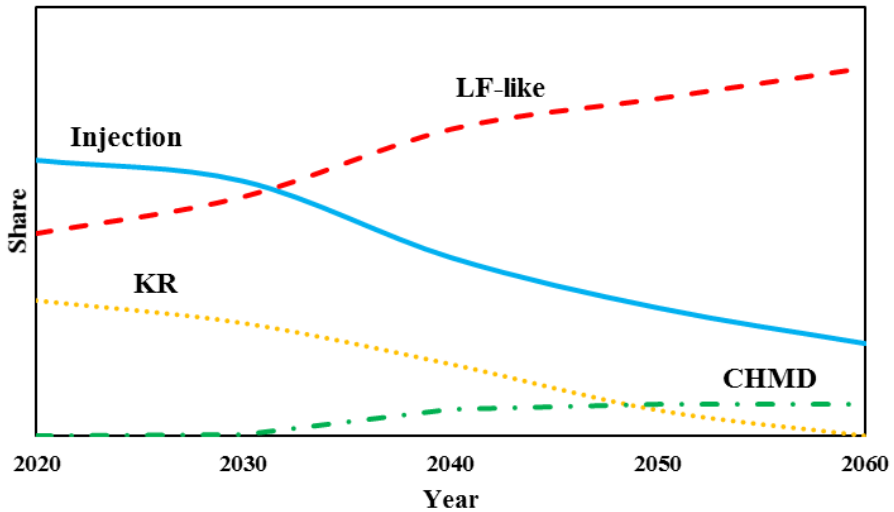


Figure 10.3: Qualitative prediction of the share of different HMD processes in steelmaking worldwide between 2020 and 2060.

It is clear that together with the steelmaking industry, desulphurisation in steelmaking will undergo a major transformation. However, the basis of desulphurisation, being binding sulphur with reagents (typically CaO and Mg), will probably not change. It is therefore likely that desulphurisation processes in the steelmaking industry can be very well understood based on the desulphurisation knowledge today.

10.6 References

- [1] “World Steel Association,” 2021. [Online]. Available: <https://www.worldsteel.org/>. [Accessed: 06-Apr-2021].
- [2] United Nations, *Paris agreement*. 2015.
- [3] “China’s Climate Goals ‘Realistic,’ ‘Ambitious,’” *VOA News on China*, 2021. [Online]. Available: <https://www.voanews.com/east-asia-pacific/voa-news-china/chinas-climate-goals-realistic-ambitious>.

Part IV Conclusions and outlook

[Accessed: 15-Jun-2021].

- [4] “China’s Biggest Steel Mill Baowu Aims to Be Carbon Neutral by 2050,” *Yicai Global*, 2021. [Online]. Available: <https://www.yicai.com/news/china-biggest-steel-mill-baowu-aims-to-be-carbon-neutral-by-2050>. [Accessed: 15-Jun-2021].
- [5] “73 Countries Commit to Net Zero CO2 Emissions by 2050,” *IISD knowledge hub*, 2019. [Online]. Available: <https://sdg.iisd.org/news/73-countries-commit-to-net-zero-co2-emissions-by-2050/>. [Accessed: 09-Apr-2021].
- [6] “Climate action,” *United Nations*, 2020. [Online]. Available: <https://www.un.org/en/climatechange/science/key-findings>. [Accessed: 09-Apr-2021].
- [7] Tata Steel Europe Ltd., “Carbon neutral steelmaking is a major challenge for the steel industry worldwide,” *Tatasteeleurope.com*, 2021. [Online]. Available: <https://www.tatasteeleurope.com/ts/sustainability/carbon-neutral-steel>. [Accessed: 02-Apr-2021].
- [8] M. Pooler, “‘Green steel’: the race to clean up one of the world’s dirtiest industries,” *Financial Times*, 2021. [Online]. Available: <https://www.ft.com/content/46d4727c-761d-43ee-8084-ee46edba491a>. [Accessed: 02-Apr-2021].
- [9] European Union, “Staal: Mondiaal Forum onderneemt belangrijke stappen om overcapaciteit aan te pakken,” *Press release*, 2018. [Online]. Available: https://ec.europa.eu/commission/presscorner/detail/nl/IP_18_5865. [Accessed: 02-Apr-2021].
- [10] M. de Roo, “Staal zit in grootste dip in tien jaar,” *De Tijd*, Nov-2019.
- [11] S. Angell, “OECD warns against steel overcapacity,” *Argus Media*, 2020. [Online]. Available: argusmedia.com/en/news/2145506-oecd-warns-against-steel-overcapacity. [Accessed: 02-Apr-2021].
- [12] European Union, “Europese klimaatwet,” *EU website*, 2021. [Online]. Available: https://ec.europa.eu/clima/policies/eu-climate-action/law_nl. [Accessed: 03-May-2021].
- [13] J.A.T. Jones, B. Bowman, and P.A. Lefranc, “Electric Furnace Steelmaking,” in *The Making Shaping and Treating of Steel*, 11th ed., R. J. Fruehan, Ed. Pittsburgh (USA), 1998, pp. 525–660.
- [14] J. Zhao, H. Zuo, Y. Wang, J. Wang, and Q. Xue, “Review of green and

- low-carbon ironmaking technology,” *Ironmak. Steelmak.*, vol. 47, no. 3, pp. 296–306, 2020, doi: 10.1080/03019233.2019.1639029.
- [15] M. Geerdes, R. Chaigneau, I. Kurunov, O. Lingiardi, and J. Ricketts, *Modern Blast Furnace Ironmaking*, 3rd ed. Delft (NL): IOS Press, 2015.
- [16] D.J. Gavel, “Shifting the limits of nut coke use in the ironmaking blast furnace,” (PhD thesis) Delft University of Technology, Delft (NL), 2020.
- [17] H.K.A. Meijer, C. Zeilstra, C. Teerhuis, M. Ouwehand, and J. van der Stel, “Developments in Alternative Ironmaking,” *Trans. Indian Inst. Met.*, vol. 66, no. 5–6, pp. 475–481, 2013, doi: 10.1007/s12666-013-0309-z.
- [18] Y. Yang, K. Raipala, and L. Holappa, “Ironmaking,” in *Treatise on Process Metallurgy*, vol. 3, S. Seetharaman, Ed. Oxford (UK): Elsevier, 2014, pp. 2–88.
- [19] L.M. Germeshuizen and P.W.E. Blom, “A techno-economic evaluation of the use of hydrogen in a steel production process, utilizing nuclear process heat,” *Int. J. Hydrogen Energy*, vol. 38, no. 25, pp. 10671–10682, 2013, doi: 10.1016/j.ijhydene.2013.06.076.
- [20] D.R. Cooper, A.C.H. Skelton, M.C. Moynihan, and J.M. Allwood, “Component level strategies for exploiting the lifespan of steel in products,” *Resour. Conserv. Recycl.*, vol. 84, pp. 24–34, 2014, doi: 10.1016/j.resconrec.2013.11.014.
- [21] “First in fossil-free steel. Using HYBRIT Technology.,” *SSAB*. [Online]. Available: <https://www.ssab.com/company/sustainability/sustainable-operations/hybrit>. [Accessed: 09-Apr-2021].
- [22] N. Thomas, D. Sheppard, and N. Hume, “The race to scale up green hydrogen,” *Financial Times*, Edinburgh (UK), [online], 2021.

Part IV Conclusions and outlook

Appendices

Appendices

Summary

In this PhD thesis, the desulphurisation in 21st century iron- and steelmaking is investigated. The current state of the art in sulphur removal in ironmaking and oxygen steelmaking is discussed (Part I of this thesis) and optimisation of the hot metal desulphurisation (HMD) slag, which is an important aspect of present day desulphurisation, is investigated (Part II of this thesis). Furthermore, since the steelmaking industry will change significantly as a result of the global climate change mitigation, desulphurisation of hot metal from HIsarna, a new low-CO₂ ironmaking process, is studied (Part III of this thesis). Finally, an overview of the main conclusions of this work, as well as an outlook about desulphurisation in iron- and steelmaking for the coming decades, based on the research presented in this thesis, is given in Part IV of this thesis.

Sulphur is an unwanted impurity in steel that lowers the formability and weldability of steel and it makes steel more brittle. Therefore, steelmakers try to limit the concentration of sulphur in the steel. In 2021, globally roughly two third of the steel is produced via the BF-BOF steelmaking process, where iron ore is reduced by carbon (coal and coke) in the blast furnace (BF), and the hot metal from the BF is refined in the basic oxygen furnace (BOF, or converter). Sulphur can be removed at different process steps in the steelmaking process chain, like at the HMD, at the converter, or at the secondary metallurgy processes. Because of the low oxygen activity in hot metal, sulphur is most efficiently removed at the HMD process. In Chapter 2, the different sulphur removal steps in the steelmaking process chain are discussed. Here also the different HMD processes that are globally being used are discussed. The two most important HMD processes are the co-injection process (where desulphurising reagents, typically Mg and CaO or CaC₂, are injected into the hot metal) and the Kanbara reactor (KR; where calcium-based reagents are mixed through the hot metal with an impellor). Currently, the co-injection process is globally the most commonly used process of the two and it is dominant in Europe and North America. Typically, magnesium and lime are used as reagents in the co-injection HMD process. Magnesium dissolves in the hot metal and reacts with the dissolved sulphur to form solid MgS. Although some lime directly reacts with the sulphur, its main task is to react with the MgS to form the more stable CaS, which moves to the slag phase. When the reagent injection is finished, the slag is removed with a skimmer.

Appendices

During the removal of the slag, some iron is lost with it. The amount of iron lost per heat is typically 0.5-2.5 wt% of the total hot metal weight, which is a major cost for the HMD process. In Chapter 3 it is explained that iron loss is governed by two mechanisms: colloidal loss (iron present in the slag in a colloidal form, which is removed together with the slag) and entrainment loss (iron being entrained with the slag during the slag removal). Entrainment loss can be minimised by optimising skimming conditions like an experienced operator, a clean skimmer paddle and a well-controlled skimmer. Colloidal loss can be minimised by decreasing the apparent viscosity of the slag, which under typical HMD conditions means that the solid fraction of the slag should be minimised. This can be achieved by either increasing the slag temperature (in practice minimising the temperature loss) or by decreasing the slag's basicity, which lowers the melting temperature of the slag. Furthermore, in Chapter 3 it is shown that the HMD slag also needs a *B2* basicity (ratio of the concentrations of CaO and SiO₂) of at least 1.1 and enough lime to convert all present sulphur to CaS, in order to have a sufficient sulphur removal capacity. The optimal HMD slag has a *B2* basicity high enough to allow all the removed sulphur to stay in the slag (sufficient sulphur removal capacity), but its basicity is low enough to keep the slag's melting temperature below the actual temperature of the slag (typically 1300-1450 °C), ensuring a mostly liquid slag, resulting in a low colloidal loss. In Chapter 4, these findings are evaluated and supported with a Monte Carlo simulation based on thermodynamic data from FactSage, melting point and viscosity measurements with artificial HMD slags and plant data analysis. The temperature of the slag has the strongest influence on the colloidal loss and total iron loss, where a lower temperature leads to a slag with a higher solid fraction and, thus, a higher iron loss. From the typical HMD slag components, MgO has the largest influence on the slag's melting temperature, where a higher concentration of MgO leads to a higher melting temperature (thus to a higher iron loss).

In an industrial setting, it is difficult to increase the temperature of the slag (which is typically 1300-1450 °C). Also, it is difficult to influence the HMD slag composition, because 60-80 wt% of the HMD slag is carryover slag from the BF (changing that would require changing the BF process) and the rest is determined by the reagents injected to remove a certain amount of sulphur (resulting in a certain amount of CaO, MgO and CaS being added to the slag). A more practical method to change the HMD slag composition for a lower viscosity is to add a slag modifier. In Chapter 5, fly ash and nepheline syenite are investigated as suitable slag modifiers for the HMD process. Fly ash contains SiO₂ and Al₂O₃ and decreases the basicity of the slag and, thus, its melting temperature. Nephelene

syenite contains SiO_2 and Al_2O_3 as well, but it also contains Na_2O , which is a basic network modifier that decreases the slag's viscosity. Melting point and viscosity experiments with synthetic HMD slags show that both fly ash and nepheline syenite are viable slag modifiers and are a good alternative to the fluoride-based slag modifiers, which are common in industry. Fluoride-based slag modifiers lower the slag's melting temperature and the viscosity of the liquid fraction. However, fluoride leads to health and environment issues and it decreases the desulphurisation efficiency of magnesium as well.

As a result of the global climate change mitigation, the steel industry has to lower its CO_2 emission. One new process that can contribute to a lower CO_2 footprint of the steelmaking industry is the HIsarna process, which is being developed at Tata Steel in IJmuiden, the Netherlands. Like a BF, HIsarna produces hot metal, but with a 20 % lower CO_2 emission. Even an 80 % lower CO_2 emission can be achieved when using carbon capture and storage or usage, due to the concentrated CO_2 off gas. Compared to a BF, HIsarna produces hot metal with a lower temperature and with lower carbon, manganese and phosphorus concentrations. HIsarna hot metal contains almost no silicon and titanium. However, compared to a BF, HIsarna produces hot metal with roughly 3-4 times more sulphur (typical sulphur concentration in hot metal is around 0.1 wt%). This means that for HIsarna hot metal more sulphur needs to be removed compared to typical BF hot metal. The consequences for desulphurisation of HIsarna hot metal are discussed in Part III of this thesis.

Typically, due to cooling, hot metal from a BF is supersaturated in carbon by the time it arrives at the HMD. This carbon supersaturation leads to graphite formation, also known as kish. The formed graphite flakes can form a layer between the slag and the hot metal. Earlier research suggested that this graphite layer could hamper the HMD process, as it would block MgS formed in the hot metal, thus it cannot reach the slag phase and form the more stable CaS . This would result in a lower desulphurisation efficiency. Since HIsarna hot metal contains less carbon, this effect could be smaller or even non-existent for desulphurisation of HIsarna hot metal. However, as is explained in Chapter 6, this hampering effect of precipitated graphite on the efficiency of the HMD process is very small, for both HIsarna and BF hot metal. Analysis of plant data shows that there is only a small correlation between expected graphite formation and HMD efficiency. Only for heats with a low initial sulphur concentration (below 225 ppm sulphur) showed a significant correlation. This means that there is no significant benefit for desulphurisation of low-carbon HIsarna hot metal, compared to carbon-saturated BF hot metal.

Appendices

The lower temperature and the higher initial sulphur concentration of HIsarna hot metal, compared to BF hot metal, do influence the HMD process, as is discussed in Chapter 7. A literature study, a thermodynamic analysis with FactSage and plant data analysis show that the lower temperature and higher initial sulphur concentration lead to a lower specific magnesium consumption. The lower temperature, typically 50 °C colder than BF hot metal, thermodynamically favours the desulphurisation reaction with magnesium. The higher initial sulphur concentration leads to a higher sulphur activity, which enhances the desulphurisation reactions. However, it should be noted that the higher efficiency caused by the initial sulphur concentration is only valid for the surplus of sulphur, compared to BF hot metal. The total amount of sulphur that has to be removed is still 3-4 times higher for HIsarna hot metal than for BF hot metal. Therefore, the total magnesium consumption for desulphurisation of HIsarna hot metal is higher as well. This also means that desulphurisation of HIsarna hot metal will take longer than desulphurisation of BF hot metal, which could lead to the HMD becoming the bottleneck in a steel plant. It is estimated that the oxygen concentration in HIsarna hot metal (~6 ppm) is roughly 5-10 times higher than in BF hot metal (0.5-1 ppm). A high oxygen concentration leads to a lower desulphurisation efficiency. However, since the oxygen concentration in HIsarna hot metal is still low, the expected extra magnesium consumption as a result of the higher oxygen concentration is limited to about 2-3 kg for a 300 t heat. The absence of silicon and titanium in the hot metal will not influence the efficiency of a magnesium-based HMD process. However, a lime-based HMD process, like KR, will have a lower efficiency, since silicon reacts with the oxygen in lime as the calcium reacts with sulphur to form CaS. Furthermore, since HIsarna produces hot metal without slag, an alternative for the carryover slag from the BF needs to be found. A slag based only on the injected magnesium and lime and the formed CaS would be solid at HMD temperatures (see Chapter 3). Therefore, the use of acidic slag additions (like SiO₂ and Al₂O₃) is required, to keep the slag liquid and minimise the iron loss. Still, the higher slag volumes as a result of more sulphur that has to be removed will lead to a higher iron loss, compared to desulphurisation of typical BF hot metal.

Because the HIsarna produces, and taps, hot metal continuously with a constant composition and temperature, it is ideal for continuous hot metal desulphurisation. Therefore, at Tata Steel in IJmuiden, the Netherlands, a new continuous hot metal desulphurisation (CHMD) process is being developed. In Chapter 8, this novel CHMD process is introduced. The CHMD process is based on the magnesium-lime co-injection HMD process. It uses several reactors in series (process simulations suggest three reactors in series are required to

desulphurise typical Hisarna hot metal to typical post-HMD sulphur concentrations), to limit the total reactor volume. The desulphurisation efficiency of the process is increased by optimising the reactor dimensions to a height to diameter ratio of 5:1, whereas a typical hot metal ladle, used for the batch HMD, has a height to diameter ratio of 1.5:1. It is expected that this leads to a reduction in reagent consumption of ~20 %. Furthermore, the continuous nature of the process allows for a foxhole-type slag skimming (separating slag and hot metal by their density difference), which will lead to an estimated 60 % lower total iron loss, compared to the skimming method of the batch HMD process (a remote-controlled skimmer arm, raking off the slag). Based on the cost estimation for iron loss and reagent costs, the cost for desulphurising one tonne hot metal with the CHMD process will be approximately € 2 lower than with the state-of-the-art batch HMD process. However, according to the current calculations, the residence time of the hot metal in the CHMD is 3-4 times longer than in a batch HMD process, leading to a higher temperature loss and, possibly, a higher CO₂ footprint, as a lower temperature allows for less scrap being charged at the converter. Given the already lower temperature of Hisarna hot metal, compared to BF hot metal, this is an issue that needs to be solved before the CHMD process can be used in industry. Currently the development of the CHMD process is still in the conceptual design phase.

The changes in the global steel industry as a result of the climate change mitigation will not stop after 2030. Finally, in 2050, the steel industry should be CO₂-neutral. In Chapter 10, an outlook is given for the expected changes in the steel industry between now and 2050 and its impact on sulphur removal in iron- and steelmaking. The amount of carbon used to reduce iron ore will gradually decrease and so will the demand for HMD, as the carbon sources coal and coke are the largest source of sulphur in hot metal. However, it is unlikely that carbon can be fully replaced by hydrogen or electricity. It is expected that in 2050 still a significant amount of steel will be produced via carbon-utilising smelting processes, like Hisarna, in combination with carbon capture and usage. Besides, scrap contains sulphur that needs to be removed as well. It is expected that the share of scrap as a source of iron in the steelmaking industry will increase in the coming decades. Therefore, steel desulphurisation will remain necessary in every steel plant and hot metal desulphurisation will be required as well for the carbon-utilising plants.

Appendices

Samenvatting

In dit proefschrift wordt de ontzwaveling in de ijzer- en staalproductie van de 21e eeuw onderzocht. De huidige stand van de techniek op het gebied van zwavelverwijdering bij de ijzer- en zuurstofstaalproductie wordt besproken in deel I van dit proefschrift en optimalisatie van de slak van ruwijzerontzwaveling (*hot metal desulphurisation*, HMD), die een belangrijk aspect van de huidige ontzwaveling is, wordt behandeld in deel II van dit proefschrift. Aangezien de staalindustrie aanzienlijk zal veranderen als gevolg van de wereldwijde beperking van de klimaatverandering, wordt in deel III de ontzwaveling bestudeerd van ruwijzer van HIsarna (een nieuw CO₂-arm ijzerproductieproces). Tenslotte wordt in deel IV van dit proefschrift een overzicht gegeven van de belangrijkste conclusies van dit werk, evenals een visie op ontzwaveling in de ijzer- en staalproductie voor de komende decennia, gebaseerd op het onderzoek dat in dit proefschrift wordt gepresenteerd.

Zwavel is een vaak ongewenst element in staal dat de vormbaarheid en lasbaarheid van staal verlaagt en het staal broser maakt. Daarom proberen staalproducenten de zwavelconcentratie in het staal te beperken. In 2021 wordt wereldwijd ongeveer twee-derde van het staal geproduceerd via het zogenaamde BF-BOF staalproductieproces, waarbij ijzererts wordt gereduceerd door koolstof (kolen en cokes) in de hoogoven (*blast furnace*, BF), en het ruwijzer uit de hoogoven wordt geraffineerd in de converter (*basic oxygen furnace*, BOF). Het ruwijzer bevat zwavel dat kan worden verwijderd bij verschillende processtappen van de staalproductieketen, zoals bij de ruwijzerontzwaveling, bij de converter of bij de secundaire metallurgieprocessen. Vanwege de lage zuurstofactiviteit in ruwijzer is de ruwijzerontzwaveling voorafgaand aan het converterproces het meest efficiënte ontzwavelingsproces. In hoofdstuk 2 worden de verschillende ontzwavelingsstappen in de staalproductieketen besproken. Hier worden ook de verschillende wereldwijd meest gebruikte ruwijzerontzwavelingsprocessen besproken. De twee belangrijkste ruwijzerontzwavelingsprocessen zijn het co-injectieproces (waarbij ontzwavelingsreagentia, over het algemeen magnesium en kalk of calciumcarbide, in het ruwijzer worden geïnjecteerd) en de Kanbara-reactor (KR; waar op calcium gebaseerde reagentia door het ruwijzer worden gemengd met een roerder). Momenteel wordt wereldwijd het co-injectieproces het meest gebruikt en is het vooral in Europa en Noord-Amerika de standaard. Gewoonlijk worden magnesium en kalk gebruikt als reagentia in het co-injectieproces. Magnesium lost op in het ruwijzer en reageert met de opgeloste

zwavel om de vaste stof magnesiumsulfide te vormen. Hoewel een deel van de kalk direct reageert met de zwavel, is de kalk vooral bedoeld om te reageren met de magnesiumsulfide om calciumsulfide te vormen, dat stabiel is en in de slak terecht komt. Wanneer de injectie van reagentia is voltooid, wordt de slak verwijderd met een afslakarm.

Bij het verwijderen van de slak gaat er ook ijzer verloren. De hoeveelheid ijzer die verloren gaat per lading is ongeveer 0,5-2,5 gew.% van het totale ruwijzer-gewicht. Dit is een grote kostenpost die het ruwijzerontzwavelingsproces veroorzaakt. In hoofdstuk 3 wordt uitgelegd dat ijzerverlies voornamelijk wordt veroorzaakt door twee mechanismen: colloïdaal verlies (ijzer aanwezig in de slak in colloïdale vorm, dat samen met de slak wordt verwijderd) en meesleurverlies (ijzer dat wordt meegeslept met de slak tijdens het afslakken). Meesleurverliezen kunnen worden geminimaliseerd door de omstandigheden van het afslakken te optimaliseren, bijvoorbeeld met een ervaren operator, een schoon afslakblad of een nauwkeurige afslakarm. Colloïdaal verlies kan worden geminimaliseerd door de schijnbare viscositeit van de slak te verlagen, hetgeen onder normale procesomstandigheden betekent dat de vaste fractie van de slak moet worden geminimaliseerd. Dit kan worden bereikt door ofwel de slaktemperatuur te verhogen (in de praktijk betekent dat het minimaliseren van het temperatuurverlies) of door de basiciteit van de slak te verlagen, waardoor de smelttemperatuur van de slak daalt. Verder wordt in hoofdstuk 3 aangetoond dat de ruwijzerontzwavelingsslak een B_2 -basiciteit (de verhouding van de concentraties kalk en siliciumoxide in de slak) van minimaal 1,1 nodig heeft, plus voldoende kalk om alle aanwezige zwavel om te zetten in calciumsulfide om voldoende zwavelverwijderingscapaciteit te hebben. De optimale ruwijzerontzwavelingsslak heeft een B_2 -basiciteit die hoog genoeg is om alle verwijderde zwavel in de slak te houden (voldoende zwavelverwijderingscapaciteit), maar de basiciteit van de slak is laag genoeg om de smelttemperatuur onder de werkelijke temperatuur van de slak te houden (over het algemeen tussen 1300 °C en 1450 °C), waardoor een overwegend vloeibare slak ontstaat, hetgeen resulteert in een laag colloïdaal verlies. In hoofdstuk 4 worden deze bevindingen geëvalueerd en ondersteund met een Monte-Carlo simulatie gebaseerd op thermodynamische gegevens van FactSage, smeltpunt- en viscositeitsmetingen met kunstmatige ruwijzerontzwavelingsslakken en analyse van fabrieksdata. De slaktemperatuur heeft de meeste invloed op het colloïdaal verlies en het totale ijzerverlies, waarbij een lagere temperatuur leidt tot een slak met een hogere fractie vaste stof en dus een hoger ijzerverlies. Van de gangbare slakcomponenten bij het ruwijzerontzwavelingsproces heeft magnesiumoxide de meeste invloed op de smelt-

temperatuur van de slak, waarbij een hogere concentratie magnesiumoxide leidt tot een hogere smelttemperatuur en dus tot een hoger ijzerverlies.

Het is moeilijk om in de oxystaalfabriek de temperatuur van de slak te verhogen. Het is ook moeilijk om de samenstelling van de ruwijzerontzwavelingsslak te veranderen, omdat 60-80 gew.% van de ruwijzerontzwavelingsslak mee is gekomen met het ruwijzer van de hoogoven. De rest van de slaksamenstelling wordt bepaald door de reagentia die worden geïnjecteerd om een bepaalde hoeveelheid zwavel te verwijderen, waardoor een bepaalde hoeveelheid kalk, magnesiumoxide en calciumsulfide aan de slak wordt toegevoegd. Het toevoegen van een slakmodifier is een praktischere methode om de slaksamenstelling zodanig te wijzigen dat de slak een lagere viscositeit heeft. In hoofdstuk 5 worden vliegas en nefeliensyeniet onderzocht als geschikte slakmodificatoren voor het ruwijzerontzwavelingsproces. Vliegas bevat SiO_2 en Al_2O_3 , wat de basiciteit van de slak, en daarmee de smelttemperatuur, vermindert. Nefeliensyeniet bevat ook SiO_2 en Al_2O_3 , maar het bevat daarnaast Na_2O , een basische netwerkmodifier die ook de viscositeit van de slak verlaagt. Smeltpunt- en viscositeits-experimenten met synthetische ruwijzerontzwavelingsslakken tonen aan dat zowel vliegas als nefeliensyeniet bruikbare slakmodificatoren zijn. Zij zijn daarmee een goed alternatief voor de slakmodificatoren op fluoridebasis, die vandaag de dag gangbaar zijn in de staalindustrie (hoewel niet in Nederland). Op fluoride gebaseerde slakmodificatoren verlagen de smelttemperatuur van de slak en de viscositeit van de vloeibare fractie. Fluoride leidt echter tot gezondheids- en milieuproblemen en het vermindert ook de ontzwavelingsefficiëntie van magnesium.

Als gevolg van de wereldwijde inspanningen om klimaatverandering te beperken, moet de staalindustrie haar CO_2 -uitstoot verlagen. Een nieuw proces dat kan bijdragen aan een lagere CO_2 -uitstoot van de staalindustrie is het HIsarna-proces dat wordt ontwikkeld bij Tata Steel in IJmuiden. Een HIsarna-reactor produceert ruwijzer, net als een hoogoven, maar wel met een 20 % lagere CO_2 -uitstoot. Door het geconcentreerde CO_2 -afgas, wat koolstofafvang en opslag of gebruik mogelijk maakt, kan zelfs een 80 % lagere CO_2 -uitstoot worden bereikt. Vergeleken met een hoogoven produceert HIsarna ruwijzer met een lagere temperatuur en met lagere koolstof-, mangaan- en fosforconcentraties. Verder bevat HIsarna-ruwijzer bijna geen silicium en titanium. In vergelijking met een hoogoven bevat HIsarna-ruwijzer ongeveer 3-4 keer meer zwavel (de typische zwavelconcentratie in het HIsarna-ruwijzer is ongeveer 0,1 gew.%). Dit betekent dat voor HIsarna-ruwijzer meer zwavel verwijderd moet worden in vergelijking met ruwijzer uit een gemiddelde hoogoven. De gevolgen voor ontzwaveling van HIsarna-ruwijzer worden besproken in deel III van dit proefschrift.

Vanwege de afkoeling is ruwijzer van een hoogoven doorgaans oververzadigd in koolstof als het bij de ruwijzerontzwavelingsinstallatie aankomt. Deze koolstof-oververzadiging leidt tot grafietvorming, dat ook wel bekend staat als kish. De gevormde grafietvlokken kunnen een laag vormen tussen de slak en het ruwijzer. Eerder onderzoek suggereerde dat deze grafietlaag het ruwijzerontzwavelingsproces zou kunnen belemmeren. De grafietlaag zou de gevormde magnesiumsulfide in het ruwijzer hinderen zodat het de slakfase niet kan bereiken en daardoor het stabielere calciumsulfide niet kan vormen. Dit zou resulteren in een lager ontzwavelingsrendement. Aangezien HIsarna-ruwijzer minder koolstof bevat, zou dit effect bij ontzwaveling van HIsarna-ruwijzer kleiner of zelfs helemaal afwezig kunnen zijn. Zoals echter in hoofdstuk 6 wordt uitgelegd, is dit belemmerende effect van neergeslagen grafiet op de efficiëntie van het ruwijzerontzwavelingsproces erg klein voor zowel HIsarna- als hoogovenruwijzer. Analyse van fabrieksdata laat zien dat er slechts een zwakke correlatie is tussen de verwachte grafietvorming en ontzwavelingsefficiëntie. Alleen voor ladingen met een initiële zwavelconcentratie lager dan 225 ppm, is er een significante correlatie. Dit betekent dat er geen significant voordeel is voor ontzwaveling van koolstofarm HIsarna-ruwijzer in vergelijking met koolstofverzadigd hoogovenruwijzer.

De lagere temperatuur en de hogere initiële zwavelconcentratie van HIsarna-ruwijzer, in vergelijking met hoogovenruwijzer, hebben wel invloed op het ruwijzerontzwavelingsproces, zoals wordt besproken in hoofdstuk 7. Een literatuurstudie, een thermodynamische analyse met FactSage en analyse van fabrieksdata laten zien dat de lagere temperatuur en hogere initiële zwavelconcentratie leiden tot een lager magnesiumverbruik per kilogram verwijderde zwavel. Deze lagere temperatuur, die ongeveer 50 °C lager is dan bij hoogovenruwijzer, is thermodynamisch gunstig voor de ontzwavelingsreactie met magnesium. De hogere initiële zwavelconcentratie leidt tot een hogere zwavelactiviteit, hetgeen de ontzwavelingsreacties versterkt. Er moet echter worden opgemerkt dat de hogere efficiëntie die wordt veroorzaakt door de initiële zwavelconcentratie alleen geldt voor het overschot aan zwavel, in vergelijking met hoogovenruwijzer. De totale hoeveelheid zwavel die verwijderd moet worden is nog steeds 3-4 keer hoger voor HIsarna-ruwijzer dan voor hoogovenruwijzer. Daarom is het totale magnesiumverbruik voor ontzwaveling van HIsarna-ruwijzer ook hoger. Dit betekent ook dat ontzwaveling van HIsarna-ruwijzer langer duurt dan ontzwaveling van hoogovenruwijzer, hetgeen ertoe zou kunnen leiden dat de ruwijzerontzwavelingsstap de bottleneck wordt in een staalfabriek. Er wordt aangenomen dat de zuurstofconcentratie in HIsarna-ruwijzer (~6 ppm) ongeveer 5-10 keer hoger is dan in hoogovenruwijzer (0,5-1,0

ppm). Een hoge zuurstofconcentratie leidt tot een lager ontzwavelingsrendement. Omdat de zuurstofconcentratie in HIsarna-ruwijzer echter nog steeds laag is, is het verwachte extra magnesiumverbruik als gevolg van de hogere zuurstofconcentratie beperkt tot ongeveer 2-3 kg voor een lading van 300 ton. De afwezigheid van silicium en titanium in het ruwijzer zal de efficiëntie van een op magnesium gebaseerd ruwijzerontzwavelingsproces niet beïnvloeden. Een ruwijzerontzwavelingsproces op basis van kalk, zoals het KR-proces, zal echter een lager rendement hebben, omdat silicium reageert met de zuurstof in de kalk terwijl het calcium reageert met de zwavel om calciumsulfide te vormen. Bovendien moet, aangezien HIsarna ruwijzer zonder slak produceert, een alternatief worden gevonden voor de slak die vanuit de hoogoven meekomt met het ruwijzer. Een slak op basis van alleen de geïnjecteerde magnesium en kalk en het gevormde calciumsulfide zou vast zijn bij de gangbare temperaturen tijdens het ruwijzerontzwavelingsproces (zie hoofdstuk 3). Daarom is het gebruik van zure slaktoevoegingen (zoals siliciumoxide en aluminiumoxide) noodzakelijk om de slak vloeibaar te houden en het ijzerverlies te beperken. Toch zullen de hogere slakvolumes als gevolg van meer zwavel dat verwijderd moet worden, leiden tot een hoger ijzerverlies, in vergelijking met ontzwaveling van gemiddeld hoogovenruwijzer.

Doordat de HIsarna continu ruwijzer met een constante samenstelling en temperatuur produceert en tapt, is het een ideaal proces voor continue ruwijzerontzwaveling. Daarom wordt bij Tata Steel in IJmuiden een nieuw continu ruwijzerontzwavelingsproces ontwikkeld: het *Continuous hot metal desulphurisation process* (CHMD). In hoofdstuk 8 wordt dit nieuwe CHMD-proces geïntroduceerd. Het CHMD-proces is gebaseerd op het ruwijzerontzwavelingsproces met co-injectie van magnesium en kalk. Het maakt gebruik van verschillende reactoren in serie om het totale reactorvolume te beperken. Volgens processimulaties zijn er drie reactoren in serie nodig om HIsarna ruwijzer te ontzwellen tot dezelfde zwavelconcentraties die gebruikelijk zijn na het standaard ruwijzerontzwavelingsproces. Bij dit proces wordt de ontzwavelingsefficiëntie verhoogd door de afmetingen van de reactoren te optimaliseren tot een hoogte-diameterverhouding van 5:1. Ter vergelijking, een gewone ruwijzerpan die gebruikt wordt in het batch ruwijzerontzwavelingsproces heeft een hoogte-diameterverhouding van 1,5:1. De optimale reactordimensies zouden moeten leiden tot een ~20 % lager reagensverbruik. Bovendien maakt het continue aspect van dit proces afslakken met een zogenaamd vossenhol mogelijk (slak en ruwijzer worden gescheiden op basis van hun dichtheidsverschil). Dit zal leiden tot ongeveer 60 % minder ijzerverlies in vergelijking met de afslakmethode van het batch ruwijzerontzwavelingsproces. De kostenraming voor

ijzerverlies en reagenskosten laat zien dat de kosten voor het ontzwavelen van één ton ruwijzer met het CHMD-proces ongeveer € 2 lager zijn dan met het state-of-the-art batch ruwijzerontzwavelingsproces. Volgens de laatste berekeningen is de verblijftijd van het ruwijzer in de CHMD echter 3-4 keer hoger dan in het batch ruwijzerontzwavelingsproces, hetgeen leidt tot een hoger temperatuurverlies en mogelijk ook een hogere CO₂-voetafdruk (omdat een lagere temperatuur ervoor zorgt dat er minder schroot in de converter kan worden ingezet). Gezien de toch al lagere temperatuur van HIsarna-ruwijzer, in vergelijking met hoogovenruwijzer, moet dit probleem worden opgelost voordat het CHMD-proces op industriële schaal kan worden ingezet. Op dit moment bevindt de ontwikkeling van het CHMD-proces zich nog in de conceptuele ontwerpfase.

De veranderingen in de wereldwijde staalindustrie als gevolg van de beperking van klimaatverandering zullen niet stoppen na 2030. In 2050 moet de staalindustrie CO₂-neutraal zijn. In hoofdstuk 10 wordt vooruitgeblikt op de verwachte veranderingen in de staalindustrie tussen nu en 2050, en de impact ervan op de ontzwaveling in de ijzer- en staalproductie. De hoeveelheid koolstof die wordt gebruikt om ijzererts te reduceren, zal geleidelijk afnemen. Daarmee neemt ook de vraag naar ruwijzerontzwaveling af, aangezien steenkool en kooks de belangrijkste bron van het zwavel in ruwijzer zijn. Het is echter onwaarschijnlijk dat koolstof volledig kan worden vervangen door waterstof of elektriciteit. De verwachting is dat in 2050 nog steeds een aanzienlijke hoeveelheid staal zal worden geproduceerd via (deels) op koolstof gebaseerde smeltprocessen, zoals HIsarna, in combinatie met CO₂ afvang en gebruik. Bovendien bevat schroot ook zwavel dat verwijderd moet worden. De verwachting is dat het aandeel van schroot als ijzerbron in de staalindustrie de komende decennia zal toenemen. Daarom blijft ontzwaveling van staal nodig in elke staalfabriek en zal ontzwaveling van ruwijzer ook nodig zijn voor de fabrieken die koolstof blijven gebruiken voor ijzerreductie.

Nomenclature

Symbols

a_x	Activity of component x	-
B_2	Basicity CaO/SiO ₂	-
B_4	Basicity based on CaO, MgO, SiO ₂ and Al ₂ O ₃	-
ΔC	Carbon undersaturation	wt%
C_S	Sulphide capacity	-
C_x	Capacity of x in the hot metal	wt%
d_{drop}	Droplet diameter	m
F_x	Volumetric flowrate of x	m ³ /s
f_x	Henrian activity coefficient of component x	-
ΔG^0	Gibbs free energy	J/mol
g	Gravity constant (9.81)	m·s ⁻²
ΔH	Enthalpy	J/mol
h_x	Height of x	m
K_x	Equilibrium constant for reaction x	-
L_S	Sulphur distribution ratio	-
M_x	Molar concentration of x	mol/m ³
m_x	Mass of component x	kg
\dot{m}_{Mg}	Specific magnesium consumption	-
\dot{m}'_{Mg}	Adjusted specific magnesium consumption	-
n	Constant (typically 2.5)	-
P_x	Solubility product of x	-
p_x	Partial pressure of x	Pa
R_x	Radius of x	m
r_x^{app}	Apparent reaction rate of reaction x	mol·s ⁻¹ ·m ⁻³
ΔS	Entropy	J/mol·K
S_{in}	Initial sulphur concentration	ppm
T	Temperature	K or °C
T_{break}	Break temperature	°C
T_{liq}	Liquidus temperature	°C
T_{melt}	Melting temperature	°C
Tor	Measured torque	N·m
t_{settle}	Settling time	s
V_R	Reactor volume	m ³
v_{drop}	Settling speed droplet	m·s ⁻¹

Appendices

X_x	Concentration of component x or weight percentage of phase x	wt%
α	Maximum solid fraction	-
$\dot{\gamma}$	Shear rate	s^{-1}
$\gamma_{[C],meas}$	Measured carbon concentration in hot metal	wt%
η_0	Viscosity of the liquid fraction of the slag	Pa·s
η_{slag}	Apparent viscosity of the slag	Pa·s
A	Optical basicity	-
ρ_x	Density of x	$kg \cdot m^{-3}$
τ	Ratio of shear stress	Pa
$\varphi_{s,slag}$	Solid volume fraction of the slag	-
ω_x	Rotational speed of x	rad/s
[x]	Indicates component x is dissolved in hot metal	
(x)	Indicates component x is in the slag phase	

Abbreviations

BF	Blast furnace
BOF	Basic oxygen furnace, or converter
CCF	Cyclone converter furnace, or smelting cyclone (upper part of HIsarna)
CCS	Carbon capture and storage
CCU	Carbon capture and usage
CHMD	Continuous hot metal desulphurisation
CM	Casting machine
CSTR	Continuously stirred tank reactor, ideal reactor
DRI	Direct reduced iron
EAF	Electric arc furnace
EMF	Electromagnetic force
HIC	Hydrogen induced cracking
HM	Hot metal
HMD	Hot metal desulphurisation
HMP	Hot metal pit
KR	Kanbara reactor, alternative HMD process
LD	Linz-Donawitz, alternative name for BOF or converter
LF	Ladle furnace
MCS	Monte Carlo simulation
MMI	Magnesium mono-injection, or Ukraina-Desmag process, alternative HMD process
NS	Nepheline syenite

PCI	Pulverised coal injection
PFA	Pulverised fuel ash, or fly ash
PFR	Plug flow reactor, ideal reactor
RFM	Random forest model
SM	Secondary metallurgy
SRV	Smelting reduction vessel (lower part of HIsarna)
tHM	Tonne hot metal
tLS	Tonne liquid steel
VD	Vacuum degasser
VOD	Vacuum oxygen decarburisation station
WD-XRF	Wavelength dispersive X-ray fluorescence spectroscopy
XRF	X-ray fluorescence

Appendices

Curriculum vitae

Frank Nicolaas Hermanus Schrama was born 4 March 1986 in Enschede, the Netherlands. In 2004 he graduated with a Gymnasium diploma from *het Stedelijk Lyceum, Zuid*, in Enschede. The same year he started with his study Chemical Engineering at the *University of Twente* in Enschede, where he received his Bachelor degree in 2009, with a minor in Industrial Engineering and Management. In 2010, Frank did an internship at *Eskom*, Johannesburg, South Africa, and the *University of the Western Cape*, Cape Town, South Africa, to work on underground coal gasification for power generation. During his study, Frank organised, among others, a study tour to Mexico and was chief editor (and cartoonist) of student magazine *The Cat*. In 2011, Frank graduated from the *University of Twente* with a Master degree in Chemical Engineering (Process Technology track). He did his Master assignment at the *Sustainable Process Technology* group, researching “Supercritical water gasification (SCWG) of pyrolysis condensate: The influence of operating parameters”.

After his graduation, Frank remained at the *University of Twente* as a researcher to work on the absorption of CO₂ in amine solutions, in cooperation with *TNO* in Delft, the Netherlands. In 2012, Frank started as a process engineer at *Danieli Corus* in Velsen-Noord, the Netherlands, where he worked, amongst others, on hot metal desulphurisation (design, sales and commissioning), converter control models and a logistic simulation model for steel plants.

In 2015, Frank started at the *Metals Production, Refining and Recycling* group at *Delft University of Technology* with his PhD study on “Sulphur removal in 21st century iron- and steelmaking”, part-time, initially next to his job at *Danieli Corus* and later next to his job at *Tata Steel*. Frank started working for *Tata Steel R&D* in IJmuiden, the Netherlands, in 2016 as a principal researcher. His expertise lays in the field of hot metal desulphurisation, the BOF converter process and, more recently, scrap analysis, preparation and utilisation. He works on projects for the steel plants of *Tata Steel* in IJmuiden and Port Talbot, United Kingdom, as well as projects for *Hisarna*. In 2018, Frank received the Williams Award from the British *IOM3* for his paper “Sulphur removal in ironmaking and oxygen steelmaking”.

Frank is married and has two children.

Appendices

List of publications

Publications that are a part of this PhD study are marked with an asterisk (*). It is indicated when a chapter of this thesis is based on a publication.

Journal publications

1. **F.N.H. Schrama**, E.M. Beunder, S.K. Panda, H.-J. Visser, J. Sietsma, R. Boom and Y. Yang, “Optimal hot metal desulphurisation slag considering iron loss and sulphur removal capacity part I: Fundamentals”, Vol. 48, No. 1, *Ironmaking and Steelmaking*, **2021**, p 1-13. (*Chapter 3*)*
2. **F.N.H. Schrama**, E.M. Beunder, S.K. Panda, H.-J. Visser, A. Hunt, J. Sietsma, R. Boom and Y. Yang, “Optimal hot metal desulphurisation slag considering iron loss and sulphur removal capacity part II: Evaluation”, Vol. 48, No. 1, *Ironmaking and Steelmaking*, **2021**, p 14-24. (*Chapter 4*)*
3. N. Madhavanpillaisajee, G.A. Brooks, M.A. Rhamdhani, B.K. Rout, **F.N.H. Schrama**, A. Overbosch, “General Mass Balance for Oxygen Steelmaking”, *Ironmaking and Steelmaking*, Vol. 48, No. 1, **2021**, p 40-54.
4. B.K. Rout, E.M. Beunder, A. Overbosch, W. van der Knoop, J. Sun, **F.N.H. Schrama**, “Understanding the Dynamics of Slag Evolution and Its Influence on Hot Metal Refining in a BOF Process”, *Iron & Steel Technology*, Vol. 18, No. 4, **2021**, p 66-75.
5. **F.N.H. Schrama**, F. Ji, A. Hunt, E.M. Beunder, R. Woolf, A. Tuling, P. Warren, J. Sietsma, R. Boom, Y. Yang, “Lowering iron losses during slag removal in hot metal desulphurisation without using fluoride”, *Ironmaking and Steelmaking*, Vol. 47, No. 5, **2020**, p 464-472. (*Chapter 5*)*
6. **F.N.H. Schrama**, E.M. Beunder, H.-J. Visser, J. Sietsma, R. Boom, Y. Yang, “The hampering effect of precipitated carbon on hot metal desulfurization with magnesium”, *Steel Research International*, Vol. 91, No. 11, **2020**, 1900441. (*Chapter 6*)*
7. B.K. Rout, G. Brooks, M.A. Rhamdhani, Z. Li, **F.N.H. Schrama**, J. Sun, “Dynamic Model of Basic Oxygen Steelmaking Process Based on Multi-zone Reaction Kinetics: Model Derivation and Validation”,

- Materials and Metallurgical Transactions B*, Vol. 49, No. 2, **2018**, p 537-557.
8. B.K. Rout, G. Brooks, M.A. Rhamdhani, Z. Li, **F.N.H. Schrama**, A. Overbosch, “Dynamic Model of Basic Oxygen Steelmaking Process Based on Multi-zone Reaction Kinetics: Modelling of Decarburization”, *Materials and Metallurgical Transactions B*, Vol. 49, No. 3, **2018**, p 1022-1033.
 9. B.K. Rout, G. Brooks, M.A. Rhamdhani, Z. Li, **F.N.H. Schrama**, W. van der Knoop, “Dynamic Model of Basic Oxygen Steelmaking Process Based on Multi-zone Reaction Kinetics: Modelling of Manganese Removal”, *Materials and Metallurgical Transactions B*, Vol. 49, No. 5, **2018**, p 2191-2208.
 10. **F.N.H. Schrama**, E.M. Beunder, B. van den Berg, Y. Yang and R. Boom, “Sulphur removal in ironmaking and oxygen steelmaking”, *Ironmaking and Steelmaking*, Vol. 44, No. 5, **2017**, p 333-343.
(Chapter 2)*
 11. **F. Schrama**, B. van den Berg, G. van Hattum, “Comparing hot metal desulphurisation methods”, *Steel Times International*, Vol. 39, No. 4, **2015**, p 42-49.
 12. **F. Schrama**, D. Merkenstein, M. Jansen, W. Vortrefflich, B. van den Berg, “Steel plant model for optimization of steel plant logistics”, *Millennium Steel India*, **2014**, p 43-47.
(the same article is published in *Millennium Steel International*, Vol. 16, **2015**, p 55-59 and, translated in Chinese as “实现钢厂物流优化的钢厂模型”, in *Millennium Steel China*, **2015**)
 13. **F. Schrama**, B. van den Berg, “Comparison of Kanbara reactor, magnesium mono-injection and lime magnesium co-injection for hot metal desulphurization”, *Millennium Steel India*, **2014**, p 26-31.
(the same article is published in *Millennium Steel International*, Vol. 16, **2015**, p 26-33 and, translated in Chinese as “KR搅拌法、单喷镁和复合喷石灰-镁铁水脱硫”, in *Millennium Steel China*, **2015**)
 14. E. Sanchez Fernandez, K. Hefferman, L.V. van der Ham, M.J.G. Linders, E. Eggink, **F.N.H. Schrama**, D.W.F. Brilman, E.L.V. Goetheer, T.J.H. Vlugt, “Conceptual Design of a Novel CO₂ Capture Process Based on Precipitating Amino Acid Solvents”, *I&EC Research*, Vol. 52, **2013**, p 12223-12235.

Publications in conference proceedings

15. **F.N.H. Schrama**, A. Emami, E.M. Beunder, J.L.T. Hage, J.W.K. van Boggelen, P. Broersen, “Continuous hot metal desulphurisation: a new cost-efficient process with a lower environmental footprint”, *Estad*, Online, **2021**, #32157. (only an abstract and a pre-recorded presentation)*
16. **F.N.H. Schrama**, E.M. Beunder, S.K. Panda, E. Moosavi-Khoonsari, R. Boom, J. Sietsma, Y. Yang, “How to Design Hot Metal Desulphurisation Slag with a High Sulphur Capacity and Low Iron Entrapment?”, *Molten*, Online, **2021**, P0956.*
17. B.K. Rout, E.M. Beunder, A. Overbosch, W. van der Knoop, J. Sun, **F.N.H. Schrama**, “Understanding the Dynamics of Slag Evolution and Its Influence on Hot Metal Refining in a BOF Process”, *AISTech*, Online, **2020**, p 704-714.
18. **F.N.H. Schrama**, E.M. Beunder, H.-J. Visser, R. Boom, J. Sietsma, Y. Yang, “Effect of graphite on hot metal desulphurisation”, *METEC/Estad*, Düsseldorf (Ger.), **2019**, P308.*
19. **F.N.H. Schrama**, E.M. Beunder, F. Ji, R. Woolf, C. Barnes, J. Sietsma, R. Boom, Y. Yang, “Effect of KAlF₄ on the efficiency of hot metal desulphurisation with magnesium”, *EOSC*, Taranto (It.), **2018**, EOSC021.*
20. E.M. Beunder, A. Overbosch, **F.N.H. Schrama**, H.-J. Visser, K. Gu, N. Dogan, K.S. Coley, “Steel and slag analysis during converter blowing compared to model calculations”, *EOSC*, Taranto (It.), **2018**, EOSC023.
21. B.K. Rout, G. Brooks, M.A. Rhamdhani, **F.N.H. Schrama**, W. van der Knoop, “Dynamic modelling of dephosphorization kinetics in BOF process by using bloated droplet mechanism”, *EOSC*, Taranto (It.), **2018**, EOSC017.
22. **F.N.H. Schrama**, E. Moosavi-Khoonsari, E.M. Beunder, C. Kooij, R. Boom, J. Sietsma, Y. Yang, “Slag optimisation considering iron loss and sulphide capacity in hot metal desulphurisation”, *ICS*, Venice (It.), **2018**, ICS131.*
23. G. Brooks, M. Rhamdhani, B. Rout, Z. Li, **F. Schrama**, A. Overbosch, “Dynamic Modeling of the BOF Process: Comparison of Model Performance With Plant Data”, *AISTech*, Philadelphia (USA), **2018**, p 981-991.
24. **F.N.H. Schrama**, E.M. Beunder, J.W.K. van Boggelen, R. Boom, Y. Yang, “Desulphurisation of Hisarna hot metal - a comparison study based on plant data”, *STIS*, Kanpur (Ind.), **2017**, p 419-422.*

Appendices

25. M. Schlautmann, B. Kleimt, S. Khadraoui, K. Hack, P. Monheim, B. Glaser, R. Antonic, M. Adderley, **F. Schrama**, “Dynamic On-line Monitoring and End Point Control of Dephosphorisation in the BOF Converter”, *Estad*, Vienna (Aut.), **2017**, p 1038-1049.
26. **F. Schrama**, G. van Hattum, B. van den Berg, “The Leading Hot Metal Desulfurization Methods - A Comparison Between KR, MMI and Co-injection”, *ABM Week*, Rio de Janeiro (Br.). **2015**, p 323-332.
27. **F. Schrama**, D. Merkenstein, M. Jansen, W. Vortrefflich, B. van den Berg, “Steel Plant Model for Solving Logistic Bottlenecks with Advanced Plant Simulation”, *ABM Week*, Rio de Janeiro (Br.). **2015**, p 298-306.
28. **F. Schrama**, B. van den Berg, D. Merkenstein, M. Jansen, W. Vortrefflich, “Solving logistic bottlenecks with advanced plant simulation - Steel Plant Model”, *METEC/Estad*, Düsseldorf (Ger.), **2015**.
29. **F. Schrama**, D. Merkenstein, M. Jansen, W. Vortrefflich, B. van den Berg, “Steel Plant Model for Optimization of Steel Plant Logistics”, *ICS*, Beijing (Chn.), **2015**, p 204-207.
30. **F. Schrama**, B. van den Berg, G. van Hattum, “A Comparison of the Leading Hot Metal Desulphurization Methods”, *ICS*, Beijing (Chn.), **2015**, p 61-66.
31. **F. Schrama**, D. Merkenstein, M. Jansen, W. Vortrefflich, B. van den Berg, “Steel Plant Model - The Comprehensive Solution for Steel Plant Logistics”, *EOSC*, Trinec (Cz.), **2014**.
32. **F. Schrama**, B. van den Berg, “A Study of Hot Metal Desulphurization Methods Based on Metallurgy Performance and Operational Costs”, *EOSC*, Trinec (Cz.), **2014**.

Patents

33. A. Emami, **F.N.H. Schrama**, J.W.K. van Boggelen, “Device and method for continuous desulphurisation of liquid hot metal”, **2020**, WO2020239554A1.

History and acknowledgements

History

Although I already attended my first PhD defence at the age of 5, which was the defence of my father at the University of Twente [1], and I have since witnessed the PhD defences of many friends, colleagues and relatives, including the defence of my wife at Leiden University [2], I never thought of doing a PhD study myself until I was already working at Danieli Corus. There I was introduced to every aspect of hot metal desulphurisation and I got enthusiastic about this elegant process. Luckily, I was able to convince the board of Danieli Corus to support a part-time PhD study in Delft on hot metal desulphurisation. In June 2015, I started to work on my PhD study at Delft University of Technology. The study was initially planned for one day per week for the period of six years.

Unfortunately, Danieli Corus had to reorganise due to financial reasons a year later, leading to my resignation there and a direct end to the funding of my PhD study. Luckily, I could start at the R&D department of Tata Steel in IJmuiden almost immediately. Tata Steel was very interested in the topic of my PhD study and, therefore, took over the funding of the (still) one-day-per-week study. The only change was that the desulphurisation of Hisarna hot metal was included in the study. Starting at the steelmaking and casting group of Tata R&D (and sharing the hallway with Centre of Expertise steelmaking) was like a warm bath. There are few hallways in the world with a higher concentration of knowledge and expertise on steelmaking. Also, many colleagues did a part-time PhD study next to their regular job before, so I could learn from their experience as well. Because of the interesting topic and the ideal atmosphere in IJmuiden and Delft, combining a PhD study and a full-time research job did not feel like hard working at all.

In 2017, I got married to Jantsje, followed in 2018 by the birth of our son Rein and in 2020 by the birth of our daughter Wende. To fully enjoy my new role as a father, I decided to work one day less per week to fully dedicate to the children. Something I have not regretted since. Meanwhile, the PhD study remained a source of inspiration to me. Especially because towards the end of the PhD study, more and more results of the research lead to a practical application in the steel plant. Even the corona crisis could not lower my enthusiasm for this PhD study.

Therefore, I am proud to present this thesis. A thesis that would not have been there without the help and efforts of many people who I will try to give their well-deserved acknowledgements.

Acknowledgements

First of all, I want to thank my promotors and supervisors. Thank you Yongxiang and Jilt, for being my promotors, for constantly challenging me to dive deeper into the subject and to improve the value of my work with your sharp and critical, but fair, feedback. Yongxiang, thank you for all the great suggestions and advice throughout this study. I could always count on you whenever I got stuck. Jilt, your often fresh look on the topic has prevented me from making a mistake more than once. Also your comments on statistics or reasoning were very helpful. I also thank my supervisors Rob and Liesbeth, for guiding me through this PhD study and sharing all their valuable knowledge. Rob, discussions with you were a real pleasure and your clear love for the field of steelmaking is an inspiration to me. Liesbeth, whether we work together at Tata or in this PhD study, I always think we form a perfect team. I am looking forward to working together with you for many years to come.

I also thank my friends and (also former) colleagues of the Metals, Production, Recycling and Refining group in Delft: Sander, Prakash, Sebastiaan, Aida, Xiaoling, Ashkan, Devi, Jim, Shoshan, Tim, Evangelos, Zhiyuan, Chenna, Allert, Prisca and Saskia. A special word for my good friend Dharm Jeet, with whom I shared my office in Delft for almost 5 years: I really enjoyed all our talks about steelmaking, different cultures, cricket or whatever we talked about. I am happy we are now also colleagues at Tata Steel.

This whole PhD study started when I was still working for Danieli Corus. I want to thank the company for initially giving me the opportunity to pursue my goal. Bart van den Berg taught me everything about steelmaking in general, and in particular hot metal desulphurisation. Thank you Bart, you have been a great mentor to me. I also want to thank all my former colleagues at Danieli Corus; I truly enjoyed working with you.

My colleagues at the steelmaking and casting departments in R&D and CoE made me feel at home the moment I started at Tata Steel. Thank you Rudi, also for your support, Gert, also for getting me on board, Bapin, also for our sometimes almost philosophical discussions, Begoña, Stefan, Pieter, Kateryna, Wouter, Ali, also for our deep and sharp discussions about hot metal desulphurisation (and many other things), Aart, also for your insightful and pragmatic comments, Willem, Jianjun, Sourav, also for your great help with thermodynamics, Erwin, Claire, Aida

(again), Fokke, Wouter, Frank, Jan, also for your enthusiasm about a PhD study and Leiden, Ton, Huijuan, also for being the first enthusiastic supporter of my PhD study, already when we were still office mates at Danieli Corus, Arnoud, Arthur, Alma, Steve and Liesbeth (again), for all your support, help, critique, advice and the great atmosphere in our hallway.

Many more people in Tata Steel have made this thesis possible. Although I will never be able to complete the following list, I want to thank, within R&D, Tim, Jan, Hans, Thong, Yanping, Dirk, Sjaak, Kumar, Sieger, Chris, James, Enno, Elmira, Menno, Nick and Ben. Also at the OSF2 steel plant many people have supported me during this study. Manuel, Sander, Rob, Marcel, Liesbeth (again), San, Elizabeth, Franka, Jasper, many operators, Ibrahim, Karina and Rukiye, thank you. The HISarna process is an important part of this thesis and that could not have been written without the help of my colleagues from HISarna Johan, Koen, Chris, Christiaan, Hans (again), Dharm Jeet (again), Erik and Melissa. My colleagues in Wales (UK), at the Port Talbot steel plant and at the R&D centre in Swansea made important contributions to this PhD study as well. Thank you John, Liam, Chris (again), Alison, also for setting up the trials to prove fly ash works as slag modifier and the photos in Chapter 1, Rhian, Heather, Ciaran, Gaj, Daniel and Shahid. Special thanks to Hessel-Jan, my predecessor in doing a PhD research about desulphurisation at Tata, for all your support and critical questions. Of course, I also thank the company Tata Steel in IJmuiden, for taking over the full support of the PhD when I started working there.

People from other institutes have also contributed to this study, as co-authors or co-workers. Thank you Fuzhong, Adam, Peter and Richard from the Materials Processing Institute in Middlesbrough (UK) and Hans and Kay from Eindhoven University.

A special thank you to my paranymphs Chris and Ali (again), for supporting me on the day of the defence. I count on you guys!

Finally, I also thank my family and friends for supporting me all these years and for simply being there for me. I am grateful to my parents, Angelique and Geerten, for all their love and for making me the person I am today. Also, Suus deserves to be mentioned here for all her support. I dedicate this thesis to my wife, Jantsje, and my children, Rein and Wende. Your love and support are invaluable to me. I cannot describe how much you mean to me, so I will simply say: I love you.

References

- [1] G.J.I. Schrama, “Keuzevrijheid in organisatievormen. Strategische keuzes rond organisatiestructuur en informatietechnologie bij het invoeren van een personeelsinformatiesysteem bij grote gemeenten,” (PhD thesis) University of Twente, Enschede (NL), 1991.
- [2] J.H. Pasma, “Impaired standing balance: Unraveling the underlying cause in elderly,” (PhD thesis) Leiden University, Leiden (NL), 2015.

Stellingen

behorende bij het proefschrift

Desulphurisation in 21st century iron- and steelmaking

door

Frank N.H. Schrama

1. Ontzwaveling van HIsarna-ruwijzer zal efficiënter zijn dan ontzwaveling van hoogoven-ruwijzer, hoewel de procestijd en het totale reagentverbruik zullen toenemen.
2. De grafitlaag die bij ontzwaveling van in koolstof oververzadigd ruwijzer wordt gevormd tussen het ruwijzer en de slak, zal niet leiden tot een significante vermindering van de ontzwavelingsefficiëntie.
3. Om ijzerverliezen tijdens het ruwijzerontzwavelingsproces te verminderen zouden fabrieken netwerkvormende stoffen moeten toevoegen aan de slak zodat de schijnbare viscositeit ervan verlaagd wordt.
4. De toekomst van een continu ruwijzerontzwavelingsproces op industriële schaal hangt minder af van het overwinnen van de technische uitdagingen dan van het overtuigen van de conservatieve staalindustrie.
5. Stellen dat co-injectie dan wel het Kanbara reactor proces universeel de beste ruwijzerontzwavelingsmethode is, is een ongelukkige oversimplificatie of een verkooptruc.
6. De huidige wereldwijde klimaatontwikkelingen zullen niet leiden tot het verdwijnen van de staalindustrie, maar wel tot de grootste verandering ervan sinds de industriële revolutie.
7. Ruwijzerontzwaveling kan beschouwd worden als het FC Twente van de staalfabriek: het valt net buiten de ‘traditionele top drie’ van converterproces, secundaire metallurgie en gieten, en krijgt derhalve niet altijd de aandacht die het verdient.
8. Ongeacht de enorme veranderingen die in de staalindustrie de komende jaren verwacht worden, zal ontzwavelingskennis zelfs over 50 jaar nog steeds relevant zijn.
9. Luiheid is de drijvende kracht achter innovatie; in een samenleving met uitsluitend harde werkers zou men nog in beestenvellen rondlopen.
10. De stelling van striptekenaar Hergé dat een goede tekening nooit teveel laat zien, is ook toepasbaar op figuren in de wetenschappelijke literatuur, maar wordt helaas regelmatig genegeerd.

Stellingen 1-4 hebben betrekking op het proefschrift.

Deze stellingen worden oponeerbaar en verdedigbaar geacht en zijn als zodanig goedgekeurd door de promotoren dr. Yongxiang Yang en prof.dr.ir. Jilt Sietsma.

Propositions

accompanying the dissertation

Desulphurisation in 21st century iron- and steelmaking

by

Frank N.H. Schrama

1. Desulphurisation of Hisarna hot metal will be more efficient than desulphurisation of blast furnace hot metal, although the process time and total reagent consumption will increase.
2. The graphite layer that is formed during the desulphurisation of carbon-supersaturated hot metal between the slag and hot metal, will not lead to a significantly lower desulphurisation efficiency.
3. In order to lower the iron losses during the industrial hot metal desulphurisation process, network-forming compounds should be added, in order to reduce the slag's apparent viscosity.
4. The future of the continuous hot metal desulphurisation process on industrial scale depends less on overcoming the technical challenges than on convincing the conservative steel industry.
5. Claiming that either co-injection process or the Kanbara reactor process is universally the best hot metal desulphurisation process, is either an unfortunate oversimplification or a sales trick.
6. The current global developments around climate change will not mean the end of the steelmaking industry, but rather its greatest transformation since the industrial revolution.
7. Hot metal desulphurisation can be considered as the FC Twente of the steel plant: it falls just outside the top-3 of converter process, secondary steelmaking and casting, and therefore it does not always receive the attention it deserves.
8. Despite the enormous changes expected for the steel industry the coming years, knowledge of desulphurisation will still be relevant even 50 years from now.
9. Laziness is the driving force behind innovation: in a society consisting of only hard workers, people would still wear animal skins.
10. The statement of comic artist Hergé that a good drawing never shows too much is applicable for figures in scientific literature as well, but is, unfortunately, often neglected.

Propositions 1-4 pertain to this dissertation.

These propositions are regarded as opposable and defensible, and have been approved as such by the promoters dr. Yongxiang Yang and prof.dr.ir. Jilt Sietsma.